Johannes Zschocke
Matthias Baumgartner
Eva Morava
Marc Patterson
Shamima Rahman
Verena Peters *Editors*

# JIMD Reports

Volume 23

SSIEM

Springer

JIMD Reports
Volume 23

Johannes Zschocke
Editor-in-Chief

Matthias Baumgartner · Eva Morava ·
Marc Patterson · Shamima Rahman
Editors

Verena Peters
Managing Editor

# JIMD Reports
# Volume 23

Springer

SSIEM

ISSN 2192-8304 ISSN 2192-8312 (electronic)
JIMD Reports
ISBN 978-3-662-47466-2 ISBN 978-3-662-47467-9 (eBook)
DOI 10.1007/978-3-662-47467-9

Springer Heidelberg New York Dordrecht London


Printed on acid-free paper

Springer-Verlag GmbH Berlin Heidelberg is part of Springer Science+Business Media (www.springer.com)

# Contents

**Arginine Functionally Improves Clinically Relevant Human Galactose-1-Phosphate Uridylyltransferase (GALT) Variants Expressed in a Prokaryotic Model** . . . . . 1
Ana I. Coelho, Matilde Trabuco, Maria João Silva, Isabel Tavares de Almeida, Paula Leandro, Isabel Rivera, and João B. Vicente

**Effect and Tolerability of Agalsidase Alfa in Patients with Fabry Disease Who Were Treatment Naïve or Formerly Treated with Agalsidase Beta or Agalsidase Alfa** . . . 7
Ozlem Goker-Alpan, Khan Nedd, Suma P. Shankar, Yeong-Hau H. Lien, Neal Weinreb, Anna Wijatyk, Peter Chang, and Rick Martin

**Niemann-Pick Type C-2 Disease: Identification by Analysis of Plasma Cholestane-3β,5α,6β-Triol and Further Insight into the Clinical Phenotype** . . . . . 17
J. Reunert, A.S. Lotz-Havla, G. Polo, F. Kannenberg, M. Fobker, M. Griese, E. Mengel, A.C. Muntau, P. Schnabel, O. Sommerburg, I. Borggraefe, A. Dardis, A.P. Burlina, M.A. Mall, G. Ciana, B. Bembi, A.B. Burlina, and T. Marquardt

**The Modulatory Effects of the Polymorphisms in *GLA* 5′-Untranslated Region Upon Gene Expression Are Cell-Type Specific** . . . . . 27
Susana Ferreira, Carlos Reguenga, and João Paulo Oliveira

**The Kuvan® Adult Maternal Paediatric European Registry (KAMPER) Multinational Observational Study: Baseline and 1-Year Data in Phenylketonuria Patients Responsive to Sapropterin** . . . . . 35
Friedrich K. Trefz, Ania C. Muntau, Florian B. Lagler, Flavie Moreau, Jan Alm, Alberto Burlina, Frank Rutsch, Amaya Bélanger-Quintana, and François Feillet

**Postmortem Findings and Clinical Correlates in Individuals with Infantile-Onset Pompe Disease** . . . . . 45
Loren D.M. Pena, Alan D. Proia, and Priya S. Kishnani

**Clinical Severity of PGK1 Deficiency Due To a Novel p.E120K Substitution Is Exacerbated by Co-inheritance of a Subclinical Translocation t(3;14)(q26.33;q12), Disrupting *NUBPL* Gene** . . . . . 55
Dezső David, Lígia S. Almeida, Maristella Maggi, Carlos Araújo, Stefan Imreh, Giovanna Valentini, György Fekete, and Irén Haltrich

**Abnormal Newborn Screening in a Healthy Infant of a Mother with Undiagnosed Medium-Chain Acyl-CoA Dehydrogenase Deficiency** . . . . . 67
Lise Aksglaede, Mette Christensen, Jess H. Olesen, Morten Duno, Rikke K.J. Olsen, Brage S. Andresen, David M. Hougaard, and Allan M. Lund

**Cobalamin C Disease Missed by Newborn Screening in a Patient with Low Carnitine Level** . . . . . 71
Rebecca C. Ahrens-Nicklas, Esra Serdaroglu, Colleen Muraresku, and Can Ficicioglu

**Adverse Effects of Genistein in a Mucopolysaccharidosis Type I Mouse Model** . . . 77
Sandra D.K. Kingma, Tom Wagemans, Lodewijk IJlst, Jurgen Seppen, Marion J.J. Gijbels, Frits A. Wijburg, and Naomi van Vlies

**Expanding the Clinical and Magnetic Resonance Spectrum of Leukoencephalopathy with Thalamus and Brainstem Involvement and High Lactate (LTBL) in a Patient Harboring a Novel *EARS2* Mutation** . . . . . 85
Roberta Biancheri, Eleonora Lamantea, Mariasavina Severino, Daria Diodato, Marina Pedemonte, Denise Cassandrini, Alexandra Ploederl, Federica Trucco, Chiara Fiorillo, Carlo Minetti, Filippo M. Santorelli, Massimo Zeviani, and Claudio Bruno

**Mitochondrial DNA Depletion and Deletions in Paediatric Patients with Neuromuscular Diseases: Novel Phenotypes** . . . . . 91
Tuomas Komulainen, Milla-Riikka Hautakangas, Reetta Hinttala, Salla Pakanen, Vesa Vähäsarja, Petri Lehenkari, Päivi Olsen, Päivi Vieira, Outi Saarenpää-Heikkilä, Johanna Palmio, Hannu Tuominen, Pietari Kinnunen, Kari Majamaa, Heikki Rantala, and Johanna Uusimaa

**Medium-Chain Acyl-CoA Dehydrogenase Deficiency: Evaluation of Genotype-Phenotype Correlation in Patients Detected by Newborn Screening** . . . . . 101
Gwendolyn Gramer, Gisela Haege, Junmin Fang-Hoffmann, Georg F. Hoffmann, Claus R. Bartram, Katrin Hinderhofer, Peter Burgard, and Martin Lindner

**Rhabdomyolysis-Associated Mutations in Human *LPIN1* Lead to Loss of Phosphatidic Acid Phosphohydrolase Activity** . . . . . 113
George G. Schweitzer, Sara L. Collier, Zhouji Chen, James M. Eaton, Anne M. Connolly, Robert C. Bucelli, Alan Pestronk, Thurl E. Harris, and Brian N. Finck

**Dup-24 bp in the *CHIT1* Gene in Six Mexican Amerindian Populations** . . . . . 123
T.D. Da Silva-José, K.J. Juárez-Rendón, J.A. Juárez-Osuna, A. Porras-Dorantes, A. Valladares-Salgado, M. Cruz, M. Gonzalez-Ibarra, A.G. Soto, M.T. Magaña-Torres, L. Sandoval-Ramírez, and José Elías García-Ortiz

JIMD Reports
DOI 10.1007/8904_2015_420

RESEARCH REPORT

# Arginine Functionally Improves Clinically Relevant Human Galactose-1-Phosphate Uridylyltransferase (GALT) Variants Expressed in a Prokaryotic Model

**Ana I. Coelho • Matilde Trabuco • Maria João Silva • Isabel Tavares de Almeida • Paula Leandro • Isabel Rivera • João B. Vicente**

Received: 30 October 2014 / Revised: 28 January 2015 / Accepted: 09 February 2015 / Published online: 27 March 2015


**Abstract** Classic galactosemia is a rare genetic disease of the galactose metabolism, resulting from deficient activity of galactose-1-phosphate uridylyltransferase (GALT). The current standard of care is lifelong dietary restriction of galactose, which however fails to prevent the development of long-term complications. Structural-functional studies demonstrated that the most prevalent *GALT* mutations give rise to proteins with increased propensity to aggregate in solution. Arginine is a known stabilizer of aggregation-prone proteins, having already shown a beneficial effect in other inherited metabolic disorders.

Herein we developed a prokaryotic model of galactose sensitivity that allows evaluating in a cellular context the mutations' impact on GALT function, as well as the potential effect of arginine in functionally rescuing clinically relevant variants.

This study revealed that some hGALT variants, previously described to exhibit no detectable activity in vitro, actually present residual activity when determined in vivo. Furthermore, it revealed that arginine presents a mutation-specific beneficial effect, particularly on the prevalent p.Q188R and p.K285N variants, which led us to hypothesize that it might constitute a promising therapeutic agent in classic galactosemia.

Communicated by: Gerard T. Berry, M.D.

Competing interests: None declared

A.I. Coelho · M. Trabuco · M.J. Silva · I.T. de Almeida · P. Leandro · I. Rivera · J.B. Vicente (✉)
Metabolism and Genetics Group, Research Institute for Medicines (iMed.ULisboa), Faculty of Pharmacy, University of Lisbon, 1649-003 Lisbon, Portugal
e-mail: joaovicente@ff.ulisboa.pt

M.J. Silva · I.T. de Almeida · P. Leandro · I. Rivera · J.B. Vicente
Department of Biochemistry and Human Biology, Faculty of Pharmacy, University of Lisbon, 1649-003 Lisbon, Portugal

A.I. Coelho
Department of Pediatrics/Laboratory of Genetic Metabolic Diseases, Maastricht University Medical Center, 6202 Maastricht, The Netherlands

## Introduction

Classic galactosemia (OMIM #230400) is a rare metabolic disease resulting from deficient activity of galactose-1-phosphate uridylyltransferase (GALT, EC 2.7.7.12), the second enzyme of the Leloir pathway (Fridovich-Keil and Walter 2008). This inherited metabolic disorder is a potentially lethal disease that develops in the neonatal period, upon exposure to galactose in milk (Berry and Walter 2012; Fridovich-Keil and Walter 2008). The present standard of care is a lifelong galactose-restricted diet, which, notwithstanding its irrefutable life-saving role in the neonatal period, fails to prevent long-term cognitive, motor, and fertility impairments (Bosch 2006; Fridovich-Keil and Walter 2008; Waggoner et al. 1990), and thus intense research has been dedicated to the pursuit of a more effective therapy.

Classic galactosemia is caused by mutations in the *GALT* gene, and more than 260 variations have already been described, the majority being missense mutations (>60%) (Calderon et al. 2007; Leslie et al. 1992). Structural and functional studies demonstrated that clinically relevant *GALT* mutations result in misfolded protein variants (Coelho et al. 2014; McCorvie et al. 2013). A decrease in thermal and conformational stability has been observed for several GALT variants (McCorvie et al. 2013), although the most frequent *GALT* mutations actually affect the variants' aggregation propensity, particularly the p.Q188R variant,

responsible for >60% of galactosemic phenotypes (Coelho et al. 2014; Suzuki et al. 2001).

Arginine has been previously described as therapeutically beneficial for a pyruvate dehydrogenase complex-deficient patient whose biochemical and clinical symptoms significantly improved upon arginine aspartate intake (Silva et al. 2009). A positive role of arginine has also been observed in the peroxisome function of cultured cells from peroxisome biogenesis disorder patients with mutations in *PEX1*, *PEX6*, and *PEX12* (Berendse et al. 2013). Furthermore, arginine is a long-recognized protein stabilizer that has been proposed to exert an anti-aggregation effect by increasing the activation energy of protein aggregation (Baynes et al. 2005). In line with this, we sought to evaluate whether arginine exerts a protective stabilizing effect towards clinically relevant GALT variants. Accordingly, this study aimed to evaluate the effect of arginine on rescuing variant GALT function and alleviating galactose-induced toxicity in a prokaryotic model of galactose sensitivity.

## Materials and Methods

### Cloning and Mutagenesis

The *Escherichia* (*E.*) *coli* K-12Δ*galT* strain (JW0741-1;Δ*galT730*::*kan*), with a deletion of the endogenous *galT* gene, was purchased from the Coli Genetic Stock Center (Baba et al. 2006). The human *GALT* (*hGALT*) cDNA sequence, including an N-terminal hexa-histidyl tag-encoding sequence, was cut from the pET24b-based construct reported in (Coelho et al. 2014) with the BamHI and HindIII restriction enzymes and cloned into the pTrcHisA expression vector (Invitrogen). The mutations originating the studied variants (p.S135L, p.G175D, p.P185S, p.Q188R, p.R231C, pR231H, p.K285N, and p.N314D) were introduced by site-directed mutagenesis, as previously described (Coelho et al. 2014), and confirmed by direct sequencing. As a negative control, we employed a pTrcHisA-based vector containing the cDNA encoding the human enzyme phenylalanine hydroxylase (hPAH) (Leandro et al. 2000).

### Cell Cultures and Growth Media

Non-transformed and wild-type *hGALT*-transformed *E. coli* Δ*galT* were first grown in M9 minimal medium (Maniatis et al. 1982) containing either 1% glucose (with or without 1% galactose), 1% glycerol, or 1% galactose as carbon sources, to evaluate the ability of wild-type hGALT to alleviate galactose toxicity.

Cultures expressing all hGALT variants and hPAH were grown at 37°C in M9 minimal medium (Maniatis et al. 1982) containing glycerol (1%) as sole carbon source, from a starting optical density at 600 nm ($OD_{600nm}$) of 0.05. At $OD_{600nm} = 0.3$, 250 μM isopropyl-D-thiogalactoside (IPTG) was added to all cultures to induce protein expression, as well as 25 mM arginine to cultures III and IV (Table 1). After 1 h of protein expression induction, 1% galactose was added to cultures II and IV (Table 1). Cultures growth was followed by hourly measurements of $OD_{600nm}$, starting at induction time ($t = 0$ h) and up to 9 h.

**Table 1** Cell culture conditions to evaluate the ability of GALT variants to alleviate galactose toxicity and the effect of arginine

| | Supplementation[a] | |
|---|---|---|
| | Galactose | Arginine |
| I | − | − |
| II | + | − |
| III | − | + |
| IV | + | + |

[a] All cultures were grown in M9 minimal medium containing 1% glycerol as carbon source, supplemented with 100 μM ferrous sulfate and 100 μM zinc sulfate

Growth curves were obtained from plotting $OD_{600nm}$ from cultures I and II (Table 1) as a function of time (Figs. 1, 2, and 3 show representative graphics from multiple independent experiments). To directly evaluate the arginine effect on the rescue from galactose toxicity, ratios $r$ and $r_{arg}$ were calculated according to Eqs. (1) and (2), respectively, and were plotted as a function of time (Figs. 2 and 3 show representative graphics from multiple independent experiments). Recombinant production of hGALT and hPAH was confirmed by immunoblotting analysis, using, respectively, the anti-GALT and anti-His primary antibodies (sc-365577, Santa Cruz Biotechnology; 27-4710-01, GE Healthcare Biosciences).

$$r = \frac{OD_{600nm}\text{gal (II)}}{OD_{600nm}\text{gly (I)}}, \quad (1)$$

$$r_{arg} = \frac{OD_{600nm}\text{gal} + \text{arg (IV)}}{OD_{600nm}\text{gly} + \text{arg (III)}}. \quad (2)$$

## Results and Discussion

We have developed a prokaryotic model of galactose sensitivity using the *E. coli* Δ*galT* strain, with a deletion of the endogenous *galT* gene (Baba et al. 2006). Expressing hGALT variants in this *E. coli* strain, and assaying the cultures sensitivity to galactose in the culture medium, allows evaluating the mutations severity in a cellular context, as well as testing stabilizing compounds. Previous studies reported a yeast model of galactose sensitivity

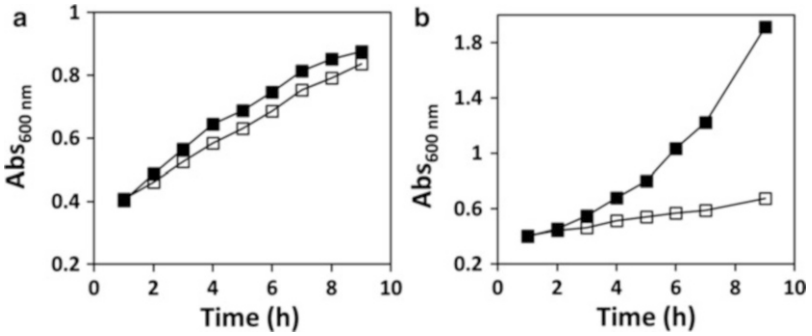


**Fig. 1** Galactose toxicity is alleviated by expression of human GALT. Growth profiles of *Escherichia coli* Δ*galT* transformed with vectors encoding wild-type hGALT (Panel **a**, positive control) or wild-type hPAH (Panel **b**, negative control), in the absence or presence of galactose. Bacteria were grown at 37°C in M9 minimal medium with 1% glycerol as carbon source. At $OD_{600nm}$ =0.3, protein expression was induced with 250 μM IPTG. After 1 h, vehicle (water, full squares) or 1% galactose (hollow squares) was added to the cultures, and the growth was followed by hourly measurements of $OD_{600nm}$ up to 9 h. Growth curves are representative graphics from several independent experiments ($n = 12$ for wild-type hGALT and $n = 12$ for PAH)

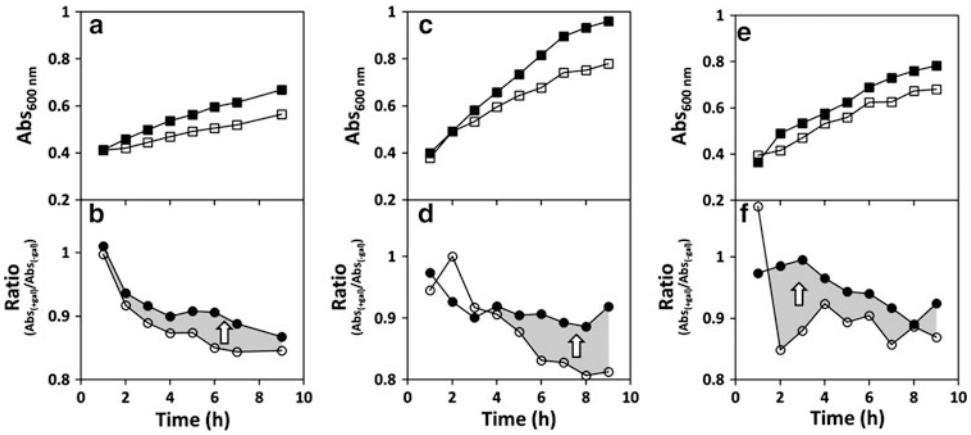


**Fig. 2** Arginine improves the function of p.Q188R, p.K285N, and p.G175D hGALT. Growth profiles of *Escherichia coli* Δ*galT* expressing the p.Q188R, p.K285N, and p.G175D hGALT variants (Panels **a**, **c,** and **e**, respectively) in the absence or presence of galactose. Bacteria were grown at 37°C in M9 minimal medium with 1% glycerol as carbon source. At $OD_{600nm}$ =0.3, protein expression was induced with 250 μM IPTG. After 1 h, vehicle (water, full squares) or 1% galactose (hollow squares) was added to the cultures, and the growth was followed by hourly measurements of $OD_{600nm}$ up to 9 h. Simultaneously with water/galactose, 25 mM arginine or vehicle (water) was added to the cultures. Panels **b**, **d,** and **f** depict the ratio curves for bacteria expressing, respectively, p.Q188R, p.K285N, and p.G175D hGALT, obtained by dividing, at each time point, the $OD_{600nm}$ in the presence or absence of galactose (*black circles*, in the presence of 25 mM arginine; *hollow circles*, absence of arginine). The *gray-shaded areas* and the *white arrows* depict the effect of arginine in improving the ability of these variants to alleviate galactose toxicity, highlighted by *white arrows*. Growth curves are representative graphics from several independent experiments ($n = 4$ for p.Q188R and $n = 3$ for p.G175D and p.K285N)

(Riehman et al. 2001; Ross et al. 2004), which is however technically more demanding and time-consuming comparatively to *E. coli*.

## Effect of Carbon Sources upon the Growth of Non-transformed and Wild-Type *hGALT*-Transformed *E. coli* Δ*galT*

Non-transformed and wild-type *hGALT*-transformed *E. coli* Δ*galT* were initially grown in the presence of different carbon sources. For non-transformed *E. coli* Δ*galT* cultured under glucose or glucose plus galactose, the growth curves were indistinguishable, since glucose is the preferred carbon source and galactose represents no toxicity in the presence of this hexose. This absent toxicity of galactose likely results from carbon catabolite repression exerted by glucose, which represses the galactose uptake systems GalP and Mgl (Görke and Stülke 2008; Misko et al. 1987; Shimizu 2013; Steinsiek and Bettenbrock 2012). In the presence of glycerol, transported into *E. coli* through facilitated diffusion (Chu et al. 2002), the growth rate was approximately half of that observed in the presence of glucose, confirming that this polyol is not as efficient as glucose as a carbon source, as previously described (Chu et al. 2002). In the presence of galactose, the growth was practically arrested, indicating the inability of this strain to

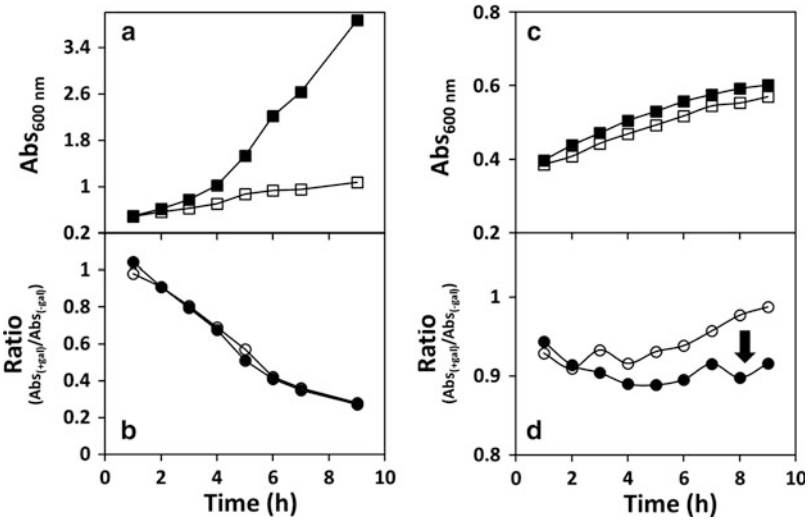


**Fig. 3** Absent or negative effect of arginine on p.P185S and p.R231C hGALT function. Growth profiles of *Escherichia coli* Δ*galT* expressing the p.P185S and p.R231C hGALT variants (Panels **a** and **c**, respectively), in the absence or presence of galactose. Bacteria were grown at 37°C in M9 minimal medium with 1% glycerol as carbon source. At $OD_{600nm}$ =0.3, protein expression was induced with 250 μM IPTG. After 1 h, vehicle (water, *full squares*) or 1% galactose (*hollow squares*) was added to the cultures, and the growth was followed by hourly measurements of $OD_{600nm}$ up to 9 h. Simultaneously with water/galactose, 25 mM arginine or vehicle (water) was added to the cultures. Panels **b** and **d** depict the ratio curves for bacteria expressing, respectively, p.P185S and p.R231C hGALT, obtained by dividing, at each time point, the $OD_{600nm}$ in the presence or absence of galactose (*black circles*, in the presence of 25 mM arginine; *hollow circles*, absence of arginine). Growth curves of *E. coli* Δ*galT* cultures expressing the p.P185S variant (Panel **a**) suggest a galactose-sensitivity profile similar to that of hPAH (negative control), and the ratio curves (Panel **b**) show complete functional unresponsiveness to arginine supplementation. Growth curves of Δ*galT E. coli* expressing p.R231C (Panel **c**) suggest a very mild galactose-sensitivity profile, and the ratio curves (Panel **d**) show a puzzlingly negative effect of arginine. Growth curves are representative graphics from several independent experiments ($n = 2$ for p.P185S and $n = 3$ for p.R231C)

use galactose as carbon source and/or its high toxicity. In turn, *E. coli* Δ*galT* expressing wild-type hGALT presented growth curves identical to the non-transformed strain in all conditions, except when galactose was the single carbon source, in which the growth was significantly higher than that of the non-transformed bacteria. This strongly suggests that the expression of hGALT enables the utilization of galactose as a carbon source and/or abolishes the galactose sensitivity of the *E. coli* Δ*galT* strain (Fig. 1a).

## Galactose Sensitivity of Bacteria Expressing Different hGALT Variants

To evaluate the ability of the studied hGALT variants to sustain growth in the presence of galactose when expressed in *E. coli* Δ*galT*, the bacteria expressing wild-type hGALT were used as the positive control, whose growth was barely affected by the presence of 1% galactose (Fig. 1a). Bacteria expressing wild-type hPAH were used as the negative control, with galactose severely arresting the culture growth (Fig. 1b). Taken together, these observations confirm the toxicity of galactose in our model, since the PAH-expressing cells are still able to use glycerol as carbon source, while being severely affected by galactose. By expressing an unrelated protein, we aimed to subject the control bacterial cultures to the same metabolic demands associated with protein production as the cultures expressing hGALT. Interestingly, using glycerol as sole carbon source (condition I, Table 1), the hPAH-producing culture exhibited a much higher growth rate than hGALT (wild-type and variants) cultures in the same conditions (Fig. 1b, upper panel). This may arise from the fact that producing different recombinant proteins has different energy costs to the bacterial cells.

Bacterial cultures expressing the variants p.N314D, p.S135L, and p.R231H showed essentially no growth arrest upon galactose addition, presenting a galactose growth curve essentially superimposable to that of glycerol alone (not shown). Cells expressing the p.Q188R, p.K285N, p.G175D, and p.R231C variants exhibited variable levels of galactose toxicity (Figs. 2a, c, e and 3c). On the other hand, cultures expressing p.P185S showed a highly galactose-sensitive profile, similarly to the negative control (Fig. 3a). No clear correlation could be established between the variants' toxicity and the in vitro specific activity (Coelho et al. 2014), suggesting that some hGALT variants

present some residual activity in vivo that, however, is not detectable in vitro, particularly p.K285N, p.R231C, and p.R231H (Coelho et al. 2014).

### Arginine Rescue of the hGALT Variants

Wild-type hGALT ratio curves ($r$ and $r_{arg}$) revealed a slight degree of response to the medium supplementation with arginine (not shown), which is not surprising since it has been described that arginine is also able to stabilize the proteins' native state (Arakawa and Tsumoto 2003). In contrast, wild-type hPAH ratio curves ($r$ and $r_{arg}$) are superimposable, which rules out any indirect effect of arginine in improving the growth profiles of the cultures expressing the hGALT variants.

Interestingly, p.N314D, which is believed to be the ancestral allele (Carney et al. 2009), appears to be insensitive to arginine, as well as p.S135L and p.R231H which show essentially overlapping ratio curves. Notably, the p.Q188R, p.K285N, and p.G175D variants were partially rescued by arginine, with $r_{arg} > r$ (Fig. 2b, d and f). The rescue of p.Q188R is remarkable, due to its high prevalence and to its classification as a severe mutation particularly prone to aggregation (Coelho et al. 2014; Shield 2000; Suzuki et al. 2001). Immunoblotting analysis of the soluble lysate revealed that this variant is actually highly expressed (higher than the wild type or any other variant), which may account for the unexpected high tolerance of the cultures even in the absence of arginine (not shown). The p.R231C variant displays ratio curves with the puzzling feature of a slightly increased toxicity in the presence of arginine (Fig. 3d). In turn, p.P185S ratio curves are very similar to the hPAH negative control, revealing its severe functional impairment and unresponsiveness to the potential stabilizing effect of arginine (Fig. 3b and d).

The reproducibility of the ratio curves clearly indicates that arginine's mode of action is mutation specific, showing it is indeed functionally improving variants p.Q188R, p.K285N, and p.G175D in alleviating the galactose toxicity.

## Conclusion

We have developed a prokaryotic model of galactose sensitivity that allows evaluating the impact of human *GALT* mutations on the function of GALT variants, with the additional advantage of being assessed in a cellular context. In fact, this study has revealed that some hGALT variants present residual activity in cell cultures that, however, is not detectable when determined in vitro with the recombinant protein (Coelho et al. 2014). Additionally, this bacterial model of galactose sensitivity has also proven useful in evaluating potential therapeutic agents for new therapeutic approaches against classic galactosemia. Previous studies on the molecular basis of classic galactosemia associated with missense mutations reported that the main pathogenic mechanism relates to protein misfolding, resulting in increased protein aggregation (Coelho et al. 2014) or decreased thermal and conformational stability (McCorvie et al. 2013). Accordingly, we have studied the potential beneficial effect of arginine, a well-established suppressant of protein aggregation (Baynes et al. 2005). Arginine has shown a mutation-specific effect, with p.Q188R, p.K285N, and p.G175D variants being rescued, suggesting that this amino acid could be of some therapeutic benefit in patients carrying these mutations. Notably, p.Q188R results from the most prevalent mutation in Western countries, accounting for over 60% of *GALT* mutant alleles (Suzuki et al. 2001), which entails a great therapeutic impact of arginine in classic galactosemia.

These results lay a foundation for future studies using the prokaryotic model of galactose sensitivity and put forward the hypothesis that arginine might be of some benefit in classic galactosemia, setting the stage for further studies.

**Acknowledgments** This work was supported by Fundação para a Ciência e Tecnologia (SFRH/BD/48259/2008 to AIC and PEst-OE/SAU/UI4013/2011) and by Sociedade Portuguesa de Doenças Metabólicas Grant to IR.

## Synopsis

Arginine supplementation functionally improves, in a mutation-specific manner, clinically relevant human GALT variants expressed in a bacterial model of galactose sensitivity, opening new perspectives towards the therapeutic potential of arginine for classic galactosemia.

## Compliance with Ethics Guidelines

### Conflict of Interest

All the authors, Ana I. Coelho, Matilde Trabuco, Maria João Silva, Isabel Tavares de Almeida, Paula Leandro, Isabel Rivera, and João B. Vicente, declare that they have no conflict of interest.

### Informed Consent

No patients were included in this study.

## Animal Rights

This article does not contain any studies with human or animal subjects performed by any of the authors.

## Contributions

Experimental design – AI Coelho, MJ Silva, I Tavares de Almeida, P Leandro, I Rivera, JB Vicente

Experimental work – AI Coelho, M Trabuco, JB Vicente

Data analysis and interpretation – AI Coelho, P Leandro, I Rivera, JB Vicente

Writing of the manuscript – AI Coelho, P Leandro, I Rivera, JB Vicente

## References


Arakawa T, Tsumoto K (2003) The effects of arginine on refolding of aggregated proteins: not facilitate refolding, but suppress aggregation. Biochem Biophys Res Commun 304:148–152

Baba T, Ara T, Hasegawa M et al (2006) Construction of *Escherichia coli* K-12 in-frame, single-gene knockout mutants: the Keio collection. Mol Syst Biol 2:1–11

Baynes BM, Wang DIC, Trout BL (2005) Role of arginine in the stabilization of proteins against aggregation. Biochemistry 44:4919–4925

Berendse K, Ebberink MS, IJlst L, Wanders RJ, Waterham HR (2013) Arginine improves peroxisome functioning in cells from patients with a mild peroxisome biogenesis disorder. Orphanet J Rare Dis 8:138–145

Berry GT, Walter JH (2012). Disorders of galactose metabolism. In: Saudubray JM, van den Berghe G, Walter JH (eds). Inborn metabolic diseases: diagnosis and treatment. Springer, Germany

Bosch AM (2006) Classical galactosaemia revisited. J Inherit Metab Dis 29:516–525

Calderon FR, Phansalkar AR, Crockett DK, Miller M, Mao R (2007) Mutation database for the galactose-1-phosphate uridyltransferase (*GALT*) gene. Hum Mutat 28:939–943

Carney AE, Sanders RD, Garza KR et al (2009) Origins, distribution and expression of the Duarte-2 (D2) allele of galactose-1-phosphate uridylyltransferase. Hum Mol Genet 18:1624–1632

Chu C, Han C, Shimizu H, Wong B (2002) The effect of fructose, galactose, and glucose on the induction of β-galactosidase in *Escherichia coli*. J Exp Microbiol Immunol 2:1–5

Coelho AI, Trabuco M, Ramos R et al (2014) Functional and structural impact of the most prevalent missense mutations in classic galactosemia. Mol Genet Genomic Med 2:484–496

Fridovich-Keil JL, Walter JH (2008) Galactosemia. In: Valle D, Beaudet AL, Vogelstein B, Kinzler KW, Antonarakis SE, Ballabio A (eds) The online metabolic and molecular bases of inherited disease. Mc-Graw Hill, New York, pp 1–92

Görke B, Stülke J (2008) Carbon catabolite repression in bacteria: many ways to make the most out of nutrients. Nat Rev Microbiol 6:613–624

Leslie ND, Immerrman EB, Flach JE, Florez M, Fridovich-Keil JL, Elsas LJ II (1992) The human galactose-1-phosphate uridyltransferase gene. Genomics 14:474–480

Maniatis T, Fritsch EF, Sambrook J (1982) Molecular cloning. A laboratory manual. Cold Spring Harbor, New York

McCorvie TJ, Gleason TJ, Fridovich-Keil JL, Timson DJ (2013) Misfolding of galactose 1-phosphate uridylyltransferase can result in type I galactosemia. Biochim Biophys Acta 1832:1279–1293

Misko TP, Mitchell W, Meadow N, Roseman S (1987) Sugar transport by the bacterial phosphotransferase system. Reconstitution of inducer exclusion in *Salmonella typhimurium* membrane vesicles. J Biol Chem 262:16261–16266

Riehman K, Crews C, Fridovich-Keil JL (2001) Relationship between genotype, activity, and galactose sensitivity in yeast expressing patient alleles of human galactose-1-phosphate uridylyltransferase. J Biol Chem 276:10634–10640

Ross KL, Davis CN, Fridovich-Keil JL (2004) Differential roles of the Leloir pathway enzymes and metabolites in defining galactose sensitivity in yeast. Mol Genet Metab 83:103–116

Shield JPH (2000) The relationship of genotype to cognitive outcome in galactosaemia. Arch Dis Child 83:248–250

Shimizu K (2013) Metabolic regulation of a bacterial cell system with emphasis on *Escherichia coli* metabolism. ISRN Biochem 2013:645983:1–645983:47

Silva MJ, Pinheiro A, Eusebio F, Gaspar A, Tavares de Almeida I, Rivera I (2009) Pyruvate dehydrogenase deficiency: identification of a novel mutation in the PDHA1 gene which responds to amino acid supplementation. Eur J Pediatr 168:17–22

Steinsiek S, Bettenbrock K (2012) Glucose transport in *Escherichia coli* mutant strains with defects in sugar transport systems. J Bacteriol 194:5897–5908

Suzuki M, West C, Beutler E (2001) Large-scale molecular screening for galactosemia alleles in a pan-ethnic population. Hum Genet 109:210–215

Waggoner DD, Buist NRM, Donnel GN (1990) Long-term prognosis in galactosaemia: results of a survey of 350 cases. J Inherit Metab Dis 13:802–818

JIMD Reports
DOI 10.1007/8904_2015_422

RESEARCH REPORT

# Effect and Tolerability of Agalsidase Alfa in Patients with Fabry Disease Who Were Treatment Naïve or Formerly Treated with Agalsidase Beta or Agalsidase Alfa

**Ozlem Goker-Alpan • Khan Nedd • Suma P. Shankar • Yeong-Hau H. Lien • Neal Weinreb • Anna Wijatyk • Peter Chang • Rick Martin**

Received: 01 October 2014 / Revised: 22 January 2015 / Accepted: 12 February 2015 / Published online: 31 March 2015


**Abstract** *Objectives*: In a multicenter, open-label, treatment protocol (HGT-REP-059; NCT01031173), clinical effects and tolerability of agalsidase alfa (agalα; 0.2 mg/kg every other week) were evaluated in patients with Fabry disease who were treatment naïve or switched from agalsidase beta (switch). Over 24 months, data were collected on the safety profile; renal and cardiac parameters were assessed using estimated glomerular filtration rate (eGFR), left ventricular mass index (LVMI), and midwall fractional shortening (MFS).

*Results*: Enrolled patients included 71 switch (median [range] age, 46.6 [5–84] years; male to female [M:F], 40:31) and 29 treatment naïve (38.7 [12–74] years; M:F, 14:15). Adverse events (AEs) were consistent with the known safety profile of agalα. Two switch patients had hospitalization due to possibly/probably drug-related serious AEs (one with transient ischemic attack, one with infusion-related AEs). One switch and two treatment-naïve patients discontinued treatment because of AEs. Three patients (one each switch, treatment naïve, and previous agalα) died; no deaths were considered drug-related. There was no significant change from baseline in LVMI or MFS in either group. Similarly, eGFR remained stable; mean ± standard error annualized change in eGFR (mL/min/1.73 $m^2$) was −2.40 ± 1.04 in switch and −1.68 ± 2.21 in treatment-naïve patients.

*Conclusions*: This is the largest cohort of patients with Fabry disease who were started on or switched to agalα in an FDA-accepted protocol during a worldwide supply shortage of agalsidase beta. Because this protocol was primarily designed to provide access to agalα, there were limitations, including not having stringent selection criteria and the lack of a placebo group.

Communicated by: Markus Ries, MD, PhD, MHSc, FCP

Competing interests: None declared

O. Goker-Alpan (✉)
Lysosomal Disorders Unit, O&O ALPAN LLC, Fairfax, VA, USA
e-mail: ogokeralpan@oandoalpan.com

K. Nedd
Infusion Associates, Grand Rapids, MI, USA

S.P. Shankar
Department of Human Genetics and Ophthalmology, School of Medicine, Emory University, Atlanta, GA, USA

Y.-H.H. Lien
Arizona Kidney Disease and Hypertension Center, Tucson, AZ, USA

N. Weinreb
University Gaucher Disease–Fabry Disease Treatment Center, University Research Foundation for Lysosomal Storage Disorders, Coral Springs, FL, USA

A. Wijatyk
Global Clinical Development, Shire, Lexington, MA, USA

P. Chang
Biometrics, Shire, Lexington, MA, USA

R. Martin
Global Medical, Shire, Lexington, MA, USA

## Introduction

Fabry disease (FD; OMIM number 301500) is a rare, X-linked disorder caused by deficiency of the lysosomal enzyme alpha-galactosidase A (Enzyme Commission number 3.2.1.22) that hydrolyzes the terminal alpha-galactosyl moieties from glycolipids and glycoproteins. FD is a chronic and progressive multiorgan disorder with considerable morbidity and early mortality in both men and clinically affected women (MacDermot et al. 2001). Signs and symptoms of FD include progressive renal insuffi-

ciency and cardiovascular, cerebrovascular, dermatologic, ocular, auditory, and neurologic complications, with consequent reductions in quality of life.

Enzyme replacement therapy (ERT) with agalsidase alfa (agalα) alleviates many of the renal and cardiac signs and symptoms of FD, decreases pain and gastrointestinal symptoms, and improves overall quality of life (Dehout et al. 2003; Beck et al. 2004; Schwarting et al. 2006; Choi et al. 2008; Mehta et al. 2009). In December 2009, because of a worldwide supply shortage of agalsidase beta (agalβ), the only ERT then marketed in the United States, the US Food and Drug Administration approved HGT-REP-059, a protocol to allow access to agalα for FD patients who were left without a therapeutic option. FD patients who were ERT treatment naïve ("naïve"), or who were previously treated with agalβ ("switch"), were included. Outcome measures focused on agalα safety and tolerability and renal, cardiac, biomarker, and pharmacodynamic parameters. This report of up to 24-month results from HGT-REP-059 is the largest agalβ-to-agalα switch experience to date and presents reasonable expectations for FD treatment in real-life clinical settings.

## Patients and Methods

### Treatment Protocol Design and Data Collection

HGT-REP-059 was a US multicenter, open-label treatment protocol for patients with FD (funded by Shire; ClinicalTrials.gov identifier: NCT01031173). Inclusion criteria were a confirmation of FD diagnosis biochemically (for males) or genetically (for males or females) and required the use of approved birth control methods (if female of childbearing potential) throughout the study and for at least 30 days after the final infusion. Exclusion criteria included prior anaphylactic, anaphylactoid, or other significant infusion-related reactions with agalβ; current pregnancy or breastfeeding; the use of another investigational drug or device within 30 days prior to study entry; concomitant agalβ therapy; failure to provide written informed consent; or otherwise considered unsuitable for the study in the judgment of the investigators.

Regardless of prior treatment status, dose, or schedule of administration, patients in these analyses were treated with agalα (0.2 mg/kg body weight, infused intravenously over a 40-min period every other week). The study duration was planned to be 12 months with an option to extend. Thus, data were collected and assessed for up to 24 months of agalα treatment in the safety population (defined as all enrolled patients who received at least one full or partial dose of agalα). The study was initiated in February 2010 and terminated by the sponsor in July 2012.

Clinical effect parameters are presented only for "naïve" patients with no history of prior ERT for FD and for "switch" patients who were treated with agalβ before study entry for whom detailed information on prior dosing, gaps in treatment, and prior clinical history was not available.

Adverse events (AEs) in the safety population were recorded and coded using the Medical Dictionary for Regulatory Activities (http://www.meddramsso.com/) from baseline through the end of study. AEs were rated by severity and potential relationship to study drug. Possibly or probably drug-related AEs were considered infusion-related (IRAEs) if they occurred within 12 h from the start of an infusion. Serious AEs (SAEs; i.e., AEs that resulted in death, were life-threatening, caused new or prolonged hospitalization, led to persistent disability or congenital abnormality, or were considered SAEs by the treating investigator) and discontinuations due to AEs were recorded. Blood samples were collected at baseline and months 6, 18, and 24 to analyze for serum antibodies (Abs) against agalα (all assessments) and agalβ (at baseline only), using an enzyme-linked immunosorbent assay. Ab-positive samples were isotyped for immunoglobulin (Ig) G, IgA, IgM, and IgE and tested for enzyme-neutralizing activity using an in vitro assay (Schiffmann et al. 2001).

### Clinical and Pharmacodynamic Parameters

Renal function was assessed at baseline and at months 1, 3, 6, 9, 12, 18, and 24 using estimated glomerular filtration rate (eGFR) calculated with the Modification of Diet for Renal Disease equation (Levey et al. 2006) or, in patients <18 years of age, the Counahan-Barratt equation (Counahan et al. 1976). Patients were classified at baseline into chronic kidney disease (CKD) stage: 1b (normal kidney function), 2 (mildly reduced kidney function), 3 (moderately reduced kidney function), or 4 (severely reduced kidney function) (Levey et al. 2003). Patients with eGFR >130 ml/min/1.73 $m^2$ were classified as hyperfiltrators (CKD stage 1a) (Magee et al. 2009). The first morning's spot urine sample and 24-h urine sample were used to calculate protein-to-creatinine ratio. Patients were evaluated in subgroups of <200 or ≥200 mg 24-h urine protein at baseline.

Cardiac structure and function were assessed using left ventricular mass indexed to height (LVMI) and midwall fractional shortening (MFS). Echocardiograms at baseline (or within 60 days of the first infusion) and at months 12, 18, and 24 were assessed at a central laboratory. Left ventricular hypertrophy (LVH) was defined as LVMI values >51 g/$m^{2.7}$ in males or >48 g/$m^{2.7}$ in females.

Samples for accumulation of globotriaosylceramide ($Gb_3$) and globotriaosylsphingosine (lyso-$Gb_3$) were obtained

after 8 h of fasting. Both plasma and urine samples ($Gb_3$ only) were analyzed with liquid chromatography–tandem mass spectrometry using a validated assay (Krüger et al. 2010, 2011).

Data and Statistical Analyses

Baseline demographic and other clinical characteristics were summarized with descriptive statistics. A Wilcoxon signed-rank test at 5% significance level was used to analyze the change from baseline through 24 months in the parameters of interest for each of the subpopulations for previous ERT status. No multiplicity adjustment was made. Similar analyses were performed to assess effects within each population stratified by CKD stage (1a, 1b, 2, 3, and 4) for eGFR and by presence or absence of baseline proteinuria (24-h urine protein ≥200 mg) and LVH. To calculate an annualized rate of eGFR change, a statistical model was used to take into account all repeated measurements of eGFR over time (not just computed from the baseline and the last measurement), and the model assumed a linearity of change over time.

## Results

Patient characteristics are shown in Table 1. The safety population comprised 132 patients, including 29 naïve and 71 switch patients, plus 32 patients previously treated with either agalα ($n = 22$) or with both agalα and agalβ ($n = 10$). Female representation was substantial and comparable in naïve and switch patients. Switch patients tended to be older than naïve patients. In patients with available information on date of diagnosis of FD, the median years

**Table 1** Baseline demographic and clinical characteristics

| Baseline characteristic | Naïve ($n = 29$) | Switch ($n = 71$) | Safety population ($N = 132$)[a] |
|---|---|---|---|
| Age, years, median (range) | 38.7 (12–74) | 46.6 (5–84) | 45.1 (5–84) |
| Sex, *n* (%) | | | |
| Male | 14 (48.3) | 40 (56.3) | 81 (61.4) |
| Female | 15 (51.7) | 31 (43.7) | 51 (38.6) |
| Race, *n* (%) | | | |
| Caucasian | 26 (89.7) | 71 (100.0) | 128 (97.0) |
| African-American | 1 (3.4) | 0 | 1 (0.8) |
| Asian | 2 (6.9) | 0 | 2 (1.5) |
| Other | 0 | 0 | 1 (0.8) |
| Years since Fabry diagnosis, median (range) | 1.1 (0.1–27.4), $n = 28$ | 7.2 (0.9–49.3), $n = 70$ | 7.1 (0.1–49.3), $n = 125$ |
| Years of previous agalβ treatment, median (range) | NA | 4.6 (0.3–12.2) | 5.2 (0.3–12.2), $n = 81$ |
| Years of previous agalα treatment, median (range) | NA | NA | 7.60 (0.4–12.2), $n = 29$ |
| CKD stage, *n* (%)[b] | | | |
| 1A | 3 (10.3) | 5 (7.0) | 16 (12.1) |
| 1B | 12 (41.4) | 27 (38.0) | 50 (37.9) |
| 2 | 7 (24.1) | 21 (29.6) | 28 (21.2) |
| 3 | 4 (13.8) | 9 (12.7) | 23 (17.4) |
| 4 | 3 (10.3) | 9 (12.7) | 15 (11.4) |
| LVH, *n* (%)[c] | | | |
| Yes | 10 (34.5) | 27 (38.0) | 47 (35.6) |
| No | 15 (51.7) | 25 (35.2) | 55 (41.6) |
| Data not available | 4 (13.8) | 19 (26.8) | 30 (22.7) |

[a] The safety population also includes patients who previously received either agalα or both agalα and agalβ prior to baseline. However, these patients were not evaluated as separate subgroups, because of low patient numbers and insufficient pre-baseline data

[b] CKD stages were defined by eGFR (ml/min/1.73 $m^2$) standards as follows: stage 1A (>130), stage 1B (90–130), stage 2 (60–89), stage 3 (30–59), and stage 4 (15–29)

[c] Patients ($n = 52$ switch and 25 naïve) had sufficient echocardiographic measurements or urine samples to assess baseline LVH or urine protein data, respectively

*agal*α agalsidase alfa, *agal*β agalsidase beta, *CKD* chronic kidney disease, *eGFR* estimated glomerular filtration rate, *LVH* left ventricular hypertrophy, *NA* not applicable, *naïve* treatment naive prior to baseline, *switch* patients formerly treated with agalβ

elapsed since diagnosis of FD were considerably fewer in naïve patients compared with switch patients. The majority of both naïve and switch patients had CKD stage 1b or stage 2. Hyperfiltrators (CKD stage 1a) were uncommon (Fig. 1a).

## Safety and Tolerability

In the safety population, most patients experienced treatment-emergent AEs ($n = 131$ [99.2%]); however, the majority were considered mild ($n = 23$ [17.4%]) or moderate ($n = 66$ [50.0%]) in severity. Treatment-emergent AEs (TEAEs) occurring in ≥15% included nasopharyngitis, nausea, headache, dizziness, fatigue, and vomiting. Approximately half of TEAEs were considered to be possibly or probably drug-related, and approximately one third were deemed IRAEs.

Serious AEs occurred in 47 (35.6%) patients in the safety population; the most common were pneumonia ($n = 5$ [4.3%]); cerebrovascular accident ($n = 4$ [3.4%]); and anemia, congestive cardiac failure, vomiting, asthenia, transient ischemic attack, confusion, and renal impairment (each $n = 3$ [2.6%]). Hospitalizations in two adult switch patients were reported as SAEs possibly or probably drug-related, per investigators. One patient had a transient ischemic attack 13 days after the last agalα infusion; the second patient had an IRAE, with vomiting, asthenia, chills, and increased blood pressure. Both SAEs resolved without sequelae. With respect to AE severity, 31% of the safety population experienced AEs that were reported as severe or life-threatening in intensity (naïve $n = 11$ [37.9%], switch $n = 21$ [29.6%], previous agalα $n = 6$ [27.3%]).

Three adult patients discontinued treatment due to AEs: two naïve patients ($n = 1$ each with arthralgia or chest discomfort and face swelling) and one switch patient (psychotic disorder). Three patients died: a 68-year-old man (naïve) with cardiorespiratory arrest following methicillin-resistant *Staphylococcus aureus* bacteremia; a 55-year-old man (switch) with cardiac arrest; and a 55-year-old man (previous agalα) with cardiorespiratory arrest subsequent to cerebrovascular accident. All three patients had advanced heart and kidney disease at baseline, and no deaths were deemed drug-related.

Treatment adherence was high, with 94 of 132 patients (71.2%) missing no more than one agalα infusion. The mean number of completed infusions per patient was 45.5, with a mean total exposure duration of 638.5 days.

## Immunogenicity and Other Safety Parameters

No clinically meaningful changes occurred in laboratory values, vital signs, or physical examination findings in any study subpopulation. Table 2 summarizes agalα antibody status in patients with available data; 28 of 28 naïve patients were Ab negative at baseline. Two (7.1%) naïve patients converted from seronegative to seropositive during the study without experiencing IRAEs. One naïve patient lacking Ab data had an IRAE.

At baseline, 54.9% of switch patients had anti-agalβ Abs. Also at baseline, 35.2% of these anti-agalβ Ab-positive switch patients had anti-agalα Abs, and 22.5% had neutralizing Abs despite no prior agalα exposure (Table 2). Among patients who were agalα Ab negative at baseline, 19.6% (9/46) transiently or persistently seroconverted to IgM or IgG, but none developed neutralizing Abs. IRAEs occurred in 27 switch patients overall, and 15 of these were agalα Ab positive at some point.

## Renal Function and Cardiac Structure/Function

At month 24, kidney function as assessed by eGFR remained clinically stable in both the naïve and switch subgroups (Fig. 1b). Among those with no dialysis or kidney transplant experience, baseline mean ± SE eGFR (ml/min/1.73 $m^2$) values were 94.20 ± 7.65 in naïve ($n = 27$) and 87.45 ± 4.40 in switch ($n = 59$) patients. The mean ± SE annualized rates of eGFR change (ml/min/1.73 $m^2$/year) were switch −2.40 ± 1.04 ($n = 59$) and naïve −1.68 ± 2.21 ($n = 27$). In the total safety population, patients in most CKD stages showed relatively stable eGFR, except for CKD stage 1a (the hyperfiltrator group) and CKD stage 3 (Fig. 1a). The decline in the hyperfiltrator group suggests a trend toward a normal eGFR. There were no significant changes in measures of proteinuria in either naïve or switch patients, regardless of whether baseline 24-h urine protein was less than or greater than 200 mg (Fig. 1c). Mean echocardiographic measurements (LVMI, MFS) did not change significantly in any patient subgroup (Fig. 1d, e). Mean LVMI did not change significantly in patients with or without LVH at baseline (Fig. 1f).

## Plasma and Urine Biomarkers

Previous assessments in healthy volunteers have shown that the mean ± 2 standard deviations normal plasma $Gb_3$ (nmol/mL) was 4.55 ± 3.90 (observed range, 1.96–7.70; $n = 60$). For naïve patients, mean ± SE baseline plasma $Gb_3$ levels (nmol/mL) were 19.02 ± 3.11 for male patients and 13.76 ± 2.32 for female patients. For switch patients, mean ± SE baseline plasma $Gb_3$ levels (nmol/mL) were 13.36 ± 0.86 for male patients and 11.46 ± 0.96 for female patients. There was a trend of reduction from baseline in plasma $Gb_3$ levels in naïve male patients, but not in switch male nor in all female patients (Fig. 2a).

The normal range for creatinine-normalized urine $Gb_3$ in healthy volunteers is <0.03 nmol/mg creatinine ($n = 60$;

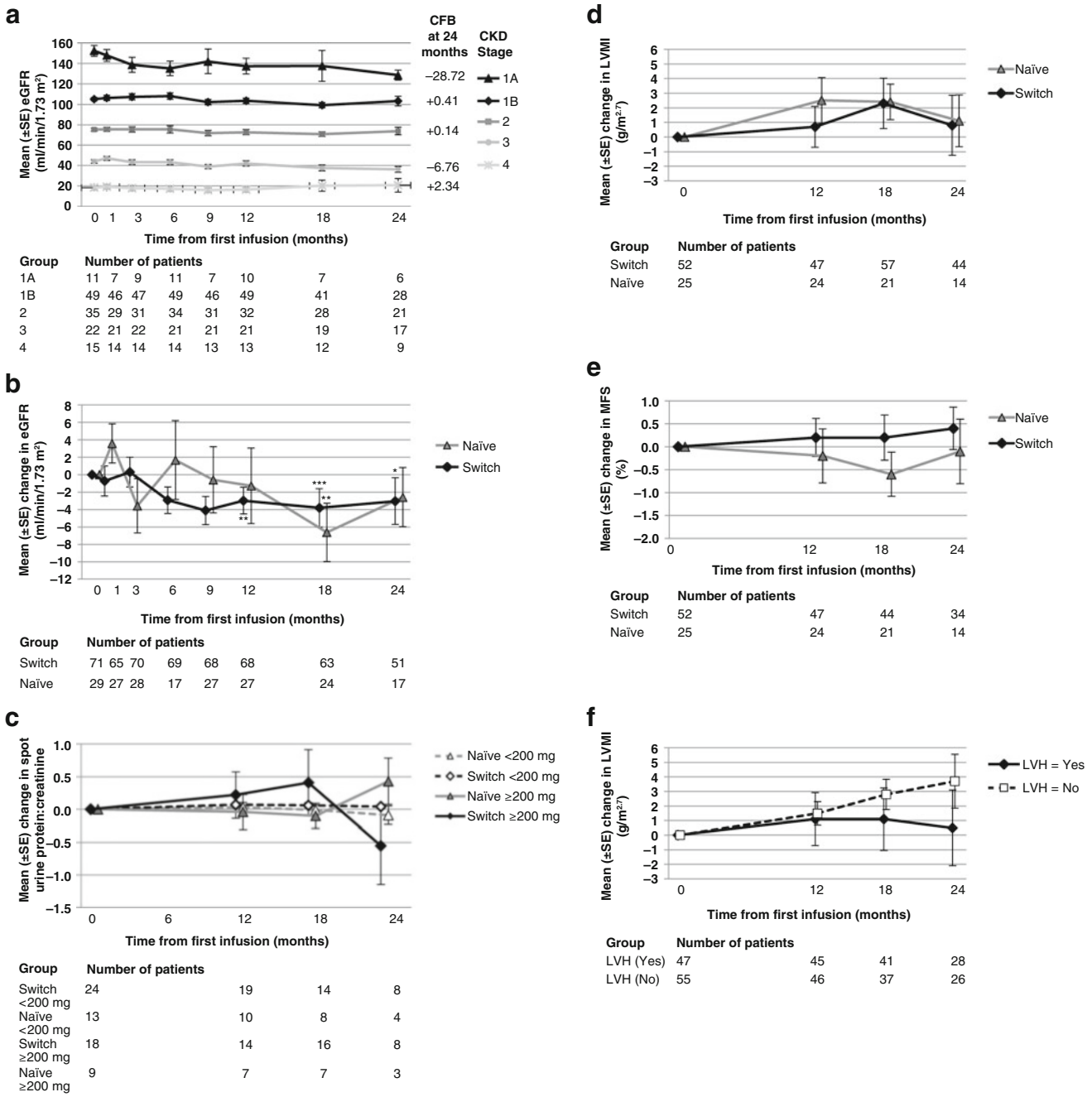


**Fig. 1** Renal and cardiac parameters in the safety population. Renal parameters included change over time by treatment group by (**a**) CKD stage, (**b**) mean ± SE eGFR, and (**c**) early-morning spot urine protein-to-creatinine ratio in patients with baseline 24-h urine protein <200 or ≥200 mg. CKD stages defined by eGFR (in ml/min/1.73 $m^2$) standards as follows: stage 1A (>130 [hyperfiltrators]), stage 1B (90–130 [normal kidney function]), stage 2 (60–89 [mildly reduced kidney function]), stage 3 (30–59 [moderately reduced kidney function]), and stage 4 (15–29 [severely reduced kidney function]). eGFR was calculated with the Modification of Diet for Renal Disease or Counahan-Barratt equation in patients aged <18 years. Cardiac parameters as measured by echocardiography by treatment group included (**d**) mean ± SE LVMI ($g/m^{2.7}$) change over time and (**e**) mean change over time in MFS (%), as well as by (**f**) presence or absence of baseline LVH. *$p < 0.05$, **$p < 0.01$, ***$p < 0.001$; other data points (without footnotes indicating $p$-values) were $p \geq 0.05$ versus baseline. *agalα* agalsidase alfa, *CFB* change from baseline, *CKD* chronic kidney disease, *eGFR* estimated glomerular filtration rate, *LVH* left ventricular hypertrophy, *LVMI* left ventricular mass index, *MFS* midwall fractional shortening, *naïve* treatment naïve prior to baseline, *SE* standard error, *switch* patients formerly treated with agalsidase beta

**Table 2** Anti-agalsidase alfa antibody status over time by previous treatment group

| Status | Baseline | | Month 6 | | Month 12 | | Month 24 | |
|---|---|---|---|---|---|---|---|---|
| | Anti-agalα Ab *n* (%) | NAb *n* (%) | Anti-agalα Ab *n* (%) | NAb *n* (%) | Anti-agalα Ab *n* (%) | NAb *n* (%) | Anti-agalα Ab *n* (%) | NAb *n* (%) |
| Naïve ($n = 28$)[a] | | | | | | | | |
| Ab negative | 28 (96.6) | 28 (96.6) | 27 (93.1) | 27 (93.1) | 25 (86.2) | 26 (89.7) | 9 (31.0) | 9 (31.0) |
| Ab positive | 0 | 0 | 0 | 0 | 2 (6.9) | 1 (3.4) | 0 | 0 |
| Switch ($n = 71$) | | | | | | | | |
| Ab negative | 46 (64.8) | 55 (77.5) | 44 (62.0) | 59 (83.1) | 45 (63.4) | 54 (76.1) | 25 (35.2) | 35 (49.3) |
| Ab positive | 25 (35.2) | 16 (22.5) | 25 (35.2) | 10 (14.1) | 21 (29.6) | 12 (16.9) | 15 (21.1) | 5 (7.0) |
| Safety population ($n = 132$) | | | | | | | | |
| Ab negative | 98 (74.2) | 112 (84.8) | 92 (69.7) | 115 (87.1) | 91 (68.9) | 108 (81.8) | 36 (27.3) | 49 (37.1) |
| Ab positive | 33 (25.0) | 19 (14.4) | 36 (27.3) | 13 (9.8) | 32 (24.2) | 15 (11.4) | 20 (15.2) | 7 (5.3) |

The assays were performed by a central laboratory. Samples were analyzed using an enzyme-linked immunosorbent assay

[a] Antibody data were not available for one naïve patient. *Ab* antibody, *agalα* agalsidase alfa, *NAb* antibody with enzyme-neutralizing activity, *naïve* treatment naive prior to baseline, *switch* patients formerly treated with agalsidase beta

per internal validation). For naïve patients, mean ± SE baseline creatinine-normalized urine $Gb_3$ levels (nmol/mg) were 3.78 ± 0.83 for male patients and 2.48 ± 1.82 for female patients. For switch patients, mean ± SE baseline creatinine-normalized urine $Gb_3$ levels (nmol/mg) were 2.74 ± 0.51 for male patients and 0.16 ± 0.049 for female patients. The only significant change from baseline over time was a reduction at month 12 in male switch patients (Fig. 2b).

For naïve patients, mean ± SE baseline plasma lyso-$Gb_3$ levels (nM) were 102.67 ± 19.09 for male patients and 27.59 ± 15.40 for female patients. For switch patients, mean ± SE baseline plasma lyso-$Gb_3$ levels (nM) were 57.94 ± 5.11 for male patients and 13.82 ± 1.16 for female patients. Naïve male patients demonstrated a significant reduction from baseline in mean plasma lyso-$Gb_3$ levels (nM) at months 12, 18, and 24; a similar pattern was observed for naïve female patients at month 18 ($n = 11$) and 24 ($n = 3$). Other changes over time were not significant (Fig. 2c).

## Discussion

The primary objective of this FD study, the largest agalα clinical trial to date, was to evaluate the safety and tolerability of agalα in an open-label scenario in both naïve and previously treated male and female patients lacking access to a therapeutic alternative. The findings are consistent with the previously reported safety profile of agalα (European Medicines Agency 2014). No new or unexpected safety concerns emerged during the 24 months of treatment. In FD, chronic protean signs and symptoms usually predate initiation of treatment and may persist or even progress despite ERT. Thus, it is not surprising that most patients experienced one or more treatment-emergent AEs, the majority of which were mild or moderate in intensity, consistent with events observed during disease progression, consistent with events documented during agalsidase alfa clinical trials, and consistent with events recorded in post-marketing safety surveillance.

Also consistent with past experience, IRAEs occurred in approximately one third of patients. The SAEs and deaths mostly encompassed renal, cardiac, and cerebrovascular etiologies in males with classical phenotypes and preexisting advanced heart and kidney disease. These were judged to be natural morbidity of FD rather than drug-related and support the hypothesis that initiating ERT before end-organ damage occurs is key to attaining favorable long-term outcomes.

There was little measurable change in renal function or proteinuria during this 24-month study. Naïve and switch patients had an annualized mean eGFR (ml/min/1.73 $m^2$/year) change of −1.68 and −2.40, respectively. Given the substantial heterogeneity in our patient population and lack of pre-enrollment renal history, it is difficult to compare these outcomes with those reported in previous clinical trials and observational studies of either agalα or agalβ. However, our results are generally similar to those from previous studies with agalα or agalβ, which have shown positive effects of ERT to slow down the decline of eGFR (Banikazemi et al. 2007; Germain et al. 2007; Mehta et al. 2009; West et al. 2009; Rombach et al. 2013; Weidemann et al. 2013; Anderson et al. 2014).

Cardiac structure and function remained relatively stable in patients with or without LVH for both switch and naïve patients. Like stabilization of renal function, maintenance of cardiac structure and function is critical with respect to

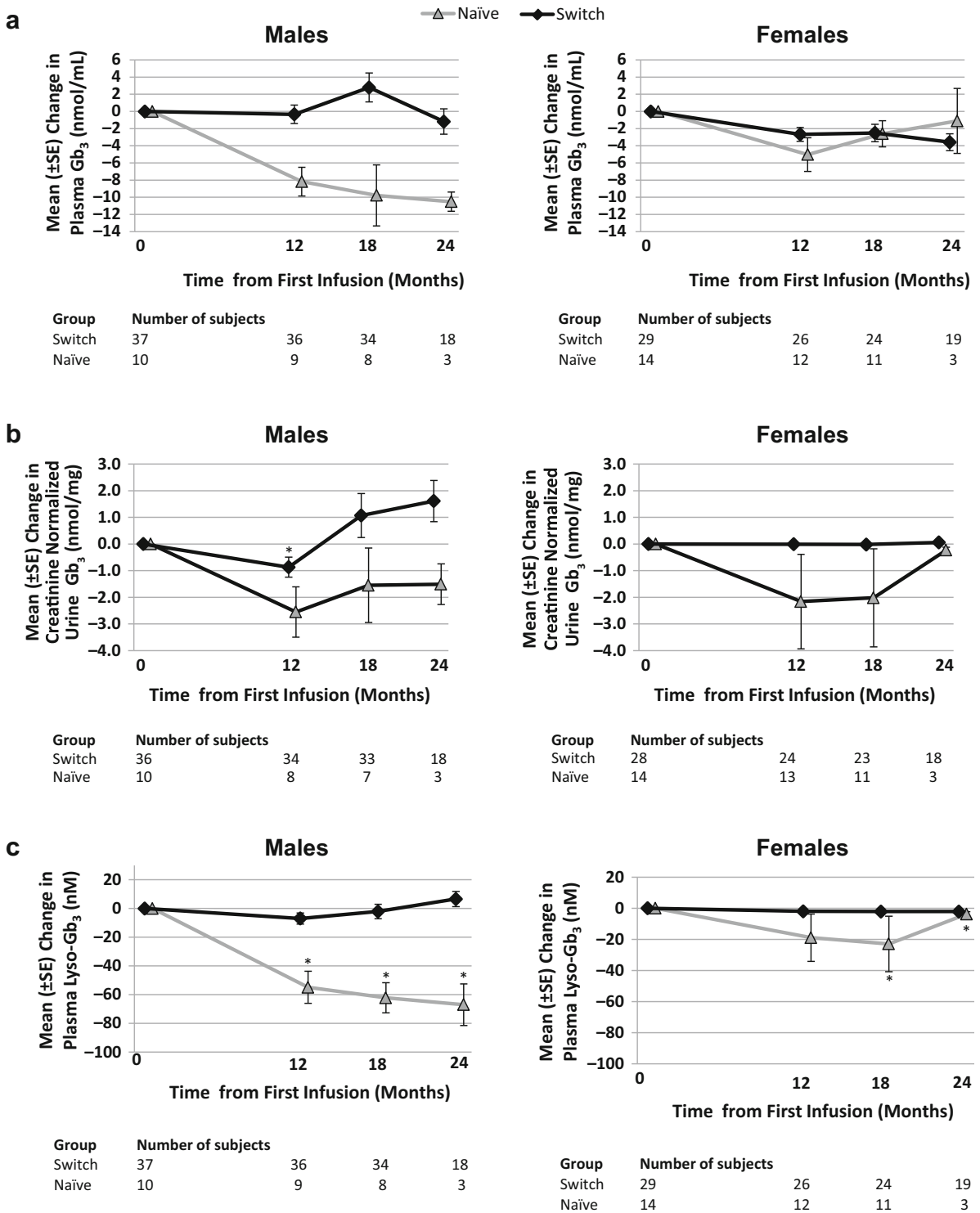


**Fig. 2** Mean ± SE change over time by sex and by treatment group in (**a**) plasma $Gb_3$, (**b**) creatinine-normalized urinary $Gb_3$, and (**c**) plasma lyso-$Gb_3$. Both plasma and urine $Gb_3$ and plasma lyso-$Gb_3$ levels were measured using a liquid chromatography–tandem mass spectrometry assay. *agalα* agalsidase alfa, *$Gb_3$* globotriaosylceramide, *lyso-$Gb_3$* globotriaosylsphingosine, *naïve* treatment naïve prior to baseline, *SE* standard error, *switch* patients formerly treated with agalsidase beta. *Mean values significantly different from baseline based on 95% confidence intervals

long-term outcomes and is relevant to both groups in this study, given that the annual mean increase in cardiac mass for untreated Fabry patients is 4.07 g/m$^{2.7}$ in males and 2.31 g/m$^{2.7}$ in females and even higher (6.59 g/m$^{2.7}$ in males and 3.77 g/m$^{2.7}$ in females) in those with LVH at baseline (Kampmann et al. 2008).

The infrequency of seroconversion in naïve (7.1%) and switch (19.6%) patients is consistent with previous agalα clinical trial experience (Keating 2012). More than half of the switch patients had agalβ Abs at baseline, whereas only 35% had agalα Abs, showing that although cross-reactivity is common, it is not inevitable as previously postulated (Linthorst et al. 2004). Antibody status, including presence of neutralizing Abs (found in 15–20% of switch patients), may have affected the glycosphingolipid biomarker response and could, therefore, possibly be clinically relevant.

Baseline plasma $Gb_3$ and lyso-$Gb_3$ levels were lower in switch patients versus naïve patients. Although we have no record of biomarker levels when previous agalβ treatment was terminated in the switch patients or during treatment lapses, it was similarly reported that even after agalβ interruptions or dose reductions of 1.0–1.5 years, plasma lyso-Gb3 does not return to pretreatment values (Smid et al. 2011). In general with initiation of agalα, there were significant reductions in mean plasma lyso-Gb3 levels only in naïve male patients; other changes in plasma and urinary biomarkers in switch and naïve patients were inconsistent and generally not significant. These results may be in part attributable to the relative refractoriness of agalα-Ab-positive patients (30–35% of the total at all assessment time points), as reviewed and reported by Rombach and colleagues (Rombach et al. 2012), but results in previously treated patients should be interpreted with caution as the prior treatment may have caused a reduction in "baseline" levels.

The aims and scientific design of this study are limited by its primary purpose as a vehicle to ensure continuity of treatment for a large, varied, at-risk patient population who unexpectedly lacked a therapeutic alternative. Liberal inclusion and exclusion criteria created a clinically heterogeneous population regarding gender, genotype, duration and severity of symptoms, end-organ damage, and comorbidities. There was no control group and no reliable access to clinical or treatment history prior to enrollment, and patient numbers were insufficient for matching analyses. Some patients did not complete 24 months of therapy before the study was terminated, and only half had a formal end-of-study visit. However, over 80% of patients were enrolled at the time of termination, and ~60% received all expected infusions. For a chronic disorder such as FD, a 2-year study without even more extended follow-up is somewhat limited in its ability to ascertain long-term key renal, cardiac, neurologic, and patient-reported outcomes such as health-related quality of life.

Our results show that for up to 24 months of treatment, agalα was well tolerated in a heterogeneous population of treatment-naïve and switch patients, no new or unexpected safety or immunogenicity concerns emerged, mean surrogate plasma and urine biomarkers ($Gb_3$ and lyso-$Gb_3$) showed consistent and significant reductions only in plasma lyso-$Gb_3$ levels in naïve male patients, and renal and cardiac functions generally remained stable.

**Acknowledgments** This study was funded by Shire. The authors thank Drs Bruce A. Barshop, Ellen Boyd, Alpana Desai, Richard Forte, Myrl Holida, Richard Hillman, Jennifer Ibrahim, Rebecca Mardach, Barbara Rever, and Neal Weinreb for their contributions to data collection and input for study HGT-REP-059. Medical writing support for this manuscript was provided by Ray Beck, Jr, PhD, and Margit Rezabek, DVM, PhD, of Excel Scientific Solutions, which was funded by Shire.

## Synopsis

In this cohort of patients with Fabry disease who were treatment naïve or switched from agalβ, agalα was generally well tolerated and stabilized renal and cardiac parameters.

## Compliance with Ethics Guidelines

### Conflicts of Interest

Ozlem Goker-Alpan has received research support from Actelion, Shire, Genzyme Corp, Amicus, and Pfizer-Protalix Biotherapeutics, as well as payments for consultancy from Actelion, Shire, and Pfizer-Protalix Biotherapeutics and payments for speaker bureaus from Actelion, Genzyme Corp, and Shire.

Suma P. Shankar has been site primary investigator in clinical trials and received research support and educational grants from Genzyme, Shire, Protalix, Actelion, and Amicus and has served on speakers bureaus for Genzyme and Shire.

Yeong-Hau H. Lien has received research support from Shire.

Neal Weinreb has received research support and honoraria from Genzyme-Sanofi and Shire and has served on advisory boards for Genzyme-Sanofi, Shire, and Pfizer-Protalix Biotherapeutics and served on speakers bureaus for Genzyme-Sanofi, Actelion, Shire, and Pfizer.

Anna Wijatyk, Peter Chang, and Rick Martin are employees of and hold stock options in Shire.

Khan Nedd declares no potential competing interests.

## Patient Consent Statement

All procedures followed were in accordance with the ethical standards of the responsible committee on human experimentation (institutional and national) and with the Helsinki Declaration of 1975, as revised in 2000. Informed consent was obtained from all patients for being included in the study.

## Details of the Contributions of Individual Authors

Anna Wijatyk, Peter Chang, and Rick Martin were involved in the study planning. Ozlem Goker-Alpan was the Principal Investigator and signed off on the protocol. Ozlem Goker-Alpan, Khan Nedd, Suma P. Shankar, Yeong-Hau Lien, and Neal Weinreb were involved in the study conduct. Peter Chang conducted the statistical analyses. All authors contributed to the first draft of the manuscript, were involved in the critical review and revision of subsequent drafts, and approved the final draft for submission.

## References


Anderson LJ, Wyatt KM, Henley W et al (2014) Long-term effectiveness of enzyme replacement therapy in Fabry disease: results from the NCS-LSD cohort study. J Inherit Metab Dis 37:969–978

Banikazemi M, Bultas J, Waldek S et al (2007) Agalsidase-beta therapy for advanced Fabry disease: a randomized trial. Ann Intern Med 146:77–86

Beck M, Ricci R, Widmer U et al (2004) Fabry disease: overall effects of agalsidase alfa treatment. Eur J Clin Invest 34:838–844

Choi JH, Cho YM, Suh KS et al (2008) Short-term efficacy of enzyme replacement therapy in Korean patients with Fabry disease. J Korean Med Sci 23:243–250

Counahan R, Chantler C, Ghazali S, Kirkwood B, Rose F, Barratt TM (1976) Estimation of glomerular filtration rate from plasma creatinine concentration in children. Arch Dis Child 51:875–878

Dehout F, Schwarting A, Beck M et al (2003) Effects of enzyme replacement therapy with agalsidase alfa on glomerular filtration rate in patients with Fabry disease: preliminary data. Acta Paediatr Suppl 92:14–15, discussion 15

European Medicines Agency (2014) Replagal Summary of Product Characteristics. http://www.ema.europa.eu/docs/en_GB/document_library/EPAR_-_Product_Information/human/000369/WC500053612.pdf. Accessed 7 July 2014

Germain DP, Waldek S, Banikazemi M et al (2007) Sustained, long-term renal stabilization after 54 months of agalsidase beta therapy in patients with Fabry disease. J Am Soc Nephrol 18:1547–1557

Kampmann C, Linhart A, Baehner F et al (2008) Onset and progression of the Anderson-Fabry disease related cardiomyopathy. Int J Cardiol 130:367–373

Keating GM (2012) Agalsidase alfa: a review of its use in the management of Fabry disease. BioDrugs 26:335–354

Krüger R, Bruns K, Grunhage S et al (2010) Determination of globotriaosylceramide in plasma and urine by mass spectrometry. Clin Chem Lab Med 48:189–198

Krüger R, Tholey A, Jakoby T et al (2011) Quantification of the Fabry marker lysoGb3 in human plasma by tandem mass spectrometry. J Chromatogr B Analyt Technol Biomed Life Sci 883–884:128–135

Levey AS, Coresh J, Balk E et al (2003) National Kidney Foundation practice guidelines for chronic kidney disease: evaluation, classification, and stratification. Ann Intern Med 139:137–147

Levey AS, Coresh J, Greene T et al (2006) Using standardized serum creatinine values in the modification of diet in renal disease study equation for estimating glomerular filtration rate. Ann Intern Med 145:247–254

Linthorst GE, Hollak CE, Donker-Koopman WE, Strijland A, Aerts JM (2004) Enzyme therapy for Fabry disease: neutralizing antibodies toward agalsidase alpha and beta. Kidney Int 66:1589–1595

MacDermot KD, Holmes A, Miners AH (2001) Anderson-Fabry disease: clinical manifestations and impact of disease in a cohort of 60 obligate carrier females. J Med Genet 38:769–775

Magee GM, Bilous RW, Cardwell CR, Hunter SJ, Kee F, Fogarty DG (2009) Is hyperfiltration associated with the future risk of developing diabetic nephropathy? A meta-analysis. Diabetologia 52:691–697

Mehta A, Beck M, Elliott P et al (2009) Enzyme replacement therapy with agalsidase alfa in patients with Fabry's disease: an analysis of registry data. Lancet 374:1986–1996

Rombach SM, Aerts JM, Poorthuis BJ et al (2012) Long-term effect of antibodies against infused alpha-galactosidase A in Fabry disease on plasma and urinary (lyso)Gb3 reduction and treatment outcome. PLoS One 7:e47805

Rombach SM, Smid BE, Bouwman MG, Linthorst GE, Dijkgraaf MG, Hollak CE (2013) Long term enzyme replacement therapy for Fabry disease: effectiveness on kidney, heart and brain. Orphanet J Rare Dis 8:47

Schiffmann R, Kopp JB, Austin HA 3rd et al (2001) Enzyme replacement therapy in Fabry disease: a randomized controlled trial. JAMA 285:2743–2749

Schwarting A, Dehout F, Feriozzi S et al (2006) Enzyme replacement therapy and renal function in 201 patients with Fabry disease. Clin Nephrol 66:77–84

Smid BE, Rombach SM, Aerts JM et al (2011) Consequences of a global enzyme shortage of agalsidase beta in adult Dutch Fabry patients. Orphanet J Rare Dis 6:69. doi:10.1186/1750-1172-1186-1169

Weidemann F, Niemann M, Stork S et al (2013) Long-term outcome of enzyme-replacement therapy in advanced Fabry disease: evidence for disease progression towards serious complications. J Intern Med 274:331–341

West M, Nicholls K, Mehta A et al (2009) Agalsidase alfa and kidney dysfunction in Fabry disease. J Am Soc Nephrol 20:1132–1139

JIMD Reports
DOI 10.1007/8904_2015_423

RESEARCH REPORT

# Niemann-Pick Type C-2 Disease: Identification by Analysis of Plasma Cholestane-3β,5α,6β-Triol and Further Insight into the Clinical Phenotype

**J. Reunert · A.S. Lotz-Havla · G. Polo · F. Kannenberg · M. Fobker · M. Griese · E. Mengel · A.C. Muntau · P. Schnabel · O. Sommerburg · I. Borggraefe · A. Dardis · A.P. Burlina · M.A. Mall · G. Ciana · B. Bembi · A.B. Burlina · T. Marquardt**

Communicated by: Maurizio Scarpa, MD, PhD

Competing interests: None declared

J. Reunert · T. Marquardt (✉)
Department of Pediatrics, University Hospital of Muenster, Muenster, Germany
e-mail: marquat@uni-muenster.de

A.S. Lotz-Havla · A.C. Muntau · I. Borggraefe
Dr. von Hauner Children's Hospital, Ludwig Maximilians University, Munich, Germany

G. Polo · A.B. Burlina
Division of Metabolic Diseases, Department of Woman and Child Health, University Hospital of Padua, Padua, Italy

F. Kannenberg · M. Fobker
Center of Laboratory Medicine, University Hospital of Muenster, Muenster, Germany

M. Griese
Pediatric Pulmonology, Dr. von Hauner Children's Hospital, Ludwig Maximilians University, Member of the German Center for Lung Research (DZL), Munich, Germany

E. Mengel
Villa Metabolica, Center for Pediatric and Adolescent Medicine, University Medical Center of the Johannes Gutenberg University Mainz, Mainz, Germany

P. Schnabel
Department of General Pathology, University Hospital of Heidelberg, Heidelberg, Germany

O. Sommerburg · M.A. Mall
Department of Translational Pulmonology and Division of Pediatric Pulmonology and Allergy and Cystic Fibrosis Center, University of Heidelberg, Heidelberg, Germany

A. Dardis · G. Ciana · B. Bembi
Regional Coordinator Centre for Rare Diseases, University Hospital Santa Maria della Misericordia, Udine, Italy

A.P. Burlina
Neurological Unit, St. Bassiano Hospital, Bassano del Grappa, Italy

P. Schnabel · O. Sommerburg · M.A. Mall
Translational Lung Research Center Heidelberg (TLRC), Member of German Center for Lung Research (DZL), University of Heidelberg, Heidelberg, Germany

Received: 18 November 2014 / Revised: 26 January 2015 / Accepted: 13 February 2015 / Published online: 13 March 2015


**Abstract** *Introduction*: Niemann-Pick type C disease is a rare disorder caused by impaired intracellular lipid transport due to mutations in either the *NPC1* or the *NPC2* gene. Ninety-five % of NPC patients show mutations in the *NPC1* gene. A much smaller number of patients suffer from NPC2 disease and present respiratory failure as one of the most frequent symptoms. Several plasma oxysterols are highly elevated in NPC1 and can be used as a biomarker in the diagnosis of NPC1.

*Methods*: Plasma cholestane-3β,5α,6β-triol was evaluated as biomarker for NPC2 by GC/MS and LC-MS/MS analysis. The diagnosis was confirmed by Sanger sequencing and filipin staining.

*Results*: We report three NPC2 patients with typical respiratory problems and a detailed description of the nature of the lung disease in one of them. All patients had elevated levels of plasma cholestane-3β,5α,6β-triol. In two of these patients, the positive oxysterol result led to a rapid diagnosis of NPC2 by genetic analysis. The phenotype of the third patient has been described previously. In this patient a cholestane-3β,5α,6β-triol concentration markedly above the reference range was found.

*Conclusions*: Measurement of plasma cholestane-3β,5α,6β-triol enables to discriminate between controls and NPC1 and NPC2 patients, making it a valuable biomarker for the rapid diagnosis not only for NPC1 but also for NPC2 disease.

The measurement of oxysterols should be well kept in mind in the differential diagnosis of lysosomal diseases, as the elevation of oxysterols in plasma may speed up the diagnosis of NPC1 and NPC2.

## Introduction

Niemann-Pick type C disease (NPC; OMIM 257220; OMIM 607625) is a rare autosomal recessive lysosomal storage disorder affecting the intracellular trafficking of unesterified cholesterol and other lipids (for review, see Mengel et al. 2013). Two disease-causing genes have been identified, *NPC1* (MIM#607623) and *NPC2* (MIM#601015), encoding two proteins, that are involved in the transport of cholesterol and other lipids out of late endosomes and lysosomes. As a consequence, unesterified cholesterol accumulates within these compartments. NPC1 is a large membrane spanning glycoprotein mainly located in the late endosomes (Carstea et al. 1997; Higgins et al. 1999). NPC2 is a small soluble protein, binding nonesterified cholesterol with high affinity (Okamura et al. 1999; Storch and Xu 2009).

The majority of NPC patients have a defect in *NPC1* (95%), while only 5% of the NPC cases are due to mutations in *NPC2*. To date, more than 300 mutations have been described in the *NPC1* gene; about 20 mutations have been reported in the *NPC2* gene. Most NPC2 mutations lead to a severe phenotype, frequently presenting with pronounced pulmonary involvement (Millat et al. 2001; Verot et al. 2007).

The onset of symptoms may vary from early infancy to late adulthood, and clinical manifestations are extremely heterogeneous. Systemic symptoms include isolated spleno- or hepatosplenomegaly in infancy or childhood and precede the onset of neurological signs. Characteristic neurological manifestations include saccadic eye movement abnormalities, cerebellar signs (ataxia, dystonia/dysmetria, dysarthria), gelastic cataplexy, and epileptic seizures. Pulmonary infiltration with foam cells is usually restricted to patients with early onset disease and is more frequent in patients with severe *NPC2* mutations.

The current diagnostic screening methods for NPC include biochemical testing, such as filipin staining in fibroblasts, and measuring the plasma chitotriosidase activity followed by a mutation analysis of the *NPC1* and *NPC2* genes. No specific biomarker was available for NPC until Porter et al. (2010) demonstrated the usefulness of cholesterol oxidation products in human plasma as new biomarker for NPC1. In NPC1 cells, cholesterol accumulation is associated with oxidative stress (Reddy et al. 2006; Zampieri et al. 2009), resulting in increased non enzymatic oxidation of cholesterol in different tissues (Porter et al. 2010). Therefore, a small fraction of the cholesterol is oxidized to so-called oxysterols, which can be measured in EDTA plasma and serum by GC/MS and LC-MS/MS. In plasma of NPC1 patients, cholesterol oxidation products such as 7-ketocholesterol and cholestane-3β,5α,6β-triol are significantly elevated (Porter et al. 2010). In fact, the plasmatic levels of these oxysterols allow distinguishing between NPC1 patients and controls. Only one NPC2 patient has been detected after oxysterol analysis so far (Boenzi et al. 2014).

We report three NPC2 patients with elevated plasma cholestane-3β,5α,6β-triol levels; in two of them a genetic analysis was initiated after positive oxysterol results, leading to a rapid diagnosis of NPC2. The clinical phenotype of the first patient gives new insights into the physiology of the lung disease in NPC2. The third NPC2 patient has already been described by Griese et al. (2010). We show that this patient also had an elevated cholestane-3β,5α,6β-triol plasma concentration.

## Materials and Methods

### LC-MS/MS

The concentration of cholestane-3β,5α,6β-triol was determined in 50 µl plasma. Cholestane-3β,5α,6β-triol D7 (TRC) was used as internal standard. The analytes were derivatized into dimethylglycine esters based on the method of Jiang et al. (2011). The chromatographic separation was performed on a column Symmetry C18 (2.1 × 50 mm 3.5 µm) using a linear gradient of water and acetonitrile (pH 3; 1 mM ammonium formate). The mass spectrometer Waters Xevo TQ MS was used as detector, and quantification was based on an 8-point calibration curve. The cutoff value for the LC-MS/MS method was 30 ng/ml.

### GC/MS

10 ng of d7-cholestane-3β,5α,6β-triol (Santa Cruz) as an internal standard (IS) was added to 100 µL of plasma or serum. Alkaline saponification and lipid extraction were performed using the method of Klansek et al. (1995) with some modifications: plasma or serum was subjected to alkaline saponification with potassium hydroxide/isopropanol followed by extraction of the free triol with carbon tetrachloride and derivatization with *N*-Methyl-*N*-(trimethylsilyl)trifluoroacetamide/1-methylimidazole (19:1 v/v). 1 µL was analyzed isothermal at 280°C by gas chromatography-mass spectrometry (GC/MS) using a Shimadzu QP2010Plus with an Rtx-200MS-column (Restek, 30 m, 0.25 mm, 0.5 µm). For quantification, the triols were monitored with ions *m/z* 403 and *m/z* 410 in EI-SIM-mode. Concentrations were calculated from the linear response

range of standard curve established for cholestane-3β,5α,6β-triol/IS (Porter et al. 2010). The cutoff value for the GC/MS method was 50 ng/ml.

### Mutation Analysis

All exons of *NPC1* (NM_000271) and *NPC2* (NM_006432) and their flanking intronic sequences were amplified by PCR and analyzed by Sanger sequencing. Primer sequences and PCR conditions are available upon request. Putative mutations were confirmed by sequencing duplicate PCR products and by the DNA analysis from parents.

### Filipin Staining

Intracellular accumulation of unesterified cholesterol was analyzed in cultured fibroblasts by filipin staining as previously described (Blanchette-Mackie et al. 1988).

### Chitotriosidase Activity

The chitotriosidase activity was measured as described earlier (Hollak et al. 1994). Plasma samples were diluted 1:10, 1:20, 1:40, and 1:80 with demineralized water before incubation. The reaction was stopped with 2 ml ethylenediamine (Fluka 03550) after 15 min. The product of the enzymatic reaction, fluorescent 4-methylumbelliferone, was measured using a spectral fluorophotometer at 360 and 450 nm. The enzyme activity was expressed in nmol/h/ml (normal 100 nmol/h/ml).

## Results

### Case Reports

#### *Patient 1*

The first patient was born at term (38 + 4 gestational weeks) with a weight of 3,360 g, a length of 51 cm, and a head circumference of 35 cm. Pregnancy and postpartum adaptation were uneventful. There was no history of neonatal cholestasis. The girl was the second child of healthy parents, both of German origin. The family history was unremarkable; the older brother of the patient is healthy.

The patient was first admitted to a hospital at 10 weeks of age for further workup for failure to thrive and respiratory difficulties. Furthermore, the patient was found to have mild hepatosplenomegaly. There was a rapid progression of respiratory insufficiency with recurrent atelectasis. From the age of 4 months on, continuous artificial ventilation was required. Repeated bronchoalveolar lavage did not improve the respiratory situation. At 5 months of age, lateral thoracotomy with biopsy and partial resection of segments 5 and 9 of the right lung was performed. However, the respiratory situation did not improve. At 7 months of age, the patient was transferred to a specialized hospital for further workup. CT scans revealed ground glass-shading of both lungs in CT scan (Fig. 1a), and pathological surfactant protein composition (protein C deficiency) similar to alveolar proteinosis was found in bronchoalveolar lavage fluid (Fig. 1c). Alveolae were filled with fine granular material and foam cells (Fig. 1b, d). Abdominal ultrasound confirmed mild hepatosplenomegaly (liver in anterior axillary line 9.2 cm, spleen 7 cm), both with normal parenchyma. There were no signs of cholestasis.

Due to the combination of severe respiratory disease with hepatosplenomegaly, metabolic workup was initiated showing elevated plasma oxysterols (150 ng/ml, measured by GC/MS) and chitotriosidase activity (415 nmol/h/ml), suspicious for Niemann-Pick type C disease. The diagnosis of Niemann-Pick type C-2 was confirmed by a genetic analysis of the *NPC2* gene revealing the homozygous mutation c.352G>T (p.E118X). This mutation leads to a premature stop codon and has been associated with a severe phenotype of Niemann-Pick type C-2 before (Millat et al. 2001; Schofer et al. 1998).

Considering bone marrow transplant as therapeutic option (Breen et al. 2013), extensive neurological workup was performed after diagnosis at 8 months of age. High-resolution 3T MRI of the brain revealed hypomyelinization and global brain atrophy with enlarged inner and outer cerebrospinal fluid space (Fig. 2a–c). Electroencephalography detected multiregional epileptiform discharges regardless of high dosages of benzodiazepines reflecting increased cortical excitability (Fig. 2d). Evaluation of development revealed general psychomotor retardation with muscular hypotonia (as far as possible to judge due to sedatives). Gross motor movement was unfocused without active grasping for objects, hand-knee contact, or changing of objects between hands. Major developmental milestones as sitting were not reached. Spontaneous ocular fixation and eye contact were possible though without appropriate endurance. Mild horizontal saccades, end-position nystagmus, and intermittent irregular myocloni were present. Considering these results, decision was made together with the parents for palliative care management. The patient died at 11 months of age after rapid respiratory deterioration.

#### *Patient 2*

The second patient was born as the third child from Tunisian consanguineous parents (first cousins). The boy was born at term with a weight of 3,320 g; Apgar scores

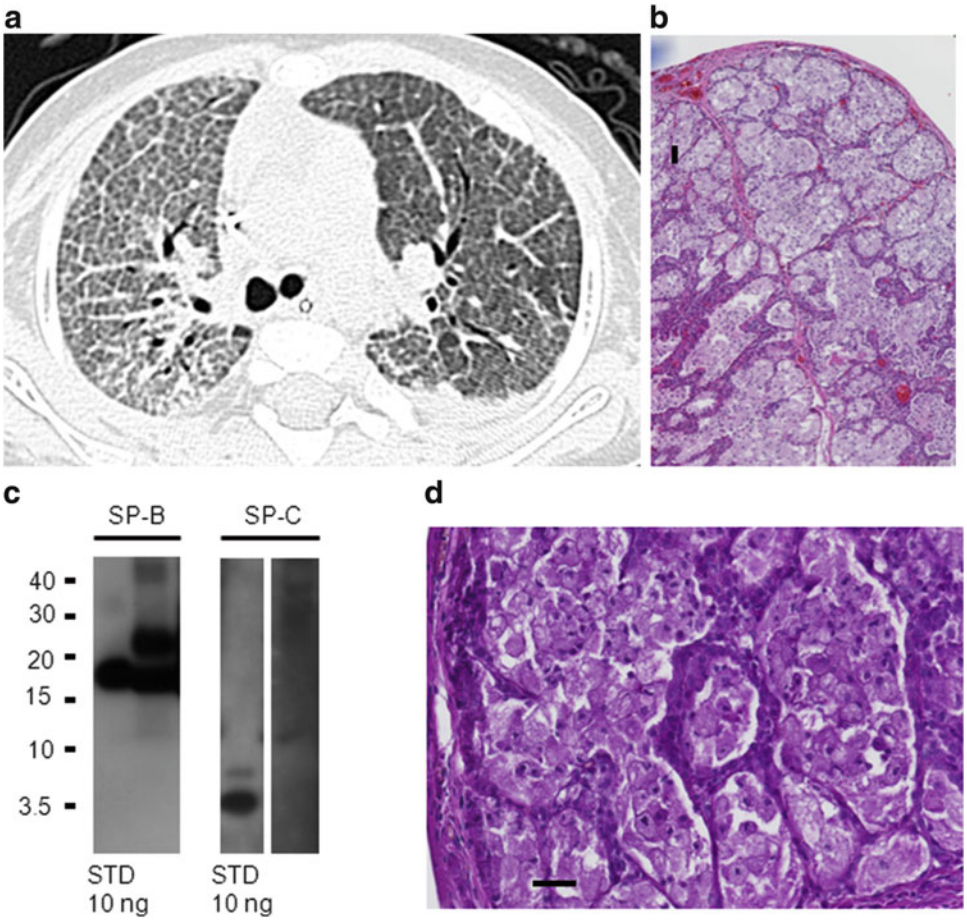


**Fig. 1** Patient 1 at the age of 7 months: (**a**) Upper left: CT scan showing crazy-paving pattern with pronounced inter- and intralobar septi, particular on the right side; left side after therapeutic lavage. (**b**) Upper right and (**d**) lower right: Lung biopsy (hematoxylin and eosin stain, 40-fold) showing alveolar filling with fine granular material. PAS-positive material (100 fold) mainly foamy macrophages and some extracellular surfactant material. (**c**) Lower left: Western blotting of bronchoalveolar lavage for surfactant protein B (SP-B) and SP-C. 5 μg of total protein of lavage fluid per lane was added and the respective standards (STD). After SDS-PAGE and transfer, the membranes were probed with antibodies against SP-B and SP-C. Molecular weights (kDa) are indicated on the left side. All bands were analyzed under nonreducing conditions. SP-B was detected as dimers (typical bands at 16 kDa; compare to standard STD of 10 ng applied to lane 1) and some higher molecular forms (bands at 24 kDa); such forms are of interest, as often seen in patients with alveolar proteinosis. No monomers or degradation products were detected. SP-C was absent at molecular weight of about 4 kDa (usually SP-C is present in amounts at least about 50% of SP-B)

were 8 and 9 at 5 and 10 min. At the fourth day of life, the neonate presented with hyperbilirubinemia: total bilirubin 135 μmol/L (nv 1.7–17 μmol/L), conjugated bilirubin 89 μmol/L (nv 0–3.4 μmol/L), impaired liver function (albumin 2.8%, INR 1.47), and severe splenomegaly. Initial chest X-ray and neurological examination were normal. Also blood and urine metabolic screenings were normal. After 20 days, he showed persistent hyperbilirubinemia, total bilirubin 104.7 μmol/L (nv 1.7–17 μmol/L), conjugated bilirubin 72 μmol/L (nv 0–3.4 μmol/L), and splenomegaly. Lysosomal investigations including urinary mucopolysaccharides and oligosaccharides were normal. Due to the persistent hyperbilirubinemia, oxysterol analysis was performed in EDTA plasma, showing abnormal values (515 ng/ml, measured by LC-MS/MS). The test led to the suspicion of Niemann-Pick type C. Since pulmonary involvement is a common feature of NPC2 patients, molecular analysis of the *NPC2* gene was performed, and the previously described mutation c.436C>T (p.Q146X) was found in a homozygous state (Millat et al. 2005).

Filipin staining of cultured fibroblasts showed a massive intracellular accumulation of unesterified cholesterol (Fig. 3a). The chitotriosidase activity was elevated to 169.3 nmol/h/ml. A therapy with miglustat was started at the dose of 50 mg once a day at 4 weeks of life.

A few days after discharge, the patient developed bronchiolitis. The chest X-ray showed bilateral micronodular infiltrates in both lungs, more pronounced in the

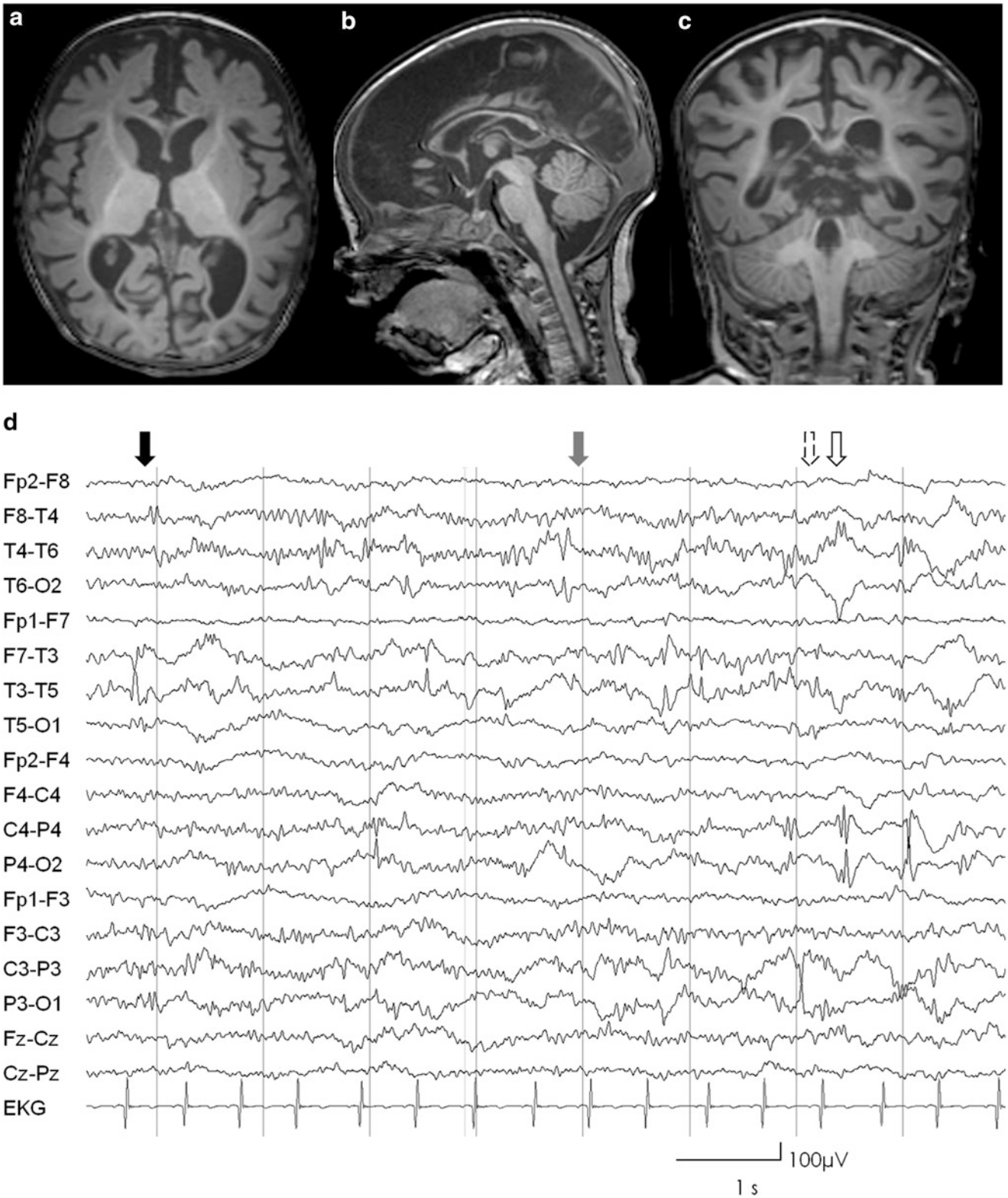


**Fig. 2** (**a**–**c**) Axial sagittal and coronal T1-weighted cranial MRI slices of patient 1, showing delayed myelinization sparing the frontal and posterior subcortical white matter and global brain atrophy; (**d**) EEG performed with current application of high doses of midazolam showing multiregional epileptiform discharges temporal left (*black arrow*), right (*gray arrow*), parietal left (*lined arrow*), and right (*bare arrow*). In addition, excessive beta-activity reflecting benzodiazepine effect is evident

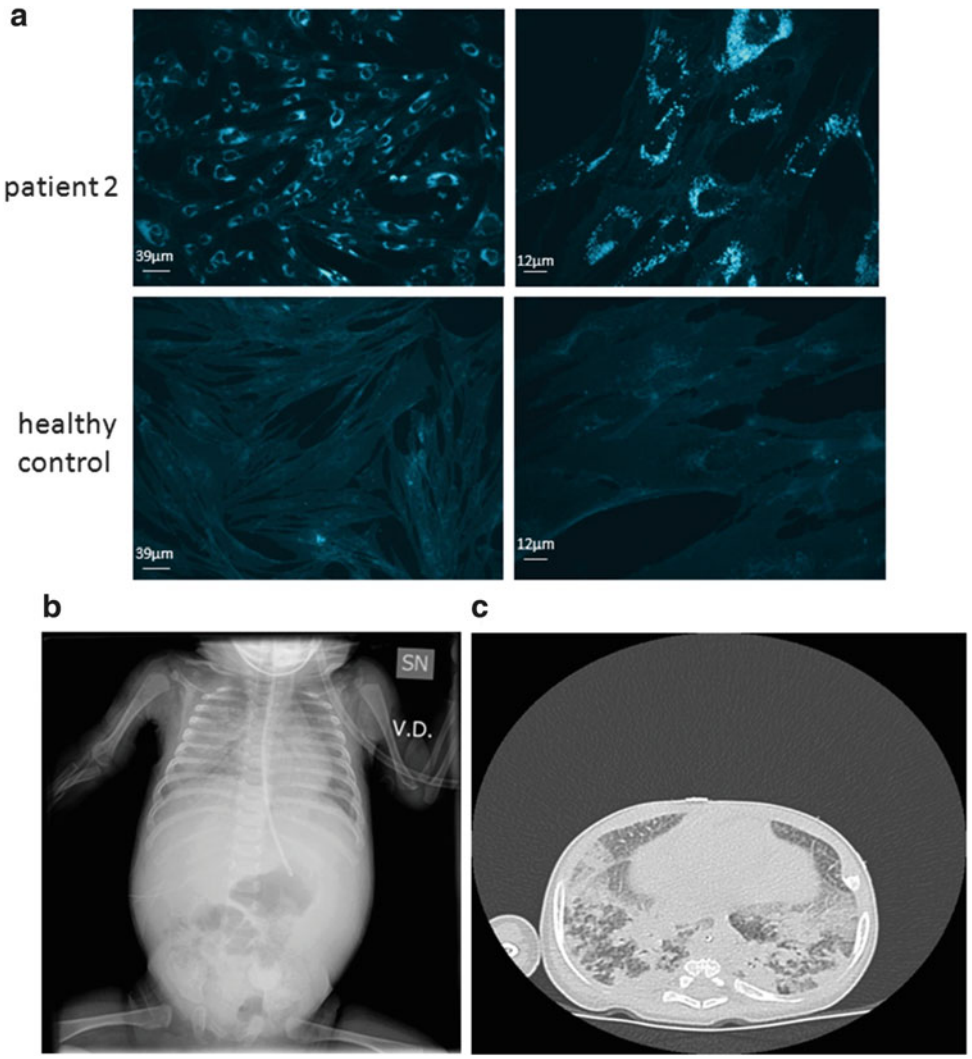


**Fig. 3** (**a**) Filipin staining of cultured fibroblasts in patient 2, showing a massive intracellular accumulation of unesterified cholesterol. (**b**, **c**) Chest X-ray and high-resolution CT of patient 2, showing diffuse hypo-diaphaneity with air bronchogram in the whole right pulmonary field and in the left inferior field (**b**) and smooth septal thickening and ground glass opacities in intermixed pattern (**c**)

right field. Due to a mean poor weight gain, miglustat was stopped at 2 and a half months of age and never recommenced. Ophthalmologic evaluation showed a regular fundus. The baby presented generalized hypotonia, with reduced spontaneous motility and poor visual contact. The baby was discharged with antibiotics and salbutamol aerosol.

He was readmitted about 1 month later with respiratory distress that needed high oxygen supply. Chest X-ray images were dramatically altered with diffuse hypo-diaphaneity and air bronchogram in the whole right pulmonary field and in the left inferior field. High-resolution CT showed smooth septal thickening and ground glass opacities in intermixed pattern (Fig. 3b, c). Cholestatic disease was stable. Although intensive respiratory therapy was initiated, the patient gradually deteriorated and died 1 month after admission, at the age of four months and a half.

*Patient 3*

The third patient was already described in detail by Griese et al. (2010). The baby girl was born at term after an uneventful pregnancy as the second child. She presented with progressive tachypnea, failure to thrive, and poor feeding since the second month of life. The X-ray showed bilateral micronodular infiltrates especially in the lower left lung and apical right lobe. Hepatosplenomegaly was present with the liver enlarged to 4 cm and the spleen enlarged to 5 cm below the costal margin. Neurological development and blood and urine metabolic screening were normal. The

suspicion for NPC was confirmed by a genetic analysis which revealed a homozygous deletion (c.408_409delAA) in *NPC2*, leading to a frame shift and an elongated protein with additional 80 amino acids (Griese et al. 2010). Treatment of the pulmonary alveolar proteinosis with GM-CSF and half lung lavages did not improve the patient's general condition. She died after the fifth lavage after developing a pneumothorax (Griese et al. 2010). The oxysterol amount in a preserved serum sample of this patient was highly elevated to 226 ng/ml.

## Discussion

The heterogeneous phenotype and the variable progression of Niemann-Pick type C disease often lead to a delay of diagnosis. Available screening methods are limited to filipin staining of unesterified cholesterol in cultured fibroblasts, measurement of chitotriosidase activity, and genetic analysis of the *NPC1* and *NPC2* genes. Filipin staining of fibroblasts is currently the most specific diagnostic method for NPC (Wraith et al. 2009; Patterson et al. 2012), showing the classical storage pattern, characterized by massive accumulation of unesterified cholesterol in 85% of NPC patients. However, 15% of patients present the so-called variant biochemical phenotype, characterized by mild to moderate intracellular cholesterol accumulation. In these cases the diagnosis of NPC might still be uncertain (Vanier et al. 1991; Wraith et al. 2009; Patterson et al. 2012). Since filipin staining requires living cells, a skin biopsy is needed, and the procedure is time-consuming. Chitotriosidase activity may be a useful indication for NPC, but is not sensitive or specific for NPC (Ries et al. 2006) and often normal in adults. In order to speed up the diagnosis, Porter et al. (2010) published a sensitive and specific biomarker by measuring plasma oxysterols in NPC1 patients. The elevation of several oxysterols in plasma of NPC patients was used to distinguish NPC1 patients from controls.

Our data show that the oxidized cholesterol derivate cholestane-3β,5α,6β-triol may also be used as appropriate biomarker for identification of NPC2 patients (Fig. 4). Patients 1 and 2 presented with an elevated plasma cholestane-3β,5α,6β-triol concentration. The diagnosis of NPC2 was then confirmed by a genetic analysis. The third patient was already diagnosed with NPC2 but also showed elevated amounts of cholestane-3β,5α,6β-triol. The cholestane-3β,5α,6β-triol levels in plasma of the NPC2 patients show a clear discrimination from 50 plasma samples that have been in normal range. In contrast, the NPC2 patients could not be discriminated from 20 genetically confirmed NPC1 patients by measuring plasma cholestane-3β,5a,6β-triol (see Fig. 4). These data demonstrate the eligibility of cholestane-3β,5α,6β-triol as biomarker not only for NPC1

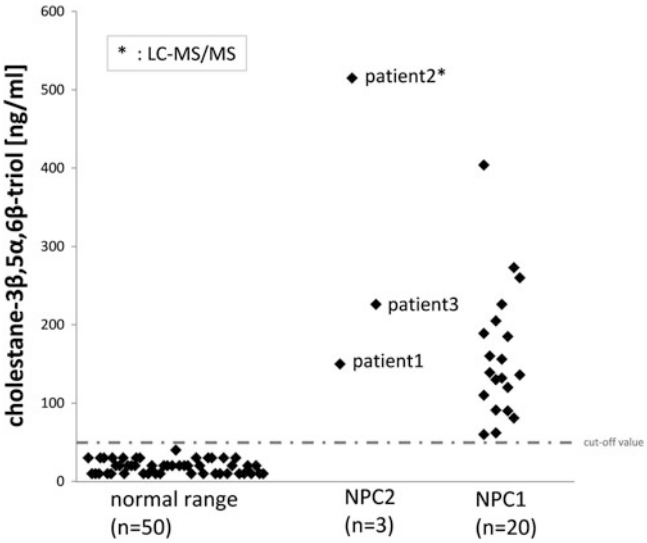


**Fig. 4** Cholestane-3β,5α,6β-triol levels in plasma of patients with genetically confirmed NPC2 ($n = 3$) showing a clear discrimination from 50 plasma samples in normal range. The patients with confirmed NPC2 mutations show similar cholestane-3β,5α,6β-triol levels as NPC1 ($n = 20$) patients. The *dotted line* indicates the cutoff value for the GC/MS method (50 ng/ml)

but also for NPC2. The specificity of oxysterols as biomarker for other lysosomal diseases with a similar clinical phenotype has already been investigated by Porter et al. (2010) and Lin et al. (2014). Porter et al. (2010) showed that cholestane-3β,5α,6β-triol and 7-ketocholesterol can be used to distinguish between patients suffering from NPC and patients suffering from other lysosomal diseases (infantile neuronal ceroid lipofuscinosis (INCL), GM-1 gangliosidosis, GM-2 gangliosidosis, and Gaucher disease (GD)), where the plasma oxysterols showed normal levels.

Lin et al. (2014) additionally demonstrated that 7-ketocholesterol was not elevated in glycogen storage disorder type II (GSDII), Krabbe disease (KD), metachromatic leukodystrophy (MLD), and mucopolysaccharidosis type II (MPSII). A limitation in specificity of oxysterols as biomarkers for NPC becomes evident in the elevation of 7-ketocholesterol in the plasma of patients with a defect in the acid sphingomyelinase (Niemann-Pick A/B). This might also apply for plasma cholestane-3β,5α,6β-triol. It has been shown for at least one NPB patient (SSIEM 2014 Annual Symposium: Abstracts suppl: S150, 2014). In their publication, Lin et al. (2014) stated that cholestane-3β,5α,6β-triol was not detectable by ESI-MS due to the relatively low ionization efficiency.

NPC2 patients usually present with early pulmonary involvement and progression to severe respiratory disease. Although minimizing diagnostic delay is an important factor for all NPC patients, it is particularly critical for NPC2

patients with severe lung problems, in whom immediate causative treatment is of great importance. Indeed, in one NPC2 patient, early bone marrow transplantation improved the respiratory illness and the general developmental outcome (Bonney et al. 2010; Breen et al. 2013).

In patient 1, metabolic workup was already done at 3 month of age, showing mildly elevated chitotriosidase activity up to 117 nmol/ml/h (normal <100 nmol/ml/h) suggesting a lysosomal storage disease. A subsequent investigation for lysosomal diseases, such as Gaucher and Niemann-Pick A/B, was done by enzymatic analyses, showing negative results. Further testing for NPC was not performed. If the oxysterols would have been tested at the initial clinic suspicion, the diagnosis would have been confirmed earlier, and further diagnostics would have been spared (multiple genetic analysis, whole exome sequencing, lung biopsy).

In patient 2 the prolonged neonatal cholestatic jaundice together with a splenomegaly suggested an early neonatal lysosomal disease. In the metabolic investigation protocol, oxysterol analysis was recently included as it allows a rapid screening of NPC. The diagnosis in patient 2 was puzzling for the lack of inflammatory lung disease. Nevertheless, oxysterol analysis established the correct diagnosis.

Other patients with the same mutation as patients 1 and 2 have been described before. One patient carrying the homozygous p.E118X mutation also came from Germany and showed a similar clinical phenotype (Schofer et al. 1998; Millat et al. 2001). An Algerian patient described by Verot et al. (2007) with the same mutation as patient 2 did not show a pronounced pulmonary involvement.

In all three patients, *NPC2* mutations were deleterious, leading to death in the first year of life, mainly due to respiratory manifestations. Usually, NPC2 patients present with a broad spectrum of clinical severity including progressive neurological dysfunction (Millat et al. 2001; Verot et al. 2007; Alavi et al. 2013; Klünemann 2002). However, in these cases, initial neurological symptoms were unspecific and did not lead to NPC diagnosis. Since systemic symptoms precede neurological signs, it is likely that these patients did not live long enough to develop characteristic neurological symptoms. These findings were also mentioned by Millat et al. (2001), who described six NPC2 patients having a short lifespan, 4 of those did not show any neurological symptoms and died of respiratory failure in the first year of life. Two other patients were described who survived until 19 month and 4 years, respectively. These two patients developed neurological disease (Millat et al. 2001).

In conclusion, the measurement of oxysterols should be well kept in mind in the differential diagnosis of lysosomal diseases. Our data confirm that the elevation of oxysterols in plasma presents a valuable tool and may speed up the diagnosis of NPC1 and NPC2. Early detection of the NPC2 diagnosis is a significant step toward slowing of disease progression and allows genetic counseling for the family.

## Compliance with Ethics Guidelines

### Conflict of Interest

The work of Thorsten Marquardt and Janine Reunert is part of an investigator-initiated study, funded by a grant from Actelion Pharmaceuticals Ltd.

The work of Matthias Griese was supported by eRARE-2009 (EUPAPNet), DFG-970/8-1, and FP7-chILD-EU. The funding sources had no involvement in the collection, analysis, and interpretation of data or in the writing of the report.

Janine Reunert has received travel reimbursements and speaker honorarium from Actelion Pharmaceuticals Ltd, Allschwil, Switzerland.

Giulia Polo has received travel reimbursements and speaker honorarium from Actelion Pharmaceuticals Ltd, Allschwil, Switzerland.

Frank Kannenberg has received speaker honorarium from Actelion Pharmaceuticals Ltd, Allschwil, Switzerland.

Eugen Mengel has received travel reimbursements and speaker honorarium from Actelion Pharmaceuticals Ltd, Allschwil, Switzerland.

Andrea Dardis has received travel reimbursements and speaker honorarium from Actelion Pharmaceuticals Ltd, Allschwil, Switzerland.

Alessandro Burlina has received travel reimbursements and speaker honorarium from Actelion Pharmaceuticals Ltd, Allschwil, Switzerland.

Bruno Bembi has received travel reimbursements and speaker honorarium from Actelion Pharmaceuticals Ltd, Allschwil, Switzerland.

Alberto Burlina has received travel reimbursements and speaker honorarium from Actelion Pharmaceuticals Ltd, Allschwil, Switzerland.

Thorsten Marquardt has received travel reimbursements and speaker honorarium from Actelion Pharmaceuticals Ltd, Allschwil, Switzerland.

Amelie Lotz-Havla, Manfred Fobker, Ania Muntau, Philipp Schnabel, Olaf Sommerburg, Ingo Borggraefe, Matthias Mall, and Giovanni Ciana declare that they have no conflict of interest. None of the authors has nonfinancial interests that may be relevant to the submitted work.

## Informed Consent

All procedures followed were in accordance with the ethical standards of the responsible committee on human experimentation (institutional and national) and with the Helsinki Declaration of 1975, as revised in 2000 (5). Informed consent was obtained from all patients for being included in the study.

## Details of the Contributions of Individual Authors

Janine Reunert: acquisition and analysis of data, drafting, and revising the manuscript.

Amelie Lotz-Havla and Andrea Dardis: acquisition and interpretation of data, involved in drafting and revising the manuscript.

Giulia Polo, Matthias Griese, Frank Kannenberg, Eugen Mengel, Manfred Fobker, Ania Muntau, Ingo Borggraefe, Philipp Schnabel, Olaf Sommerburg, Alessandro Burlina, Matthias Mall, Giovanni Ciana, and Bruno Bembi: acquisition and interpretation of data, revising the manuscript.

Alberto Burlina and Thorsten Marquardt: supervising and design of the study, acquisition and interpretation of data, revising the manuscript.

## References


Alavi A, Nafissi S, Shamshiri H, Nejad MM, Elahi E (2013) Identification of mutation in NPC2 by exome sequencing results in diagnosis of Niemann-Pick disease type C. Mol Genet Metab 110:139–144

Blanchette-Mackie EJ, Dwyer NK, Amende LM et al (1988) Type-C Niemann-Pick disease: low density lipoprotein uptake is associated with premature cholesterol accumulation in the Golgi complex and excessive cholesterol storage in lysosomes. Proc Natl Acad Sci U S A 85:8022–8026

Boenzi S, Deodato F, Taurisano R et al (2014) A new simple and rapid LC–ESI-MS/MS method for quantification of plasma oxysterols as dimethylaminobutyrate esters. Its successful use for the diagnosis of Niemann–Pick type C disease. Clin Chim Acta 437:93–100. doi:10.1016/j.cca.2014.07.010

Bonney DK, O'Meara A, Shabani A et al (2010) Successful allogeneic bone marrow transplant for Niemann–Pick disease type C2 is likely to be associated with a severe "graft versus substrate" effect. J Inherit Metab Dis 33:171–173. doi:10.1007/s10545-010-9060-3

Breen C, Wynn RF, O'Meara A et al (2013) Developmental outcome post allogenic bone marrow transplant for Niemann Pick Type C2. Mol Genet Metab 108:82–84. doi:10.1016/j.ymgme.2012.11.006

Carstea ED, Morris JA, Coleman KG et al (1997) Niemann-Pick C1 disease gene: homology to mediators of cholesterol homeostasis. Science 277:228–231. doi:10.1126/science.277.5323.228

Griese M, Brasch F, Aldana V et al (2010) Respiratory disease in Niemann-Pick type C2 is caused by pulmonary alveolar proteinosis. Clin Genet 77:119–130. doi:10.1111/j.1399-0004.2009.01325.x

Higgins ME, Davies JP, Chen FW, Ioannou YA (1999) Niemann–Pick C1 is a late endosome-resident protein that transiently associates with lysosomes and the trans-Golgi network. Mol Genet Metab 68:1–13. doi:10.1006/mgme.1999.2882

Hollak CE, van Weely S, van Oers MH, Aerts JM (1994) Marked elevation of plasma chitotriosidase activity. A novel hallmark of Gaucher disease. J Clin Invest 93:1288–1292. doi:10.1172/JCI117084

Jiang X, Sidhu R, Porter FD et al (2011) A sensitive and specific LC-MS/MS method for rapid diagnosis of Niemann-Pick C1 disease from human plasma. J Lipid Res 52:1435–1445. doi:10.1194/jlr.D015735

Klansek JJ, Yancey P, Clair RWS et al (1995) Cholesterol quantitation by GLC: artifactual formation of short-chain steryl esters. J Lipid Res 36:2261–2266

Klünemann HH, Elleder M, Kaminski WE et al (2002) Frontal lobe atrophy due to a mutation in the cholesterol binding protein HE1/NPC2. Ann Neurol 52:743–749

Lin N, Zhang H, Qiu W et al (2014) Determination of 7-ketocholesterol in plasma by LC-MS for rapid diagnosis of acid SMase-deficient Niemann-Pick disease. J Lipid Res 55:338–343. doi:10.1194/jlr.D044024

Mengel E, Klunemann H-H, Lourenco CM et al (2013) Niemann-Pick disease type C symptomatology: an expert-based clinical description. Orphanet J Rare Dis 8:166. doi:10.1186/1750-1172-8-166

Millat G, Chikh K, Naureckiene S et al (2001) Niemann-Pick disease type C: spectrum of HE1 mutations and genotype/phenotype correlations in the NPC2 group. Am J Hum Genet 69:1013–1021. doi:10.1086/324068

Millat G, Baïlo N, Molinero S et al (2005) Niemann–Pick C disease: use of denaturing high performance liquid chromatography for the detection of NPC1 and NPC2 genetic variations and impact on management of patients and families. Mol Genet Metab 86:220–232. doi:10.1016/j.ymgme.2005.07.007

Okamura N, Kiuchi S, Tamba M et al (1999) A porcine homolog of the major secretory protein of human epididymis, HE1, specifically binds cholesterol. Biochim Biophys Acta BBA Mol Cell Biol Lipids 1438:377–387. doi:10.1016/S1388-1981(99)00070-0

Patterson MC, Hendriksz CJ, Walterfang M et al (2012) Recommendations for the diagnosis and management of Niemann–Pick disease type C: an update. Mol Genet Metab 106:330–344. doi:10.1016/j.ymgme.2012.03.012

Porter FD, Scherrer DE, Lanier MH et al (2010) Cholesterol oxidation products are sensitive and specific blood-based biomarkers for Niemann–Pick C1 disease. Sci Transl Med 2:56ra81. doi:10.1126/scitranslmed.3001417

Reddy JV, Ganley IG, Pfeffer SR (2006) Clues to neuro-degeneration in Niemann-Pick type C disease from global gene expression profiling. PloS One 1:e19. doi:10.1371/journal.pone.0000019

Ries M, Schaefer E, Lührs T et al (2006) Critical assessment of chitotriosidase analysis in the rational laboratory diagnosis of children with Gaucher disease and Niemann–Pick disease type A/B and C. J Inherit Metab Dis 29:647–652. doi:10.1007/s10545-006-0363-3

Schofer O, Mischo B, Püschel W et al (1998) Early-lethal pulmonary form of Niemann-Pick type C disease belonging to a second, rare genetic complementation group. Eur J Pediatr 157:45–49. doi:10.1007/s004310050764

SSIEM (2014) Annual symposium: abstracts. J Inherit Metab Dis 37:27–185. doi:10.1007/s10545-014-9740-5

Storch J, Xu Z (2009) Niemann–Pick C2 (NPC2) and intracellular cholesterol trafficking. Biochim Biophys Acta BBA Mol Cell Biol Lipids 1791:671–678. doi:10.1016/j.bbalip.2009.02.001

Vanier MT, Rodriguez-Lafrasse C, Rousson R et al (1991) Type C Niemann–Pick disease: spectrum of phenotypic variation in disruption of intracellular LDL-derived cholesterol processing. Biochim Biophys Acta 1096:328–337

Verot L, Chikh K, Freydière E et al (2007) Niemann–Pick C disease: functional characterization of three NPC2 mutations and clinical and molecular update on patients with NPC2. Clin Genet 71:320–330. doi:10.1111/j.1399-0004.2007.00782.x

Wraith JE, Baumgartner MR, Bembi B et al (2009) Recommendations on the diagnosis and management of Niemann–Pick disease type C. Mol Genet Metab 98:152–165. doi:10.1016/j.ymgme.2009.06.008

Zampieri S, Mellon SH, Butters TD et al (2009) Oxidative stress in NPC1 deficient cells: protective effect of allopregnanolone. J Cell Mol Med 13:3786–3796. doi:10.1111/j.1582-4934.2008.00493.x

JIMD Reports
DOI 10.1007/8904_2015_424

RESEARCH REPORT

# The Modulatory Effects of the Polymorphisms in *GLA* 5′-Untranslated Region Upon Gene Expression Are Cell-Type Specific

**Susana Ferreira • Carlos Reguenga • João Paulo Oliveira**

Received: 17 September 2014 / Revised: 01 December 2014 / Accepted: 13 February 2015 / Published online: 13 March 2015


**Abstract** Lysosomal α-galactosidase A (αGal) is the enzyme deficient in Fabry disease (FD). The 5′-untranslated region (5′UTR) of the αGal gene (*GLA*) shows a remarkable degree of variation with three common single nucleotide polymorphisms at nucleotide positions c.-30G>A, c.-12G>A and c.-10C>T. We have recently identified in young Portuguese stroke patients a fourth polymorphism, at c.-44C>T, co-segregating in *cis* with the c.-12A allele. In vivo, the c.-30A allele is associated with higher enzyme activity in plasma, whereas c.-10T is associated with moderately decreased enzyme activity in leucocytes. Limited data suggest that c.-44T might be associated with increased plasma αGal activity. We have used a luciferase reporter system to experimentally assess the relative modulatory effects on gene expression of the different *GLA* 5′UTR polymorphisms, as compared to the wild-type sequence, in four different human cell lines. Group-wise, the relative luciferase expression patterns of the various *GLA* variant isoforms differed significantly in all four cell lines, as evaluated by non-parametric statistics, and were cell-type specific. Some of the post hoc pairwise statistical comparisons were also significant, but the observed effects of the *GLA* 5′UTR polymorphisms upon the luciferase transcriptional activity in vitro did not consistently replicate the in vivo observations.

These data suggest that the *GLA* 5′UTR polymorphisms are possible modulators of the αGal expression. Further studies are needed to elucidate the biological and clinical implications of these observations, particularly to clarify the effect of these polymorphisms in individuals carrying *GLA* variants associated with high residual enzyme activity, with no or mild FD clinical phenotypes.

Communicated by: Viktor Kožich

Competing interests: None declared

**Electronic supplementary material:** The online version of this chapter (doi:10.1007/8904_2015_424) contains supplementary material, which is available to authorized users.

S. Ferreira (✉) · J.P. Oliveira
Department of Genetics, Faculty of Medicine, University of Porto, Porto, Portugal
e-mail: susanadg@med.up.pt

C. Reguenga
Department of Experimental Biology, Faculty of Medicine, University of Porto, Porto, Portugal

C. Reguenga
Institute for Molecular and Cell Biology, Porto, Portugal

J.P. Oliveira
Genetics Clinic, São João Hospital Centre, Porto, Portugal

## Introduction

Insufficient activity of lysosomal alpha-galactosidase A (αGal; EC 3.2.1.22) impairs the catabolism of several neutral glycosphingolipids, particularly of trihexosylceramide (Kint 1970). Accumulation of these glycosphingolipids in the endothelium and smooth muscle cells of blood vessels, as well as in the heart, the kidney and the nervous system, is the pathologic hallmark of Fabry disease (FD, OMIM #301500) (Desnick et al. 2001). The severity of the clinical phenotype of FD is roughly related to residual enzyme activity (REA) of αGal, as assayed in vitro: the lower the REA, the earlier is the age of onset and the more severe and multi-systemic are the clinical manifestations, while in patients with higher levels of REA the resultant phenotypes are more organ restricted (Germain 2010).

The primary transcript of the αGal gene (*GLA*) contains an unusually polymorphic 5′-untranslated region (5′UTR) of 110 nucleotides, encoded by exon 1 (Nucleotide

database, National Center for Biotechnology Information – NCBI, reference sequence: NM_000169.2; http://www.ncbi.nlm.nih.gov/nuccore/NM_000169.2; National Library of Medicine, Bethesda, MD, USA). Three single nucleotide polymorphisms (SNPs) respectively identified by reference numbers rs2071225, rs3027585 and rs3027584 at the NCBI SNP database (dbSNP, http://www.ncbi.nlm.nih.gov/snp/), which result from cytosine-to-thymine (C>T) or adenine-to-guanine (G>A) transitions at cDNA nucleotide positions c.-10(C>T), c.-12(G>A) and c.-30(G>A), counting backwards from the translation initiation codon, are relatively common in several ethnically different populations (Davies et al. 1993; Saifudeen et al. 1995; Wu et al. 2011; Ferri et al. 2012), including the Portuguese (Oliveira et al. 2008a). The dbSNP lists three additional *GLA* 5′UTR SNPs, at positions c.-8(C>G), c.-18(T>C) and c.-105(A>G), respectively identified as rs371291716, rs545597063 and rs3027583, but these variants have never been reported in the Portuguese population. Another *GLA* 5′UTR variant at c.-44(C>T), not yet registered at the dbSNP, was identified in young Portuguese stroke patients (Baptista et al. 2010), co-segregating in cis with the c.-12A allele.

Compared to the wild-type (WT) allele, the c.-30A allele is associated with increased plasma αGal activity (Saifudeen et al. 1995; Fitzmaurice et al. 1997), the c.-10T allele is associated with decreased activity of αGal in leukocytes (Oliveira et al. 2008a, b) and the c.-44T allele might be associated with increased plasma αGal activity (Baptista et al. 2010). Contrastingly, the SNP c.-12(G>A) seems to have no effect upon *GLA* gene expression (Oliveira et al. 2008a).

Because the *GLA* 5′UTR contains a binding site for methylated DNA-binding protein (MDBP)/regulatory factor X (RFX) transcription factor family (Zhang et al. 1990; Samac et al. 1998), as well as partially overlapping binding motifs for the nuclear factor kappa-B (NFκB) and E-26 (Ets) transcriptional regulatory factors (Saifudeen et al. 1995; Fitzmaurice et al. 1997), it has been previously suggested that protein ligands to these sites might be involved in the regulation of *GLA* gene expression (Saifudeen et al. 1995; Fitzmaurice et al. 1997). Since the SNPs c.-10(C>T) and c.-30(G>A) involve nucleotides respectively located at each of those binding sites, they might act as polymorphic modulators of *GLA* gene expression, with possible clinical relevance particularly in males carrying *GLA* sequence variants associated with high REA.

To compare the relative impact upon in vitro gene expression of each of the *GLA* 5′UTR SNPs that have been identified in the Portuguese population, we have carried out luciferase reporter assays in several human cell lines of distinct embryological origins, representing some of the cell types that are critically involved in the pathogenesis of FD.

## Materials and Methods

A detailed description of the laboratory methods is available online (Supplementary Information and Supplementary Tables 1 and 2).

### Synopsis of the Laboratory Protocol

Five genomic DNA (gDNA) samples from adult males known to carry either the *GLA* 5′UTR WT sequence or one of the four SNPs identified in the Portuguese population were obtained from an anonymised biorepository. The five distinct isoforms were amplified by polymerase chain reaction (PCR) and the amplicons were inserted into the *HindIII* site of the pGL3-Control Vector (pGL3 Luciferase Reporter Vectors; Promega, Madison, WI, USA). The pGL3-Control Vector contains a cDNA encoding a modified firefly luciferase (luc+) under the control of the Simian virus 40 (SV40) promoter. The recombinant pGL3 vectors were transiently transfected into each of four human cell lines of different embryological origin: (1) human embryonic kidney, HEK-293 (Shaw et al. 2002); (2) human cervical carcinoma, HeLa (Macville et al. 1999); (3) human dermal microvascular endothelial cells, HDMEC (Richard et al. 1999); and (4) human T cell lymphoblast-like, Jurkat (Schneider et al. 1977). A plasmid (pCDNA3.3-LacZ; Invitrogen, Life Technologies, Carlsbad, CA, USA) containing the *Escherichia coli* (*E. coli*) β-galactosidase gene (pGAL) was used as an internal control for transfection efficiency. The relative luciferase activity (RLA) of each sample was calculated as the ratio of luciferase to β-galactosidase luminometric readings. A minimum of nine independent successful co-transfection experiments were analysed per cell type.

To allow comparisons between independent experiments in each cell type, a normalised RLA (nRLA) was calculated by dividing the RLA calculated for each sample by the average RLA of the WT construct vector samples of the corresponding experiment.

### Statistical Analyses

The non-parametric Kruskal–Wallis one-way analysis of variance by ranks was used as the first-tier statistical testing for significant differences in the nRLA raw data of the various *GLA* 5′UTR vector constructs, in each cell type.

As this test does not identify where the observed differences occur or how many differences actually occur, further statistical analyses were based on parametric testing with one-way analysis of variance (ANOVA) and post hoc Dunnett's test. To this end, outlier raw RLA data points were first excluded by the fourth-spread method, as recommended by other investigators (Jacobs and Dinman

**Table 1** Non-parametric statistical analysis by the Kruskal–Wallis test of the normalised relative luminometric activity (nRLA) of the five *GLA* 5′UTR plasmid vector constructs in four different cell lines

| | Cell lines | | | | | | | |
|---|---|---|---|---|---|---|---|---|
| | HEK-293 | | HeLa | | HDMEC | | Jurkat | |
| *GLA* 5′UTR plasmid vector constructs | *N* | Mean rank (nRLA) | *N* | Mean rank (nRLA) | *N* | Mean rank (nRLA) | *N* | Mean rank (nRLA) |
| WT | 13 | 20.54 | 16 | 38.03 | 15 | 45.23 | 15 | 45.17 |
| c.-10T | 13 | 46.62 | 16 | 48.28 | 15 | 39.77 | 15 | 27.07 |
| c.-12A | 13 | 30.92 | 16 | 28.69 | 15 | 26.73 | 15 | 27.83 |
| c.-30A | 13 | 25.96 | 12 | 10.00 | 15 | 48.60 | 9 | 23.94 |
| c.-44T | 13 | 40.96 | 16 | 60.38 | 15 | 29.67 | 15 | 46.57 |
| Total (*N*) | 65 | | 76 | | 75 | | 69 | |
| *Kruskal–Wallis test* | | | | | | | | |
| Chi-square (df = 4) | 16.652 | | 41.993 | | 11.501 | | 15.831 | |
| Asymptotic significance | 0.002 | | 0.000 | | 0.021 | | 0.003 | |

*WT* wild-type, *N* number of experiments validated per each cell line, *df* degrees of freedom

**Table 2** One-way analysis of variance (ANOVA) of the natural logarithms of the normalised relative firefly luciferase activities expressed as a percentage of the wild-type (nRLA%), comparing the means of the five *GLA* 5′UTR plasmid vector constructs in four different cell lines

| | ANOVA results | | | | | |
|---|---|---|---|---|---|---|
| Cell lines | | Sum of squares | df | Mean square | *F* | *p*-value |
| HEK-293 | Between groups | 2.184 | 4 | 0.546 | 3.615 | 0.010 |
| | Within groups | 9.062 | 60 | 0.151 | | |
| | Total | 11.246 | 64 | | | |
| HeLa | Between groups | 10.423 | 4 | 2.606 | 22.796 | 0.000 |
| | Within groups | 8.116 | 71 | 0.114 | | |
| | Total | 18.538 | 75 | | | |
| HDMEC | Between groups | 1.401 | 4 | 0.350 | 3.721 | 0.009 |
| | Within groups | 6.305 | 67 | 0.094 | | |
| | Total | 7.706 | 71 | | | |
| Jurkat | Between groups | 1.005 | 4 | 0.251 | 4.278 | 0.004 |
| | Within groups | 3.641 | 62 | 0.059 | | |
| | Total | 4.646 | 66 | | | |

*df* degrees of freedom

2004), the nRLA values were expressed as percentage of the WT nRLA (nRLA%), and the natural logarithms of the latter values were used for the statistical analyses.

A two-sided significance level of $<0.05$ was assumed for all the statistical tests except for post hoc Dunnett's test where one-sided *p*-values were used instead. All statistical analyses were performed with the SPSS software, Version 19.0.

## Results

HDMEC cells with more than 12 subculture passages showed non-uniform and significantly slower doubling rates, with more erratic transfection efficiencies (data not shown). For that reason, only the RLA assays obtained in younger cell cultures were validated for the final analyses.

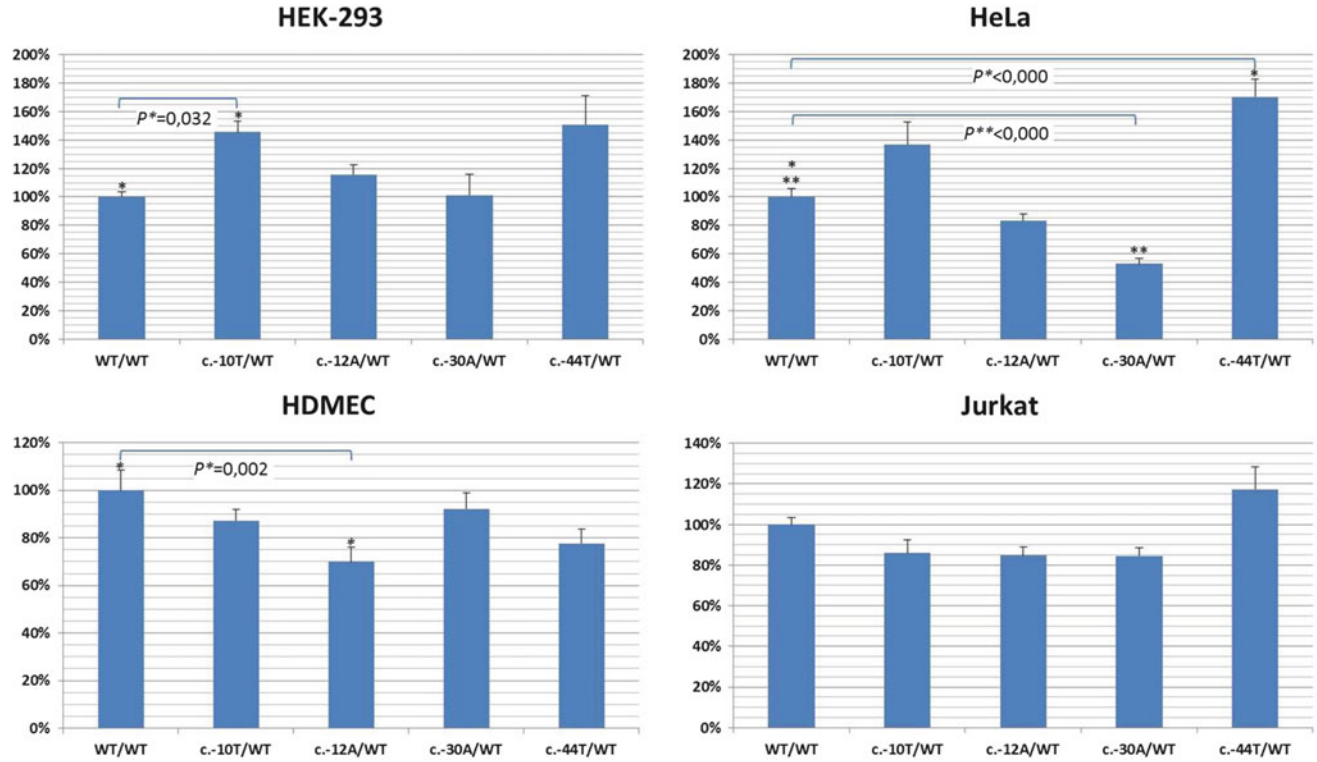


**Fig. 1** Normalised luciferase/β-galactosidase luminometric ratios of the *GLA* 5′UTR sequence variant isoforms c.-10T, c.-12A, c.-30A and c.-44T, expressed as percent of wild-type (WT), in HEK-293, HeLa, HDMEC and Jurkat human cell lines. The average bars are shown with the upper limit of the standard error of the mean. As explained in the text, the c.-44T allele was present in *cis* with the c.-12A allele. All pairwise comparisons between each of the variant alleles and the WT *GLA* 5′UTR isoform that reached statistical significance in the post hoc analyses are shown in the charts, with the corresponding one-sided Dunnett's test *p*-value

The distributions of the nRLA of the five *GLA* 5′UTR constructs, as evaluated by non-parametric statistics (Table 1), differed significantly in all cell types. By the fourth-spread method, one of the WT and one of the c.-44T allele data point values obtained in the Jurkat cells, as well as three of the c.-30A allele data point values obtained in the HDMEC cells, were classified as outliers and removed from the dataset for the subsequent parametric statistical analyses. ANOVA was performed on the normalised, log-transformed nRLA% data, with results similar to the non-parametric statistical approach (Table 2). Post hoc parametric statistical analyses showed that the SNPs c.-12 (G>A) and c.-30(G>A) were associated with significantly lower nRLA%, respectively in HDMEC ($p = 0.002$) and HeLa ($p < 0.000$) cells, while the SNPs c.-10(C>T) and c.-44(C>T) were associated with significantly higher nRLA%, respectively in HEK-293 ($p = 0.032$) and HeLa ($p < 0.000$) cells. In the Jurkat cells, none of the *GLA* SNPs was associated with a statistically significant difference in nRLA%, but both the c.-10T ($p = 0.067$) and c.-12A ($p = 0.086$) alleles showed a trend to lower activity (Fig. 1).

## Discussion

Luciferase-based genetic reporter assays are a standard in vitro approach to study DNA sequences and molecular processes that control gene expression, in various cellular contexts (Brogan et al. 2012). Herein we report the results of luciferase expression assays designed to investigate the relative efficiency of four different human *GLA* 5′UTR SNPs, in comparison to the WT sequence, as potential modulators of gene expression. One of the most common research applications of chimeric genetic reporter systems is in the analysis of *cis*-acting elements, like gene promoters; however, to the best of our knowledge, the functional consequences of the 5′UTR SNPs upon *GLA* gene expression have never been assayed in this manner. Overall, our results are consistent with the working hypothesis, based on observations in vivo that some of the minor 5′UTR SNPs alleles significantly affect αGal activity levels (Saifudeen et al. 1995; Fitzmaurice et al. 1997; Oliveira et al. 2008a, b), and provide indirect evidence that the human *GLA* 5′UTR indeed contains sequences that are involved in the regulation of gene expression. These data

also demonstrate, for the first time, that the 5′UTR-dependent modulation of *GLA* gene expression may vary among different cell types. The expression of alternative 5′UTRs represents an evolutionary gain of transcriptional and translational control pathways, allowing tissue-specific expression patterns and expanding the repertoire of expression from a single gene locus (Barrett et al. 2012). Although *GLA* is a housekeeping gene, αGal activity levels vary greatly from organ to organ and in different cell types (Brady et al. 1967; von Scheidt et al. 1991). It is possible that either transcription factors (TF) or RNA-binding proteins (RBP) that bind to specific sequences in the *GLA* 5′UTR contribute to the regulation of *GLA* gene expression in a tissue-specific manner.

The three common SNPs of the human *GLA* 5′UTR were originally described in 1993 with a combined minor allele frequency of 10% in the British population (Davies et al. 1993). Because they were neither translated nor part of the mRNA Kozak consensus sequence for translation initiation, they were regarded as biologically neutral, but subsequent studies showed that the c.-30A allele was associated with increased αGal activity in plasma (Saifudeen et al. 1995) and the c.-10T allele with decreased αGal activity in leukocytes (Oliveira et al. 2008a, b), as compared to the corresponding WT alleles. Since the *GLA* 5′UTR c.-10 and c.-30 positions are within binding sites respectively for the MDBP and the NFκB and Ets families of TF, the effect of those two nucleotide transitions upon αGal expression in vivo might be mediated by modulation of transcriptional activity.

On electrophoretic mobility shift assays (EMSA), binding of nuclear extract proteins to synthetic oligonucleotides containing the *GLA* 5′UTR NFκB/Ets binding site, either with a G or an A at the position corresponding to c.-30, was significantly less when adenine was present (Saifudeen et al. 1995), showing that the WT sequence has higher affinity to the putative NFκB/Ets ligands. Furthermore, in vitro translation of mRNAs from cloned WT and c.-30A alleles resulted in similar levels of αGal protein, indicating that the G>A transition does not enhance translation (Fitzmaurice et al. 1997), and studies performed on αGal derived from the WT and the c.-30A alleles, partially purified from plasma and lymphoblasts, revealed that the high plasma activity was not due to altered post-translational processing (Fitzmaurice et al. 1997). Overall, these findings suggest that the *GLA* 5′UTR c.-30G>A transition results in enhanced transcription, presumably by interfering with the binding of negatively acting TF which normally decrease αGal expression in various cells (Fitzmaurice et al. 1997).

Surprisingly, the c.-30A allele was not associated with higher protein expression in comparison to the WT allele, in any of the four cell types assayed in our luciferase reporter studies. Since plasma αGal most probably has a multiplicity of cellular sources (Fitzmaurice et al. 1997; Warnock 2005), a possible explanation for the inconsistency between the in vivo observations and the experimental in vitro data might be that none of the cell types used in our reporter studies is the right model to assay the 5′UTR-related modulation of *GLA* gene expression at the transcriptional level, at least for cells that most significantly contribute to the pool of circulating αGal protein. Therefore, testing additional cell types, ideally representing highly vascularised tissues that are particularly rich in αGal activity, like the spleen and the liver (Brady et al. 1967), might help to clarify these discrepancies.

Both the c.-12(A>G) and the c.-10(C>T) SNPs are located within the *GLA* 5′UTR MDBP consensus sequence, respectively, at its first and third nucleotide positions (Zhang et al. 1990), but only the c.-10(C>T) SNP seem to affect enzyme expression in vivo (Oliveira et al. 2008a). The amount of αGal identified by western blot analyses of leukocyte protein extracts was significantly lower in carriers of the c.-10T allele as compared to carriers of the WT allele (Oliveira et al. 2008b). Experimental data (Samac et al. 1998) have shown that sequence changes that increase the affinity of the *GLA* 5′UTR MDBP binding site for its cognate ligands exert a strong repressive effect upon gene expression. Furthermore, a C>T transition in the third nucleotide position of a MDBP binding site in the human cytomegalovirus significantly increased ligand binding, resulting in 10-fold reduction of reporter gene expression (Schneider et al. 1977). However, to the best of our knowledge, no EMSA studies have ever been performed with the human *GLA* 5′UTR MDBP binding site, to assess the relative affinities of the c.-10(C > T) alleles. Although the human *GLA* 5′UTR c.-12(G>A) SNP does not seem to change αGal expression in vivo, at least in plasma and leukocytes (Oliveira et al. 2008a), studies in the MDBP binding site of plasmid pBR322 have shown that the A>G transition in its first nucleotide position significantly increased the binding of MDBP extracted from the human placenta (Macville et al. 1999).

The results of our luciferase reporter assay studies are consistent with the hypothesis that the G>A transition at c.-12 has indeed a biological effect on gene expression. It is of note that in HDMEC and Jurkat cells the *GLA* c.-10T and c.-12A alleles are associated with relatively lower reporter gene expression as compared to the WT alleles, but in HEK-293 and HeLa cells the c.-10T allele is associated with increased reporter gene expression. The trend for a lower reporter gene expression associated with the c.-10T allele in the Jurkat cells is in agreement with the decreased leukocyte αGal activity observed in vivo (Oliveira et al. 2008a). The lack of statistical significance of all the post hoc analyses of the relative luciferase reporter expression

data in the Jurkat cells, as well as of some of the comparisons made in other cell types, can be attributed to statistically underpowered datasets. Confirmation of the present findings should be made using larger datasets of validated reporter gene expression readings per cell type, possibly using a dual reporter assay for better control of experimental normalisation (Jacobs and Dinman 2004).

The relative luciferase expression profile of the four human *GLA* 5′UTR SNPs, as normalised to the WT sequence, was different for each of the transfected cell lines in our experimental protocol. The diverse embryological lineages of HEK-293 (Shaw et al. 2002), HeLa (Macville et al. 1999), HDMEC (Richard et al. 1999), and Jurkat (Schneider et al. 1977) cells are a logical explanation for this finding, as the *GLA* gene may be under different constitutive expression regulation on different cells.

To identify other potential TF binding sites in the *GLA* 5′UTR, we queried the Transcription Factor Database (TRANSFAC). According to TRANSFAC, the c.-12G and the c.-10C nucleotides are both part of a consensus binding motif for zinc finger C4-type domains of nuclear receptors (ZFC4-NR), particularly the estrogen receptor alpha (ER-α), and the G>A and C>T transitions at those positions result in the loss of ZFC4-NR binding affinity. Similarly, the G>A transition at the c.-30 nucleotide, which is part of a conserved consensus binding sequence for both the Ets and the adenovirus E2 promoter binding (E2F) families of TF, also suppresses the site ligand affinity. On the other hand, the C>T transition at the c.-44 nucleotide creates a novel ZFC4-NR binding site, particularly for hepatocyte nuclear factor-4-alpha (HNF-4α). It is of note that, in the Portuguese population, the c.-44T allele has been found exclusively in *cis* with the c.-12A allele: therefore, the results of our luciferase reporter assays represent the in vitro combined effects of the two nucleotide transitions.

By predicting binding sites from position weight matrix in the database of RNA-binding specificities (RBPDB), the G>A transition at the c.-30 nucleotide results in the loss of binding affinity with the eukaryotic translation initiation factor 4B (EIF4B), but no changes are reported for the c.-10 (C>T) and the c.-12(G>A) SNPs. On the other hand a C>T transition at the c.-44 nucleotide originates a novel binding site to KH-type splicing regulatory protein. According to these results either the transcriptional machinery or post-transcriptional events, or both, might be influencing the gene expression.

In conclusion, as assessed in vitro by luciferase reporter assays, the various *GLA* 5′UTR SNPs modulate the gene expression in a manner that seems to be cell-type specific. The biological context and clinical implications of these observations are not yet clear, and further studies will be necessary to elucidate such questions. This may be of particular relevance considering the recent data suggesting that subnormal αGal activity levels above the range of enzyme insufficiency associated with FD phenotypes may be a risk factor in the pathogenesis of sporadic Parkinson disease (Wu et al. 2008, 2011) and stroke (Baptista et al. 2010). Although the 5′UTR-related modulation of *GLA* gene expression is not anticipated to be of much relevance for male patients carrying pathogenic mutations associated with very low or absent αGal activity, elucidation of the specific cellular contexts and of the molecular mechanisms underlying the effect of *GLA* 5′UTR SNPs, particularly of the negatively acting, might be clinically relevant in individuals with several other *GLA* genotypes. First: in patients with later-onset, organ-limited FD phenotypes, because most of such cases are associated with *GLA* mutations leading to altered enzyme stability (Garman 2007), which makes the final amount of αGal protein available in each tissue more dependent of the local gene expression profile. Second: in females coinheriting a negatively acting *GLA* 5′UTR SNP in *trans* with a pathogenic *GLA* mutation, the compound heterozygosity may significantly decrease the REA and aggravate the clinical phenotype since the αGal activity would be subnormal in all cells, irrespective of which of the two X chromosomes is inactivated. Third: in individuals carrying *GLA* variants associated with small decreases in REA, which otherwise would not be the cause of FD clinical phenotypes – like the p.Arg118Cys (Ferreira et al. 2015) and the p.Asp313Tyr (Yasuda et al. 2003; Niemann et al. 2013) – the additive effect of a negatively acting *GLA* 5′UTR SNP in *cis* could decrease REA into the typical range of mutations associated with later-onset phenotypic variants of FD (Ferreira et al. 2015), thereby modifying the expected phenotype. This might also affect the probability of identifying individuals carrying such mutations in large case-finding studies of FD among high-risk patients, when the primary screening method is based on αGal activity analysis. Finally, at the population level, the inadvertent inclusion of carriers of nonneutral *GLA* 5′UTR SNPs in cohorts of healthy individuals used to define the normal laboratory ranges of αGal activity will affect the values of the upper limit in plasma, like the c.-30A allele, and of the lower limit in leukocytes, like the c.-10T allele.

**Acknowledgements** These studies have been partially supported by a donation from Sanofi-Genzyme (Portugal) for research in Fabry disease. However, Sanofi-Genzyme was not involved in any way either with the design or the development of this study, including the analyses of the experimental data, or with the decision to publish their results.

We thank Deolinda Lima, M.D., Ph.D., for providing the facilities of the Laboratory of Support to Research in Molecular Medicine (LAIMM), at the Department of Experimental Biology, of the Faculty of Medicine, University of Porto (FMUP), Portugal, where most of the experimental work was performed.

We thank Ana Moço, MSc Student, from the Biocomposites Group, Institute of Biomedical Engineering (INEB), Faculty of Engineering, University of Porto (FEUP), Portugal, for generously providing the HDMEC cells; José Pedro Castro, Ph.D. Student, from the Department of Experimental Biology, Centre for Medical Research, FMUP, for generously providing the Jurkat cells; and Ana Grangeia, Ph.D., from the Genetics Department, FMUP, for generously providing the HEK-293 cells.

## Synopsis

The polymorphisms in the α-galactosidase gene (*GLA*) 5′-untranslated region have cell-type-specific modulatory effects upon gene expression.

## Compliance with Ethics Guidelines

This study was conducted according to the applicable national and institutional regulatory and ethical standards. Anonymised male genomic DNA samples were used as the source of the various polymorphic *GLA* 5′-untranslated region nucleotide sequences assayed in the luciferase reporter system experiments reported herein. The original samples had been obtained and genotyped in prior research projects carried out in the laboratory of molecular genetics of the Department of Genetics, Faculty of Medicine, University of Porto, Portugal, which were approved by the institutional Health Ethics Board and subject to written informed consent. The preservation of the anonymised genomic DNA samples was authorised by the Portuguese Data Protection Authority.

The study protocol did not involve any studies performed with human or animal subjects.

This work is part of Susana Ferreira's Ph.D. thesis, supervised by João Paulo Oliveira and co-supervised by Carlos Reguenga.

All authors were involved in the conception and design of the study, had full access to all the data and were involved in their analysis and interpretation. Susana Ferreira performed the laboratory work and, as corresponding author, had the final responsibility for the decision to submit the manuscript for publication.

The authors state that none of the material contained in the submitted manuscript has been published previously. Preliminary results of this research project were presented as posters at the European Conference of Human Genetics, Paris, June 2013, and at the Fabry Expert Lounge, Rome, March 2014.

## Conflict of Interest Declaration

Susana Ferreira has received unrestricted research grants and funding for research projects from Genzyme Corporation; conference registration fees and travel grants from Genzyme Corporation and Shire Human Genetic Therapies.

Carlos Reguenga declares no conflicts of interest related to the subject matter of this manuscript.

João Paulo Oliveira is member of the European Advisory Board of the Fabry Registry, a global observational registry of patients with Fabry disease sponsored by Genzyme Corporation. He has received unrestricted research grants and funding for research projects from Genzyme Corporation; consulting honoraria and speaker's fees from Genzyme Corporation; conference registration fees and travel grants from Genzyme Corporation, Shire Human Genetic Therapies and Amicus Therapeutics.

## References

Baptista MV, Ferreira S, Pinho EMT et al (2010) Mutations of the GLA gene in young patients with stroke: the PORTYSTROKE study–screening genetic conditions in Portuguese young stroke patients. Stroke 41:431–436

Barrett LW, Fletcher S, Wilton SD (2012) Regulation of eukaryotic gene expression by the untranslated gene regions and other non-coding elements. Cell Mol Life Sci 69:3613–3634

Brady RO, Gal AE, Bradley RM, Martensson E (1967) The metabolism of ceramide trihexosides. I. Purification and properties of an enzyme that cleaves the terminal galactose molecule of galactosylgalactosylglucosylceramide. J Biol Chem 242: 1021–1026

Brogan J, Li F, Li W, He Z, Huang Q, Li CY (2012) Imaging molecular pathways: reporter genes. Rad Res 177:508–513

Davies JP, Winchester BG, Malcolm S (1993) Sequence variations in the first exon of alpha-galactosidase A. J Med Genet 30:658–663

Desnick RJ, Ioannou YA, Eng CM (2001) α-Galactosidase A deficiency: Fabry disease In: Scriver CR, Beaudet AL, Sly WS, Valle D (eds). The metabolic and molecular basis of inherited disease. McGraw-Hill, New York, pp. 3733–3774

Ferreira S, Ortiz A, Germain DP et al (2015) The alpha-galactosidase A p.Arg118Cys variant does not cause a Fabry disease phenotype: Data from individual patients and family studies. Mol Genet Metab 114(2):248–258.

Ferri L, Guido C, la Marca G et al (2012) Fabry disease: polymorphic haplotypes and a novel missense mutation in the GLA gene. Clin Genet 81:224–233

Fitzmaurice TF, Desnick RJ, Bishop DF (1997) Human alpha-galactosidase A: high plasma activity expressed by the -30G→A allele. J Inherit Metab Dis 20:643–657

Garman SC (2007) Structure-function relationships in alpha-galactosidase A. Acta Paediatr (Suppl 96):6–16

Germain DP (2010) Fabry disease. Orphanet J Rare Dis 5:30

Jacobs JL, Dinman JD (2004) Systematic analysis of bicistronic reporter assay data. Nucleic Acids Res 32:e160

Kint JA (1970) The enzyme defect in Fabry's disease. Nature 227: 1173

Macville M, Schrock E, Padilla-Nash H et al (1999) Comprehensive and definitive molecular cytogenetic characterization of HeLa cells by spectral karyotyping. Cancer Res 59:141–150

Niemann M, Rolfs A, Giese A et al (2013) Lyso-Gb3 indicates that the alpha-galactosidase A mutation D313Y is not clinically relevant for fabry disease. JIMD Rep 7:99–102

Oliveira JP, Ferreira S, Barcelo J et al (2008a) Effect of single-nucleotide polymorphisms of the 5′ untranslated region of the human alpha-galactosidase gene on enzyme activity, and their frequencies in Portuguese caucasians. J Inherit Metab Dis 31(Suppl 2):S247–S253

Oliveira JP, Ferreira S, Reguenga C, Carvalho F, Mansson JE (2008b) The g.1170C>T polymorphism of the 5′ untranslated region of the human alpha-galactosidase gene is associated with decreased enzyme expression–evidence from a family study. J Inherit Metab Dis 31(Suppl 2):S405–S413

Richard L, Velasco P, Detmar M (1999) Isolation and culture of microvascular endothelial cells. Methods Mol Med 18:261–269

Saifudeen Z, Desnick RJ, Ehrlich M (1995) A mutation in the 5′ untranslated region of the human alpha-galactosidase A gene in high-activity variants inhibits specific protein binding. FEBS Lett 371:181–184

Samac S, Rice JC, Ehrlich M (1998) Analysis of methylation in the 5′ region of the human alpha-galactosidase A gene containing a binding site for methylated DNA-binding protein/RFX1-4. Biol Chem 379:541–544

Schneider U, Schwenk HU, Bornkamm G (1977) Characterization of EBV-genome negative "null" and "T" cell lines derived from children with acute lymphoblastic leukemia and leukemic transformed non-Hodgkin lymphoma. Int J Cancer 19:621–626

Shaw G, Morse S, Ararat M, Graham FL (2002) Preferential transformation of human neuronal cells by human adenoviruses and the origin of HEK 293 cells. Faseb j 16:869–871

von Scheidt W, Eng CM, Fitzmaurice TF et al (1991) An atypical variant of Fabry's disease with manifestations confined to the myocardium. N Engl J Med 324:395–399

Warnock DG (2005) Fabry disease: diagnosis and management, with emphasis on the renal manifestations. Curr Opin Nephrol Hypertens 14:87–95

Wu G, Yan B, Wang X et al (2008) Decreased activities of lysosomal acid alpha-D-galactosidase A in the leukocytes of sporadic Parkinson's disease. J Neurol Sci 271:168–173

Wu G, Pang S, Feng X et al (2011) Genetic analysis of lysosomal alpha-galactosidase A gene in sporadic Parkinson's disease. Neurosci Lett 500:31–35

Yasuda M, Shabbeer J, Benson SD, Maire I, Burnett RM, Desnick RJ (2003) Fabry disease: characterization of alpha-galactosidase A double mutations and the D313Y plasma enzyme pseudo-deficiency allele. Hum Mutat 22:486–492

Zhang XY, Asiedu CK, Supakar PC, Khan R, Ehrlich KC, Ehrlich M (1990) Binding sites in mammalian genes and viral gene regulatory regions recognized by methylated DNA-binding protein. Nucleic Acids Res 18:6253–6260

JIMD Reports
DOI 10.1007/8904_2015_425

RESEARCH REPORT

# The Kuvan® Adult Maternal Paediatric European Registry (KAMPER) Multinational Observational Study: Baseline and 1-Year Data in Phenylketonuria Patients Responsive to Sapropterin

**Friedrich K. Trefz • Ania C. Muntau • Florian B. Lagler • Flavie Moreau • Jan Alm • Alberto Burlina • Frank Rutsch • Amaya Bélanger-Quintana • François Feillet • On behalf of the KAMPER investigators**

Received: 19 November 2014 / Revised: 06 February 2015 / Accepted: 18 February 2015 / Published online: 31 March 2015


**Abstract** *Introduction*: Sapropterin dihydrochloride (Kuvan®), a synthetic 6R-diastereoisomer of tetrahydrobiopterin ($BH_4$), is approved in Europe for the treatment of patients aged ≥4 years with hyperphenylalaninaemia (HPA) due to $BH_4$-responsive phenylalanine hydroxylase (PAH) deficiency, in conjunction with a phenylalanine-restricted diet, and also for the treatment of patients with $BH_4$ deficiency.

*Aims/methods*: KAMPER is an ongoing, observational, multicentre registry with the primary objective of providing information over 15 years on long-term safety of sapropterin dihydrochloride treatment in patients with HPA. Here we report initial data on characteristics from patients recruited by the time of the third interim analysis and results at 1 year.

*Results*: Overall, 325 patients from 55 sites in seven European countries were included in the analysis: 296 (91.1%) patients with PAH deficiency (median [Q1, Q3] age, 10.3 [7.2, 15.0] years) and 29 (8.9%) with $BH_4$ deficiency (12.8 [6.6, 18.9] years). Fifty-nine patients (18.2%) were aged ≥18 years; 4 patients were pregnant. No elderly patients (aged ≥65 years) or patients with renal or hepatic insufficiency were enroled in the study. Twelve-month data were available for 164 patients with PAH deficiency and 16 with $BH_4$ deficiency. No new safety concerns were identified as of May 2013.

*Conclusions*: Initial data from KAMPER show that sapropterin dihydrochloride has a favourable safety profile. Registry data collected over time will provide insight into the management and outcomes of patients with PAH deficiency and $BH_4$ deficiency, including long-term safety, impact on growth and neurocognitive outcomes and the effect of sapropterin dihydrochloride treatment on populations of special interest.

Communicated by: Nenad Blau, PhD

Competing interests: None declared

**Electronic supplementary material:** The online version of this chapter (doi:10.1007/8904_2015_425) contains supplementary material, which is available to authorized users.

F.K. Trefz (✉)
Department of Pediatrics, University of Heidelberg, Germany
e-mail: friedrich.trefz@gmx.de

A.C. Muntau
University Children's Hospital, Medical Center Hamburg Eppendorf, Hamburg, Germany

F.B. Lagler
University Children's Hospital and Institute for Inborn Errors of Metabolism, Paracelsus Medical University, Salzburg, Austria

F. Moreau
EMD Serono, Inc., Billerica, MA, USA

J. Alm
Karolinska University Hospital, Stockholm, Sweden

A. Burlina
University Hospital, Padova, Italy

F. Rutsch
Münster University Children's Hospital, Münster, Germany

A. Bélanger-Quintana
Hospital Ramon y Cajal, Madrid, Spain

F. Feillet
Hôpital d'enfants Brabois, Vandoeuvre lès, Nancy, France

**Abbreviations**

| | |
|---|---|
| AE | Adverse event |
| $BH_4$ | Tetrahydrobiopterin |
| BMI | Body mass index |
| CI | Confidence interval |
| ECG | Electrocardiogram |
| HPA | Hyperphenylalaninaemia |
| ICH | International Conference on Harmonisation of Technical Requirements for Registration of Pharmaceuticals for Human Use |
| KAMPER | Kuvan® Adult Maternal Paediatric European Registry |
| PAH | Phenylalanine hydroxylase |
| Q | Quarter |
| SAE | Serious adverse event |

## Introduction

Hyperphenylalaninaemia (HPA) is characteristic of phenylalanine hydroxylase (PAH) deficiency, a disorder caused by mutations in the *PAH* gene resulting in reduction or loss of PAH enzyme activity and associated with progressive neurocognitive impairment if untreated (Blau et al. 2010). PAH deficiency is predominantly managed with a phenylalanine-restricted diet, but treatment can be supplemented with synthetic tetrahydrobiopterin ($BH_4$), an essential PAH cofactor, in $BH_4$-responsive patients (Fiege and Blau 2007; Keil et al. 2013; Kure et al. 1999).

$BH_4$ deficiencies affect 2% of individuals with HPA (Blau et al. 1996). $BH_4$ is essential for the functioning of tyrosine hydroxylase, tryptophan hydroxylase (Friedman et al. 1972; Shiman et al. 1971) and nitric oxide synthase (Marletta 1993). Patients with most $BH_4$ deficiencies require treatment with $BH_4$ and neurotransmitter precursors (5-hydroxytryptophan and levodopa) to reduce neurological deterioration (Shintaku 2002).

Randomized, placebo-controlled studies have shown that sapropterin (sapropterin dihydrochloride, Kuvan®; Merck KGaA, Darmstadt, Germany; BioMarin, Novato, California, USA; and Asubio Pharma, Kobe, Japan), a synthetic 6R-diastereoisomer of $BH_4$, can improve the control of blood phenylalanine concentration and allows greater phenylalanine consumption in $BH_4$-responsive patients (Levy et al. 2007; Trefz et al. 2009). Sapropterin has been approved for the treatment of patients with HPA due to $BH_4$-responsive PAH deficiency in the USA since December 2007, in Japan (as Biopten®) since July 2008, in Europe (for patients aged ≥4 years only) since December 2008 and in Canada since April 2010 (BioMarin Pharmaceutical Inc. 2010; Daiichi Sankyo 2013; Merck Serono 2013). Sapropterin is licensed for the treatment of patients of all ages with $BH_4$ deficiencies in Europe and Japan (Daiichi Sankyo 2013; Merck Serono 2013).

The primary objective of the Kuvan® Adult Maternal Paediatric European Registry (KAMPER) is to provide information over 15 years on the long-term safety of sapropterin in patients with HPA, in accordance with a post-approval commitment with the European Medicines Agency. It is also designed to collect information on the use of sapropterin in maternal HPA and on the effects on childhood growth and neurocognitive outcomes. We report baseline data from patients recruited by the time of the third interim analysis and results at 1 year.

## Methods

### Study Design

KAMPER is an ongoing observational, multicentre drug registry (ClinicalTrials.gov identifier NCT01016392) conducted in accordance with the protocol and protocol amendments, the International Conference on Harmonisation of Technical Requirements for Registration of Pharmaceuticals for Human Use (ICH) guideline for Good Clinical Practice (ICH Topic E6), applicable local regulations and the Declaration of Helsinki. Patients receive the standard of care for the management of HPA with no additional study-related dietary or other protocol restrictions. Patients undergo clinical assessments and receive medications and treatments as recommended by their study physician, including sapropterin treatment as per the summary of product characteristics (Merck Serono 2013).

The registry is being established in European countries where sapropterin is marketed, which reflects different geographical areas, lifestyles, genetic backgrounds and varied incidence rates of PAH deficiency and $BH_4$ deficiencies. At the time of the third interim analysis (May 2013), the registry was established in Austria, France, Germany, Italy, the Netherlands, Slovakia and Spain.

### Study Population

Patients with HPA due to PAH deficiency (including patients with mild phenylketonuria and mild HPA with phenylalanine levels >360 μmol/L) aged ≥4 years, or $BH_4$ deficiency (no age limit) and who meet the study inclusion/exclusion criteria, are being recruited from December 2009 to December 2019, with follow-up until 2025. Patients are eligible for the study if they are currently receiving sapropterin treatment at a participating centre, are responsive to $BH_4$ or sapropterin (≥30% reduction in blood phenylalanine level or attainment of physician-defined therapeutic blood phenylalanine targets) and are willing

and able to provide written, signed, informed consent (or by parent/guardian where appropriate). Exclusion criteria include known hypersensitivity to sapropterin and breast-feeding.

Eligible patients are identified at a baseline visit and followed in accordance with routine care practices of the participating sites. Eligible patients who are pregnant and unable to lower blood phenylalanine levels with a phenylalanine-restricted diet, or who become pregnant while participating in the study and decide to continue sapropterin therapy, are invited to enrol in the maternal sub-registry. Patients may have received diet therapy before sapropterin therapy and may have received $BH_4$ formulations other than sapropterin before the study.

### Study Variables

The primary endpoint is the incidence and description of adverse events (AEs) and serious AEs (SAEs), including the incidence in specific populations (elderly patients aged $\geq$65 years, paediatric patients aged $<$18 years and patients with renal or hepatic insufficiency). Secondary outcomes include study population characteristics (PAH deficiency and $BH_4$ deficiencies, PAH genotype, electrocardiogram [ECG] results), adherence to treatment (sapropterin and diet therapy), phenylalanine tolerance and metabolic control during follow-up (blood phenylalanine and tyrosine levels and long-term sensitivity to sapropterin treatment). Secondary outcomes also include auxological/nutritional outcomes (growth, clinical and biological micronutrients [including vitamin D, serum iron, serum folate and serum B12] and bone density), neurological and neuropsychiatric outcomes and maternal sub-registry outcomes. Information was also collected regarding type of treatment (PAH deficiency, sapropterin with/without diet therapy; $BH_4$ deficiencies, sapropterin with/without neurotransmitter precursors). Information regarding recommended data collection is available in Supplementary Table 1.

### Assessments

Study visits may vary widely between patients and between study years. Patients attend a baseline visit followed by quarterly to annual visits according to the routine practice at each participating centre and the individual needs of patients. For the maternal sub-registry, additional data are gathered, e.g. ultrasound results on the mother during pregnancy and foetal outcomes.

### Study Size

In total, 625 patients from 100 study sites in Europe are planned for enrolment to have an evaluable population of $\geq$500 at the end of the study. Five hundred evaluable patients are estimated to represent 20% among an initial population of 2,500 patients with HPA, which is the estimated number of patients with PKU who are sapropterin responsive (20% of total PKU population) in Europe (Burton et al. 2007).

### Minimizing Bias

To minimize selection bias, broad eligibility criteria are used, sites are expected to enrol all eligible patients treated according to the approved label for sapropterin in each country (Merck Serono 2013), and patients are recruited from a diverse pool of countries and clinical sites. To minimize measurement bias, sites receive systematic, standardized protocol training and use standardized data collection forms at enrolment and follow-up assessments.

### Statistical Analyses

This analysis included patients enrolled between 8 December 2009 and 26 November 2012 who had available baseline data. All analyses were descriptive; 95% confidence intervals (CIs) were calculated for the primary endpoint. Categorical variables were summarized as *n* (%) of patients; continuous variables were summarized using descriptive statistics (median, Quartile 1 [Q1], Quartile 3 [Q3]). No imputation for missing data was performed; for categorical variables, percentages were calculated with 'missing' as a category. Height, weight and body mass index (BMI) *Z*-scores were calculated for patients with PAH deficiency and $BH_4$ deficiencies using normative data from the World Health Organization 2007 reference population (World Health Organization 2011). Height and BMI *Z*-scores used 19-year-olds as a reference group for patients aged $>$19 years; weight *Z*-scores were calculated for patients aged $\leq$10 years only. *Z*-scores between $-2$ and 2 were considered to be within the normal range.

## Results

### Patients

Patients were recruited from 55 sites in seven European countries (Supplementary Fig. 1). In total, 329 patients were enrolled and 325 were included in the present analysis; 296 (91.1%) patients with PAH deficiency and 29 (8.9%) with a $BH_4$ deficiency (Supplementary Fig. 2). Fifty-nine patients (18.2%) were aged $\geq$18 years at enrolment, and four patients (1.2%) entered the maternal sub-registry. Two patients (0.6%) with PAH deficiency discontinued from the study: one was considered a

nonresponder after 14 months of treatment, and one pregnant patient discontinued early due to her concerns about drug use during pregnancy. No elderly patients (≥65 years of age) or patients with renal or hepatic insufficiency were enrolled. Data were available for the 1-year follow-up analysis for 180 patients (87.8%; 164 with PAH deficiency; 16 patients with a $BH_4$ deficiency).

At baseline, median (Q1, Q3) age was 10.3 (7.2, 15.0) years in patients with PAH deficiency and 12.8 (6.6, 18.9) years in patients with a $BH_4$ deficiency (Table 1). Newborn screening for HPA was performed in most patients with PAH deficiency (259/296; 87.5%) and $BH_4$ deficiencies (26/29; 89.7%), with the majority (234/296 [79.1%] and 27/29 [93.1%], respectively) undergoing confirmatory testing and approximately a third (101/296 [34.1%] and 10/29 [34.5%], respectively) undergoing a second confirmatory testing.

*PAH* gene analysis was performed in 212/296 (71.6%) patients with PAH deficiency; 91 individual mutations and 149 different genotypes were identified ($n$=210). The most frequent mutations are shown in Table 2.

Overall, 85 patients with PAH deficiency (28.7%) and six with a $BH_4$ deficiency (20.7%) had ≥1 medical condition at baseline. Intellectual disability was diagnosed in 10 patients (7 [2.4%] with PAH deficiency and 3 [10.3%] with a $BH_4$ deficiency). The majority of patients with a $BH_4$ deficiency (22/23; 95.7%) were receiving either concomitant levodopa or carbidopa/levodopa.

**Table 1** Baseline demographic characteristics

| | PAH deficiency ($n$ = 296) | $BH_4$ deficiency ($n$ = 29) | Overall ($n$ = 325) |
|---|---|---|---|
| Age, years[a] | | | |
| Median (Q1, Q3) | 10.3 (7.2, 15.0) | 12.8 (6.6, 18.9) | 10.3 (7.1, 15.5) |
| Age group, *n* | | | |
| <4 | 0 | 5 | 5 |
| 4–<8 | 100 | 7 | 107 |
| 8–<12 | 75 | 1 | 76 |
| 12–<18 | 70 | 8 | 78 |
| 18–<65 | 51 | 8 | 59 |
| Sex | | | |
| Male, *n* (%) | 150 (50.7) | 16 (55.2) | 166 (51.1) |
| Female, *n* (%) | 146 (49.3) | 13 (44.8) | 159 (48.9) |
| Male/female ratio | 1.03 | 1.23 | 1.04 |

[a] Age at informed consent; one patient was <4 years old at the time of informed consent; however, enrolment and collection of baseline data occurred after the patient turned 4 years of age
*$BH_4$* tetrahydrobiopterin, *PAH* phenylalanine hydroxylase, *Q1* Quartile 1, *Q3* Quartile 3

**Table 2** *PAH* gene mutations in patients with PAH deficiency ($N$ = 296)

| | *n* (%) |
|---|---|
| Patients with available data | 212 (71.6) |
| Patients with a classified mutation | 210 (70.9) |
| Most frequent mutations[a,b] | |
| p.L48S | 44 (14.9) |
| p.Y414C | 38 (12.8) |
| p.R261Q | 39 (13.2) |
| IVS10-11G>A | 30 (10.1) |
| Most frequent genotypes[c] | |
| p.R408W/p.Y414C | 7 (2.4) |
| p.L48S/p.L48S | 6 (2.0) |
| p.R261Q/p.R261Q | 6 (2.0) |

[a] Number of reported mutations on either allele 1 or allele 2
[b] Reported in ≥10% of patients
[c] Genotype includes allele 1-allele 2 or allele 2-allele 1 combinations of mutations, reported in ≥2% of patients
*PAH* phenylalanine hydroxylase

## $BH_4$ Responsiveness

Sapropterin/$BH_4$ response test data were available for 307 patients: 291/296 (98.3%) with PAH deficiency and 16/29 (55.2%) with a $BH_4$ deficiency. Further information regarding $BH_4$ responsiveness testing is available in Supplementary Table 2. Of 291 patients with PAH deficiency, 282 (96.9%) demonstrated ≥30% decrease in blood phenylalanine levels during the response test. Of 16 patients with $BH_4$ deficiency, 15 (93.8%) demonstrated ≥30% decrease in blood phenylalanine levels during the response test; data were missing for one patient.

## Safety

A total of 101 AEs, including 7 SAEs, were reported in 61 patients (Table 3). Headache was the most frequently reported AE, occurring in 8 (2.7%) patients with PAH deficiency and 1 (3.4%) patient with a $BH_4$ deficiency. No deaths were reported. AEs were mild or moderate in intensity, with the exception of one SAE of severe headache that led to hospitalization (PAH deficiency group) and was considered possibly related to sapropterin treatment.

In patients with PAH deficiency, 88 AEs occurred in 55 patients, including five SAEs in three patients; nine AEs were considered possibly related to sapropterin treatment (Table 3). Most AEs were mild in severity ($n$ = 65), 22 were moderate, and one was severe. The incidence of total AEs per patient-year was 19.0% (95% CI 14.1%, 25.6%) in year 1 ($n$ = 43) and 9.0% (95% CI 5.7%, 14.3%) in year

**Table 3** Frequency of adverse events and those occurring in ≥2 patients in the overall population, stratified by PAH deficiency and $BH_4$ deficiency

| | PAH deficiency ($n = 296$) | | $BH_4$ deficiency ($n = 29$) | |
|---|---|---|---|---|
| | Patients *n* (%) | Events (*n*) | Patients *n* (%) | Events (*n*) |
| Any adverse event | 55 (18.6) | 88[a,b] | 6 (20.7) | 13[c,d] |
| Headache | 8 (2.7) | 8[e] | 1 (3.4) | 1 |
| Cough | 4 (1.4) | 4 | – | – |
| Abdominal pain | 4 (1.4) | 4 | – | – |
| Nasopharyngitis | 3 (1.0) | 4 | – | – |
| Acute tonsillitis | 3 (1.0) | 3 | – | – |
| Pharyngitis | 2 (0.7) | 3 | – | – |
| Tonsillitis | 3 (1.0) | 3 | – | – |
| Gastroenteritis | 2 (0.7) | 2 | – | – |
| Weight decreased | 2 (0.7) | 2 | – | – |
| Overweight | 2 (0.7) | 2 | – | – |
| Rhinorrhoea | 2 (0.7) | 2 | – | – |
| Vomiting | 1 (0.3) | 1 | 1 (3.4) | 1 |
| Acne | 1 (0.3) | 1 | 1 (3.4) | 1 |

[a] Including five serious adverse events (tachycardia, drop attacks, unresponsive to stimuli, nephrolithiasis and headache) occurring in three patients. The events of tachycardia and drop attacks (both occurring in the same patient) were not associated with electrocardiogram abnormalities

[b] Nine adverse events in seven patients were considered possibly related to sapropterin treatment: headache (three events), abdominal pain (two events), rhinitis (one event), weight decrease (one event), hyposmia (one event) and rhinorrhoea (one event)

[c] Including two serious adverse events in two patients (epistaxis and laryngitis, both led to hospitalization)

[d] No adverse events were considered possibly related to sapropterin treatment

[e] Including one severe, possibly treatment-related headache that led to hospitalization for tests and was classified as a serious adverse event

*$BH_4$* tetrahydrobiopterin, *PAH* phenylalanine hydroxylase

2 ($n = 18$); the number of patient-years was 226.3 and 199.5, respectively.

In patients with a $BH_4$ deficiency, 13 AEs occurred in six patients, including two SAEs in two patients but no treatment-related AEs (Table 3). In terms of AE severity, five were mild, eight were moderate, and none was severe. All patients with a $BH_4$ deficiency who experienced an AE were treated concomitantly with carbidopa/levodopa; notable AEs were chorea (facial movements of a choreic nature) and tic (persistent facial tic) in one patient and hypertonia in one patient. No other relevant neurological AEs were reported in any other patients. The incidence of total AEs per patient-year was 26.7% (95% CI 12.0%, 53.9%) in year 1 ($n = 6$); the number of patient-years was 22.5.

Baseline ECG results were available for 17 patients with PAH deficiency and five with a $BH_4$ deficiency; results were normal except for one patient with PAH deficiency (sinus bradycardia) and one with a $BH_4$ deficiency (non-specific ventricular repolarization and first-degree atrioventricular block). At 1-year follow-up, data were available for eight patients with PAH deficiency and three with a $BH_4$ deficiency; all were reported to be normal and were performed in patients who had not undergone a baseline ECG assessment.

Of four pregnant patients, a term live birth was reported for three, and one pregnancy was ongoing; no development problems or AEs related to the pregnancies have been reported.

### Sapropterin Treatment

The median (Q1, Q3) sapropterin dose was 12.7 (10.0, 18.9) mg/kg/day in patients with PAH deficiency ($n = 245$) and 5.0 (3.0, 7.5) mg/kg/day in those with a $BH_4$ deficiency ($n = 25$). In the pregnant patients, one was treated with sapropterin at a dose of 3 mg/kg/day and another received 10 mg/kg/day, and there was no alteration in dose during the course of either pregnancy. Another pregnant patient received sapropterin 8 mg/kg/day initially, reduced to 4 mg/kg/day, and another received sapropterin at doses between 9 and 17 mg/kg/day.

### Blood Phenylalanine Concentrations at Baseline, 6 Months and 12 Months

In patients with PAH deficiency, median (Q1, Q3) blood phenylalanine concentration was 414 (289, 561) μmol/L before treatment with sapropterin ($n$=215), 349 (258, 503) μmol/L at 6 months ($n = 133$) and 340 (248, 486) μmol/L at 12 months ($n = 121$). Median blood phenylalanine concentration in patients with PAH deficiency varied between age groups at baseline, but observations suggest stability within age groups over 12 months (Supplementary Table 3).

In patients with a $BH_4$ deficiency, median (Q1, Q3) blood phenylalanine concentration was 91 (67, 313) μmol/L before treatment with sapropterin ($n = 20$), 103 (81, 254) μmol/L at 6 months ($n = 11$) and 89 (76, 117) μmol/L at 12 months ($n = 6$).

### Natural Protein and Actual Phenylalanine Intake at Baseline, 6 Months and 12 Months

In patients with PAH deficiency who completed their dietary records, the observed median (Q1, Q3) natural protein intake was higher at 12 months than baseline (before sapropterin treatment) (Fig. 1; Supplementary Table

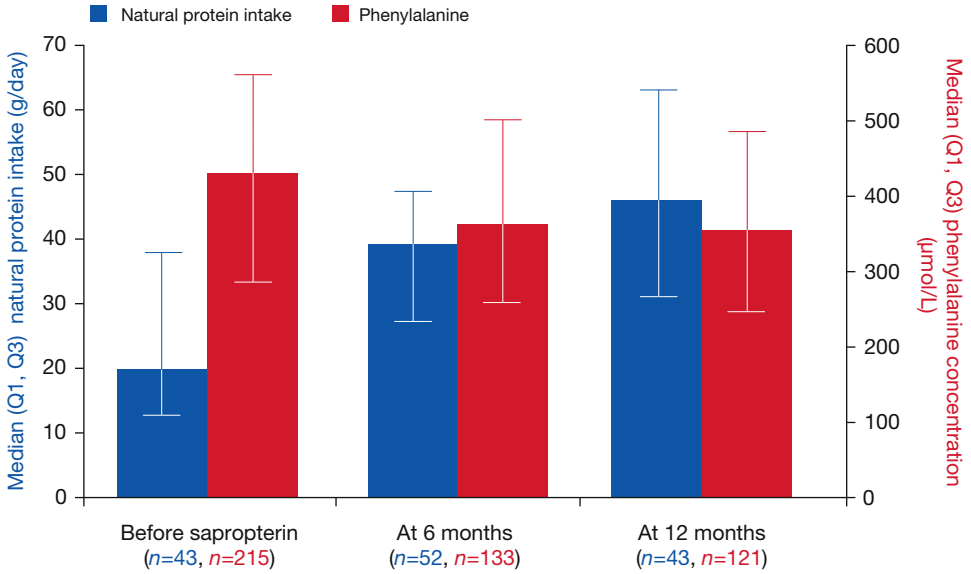


**Fig. 1** Median natural protein intake and median blood phenylalanine levels before sapropterin treatment and at 6 and 12 months in patients with PAH deficiency ($N = 296$). *PAH* phenylalanine hydroxylase, *Q1* Quartile 1, *Q3* Quartile 3

3). The observed median (Q1, Q3) dietary phenylalanine intake in patients with PAH deficiency varied over time, from 718 (385, 1514) mg/day at baseline ($n = 136$) to 1,525 mg/day (750, 2,298) at 6 months ($n = 79$) and 1,205 (600, 2,549) mg/day at 12 months ($n = 70$); however, median dietary phenylalanine intake was higher at 12 months than baseline for all age groups, including adults (Supplementary Table 3).

### Growth

Median growth measurements were considered to be within the normal range for patients with PAH deficiency and those with a $BH_4$ deficiency. In patients with PAH deficiency, median height, weight and BMI *Z*-scores were similar at baseline and 12 months. Median (Q1, Q3) *Z*-scores were: for height, −0.1 (−0.8, 0.6; $n = 244$) at baseline and −0.2 (−0.9, 0.6; $n = 115$) at 12 months; for weight, 0.3 (−0.2, 1.2; $n = 118$) at baseline and 0.4 (−0.4, 1.2; $n = 58$) at 12 months; and for BMI, 0.4 (−0.4, 1.2; $n = 244$) at baseline and 0.4 (−0.3, 1.3; $n = 115$) at 12 months. In patients with a $BH_4$ deficiency, median baseline (Q1, Q3) *Z*-scores were: for height, −0.1 (−1.4, 0.2; $n = 23$); for weight, −0.1 (−1.2, 1.0; $n = 12$); and for BMI, 0.3 (−1.3, 1.2; $n = 23$); data are not reported for 12-month follow-up owing to small patient numbers (<10).

In the 59 patients with PAH deficiency and available baseline bone density data, osteopenia was detected in five patients (ages 11.9, 17.8, 18.4, 23.9 and 27.3 years) and osteoporosis in two patients (ages 16.7 and 23.0 years). At 12 months, two cases of osteopenia and one case of osteoporosis were recorded ($n = 34$ patients with available data). Osteopenia and osteoporosis had not been recorded in these patients at baseline. Baseline bone density data were only available for one patient with a $BH_4$ deficiency; these data were normal with no osteopenia or osteoporosis detected. No follow-up data were available.

## Discussion

At the third interim analysis, KAMPER had accumulated data from 296 patients with PAH deficiency and 29 patients with a $BH_4$ deficiency, with 1-year follow-up data available for 180 patients. Most patients were <18 years of age at enrolment. No elderly patients (≥65 years) or patients with renal or hepatic insufficiency had been enrolled. As this was an analysis of baseline and 1-year data, there are currently insufficient data to make meaningful evaluations of observed long-term changes over time; however, such reporting will improve over the course of this 15-year study.

Information regarding sapropterin/$BH_4$ response testing was available for most patients. The most frequent test dose was 20 mg/kg, and most tests were conducted over a 24- to 48-h period. Test doses and test periods were consistent with a previous report of clinical practice in Europe (Keil et al. 2013) and with recommendations for assessing $BH_4$ response (Blau et al. 2009). Sapropterin test data were only available for 55% of patients with a $BH_4$ deficiency. Although more patients may have been tested during the neonatal period, data are not readily available. In addition, physicians may use other diagnostic tests, such as pterin analysis, for assessing $BH_4$ deficiency.

No new safety concerns were identified, with AEs consistent with those reported in previous studies (Levy et al. 2007; Trefz et al. 2009). While no AEs in patients with $BH_4$ deficiency were considered related to sapropterin treatment, two patients experienced neurological AEs (chorea, tic and hypertonia) that may have been a result of concomitant carbidopa/levodopa or the primary condition. The summary of product characteristics for sapropterin provides warnings and precautions regarding neurological AEs if co-administered with other medicinal products, including levodopa (BioMarin Pharmaceutical Inc. 2010; Merck Serono 2013). AEs will continue to be evaluated as follow-up data are accrued.

In the current study, four patients were pregnant. Three patients have since delivered live infants with no reported developmental issues, and the fourth pregnancy was ongoing at the time of this interim analysis. There is increasing support for the use of sapropterin during pregnancy in women with $BH_4$-responsive PAH deficiency who cannot achieve recommended blood phenylalanine concentrations, with or without diet therapy (Feillet et al. 2014; Grange et al. 2014).

Among patients with PAH deficiency and available dietary intake information, an increase from baseline in median actual phenylalanine intake was observed at 12 months in all age groups. These findings are consistent with previous studies showing that sapropterin may permit higher phenylalanine consumption (Hennermann et al. 2012; Keil et al. 2013; Lambruschini et al. 2005; Shintaku et al. 2004; Trefz et al. 2009). However, limitations related to sample size when stratified by age group and variability of dietary intake data must be considered. There are insufficient data to evaluate dietary intake in patients with $BH_4$ deficiency.

Although an observation period of 1 year is considered too short to see clinically significant changes in growth, growth was similar to the normal population in both patients with PAH deficiency and $BH_4$ deficiency; however, there were a limited number of patients with a $BH_4$ deficiency at the 1-year follow-up. The proportion of patients with osteoporosis and osteopenia was generally in line with a recent report on the prevalence of mineral bone disease in patients with PAH deficiency, in which none of the patients treated with $BH_4$ ($n = 12$), for an average of 7.1 years, developed mineral bone disease (Miras et al. 2013).

The present analysis has several limitations. As KAMPER is an observational, registry study, some follow-up assessment data, such as blood assessments, were limited; however, missing data are common in observational studies. Furthermore, collection of data not routinely obtained during the assessment of patients with PAH and $BH_4$ deficiencies (e.g. ECG data) may impede data availability, and data regarding PAH classification were unavailable at the time of the analysis. As recruitment is ongoing, any observed changes over time should be interpreted with caution. Observational cohort studies may be subject to potential bias; however, the potential for selection, measurement or information bias was minimized. Country selection included different geographic areas, lifestyles and incidence rates of PAH deficiency and $BH_4$ deficiencies to minimize selection bias, but the limited number of patients in specific subgroups may limit generalization of the results. As yet there are no patients in the special populations of interest; however, the patient population reflects real-world practice, and the short duration of the registry to date and recruitment of special populations should improve over time. Enrolment of patients aged >65 years, however, is not expected in the time span of this study.

In conclusion, the initial data obtained from KAMPER show that sapropterin has a good safety profile. Registry data collected over time will provide insight into the management and outcomes of patients with PAH deficiency and $BH_4$ deficiencies, including long-term safety, impact on phenylalanine tolerance, growth and neurocognitive outcomes and the effect of sapropterin treatment on populations of special interest.

**Acknowledgments** This study (EMR700773_001) was supported by Merck Serono SA Geneva, Switzerland, a subsidiary of Merck KGaA, Darmstadt, Germany. Writing assistance was provided by Alyson Bexfield and Jane Davies of Caudex Medical, Oxford, UK (supported by Merck Serono SA Geneva, Switzerland). The authors thank Charles Edward Jefford of EMD Serono, Inc., Billerica, MA, USA, a subsidiary of Merck KGaA, Darmstadt, Germany, for support in the development of this manuscript.

The authors would also like to thank the KAMPER study investigators: *Austria*: Michaela Brunner-Krainz, Daniela Karall and Dorothea Möslinger; *France*: Magalie Barth, Nathalie Bednarek, Antoine Bedu, Thierry Billette de Villemeur, Pierre Broué, Brigitte Chabrol, Dries Dobbelaere, Cécile Dumesnil, Didier Eyer, Alain Fouilhoux, François Labarthe, Delphine Lamireau, Gilles Morin, Jean-Claude Netter, Vassili Valayannopoulos and Kathy Wagner-Mahler; *Germany*: Philipp Guder, Julia Hennermann, Jürgen Herwig, Ralf Husain, Martin Lindner, Amelie S. Lotz-Havla, Klaus Mohnike, Alexandra Puchwein-Schwepcke, Dagmar Scheible and Michael Staudigl; *Italy*: Generoso Andria, Milva Orquidea Bal, Roberto Cerone, Daniela Concolino, Antonio Correra, Vincenzo Leuzzi, Concetta Meli, Enrica Riva and Iris Scala; *Netherlands*: Annet M Bosch, Maria Estela Rubio-Gozalbo and Ans van der Ploeg; *Slovakia*: Katarina HÄlovÄ and Ludmila Potocnakova; *Spain*: Javier Blasco Alonso, Jaume Campistol Plana, Maria Luz Couce Pico, Maria García Jimenez, David Gil Ortega, Domingo GonzÄlez-Lamuño, Mónica Ruiz Pons, Angeles Rúiz Gomez, Félix SÄnchez-Valverde and Pablo Sanjurjo Crespo.

## Synopsis

Initial data from the ongoing, 15-year, Kuvan® Adult Maternal Paediatric European Registry show that sapropterin dihydrochloride has a good safety profile in patients with phenylalanine hydroxylase deficiency or tetrahydrobiopterin deficiency.

## Compliance with Ethics Guidelines

Conflicts of Interest

F. K. Trefz has served as a member on Merck Serono SA Geneva, Switzerland, advisory boards or similar committees; has current or recent participation in a clinical trial sponsored by Merck Serono SA Geneva, Switzerland; has assisted in the design of and/or participated in clinical studies using products manufactured by Merck Serono SA Geneva, Switzerland; and has received consulting fees or other remuneration including speaker fees from Merck Serono SA Geneva, Switzerland.

A. C. Muntau has participated in strategic advisory boards for Merck Serono SA Geneva, Switzerland; has assisted in the design of and/or participated in clinical studies using products manufactured by Merck Serono SA Geneva, Switzerland; and has received honoraria as a consultant and as a speaker from Merck Serono SA Geneva, Switzerland.

F. B. Lagler has served as a member on Merck Serono SA Geneva, Switzerland, advisory boards and has received research grants from Merck GesmbH, Austria.

F. Moreau is an employee of EMD Serono, Inc., Billerica, MA, USA.

J. Alm has served as a member on Merck Serono SA Geneva, Switzerland, advisory boards or similar committees; has assisted in the design of and/or participated in clinical studies using products manufactured by Merck Serono SA Geneva, Switzerland; and has received honoraria as a consultant from Merck AB Sweden.

A. Burlina has served as a member on Merck Serono SA Geneva, Switzerland, advisory boards or similar committees; has current or recent participation in a clinical trial sponsored by Merck Serono SA Geneva, Switzerland; has assisted in the design of and/or participated in clinical studies using products manufactured by Merck Serono SA Geneva, Switzerland; and has received consulting fees or other remuneration including speaker fees from Merck Serono SA Geneva, Switzerland.

F. Rutsch has served as a member on Merck Serono SA Geneva, Switzerland, advisory boards or similar committees; has assisted in the design of and/or participated in clinical studies using products manufactured by Merck Serono SA Geneva, Switzerland; and has received consulting fees or other remuneration including speaker fees from Merck Serono SA Geneva, Switzerland.

A. Bélanger-Quintana has participated in strategic advisory boards and received grants and fees for presentations from Merck Serono SA Geneva, Switzerland, and Nutricia.

F. Feillet has served as a member on Merck Serono SA Geneva, Switzerland, advisory boards or similar committees; has current or recent participation in a clinical trial sponsored by Merck Serono SA Geneva, Switzerland; has assisted in the design of and/or participated in clinical studies using products manufactured by Merck Serono SA Geneva, Switzerland; and has received consulting fees or other remuneration including speaker fees from Merck Serono SA Geneva, Switzerland.

## Informed Consent

All procedures followed were in accordance with the ethical standards of the responsible committee on human experimentation (institutional and national), with the International Conference on Harmonisation of Technical Requirements for Registration of Pharmaceuticals for Human Use (ICH) guideline for Good Clinical Practice (ICH topic E6, 1996) and with the Helsinki Declaration. Informed consent was obtained from all patients included in the registry.

## Contributions of Individual Authors

F.K. Trefz was substantially involved in the conception and design of the study protocol; the interpretation of data; and the preparation, review and approval of the manuscript.

A.C. Muntau was substantially involved in the conception and design of the study protocol; the interpretation of data; and the preparation, review and approval of the manuscript.

F.B. Lagler was substantially involved in the conception and design of the study protocol; the interpretation of data; and the preparation, review and approval of the manuscript.

F. Moreau was substantially involved in the conception and design of the study protocol and the development of the statistical analysis plan; the analysis and interpretation of data; and the preparation, review and approval of the manuscript.

J. Alm was substantially involved in the conception and design of the study protocol; the interpretation of data; and the preparation, review and approval of the manuscript.

A. Burlina was substantially involved in the conception and design of the study protocol; the interpretation of data; and the preparation, review and approval of the manuscript.

F. Rutsch was substantially involved in collection and interpretation of data and the preparation, review and approval of the manuscript.

A. Bélanger-Quintana was substantially involved in the conception and design of the study protocol; the interpretation of data; and the preparation, review and approval of the manuscript.

F. Feillet is the principal investigator of the KAMPER study and was substantially involved in the conception and design of the study protocol; the interpretation of data; and the preparation, review and approval of the manuscript.

## References


BioMarin Pharmaceutical Inc. (2010) Kuvan (sapropterin dihydrochloride) tablets. Full Prescribing Information. http://www.kuvan.com/hcp/kuvan-full-prescribing-information.html. Accessed 21 Aug 2014

Blau N, Barnes I, Dhondt JL (1996) International database of tetrahydrobiopterin deficiencies. J Inherit Metab Dis 19:8–14

Blau N, Belanger-Quintana A, Demirkol M et al (2009) Optimizing the use of sapropterin (BH(4)) in the management of phenylketonuria. Mol Genet Metab 96:158–163

Blau N, van Spronsen FJ, Levy HL (2010) Phenylketonuria. Lancet 376:1417–1427

Burton BK, Grange DK, Milanowski A et al (2007) The response of patients with phenylketonuria and elevated serum phenylalanine to treatment with oral sapropterin dihydrochloride (6R-tetrahydrobiopterin): a phase II, multicentre, open-label, screening study. J Inherit Metab Dis 30:700–707

Daiichi Sankyo (2013) Daiichi Sankyo launches natural tetrahydrobiopterin agent Biopten® Granules 10%. http://www.daiichisankyo.com/media_investors/media_relations/press_releases/detail/006042/20131129_479_E.pdf. Accessed 21 Aug 2014

Feillet F, Muntau AC, Debray FG et al (2014) Use of sapropterin dihydrochloride in maternal phenylketonuria. A European experience of eight cases. J Inherit Metab Dis. doi:10.1007/s10545-014-9716-5

Fiege B, Blau N (2007) Assessment of tetrahydrobiopterin (BH4) responsiveness in phenylketonuria. J Pediatr 150:627–630

Friedman PA, Kappelman AH, Kaufman S (1972) Partial purification and characterization of tryptophan hydroxylase from rabbit hindbrain. J Biol Chem 247:4165–4173

Grange DK, Hillman RE, Burton BK et al (2014) Sapropterin dihydrochloride use in pregnant women with phenylketonuria: an interim report of the PKU MOMS sub-registry. Mol Genet Metab 112:9–16

Hennermann JB, Roloff S, Gebauer C, Vetter B, von Arnim-Baas A, Mönch E (2012) Long-term treatment with tetrahydrobiopterin in phenylketonuria: treatment strategies and prediction of long-term responders. Mol Genet Metab 107:294–301

Keil S, Anjema K, van Spronsen FJ et al (2013) Long-term follow-up and outcome of phenylketonuria patients on sapropterin: a retrospective study. Pediatrics 131:e1881–e1888

Kure S, Hou DC, Ohura T et al (1999) Tetrahydrobiopterin-responsive phenylalanine hydroxylase deficiency. J Pediatr 135:375–378

Lambruschini N, Perez-Duenas B, Vilaseca MA et al (2005) Clinical and nutritional evaluation of phenylketonuric patients on tetrahydrobiopterin monotherapy. Mol Genet Metab 86(Suppl 1): S54–S60

Levy HL, Milanowski A, Chakrapani A et al (2007) Efficacy of sapropterin dihydrochloride (tetrahydrobiopterin, 6R-BH4) for reduction of phenylalanine concentration in patients with phenylketonuria: a phase III randomised placebo-controlled study. Lancet 370:504–510

Marletta MA (1993) Nitric oxide synthase structure and mechanism. J Biol Chem 268:12231–12234

Merck Serono (2013) Kuvan 100 mg soluble tablets: summary of product characteristics. http://www.medicines.org.uk/emc/medicine/21362/SPC. Accessed 21 Aug 2014

Miras A, Boveda MD, Leis MR et al (2013) Risk factors for developing mineral bone disease in phenylketonuric patients. Mol Genet Metab 108:149–154

Shiman R, Akino M, Kaufman S (1971) Solubilization and partial purification of tyrosine hydroxylase from bovine adrenal medulla. J Biol Chem 246:1330–1340

Shintaku H (2002) Disorders of tetrahydrobiopterin metabolism and their treatment. Curr Drug Metab 3:123–131

Shintaku H, Kure S, Ohura T et al (2004) Long-term treatment and diagnosis of tetrahydrobiopterin-responsive hyperphenylalaninemia with a mutant phenylalanine hydroxylase gene. Pediatr Res 55:425–430

Trefz FK, Burton BK, Longo N et al (2009) Efficacy of sapropterin dihydrochloride in increasing phenylalanine tolerance in children with phenylketonuria: a phase III, randomized, double-blind, placebo-controlled study. J Pediatr 154:700–707

World Health Organization (2011) The WHO Child Growth Standards. http://www.who.int/childgrowth/en/. Accessed 21 Aug 2014

JIMD Reports
DOI 10.1007/8904_2015_426

RESEARCH REPORT

# Postmortem Findings and Clinical Correlates in Individuals with Infantile-Onset Pompe Disease

**Loren D.M. Pena · Alan D. Proia · Priya S. Kishnani**

Received: 13 November 2014 / Revised: 12 February 2015 / Accepted: 18 February 2015 / Published online: 13 March 2015


**Abstract** Pompe disease (OMIM 232300), a glycogen storage disorder caused by deficiency in the lysosomal enzyme acid alpha-glucosidase (EC 3.2.1.20), results in weakness and cardiomyopathy in infants affected with the classic form. Although the primary disease manifestations are due to glycogen accumulation in skeletal and cardiac muscle, glycogen also accumulates in a variety of additional tissues. To improve our understanding of disease pathogenesis in long-term survivors, we reviewed postmortem results for three infants with the classic form of Pompe disease. We have observed a number of new complications in long-term survivors of infantile-onset Pompe disease, and we focused this postmortem study on pathological correlates. Findings in survivors include cardiac arrhythmias, which may be related to glycogen accumulation in cardiac conduction tissue; urinary incontinence, likely due to glycogen accumulation in smooth muscle; and refractory errors, possibly related to accumulation in ocular structures. These observations provide potential pathophysiologic correlates for complications in long-term survivors of infantile Pompe disease.

**Abbreviations**

| | |
|---|---|
| AIMS | Alberta infant motor scale |
| CRIM | Cross-reactive immunological material |
| ERT | Enzyme replacement therapy |
| GAA | Acid alpha-glucosidase |
| GSD | Glycogen storage disease |
| H&E | Hematoxylin and eosin stain |
| IPD | Infantile Pompe disease |
| IVIG | Intravenous immunoglobulin |
| LOPD | Late-onset Pompe disease |
| PAS | Periodic acid-Schiff |
| PASD | Periodic acid-Schiff followed by diastase digestion |

Communicated by: Carla E. Hollak, MD

Competing interests: None declared

L.D.M. Pena (✉) · P.S. Kishnani
Division of Medical Genetics, Department of Pediatrics, Duke Medicine, 905 S. LaSalle St., GSRB1, Box 103856, Durham, NC 27710, USA
e-mail: loren.pena@duke.edu

A.D. Proia
Department of Pathology, Duke Medicine, Box 3712, Durham, NC, USA

## Introduction

Pompe disease (glycogen storage disease type II) is an autosomal recessive disorder due to deficiency of the lysosomal enzyme acid alpha-glucosidase (GAA). Infantile-onset Pompe disease (IPD) presents in the first few days to weeks of life with hypotonia, developmental delay, and cardiomyopathy. Enzyme replacement therapy (ERT) with recombinant acid alpha-glucosidase (rhGAA) improves survival in IPD (van den Hout et al. 2000; Kishnani et al. 2006). While the disorder was described decades ago, our understanding of disease complications continues to evolve, particularly as ERT has improved survival.

Recent publications highlight the need for a better understanding of disease complications in long-term survivors of IPD. Some of the complications, such as bowel and urinary incontinence, arterial aneurysms, and dysphagia, overlap with known complications in late-onset Pompe disease (LOPD) (El-Gharbawy et al. 2011; Prater et al. 2012; Hobson-Webb et al. 2012; Laforêt et al. 2008). Additional findings, such as cardiac arrhythmias and ocular

refractory errors, are emerging (Prakalapakorn et al. 2014). In addition, cognitive abnormalities have been observed in long-term survivors (Spiridigliozzi et al. 2012).

We analyzed autopsy findings in three deceased individuals with IPD, diagnosed 5–14 years ago, to explore the pathophysiology of clinical findings in long-term survivors with IPD. These observations were compared with postmortem findings in the published literature. We placed particular emphasis on glycogen accumulation in tissue with few or no previous observations, such as central and peripheral nervous system, cardiac conduction tissue, ocular structures, and smooth muscle. This knowledge expands our current understanding of complications observed among long-term survivors of infantile Pompe disease and offers additional knowledge that can guide health care supervision.

## Materials and Methods

We conducted a retrospective chart review of clinical and postmortem data in three deceased individuals with infantile Pompe disease. Chart review included notes from clinical care, radiology results, and autopsy results. The study received exempt status by the Duke Medicine Institutional Review Board for Clinical Investigations. Literature review included articles generated by a PubMed database search using the terms "Pompe disease and autopsy," "Pompe disease and postmortem," "glycogen storage disease type II and autopsy," and "glycogen storage disease type II and postmortem."

## Results

### Patient 1

This female African American infant had hypotonia and feeding difficulties at 2 months of age. She was diagnosed with Pompe disease at 6 months of age, when a diagnostic evaluation was initiated on the observation of cardiomegaly noted during a respiratory illness. Her diagnosis was made by muscle biopsy findings, reduced GAA enzyme activity, and homozygosity for the c.2560C>T mutation in the *GAA* gene. She was determined to be cross-reactive immunological material (CRIM)-negative by Western blot. Recombinant alglucosidase-alpha infusions were initiated at 6 months of age at 20 mg/kg every week. Due to CRIM-negative status, she received a course of immunomodulation therapy using rituximab, methotrexate, and intravenous immunoglobulin (IVIG) when ERT was initiated. She developed peak IgG titers of 12,800 at eight weeks after initiation of ERT. She received a second round of immunomodulation, and peak titers were 25,600 after this intervention.

She had a history of poor feeding, gastroesophageal reflux, reduced diaphragmatic muscle movement, and respiratory insufficiency and received a tracheostomy and gastrostomy tube at 7 months of age. This child was diagnosed with dysphagia at 15 months of age. Gross and fine motor development remained delayed throughout life, with scores less than 5th percentile at 15 and 22 months of age on the Alberta Infant Motor Scale (AIMS). She had osteopenia, as evidenced by a *Z*-score of −4.4 in lumbar vertebrae on a DEXA scan at 16 months of age. Cardiac function and left ventricular mass improved with enzyme replacement therapy (Table 1). However, she had electrocardiographic evidence of accelerated cardiac conduction throughout her life. She had a sudden death at 21 months of age from a presumed arrhythmia.

**Table 1** Cardiac measurements

| Time point | Age (months) | FS (%) | EF (%) | LVmass (AL)dI ($g/m^2$) |
|---|---|---|---|---|
| *Patient 1* | | | | |
| Diagnosis | 6 | 20.7 | | 351.4 |
| 6 months ERT | 12 | 39.7 | | 107.1 |
| 12 months ERT | 18 | 35.1 | | 87.2 |
| 15 months ERT | 21 | 50.8 | | 60.6 |
| *Patient 2* | | | | |
| Diagnosis | 8 | 51 | 68 | 296 |
| 1 months ERT | 9 | | 36 | 292 |
| 2 months ERT | 10 | | 34 | 239 |
| 3 months ERT | 11 | | 58 | 272 |
| *Patient 3* | | | | |
| Diagnosis | 5 | 9.6 | | |
| 0.5 months ERT | 5.5 | 27.1 | | 474.7 |
| 1 months ERT | 6 | 18.1 | | 489.8 |
| 2 months ERT | 7 | 16.3 | | 483.2 |
| 2.5 months ERT | 7.5 | 27.9 | | 463.4 |

*FS* fractional shortening, *EF* ejection fraction, *LV* left ventricle

Postmortem Examination

Autopsy findings are summarized in Table 2.

*Smooth Muscle*

Glycogen accumulation in smooth muscle was severe in the iris sphincter muscle of the eyes and in the urinary bladder and mild in the distal esophagus (Fig. 1a, b), stomach, small intestine, and colon.

*Cardiac Muscle*

There was glycogen accumulation in the cardiac conduction system, with severe vacuolization of cells at the sinoatrial node (Fig. 1c, d), atrioventricular node, and the bundle of His.

*Nervous System*

Unfixed brain weight was 1,165 g (normal for age is 1,026.6–1,154.1 g, Stocker and Dehner 2001). There was moderate ventricular dilatation. Glycogen accumulation was evident in neurons of the cortex, midbrain, pons, medulla, cerebellum, and spinal cord. There was cytoplasmic storage material in glial cells of white matter, in the temporal neocortex, and in neurons and glia of the basal ganglia and internal capsule, caudate, and thalamus. The patient also had ballooned neurons in the substantia nigra, the dorsal raphe nuclei, the pontine nuclei, and in the inferior olivary nuclei with periodic acid-Schiff (PAS) staining of the material in the cytoplasm. There were also ballooned neurons with positive PAS staining in the dentate nucleus, neurons, glial cells, and white matter of the cerebellum. Purkinje cells in the cerebellum were relatively spared of glycogen accumulation. The patient had large ballooned neurons in the anterior horns of the spinal column. There were vacuolar changes consistent with glycogen accumulation in the sural nerve and ganglia of the small intestine and colon.

*Eyes*

The patient had severe vacuolation in lens epithelial cells, moderate glycogen accumulation in retinal ganglion cells, and mild accumulation in corneal endothelial cells.

*Other Findings*

Moderate vertebral osteoporosis was present.

Patient 2

This African American female was noted to have hypotonia and poor feeding at 3 months of age. She was diagnosed with cardiomyopathy and subsequently with CRIM-negative infantile Pompe disease after presentation with a respiratory illness at 4 months of age. Her diagnosis was established by deficiency in GAA enzyme activity in muscle and fibroblasts and compound heterozygosity for mutations in the *GAA* gene: c.766_785del_ins_C (p.Tyr256fsX6) and c.2432delT (p.Leu811fsX37). As this child received a diagnosis of Pompe disease prior to regulatory approval of ERT, treatment was started at 8 months, without immunomodulation. The patient developed inhibitory antibodies four weeks after initiation of therapy and had peak titers of 102,400 at 12 weeks after initiation of ERT. She had left ventricular hypertrophy and decreased function at initiation of treatment, with minimal short-term improvement while receiving ERT (Table 1). She was diagnosed with obstructive apnea and hypoventilation and required noninvasive ventilation at 11 months of age. She had aspiration on a swallow study at 11 months of age and required nasogastric feedings. She died at almost 12 months of age after an episode of emesis and subsequent cardiopulmonary arrest.

Postmortem Examination

*Smooth Muscle*

Glycogen was present in the smooth muscle of blood vessels, gastrointestinal (Fig. 1e, f) and respiratory tracts, myometrium, iris sphincter, and ciliary body.

*Nervous System*

Unfixed brain weight was 733 g (mean for age 886 g, standard deviation 64 g, Stocker and Dehner 2001). She had unremarkable ventricles without evidence of dilatation. PAS-positive material had accumulated in the glial cells and astrocytes within the white matter and in the cytoplasm of neurons of multiple brainstem nuclei, including the oculomotor, pontine, and inferior olivary nuclei. There was glycogen accumulation in astrocytes of the cerebellar white matter, although the Purkinje cells were relatively spared. The child also had glycogen accumulation in ganglion cells of the GI tract, adrenal glands, pancreas, and anterior horn of the spinal cord (Fig. 1g, h).

*Eyes*

There was prominent vacuolization and PAS staining of the iris sphincter and lens epithelial cells, as previously described by Yanovitch et al. (2010). There was also PAS-positive material in the corneal endothelium, iris pigment and lens epithelium, retinal ganglion cells, and inner plexiform layer of the retina. Transmission electron

**Table 2** Glycogen accumulation within specific tissues

| Glycogen accumulation | Patient 1 | Patient 2 | Patient 3 |
|---|---|---|---|
| *Skeletal muscle* | | | |
| Quadriceps femoris | Severe | Severe | Moderate |
| Psoas | Severe | | |
| Sternothyroid | Severe | | |
| Proximal esophagus | Severe | | Moderate |
| Deltoid | Moderate | Severe | Mild |
| Intercostal | Moderate | | |
| Diaphragm | Moderate | Moderate | Minimal |
| Extraocular | Moderate | Moderate | Moderate |
| Smooth muscle | | | |
| Eye | | | |
| Iris sphincter | Severe | Severe | Severe |
| Ciliary body | Moderate | Mild | Mild |
| Genitourinary | | | |
| Urinary bladder | Severe | Severe | Moderate |
| Blood vessels | | | |
| Medium-sized arteries in sclera and orbit | Severe | Severe | |
| Respiratory | | | |
| Bronchi | Mild | Mild | Moderate |
| Gastrointestinal | | | |
| Esophagus | Mild | | Moderate |
| Stomach | Mild | Moderate | Moderate |
| Small intestine | Mild | Mild | None |
| Colon | Mild | Mod | Moderate |
| Heart | | | |
| Cardiac myocytes | | | |
| Outer myocardium of anterior, lateral, and posterior wall of left ventricle | Severe | Moderate | Moderate |
| Inner myocardium, subendocardium of anterior, lateral and posterior walls of LV | Moderate | Moderate | Severe |
| Mid-myocardium of anterior, lateral, posterior walls of LV | | | |
| Conduction system | Mild | Mild | Moderate |
| Sinoatrial node | | | |
| Atrioventricular node | | | |
| Bundle of His | Severe | | |
| Cardiac weight (mean for age) | Severe | | Moderate to severe |
| | Severe | | Moderate |
| | 83 g (55 g) | 120 g (49 g) | 200 g (43 g) |
| Peripheral nervous system | | | |
| Sural nerve | Moderate | Moderate | Moderate |
| Ganglion cells (neurons) | | | |
| Small intestine | Moderate | Severe | Severe |
| Colon | Moderate | Severe | Severe |
| Adrenal glands | None | Minimal | Moderate |
| Eyes | | | |
| Lens epithelial cells | Severe | Moderate | Severe |
| Retinal ganglion cells | Moderate | Moderate | Moderate |
| Corneal endothelial cells | Moderate | Moderate | Mild |

(continued)

**Table 2** (continued)

| Glycogen accumulation | Patient 1 | Patient 2 | Patient 3 |
|---|---|---|---|
| Iris pigmented epithelium | Mild | Moderate | Moderate |
| Photoreceptors | None | Moderate | Moderate |
| Optic nerve glial cells | Moderate | Moderate | Severe |

microscopy demonstrated glycogen accumulation within lysosomes of scleral fibroblasts, retinal ganglion cells, and cells of the retinal inner nuclear layer. In addition, glycogen accumulation was more prominent in bipolar and Müller cells than in amacrine and horizontal cells of the inner retinal nuclear layer.

Patient 3

This African American male infant was diagnosed at 5 months of age with Pompe disease during a hospitalization for respiratory symptoms. He was homozygous for the c.2560C>T mutation in the *GAA* gene and was determined to be CRIM-negative by Western blot. Enzyme replacement therapy at 20 mg/kg every other week and immune modulation with rituximab and methotrexate were started shortly after diagnosis. Hypertrophic cardiomyopathy and severe decrease in fractional shortening were present at diagnosis, and fractional shortening had some improvement with ERT (Table 1). Swallow study at 6 months of age demonstrated severe oropharyngeal dysphagia and aspiration with all consistencies. The child had delayed motor milestones, with an AIMS score less than 1st percentile at initial evaluation at 5.5 months of age. IgG titers remained negative during ERT. He was diagnosed with subglottic stenosis at 7 months of age and had a cardiopulmonary arrest at 7.5 months of age.

Postmortem Examination

*Smooth Muscle*

Glycogen accumulation was observed in smooth muscle of blood vessels and the respiratory and gastrointestinal tracts.

*Cardiac Muscle*

Moderate vacuolation in the specialized myocytes of the bundle of His was present (Fig. 1i, j).

*Nervous System*

Unfixed brain weighted 796 g (mean for age 767 g, standard deviation 32 g, Stocker and Dehner 2001). There was no evidence of ventricular dilatation. Glycogen accumulation was observed within cranial nerve nuclei of the mid pons and neurons of the dorsal raphe of the medulla. There was also glycogen accumulation in ganglion cells of the gastrointestinal tract and in the spinal cord. Vacuolation was present in the sural nerve.

*Other Findings*

The child had severe subglottic stenosis due to a circumferential tracheal fibrotic ridge. Glycogen accumulation in the urothelium and the eccrine glands of the skin was noted.

## Discussion

We reviewed postmortem data in three patients with infantile Pompe disease as a method to correlate pathology in deceased individuals with complications observed in long-term survivors. Postmortem findings are summarized in Table 2. Our current understanding of the natural history of infantile Pompe disease is somewhat limited by lack of pathophysiological correlates, and autopsy findings can inform clinical observations. A sample of autopsy findings in past publications is summarized in Table 3. All decedents presented in our case series were CRIM-negative, diagnosed in the first six months of life, and treated with ERT. It is unclear if ERT modified glycogen accumulation throughout the body, as serial sampling from pre-mortem tissue was not available. The cause of death varied but appeared to be a sudden cardiac death in at least two.

All of the individuals had a clinical history of oropharyngeal dysfunction and gastroesophageal reflux. Glycogen accumulation was observed in skeletal muscle of the tongue and proximal and mid esophagus in the three cases. We note a previous report of glycogen accumulation in the tongue (Araoz et al. 1974) and of tongue weakness in individuals with IPD and LOPD (Jones et al. 2010; Dubrovsky et al. 2011; Maggi et al. 2013) as a likely contributor to oropharyngeal dysfunction in the current cases. There was also glycogen accumulation in the smooth muscle of the mid and distal esophagus, and we posit that weakness of the lower esophageal sphincter could contribute to gastroesophageal reflux.

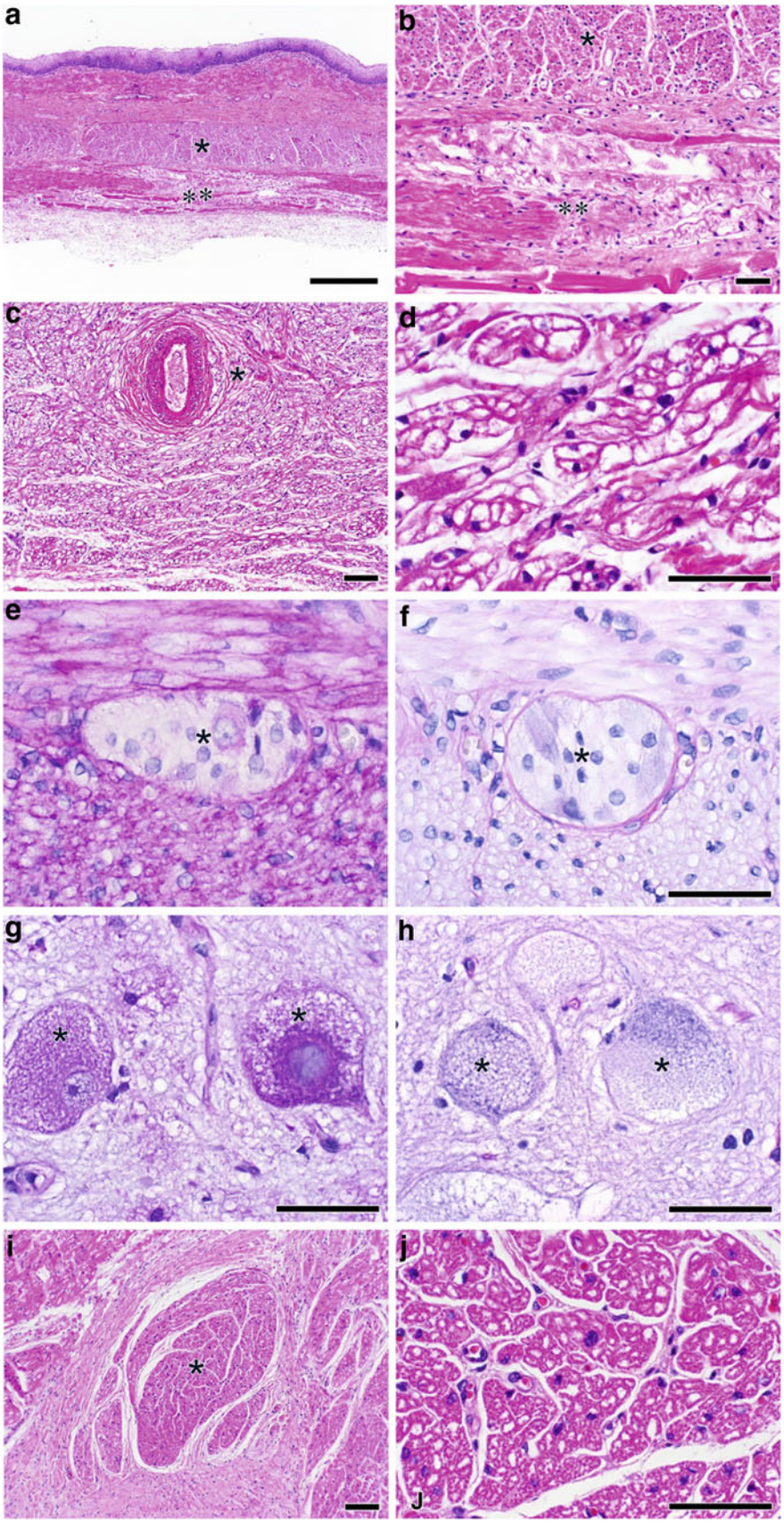


**Fig. 1** (**a**, **b**) There was mild vacuolar myopathy of smooth muscle (*) and moderate vacuolar myopathy of skeletal muscle (**) in the mid esophagus of patient 1 (hematoxylin and eosin; magnification bars = 500 μm in **a** and 100 μm in (**b**). (**c**, **d**) The sinoatrial node (*)

**Table 3** Sampling of previous autopsy reports for sites of glycogen accumulation in infantile-onset Pompe disease

| | Smooth muscle | Cardiac conduction system | Nervous system |
|---|---|---|---|
| Araoz et al. (1974) | No information | No information | PAS+, diastase-sensitive deposits in peripheral nerves, cytoplasmic glycogen accumulation in Schwann cells |
| Asukata et al. (1976) | No information | No information | PAS+ granules in GI ganglion cells |
| Nakamura et al. (1979) | Vacuolated smooth muscle in intima of muscular arteries, esophagus, and urinary bladder | Swollen myofibrils and overall shortening of the bundle of His | No information |
| Sakurai et al. (1974) | Heavy glycogen accumulation in smooth muscle of the gastrointestinal tract and arterial walls | No information | Auerbach plexus of stomach and intestine<br>CNS neurons and glial cells |
| Temple (1985) | No information | No information | No information |
| Teng et al. (2004) | No information | No information | PAS+, diastase-sensitive material in neurons of spinal cord and medulla |

The three cases presented in this series had glycogen accumulation throughout the smooth muscle of the gastrointestinal and genitourinary tracts. This finding could provide a pathophysiologic mechanism for small and large intestinal dysmotility and bowel control in this cohort. Bowel dysfunction and urinary incontinence have been reported in adults with LOPD, likely related to decreased anal sphincter pressure and fatty infiltration of pelvic floor musculature (Remiche et al. 2012; McNamara et al. 2015), along with glycogen accumulation in smooth muscle of the bladder (Hobson-Webb et al. 2012), and within neurons of the submucosal (Meissner's) and myenteric (Auerbach's) plexuses of the small and large intestines (Bernstein et al. 2010). We have observed urinary and bowel incontinence in several long-term survivors with infantile Pompe disease, an area that would benefit from long-term follow-up studies (Tan et al. 2013).

Glycogen accumulation in the smooth muscle of blood vessels was noted in the three decedents. Dilated arteriopathy has been reported in adults with LOPD (Quenardelle et al. 2014; El-Gharbawy et al. 2011), and very recently in a long-term survivor of infantile Pompe disease (Patel et al. 2013), in addition to dolichoectasia of the basilar artery and ectasia of the internal carotids (Sacconi et al. 2010; Laforêt et al. 2008). Glycogen accumulation in smooth muscle may affect cellular contractility and thus weaken blood vessel walls.

Glycogen accumulation in the cardiac conduction system in cases 1 and 3 is an interesting observation in Pompe disease that has only been reported once before (Bharati et al. 1982). A potential clinical correlate is evidence of preexcitation on electrocardiograms for case 1 and shortened conduction time in a postmortem electrogram on bundle of His tissue (Nakamura et al. 1979). Several long-term survivors have experienced arrhythmias (McDowell et al. 2008; Prater et al. 2012), and we propose that cardiac conduction is affected by glycogen accumulation within the conduction system. Glycogen accumulation in the cardiac conduction system is present in glycogen storage disease type III and in the mouse model for *PRKAG2*-caused hypertrophic cardiomyopathy (Austin et al. 2012; Arad et al. 2003). Persistence of glycogen in cardiac conduction tissue, despite ERT, suggests poor penetration and a potential cardiac cause for sudden death in cases 1 and 3.

We observed glycogen accumulation in various ocular structures. We have recently described a high prevalence of myopia and astigmatism in long-term survivors with IPD and posited various ways that glycogen accumulation in ocular tissues may contribute to these issues (Prakalapakorn et al. 2014).

There was extensive glycogen accumulation in the central and peripheral nervous systems. The pattern of accumulation included neurons and glial cells of the white matter, brainstem, and cerebellum, with relative sparing of cerebellar Purkinje cells. Glycogen accumulation has previously been reported throughout the central nervous

**Fig. 1** (continued) of patient 1 had severe vacuolation of the specialized myocytes comprising this structure, along with severe vacuolar myopathy of the right atrial cardiac myocytes (hematoxylin and eosin, magnification bars = 500 m in **c** and 50 μm in **d**). (**e**, **f**) Smooth muscle cells and some neurons within ganglia of the myenteric plexus (*; Auerbach's plexus) of the small intestine of patient 2 were laden with glycogen (**e**: periodic acid-Schiff stain and **f**: periodic acid-Schiff stain after diastase digestion of glycogen; magnification bar = 50 μm). (**g**, **h**) Anterior horn neurons (*) of the spinal cord of patient 2 exhibited prominent glycogen accumulation (**a**: periodic acid-Schiff stain and **b**: periodic acid-Schiff stain after diastase digestion of glycogen; magnification bar = 50 μm for both **g** and **h**). (**i**, **j**) The bundle of His (*) in patient 3 had moderate vacuolation of its specialized myocytes (hematoxylin and eosin; magnification bars = 100 μm in I and 50 μm in **j**)

**Table 4** Pathological – clinical correlates

| Tissue | Findings in current report | Previous reports | Clinical correlation |
|---|---|---|---|
| Cardiac conduction tissue | Vacuolation of the sinoatrial and atrioventricular nodes and the bundle of His | Thickening of the bundle of His | Supraventricular tachycardia, ventricular tachycardia, ventricular fibrillation (McDowell et al. 2008) |
| Muscular arteries | Glycogen accumulation in smooth muscle of muscular arteries | Vacuolated cells due to glycogen accumulation in intimal layer of arterial walls | Basilar artery aneurysm (Patel et al. 2013) |
| Smooth muscle | Glycogen accumulation in smooth muscle of esophagus, GI tract, and urinary bladder | As in current report | Dysphagia and GER (Prater et al. 2012); urinary incontinence (McNamara et al. 2015) |
| Peripheral nervous system | Glycogen accumulation in ganglion cells of gastrointestinal tract and sural nerve | Glycogen accumulation in myenteric plexus and peripheral nerves | Hypotonia, absent reflexes, abnormal electromyography (Burrow et al. 2010) |
| Central nervous system | Glycogen accumulation in anterior horn cells<br>Glycogen accumulation in glial cells and astrocytes of white matter, throughout nuclei of brainstem, and cerebellar white matter, with relative sparing of Purkinje cells | Glycogen accumulation in Schwann cells, cortical neurons, medulla, and anterior horn cells | Hypotonia, absent reflexes, abnormal nerve conduction studies (Bernstein et al. 2010); parenchymal volume loss (Burrow et al. 2010); cognitive effects unknown |
| Ocular tissue | Glycogen accumulation in extraocular muscles, lens epithelial cells, corneal endothelial cells, iris pigmented epithelium, retinal ganglion cells, photoreceptors, and optic nerve glial cells | Prakalapakorn et al. (2014) | Strabismus, myopia, astigmatism (Prakalapakorn et al. 2014) |

system (Araoz et al. 1974; Sakurai et al. 1974; Asukata et al. 1976; Nakamura et al. 1979; Teng et al. 2004; Thurberg et al. 2006). The decedents also had extensive accumulation in anterior horn cells of the spinal cord and in intestinal ganglion cells, as described previously (Thurberg et al. 2006; Martini et al. 2001; Teng et al. 2004). Glycogen accumulation has also been observed in peripheral nerves in LOPD (Fidziańska et al. 2011). A clinical correlate for this observation is a reduction in amplitudes and absent motor units on nerve conduction studies in a case of infantile-onset Pompe disease (Burrow et al. 2010). Glycogen accumulation in the peripheral nervous system raises the possibility that the weakness observed in affected individuals may be partly neurogenic.

While none of our three patients had pre-mortem MRI of brain, patient two in this case series had mild, diffuse volume loss on CT scan of the head at 8 months of age, and there was blurring of the gray-white differentiation for patient 3 at 5 months of age. Neuronal loss in brain and spinal cord has been described in postmortem examination (Martini et al. 2001). A recent publication noted parenchymal volume loss on brain MRI in a child with infantile Pompe disease at 2 years of age (Burrow et al. 2010). Interestingly, the oldest patient in the current case series, patient 1, had dilatation of the ventricles on postmortem examination. Ventricular dilatation was also observed in brain MRI in three of five participants who had serial MRI scanning (Chien et al. 2006). Finally, serial MRI in a CRIM-negative patient demonstrated white matter abnormalities despite normal myelination (Rohrbach et al. 2010). Glycogen accumulation in central and peripheral nervous system in the GAA knockout mouse model $6^{neo(-)}/6^{neo(-)}$ was extensive, but varied in distribution and intensity. Accumulation was progressive and included neurons, glia, and pericytes of the cerebral cortex, portions of the basal ganglia, and the brainstem. Early glycogen accumulation was present in the spinal cord, particularly in motor neurons (Sidman et al. 2008).

It is unclear whether the observed brain abnormalities can impact cognitive development in individuals affected with infantile Pompe disease. Spiridigliozzi et al. (2012) noted differences in intellectual functioning between classic and atypical Pompe disease in a CRIM-positive cohort followed prospectively. Similar data for CRIM-negative individuals, however, is lacking, and it is unclear whether the differences observed in intellectual achievement are related to glycogen accumulation in the CNS.

## Conclusion

This report expands our current understanding of pathologic correlates of clinical observations among long-term survivors (Table 4). Although limited to retrospective data, such review is nevertheless valuable in providing additional

insight into potential complications in long-term survivors of infantile Pompe disease and may provide information for health care supervision. This study also highlights the value of postmortem analysis in understanding the pathophysiology of disease manifestations.

## Synopsis

Pompe disease leads to generalized glycogen accumulation that may lead to with multi-organ complications in long-term survivors.

## Compliance with Ethics Guidelines

Conflict of Interest

Loren Pena declares that she has no conflict of interest.

Alan Proia declares that he has no conflict of interest.

Priya Kishnani has received research/grant support and honoraria from Genzyme Corporation and is a member of the Pompe Disease Advisory Board for Genzyme Corporation.

## Informed Consent

This study has been reviewed and granted exempt status by the Duke Medicine Institutional Review Board for Clinical Investigations as decedent research; hence the requirement for informed consent was waived.

## Contributions by Individual Authors

Loren Pena wrote the protocol and manuscript with guidance from Alan Proia regarding tissue findings and from Priya Kishnani regarding clinical course.

## References


Arad M, Moskowitz IP, Patel VV, Ahmad F, Perez-Atayde AR, Sawyer DB et al (2003) Transgenic mice overexpressing mutant *PRKAG2* define the cause of Wolff–Parkinson–White syndrome in glycogen storage cardiomyopathy. Circulation 107:2850–2856

Araoz C, Sun CN, Shenefelt R, White HJ (1974) Glycogenosis type II (Pompe's disease): ultrastructure of peripheral nerves. Neurology 24:739–742

Asukata I, Aizawa S, Kosakai M, Kirino Y, Ishikawa E (1976) An autopsy case of type II glycogenosis. Acta Path Jpn 26:629–635

Austin SL, Proia AD, Spencer-Manzon MJ, Butany J, Wechsler SB, Kishnani PS (2012) Cardiac pathology in glycogen storage disease type III. JIMD Rep 31:65–72

Bernstein DL, Bialer MG, Mehta L, Desnick RJ (2010) Pome disease: dramatic improvement in gastrointestinal function following enzyme replacement therapy. A report of three later-onset patients. Mol Genet Metab 101:130–133

Bharati S, Serratto M, DuBrow I et al (1982) The conduction system in Pompe's disease. Pediatr Cardiol 2:25–32

Burrow TA, Bailey LA, Kinnett DG, Hopkin RJ (2010) Acute progression of neuromuscular findings in infantile Pompe disease. Pediatr Neurol 42:455–458

Chien YH, Lee NC, Peng SF, Hwu WL (2006) Brain development in infantile-onset Pompe disease treated by enzyme replacement therapy. Pediatr Res 60:349–352

Dubrovsky A, Corderi J, Lin M, Kishnani PS, Jones HN (2011) Expanding the phenotype of late-onset Pompe disease: tongue weakness: a new clinical observation. Muscle Nerve 44:897–901

El-Gharbawy AH, Bhat G, Murillo JE et al (2011) Expanding the clinical spectrum of late-onset Pompe disease: dilated arteriopathy involving the thoracic aorta, a novel vascular phenotype uncovered. Mol Genet Metab 103:362–366

Fidziańska A, Ługowska A, Tylki-Szymańska A (2011) Late form of Pompe disease with glycogen storage in peripheral nerves axons. J Neurol Sci 301:59–62

Hobson-Webb LD, Proia AD, Thurberg BL, Banugaria S, Prater SN, Kishnani PS (2012) Autopsy findings in late-onset Pompe disease: a case report and systematic review of the literature. Mol Genet Metab 106:462–469

Jones HN, Muller CW, Lin M et al (2010) Oropharyngeal dysphagia in infants and children with infantile Pompe disease. Dysphagia 25:277–283

Kishnani PS, Nicolino M, Voit T et al (2006) Chinese hamster ovary cell-derived recombinant human acid alpha-glucosidase in infantile-onset Pompe disease. J Pediatr 149:89–97

Laforêt P, Petiot P, Nicolino M et al (2008) Dilative arteriopathy and basilar artery dolichoectasia complicating late-onset Pompe disease. Neurology 70:2063–2066

Maggi L, Salerno F, Bragato C et al (2013) Familial adult-onset Pompe disease associated with unusual clinical and histological features. Acta Myol 32:v85–v90

Martini C, Ciana G, Benettoni A et al (2001) Intractable fever and cortical neuronal glycogen storage in glycogenosis type 2. Neurology 57:906–908

McDowell R, Li JS, Benjamin DK et al (2008) Arrhythmias in patients receiving enzyme replacement therapy for infantile Pompe disease. Genet Med 10:758–762

McNamara ER, Austin S, Case L, Wiener JS, Peterson AC, Kishnani PS (2015) Expanding our understanding of lower urinary tract symptoms and incontinence in adults with Pompe disease. JIMD Rep [Epub ahead of print]

Nakamura Y, Tanimura A, Yasuoka C, Kato H (1979) An autopsy case of type II glycogenosis. Kurume Med J 26:349–354

Patel TT, Banugaria SG, Frush DP, Enterline DS, Tanpaiboon P, Kishnani PS (2013) Basilar artery aneurysm: a new finding in classic infantile Pompe disease. Muscle Nerve 47:613–615

Prakalapakorn SG, Proia AD, Yanovitch TL et al (2014) Ocular and histologic findings in a series of children with infantile Pompe disease treated with enzyme replacement therapy. J Pediatr Ophthalmol Strabismus 20:1–8

Prater SN, Banugaria SG, DeArmey SM et al (2012) The emerging phenotype of long-term survivors with infantile Pompe disease. Genet Med 14:800–810

Quenardelle V, Bataillard M, Bazin D, Lannes B, Wolff V, Echaniz-Laguna A (2014) Pompe disease presenting as an isolated generalized dilative arteriopathy with repeated brain and kidney infracts. J Neurol 262:473–475

Remiche G, Herbaut AG, Ronchi D et al (2012) Incontinence in late-onset Pompe disease: an underdiagnosed treatable condition. Eur Neurol 68:75–78

Rohrbach M, Klein A, Kohli-Wiesner A et al (2010) CRIM-negative infantile Pompe disease: 42-month treatment outcome. J Inherit Metab Dis 33:751–757

Sacconi S, Bocquet JD, Chanalet S, Tanant V, Salviati L, Desnuelle C (2010) Abnormalities of cerebral arteries are frequent in patients with late-onset Pompe disease. J Neurol 257:1730–1733

Sakurai I, Tosaka A, Mori Y, Imura S, Aoki K (1974) Glycogenosis type II (Pompe) – the fourth autopsy case in Japan. Acta Pathologica Japonica 24:829–846

Sidman RL, Taksir T, Fidler J et al (2008) Temporal neuropathologic and behavioral phenotype of 6neo/6neo Pompe disease mice. J Neuropathol Exp Neurol 67:803–818

Spiridigliozzi GA, Heller JH, Kishnani PS (2012) Cognitive and adaptive functioning of children with infantile Pompe disease treated with enzyme replacement therapy: long-term follow up. Am J Med Genet Part C 160C:22–29

Stocker JT, Dehner LP (eds) (2001) Pediatric pathology, 2nd edn. Lippincott Williams & Wilkins, Philadelphia, pp. 1444–1446, p. 1451

Tan QK, Cheah SM, DeArmey SM, Kishnani PS (2013) Low anal sphincter tone in infantile-onset Pompe disease: an emerging clinical issue in enzyme replacement therapy patients requiring special attention. Mol Genet Metab 108:142–144

Temple JK, Dunn DW, Blitzer MG, Shapira E (1985) The "muscular variant" of Pompe disease: clinical, biochemical and histologic characteristics. Am J Med Genet 21:597–604

Teng Y-T, Su W-J, Hou J-W, Huang S-F (2004) Infantile-onset glycogen storage disease type II (Pompe disease): report of a case with genetic diagnosis and pathological findings. Chang Gung Med J 27:379–384

Thurberg BL, Lynch Maloney C, Vaccaro C et al (2006) Characterization of pre- and post-treatment pathology after enzyme replacement therapy for Pompe disase. Lab Invest 86: 1208–1220

Yanovitch TL, Banugaria SG, Proia AD, Kishnani PS (2010) Clinical and histologic ocular findings in Pompe disease. J Pediatr Ophthalmol Strabismus 47:34–40

Van den Hout H, Reuser AJ, Vulto AG, Loonen MC, Cromme-Dijkhuis A, Van der Ploeg AT (2000) Recombinant human alpha-glucosidase from rabbit milk in Pompe patients. Lancet 356:397–398

JIMD Reports
DOI 10.1007/8904_2015_427

RESEARCH REPORT

# Clinical Severity of PGK1 Deficiency Due To a Novel p.E120K Substitution Is Exacerbated by Co-inheritance of a Subclinical Translocation t(3;14)(q26.33;q12), Disrupting *NUBPL* Gene

**Dezső David · Lígia S. Almeida · Maristella Maggi · Carlos Araújo · Stefan Imreh · Giovanna Valentini · György Fekete · Irén Haltrich**

Received: 25 November 2014 / Revised: 11 February 2015 / Accepted: 19 February 2015 / Published online: 27 March 2015


**Abstract** Carriers of cytogenetically similar, apparently balanced familial chromosome translocations not always exhibit the putative translocation-associated disease phenotype. Additional genetic defects, such as genomic imbalance at breakpoint regions or elsewhere in the genome, have been reported as the most plausible explanation.

By means of comprehensive molecular and functional analyses, additional to careful dissection of the t(3;14)(q26.33;q12) breakpoints, we unveil a novel X-linked PGK1 mutation and examine the contribution of these to the extremely severe clinical phenotype characterized by hemolytic anemia and neuromyopathy.

The 3q26.33 breakpoint is 40 kb from the 5′ region of tetratricopeptide repeat domain 14 gene (*TTC14*), whereas the 14q12 breakpoint is within IVS6 of nucleotide-binding protein-like gene (*NUBPL*) that encodes a mitochondrial complex I assembly factor. Disruption of *NUBPL* in translocation carriers leads to a decrease in the corresponding mRNA accompanied by a decrease in protein level. Exclusion of pathogenic genomic imbalance and reassessment of familial clinical history indicate the existence of an additional causal genetic defect. Consequently, by WES a novel mutation, c.358G>A, p.E120K, in the X-linked phosphoglycerate kinase 1 (*PGK1*) was identified that segregates with the phenotype. Specific activity, kinetic properties, and thermal stability of this enzyme variant were severely affected. The novel *PGK1* mutation is the primary genetic alteration underlying the reported phenotype as the translocation per se only results in a subclinical phenotype. Nevertheless, its co-inheritance presumably exacerbates PGK1-deficient phenotype, most likely due to a synergistic interaction of the affected genes both involved in cell energy supply.

Communicated by: Gregory Enns

Competing interests: None declared

**Electronic supplementary material:** The online version of this chapter (doi:10.1007/8904_2015_427) contains supplementary material, which is available to authorized users.

D. David (✉) · L.S. Almeida · C. Araújo
Department of Human Genetics, National Institute of Health Dr Ricardo Jorge, Lisbon, Portugal
e-mail: dezso.david@insa.min-saude.pt

M. Maggi · G. Valentini
Department of Biology and Biotechnology "L. Spallanzani", University of Pavia, Pavia, Italy

M. Maggi
Department of Molecular Medicine, Unit of Immunology and Pathology, University of Pavia, Pavia, Italy

S. Imreh
Microbiology and Tumour Biology Center, Karolinska Institute, Stockholm, Sweden

G. Fekete · I. Haltrich
II Department of Pediatrics, Semmelweis University, Budapest, Hungary

## Introduction

There is an intriguing group of apparently balanced familial chromosomal translocations characterized by phenotypic inconsistency among carriers of cytogenetically similar rearrangements.

The most fascinating explanation for this would be the co-inheritance of the chromosomal translocation with a mutation at the same or at a distinct genetic *locus*, leading to a recessive monogenic or digenic disorder. Such a case

has not yet been described so far (Schäffer 2013). On the contrary, genomic imbalance at breakpoint regions is the most plausible explanation of such phenotypic inconsistency observed among carriers of similar chromosomal translocations (De Gregori et al. 2007).

Presently, the lack of a fully annotated human genome, including a haploinsufficiency map, hinders predictability of the phenotypic consequences of balanced chromosomal translocations even when the breakpoints are identified at nucleotide resolution. Although these may considerably affect the genomic architecture at breakpoint regions, a large majority are expected to be phenotypically imperceptible or subclinical. Nevertheless, otherwise subclinical translocations may modulate clinical phenotypes.

In eukaryotes ATP synthesis relies on glycolysis and oxidative phosphorylation (OXPHOS). Phosphoglycerate kinase 1 (PGK1; ATP: 3-phosphoglycerate 1-phosphotransferase; EC 2.7.2.3) is a multifunctional protein with a key role in ATP generation during glycolysis. PGK1 deficiency (OMIM #300653) is an X-linked recessive condition characterized by variable clinical manifestations involving up to three different tissues, i.e., red blood cells (RBC), skeletal muscle, and neurological tissue. However, patients rarely show all three clinical features (Beutler 2007; Chiarelli et al. 2012). To date, 22 different mutations have been identified in *PGK1*, and 17 of them have been characterized at the protein level (Chiarelli et al. 2012; Fermo et al. 2012; Tamai et al. 2014).

Mitochondrial complex I (CI) or NADH-ubiquinone reductase (EC 1.6.5.3) is part of the electron transport chain that results in ATP synthesis through complex V or ATP synthase of the OXPHOS pathway (Fassone and Rahman 2012). At least 12 assembly factors are required for the proper assembly, stability, or maturation of this CI (Fassone and Rahman 2012). One of these assembly factors is NUBPL, the depletion of which causes CI deficiency (OMIM #252010) (Tucker et al. 2012; Kevelam et al. 2013). Incorporation of Fe/S clusters into CI subunits by NUBPL is indispensable for electron transfer activity of CI (Sheftel et al. 2009).

Here we present detailed molecular and functional analyses demonstrating that the phenotype allegedly associated with the chromosome rearrangement t(3;14)(q26.33;q12) is actually due to a novel PGK1 variant, p.E120K, resulting in severe decrease of enzyme activity and that 14q12 breakpoint disruption of mitochondrial CI assembly factor, NUBPL, presumably exacerbates the neuromuscular symptoms of the enzyme deficiency.

## Materials and Methods

### Samples, Cytogenetic Analysis, and Lymphoblastoid Cell Lines (LCLs)

The family under study is from Hungary. Blood samples were collected after informed consent; the study was carried out according to the Principles of the Declaration of Helsinki of the World Medical Association.

Cytogenetic analyses and the establishment of LCLs were performed as previously described (David et al. 2009).

### DNA extraction, flow sorting of derivative (der) chromosomes, array painting, amplification of the junction fragments, and SNP 6.0 array analysis

Genomic DNA extractions, flow sorting, and amplification of der chromosome-specific DNAs were performed as described earlier (David et al. 2009, 2013). Genomic amplicons of der(3) and der(14) chromosomes were analyzed by array painting using CytoScan HD array (Affymetrix, Santa Clara, CA, USA). The der(3) and der(14) junction fragments were amplified (see Table S1 for conditions) and sequenced by Sanger sequencing.

Genomic DNA from the index subject and his brothers (III:3 and III:6) was analyzed by Genome-Wide Human SNP 6.0 array (Affymetrix). Genotype calling was carried out using Genotyping Console software, and data was visualized using the Chromosome Analysis Suite (ChAS) software (Affymetrix).

### Whole-Exome Sequencing (WES)

Exonic targets were captured and enriched using the SureSelect Human All Exon 50 Mb Kit from Agilent Technologies (Santa Clara, CA, USA) and sequenced on a HiSeq2000 instrument (Illumina, San Diego, CA) following the manufacturer's instructions. Variants were annotated, and known SNPs as well as novel genetic alterations were identified.

### RNA Extraction and Expression Studies

Extraction of RNA samples from LCLs and reverse transcription (RT) reactions were performed as described earlier (David et al. 2013). For real-time quantitative PCR (RT-qPCR), see supplementary material.

Expression profiling of LCLs from the index subject and III:3 was carried out using the Human Gene 1.0 ST expression array (Affymetrix), and data analysis was performed as previously described (David et al. 2013).

### Construction of the Expression Vector Coding for PGK1 p.E120K Variant

The vector encoding PGK1-E120K variant was obtained by subjecting pMM1 to site-directed mutagenesis using Quick Change XL site-directed mutagenesis kit (Stratagene, La Jolla, CA, USA) (Chiarelli et al. 2012). Mutagenic oligonucleotides are available in supplementary material.

### Expression, Purification, and Characterization of the PGK1-E120K Variant

The PGK1-E120K was expressed in *E. coli* BL21(DE3) pLysS cells grown on ZYP-5052 autoinducing medium. The expressed enzyme variant was purified essentially as previously described (Chiarelli et al. 2012). Enzymatic activity and kinetic and thermal stability analyses have been performed (see the supplementary material).

### SDS-PAGE and Immunodetection

SDS-PAGE analysis was performed in control and subjects' LCL's pellets (15 μg protein). For immunodetection the following antibodies were used: rabbit anti-NUBPL (Mitosciences, Eugene, OR, USA), mouse anti-tubulin (Sigma, St. Louis, USA), and MitoProfile Total OXPHOS antibody cocktail (Mitosciences, Eugene, OR, USA). Quantification was performed using the Quantity One (BioRad) software.

## Results

### Clinical Report

The first reported symptom of the index subject (Fig. 1, III:5) was neonatal hyperbilirubinemia. Transfusion therapy was necessary at the age of eight months because of severe anemia, jaundice, and hepatomegaly, leading to the diagnosis of idiopathic hemolytic anemia. His dysmorphic features resembled those of his affected brother III:4 (Supplementary Material and Table S2), but, additionally, brachycephaly, short neck, reduced length of phalanges, four-digit crease on the right palm, cutaneous syndactyly II/III of the feet, and severe hypotonia were also reported (Fig. S2C). Repeated therapy-resistant seizures started at one year of age, and his unconscious stage resulted in a suspected but unconfirmed diagnosis of meningoencephalitis. Besides epilepsy, one of the hemolytic events caused stroke and hemiparesis of the left side. Cognitive and somatic development of the child stopped at the age of one year and 6 months: he did not walk and could not speak, but he had no hearing loss. Swallowing difficulties became more and more pronounced; gastrostoma and tube feeding were initiated from the age of 2 years. Severe recurrent hemolytic crises led to a partial splenectomy at the age of four and a half years. Positron emission tomography revealed Rasmussen's encephalitis at 5 years of age. At 6 years of age, ketogenic diet was initiated.

At the age of thirteen years, in 2013, he presented total body muscle atrophy, generalized somatic hypotrophy, diminished joint movements, muscle contractures, severe somato-mental retardation, no speech and no personal contact with other individuals, multiple dental caries, and bilateral cryptorchidism. The eyes are "swimming."

Two of his brothers (Fig. 1, III:3 and III:6) are healthy. In general, psychomotor development of III:3 was normal. He did not present any dysmorphic features. Reportedly, with physical effort, he shows signs of weakness and premature fatigue, well before his age-matched coworkers (Table 1).

Both parents are healthy, but the mother (II:5), in addition to anemia during pregnancies, also presents signs of fatigue.

During the course of this study, a maternal male cousin (Fig. 1, III:2), who died after falling down the stairs at the age of 7 years, was reported to have symptoms similar to his cousins.

His mother (II:3) and the remaining relatives (I:2, II:1, III:1) are all healthy. For additional clinical description, including subjects III:4 and III:2, see supplementary material.

### Cytogenetic Analysis

Cytogenetic analysis of GTL-banded metaphase chromosomes performed on subject III:4 revealed an apparently balanced reciprocal chromosome translocation between the long arms of chromosomes 3 and 14 [46,XY,t(3;14)(q26.3;q12)] (Fig. S2A and B). Furthermore, his healthy mother (II:5) and two of his brothers (III:3 and III:5) were also carriers of a similar translocation (Fig. 1a).

No perfect co-segregation between the translocation and the reported phenotype could be observed; therefore, we hypothesized that an additional genomic or genetic defect might also segregate in this family.

### Breakpoints and Candidate Genes

Genomic amplicons of flow-sorted der chromosomes were analyzed by array painting, and the breakpoints were narrowed to few kb regions (data not shown). Primers flanking the predicted breakpoints were designed, and the junction fragments were amplified and sequenced (Table S1). The alterations revealed by sequence alignments of the junction fragments are summarized in Fig. S1.

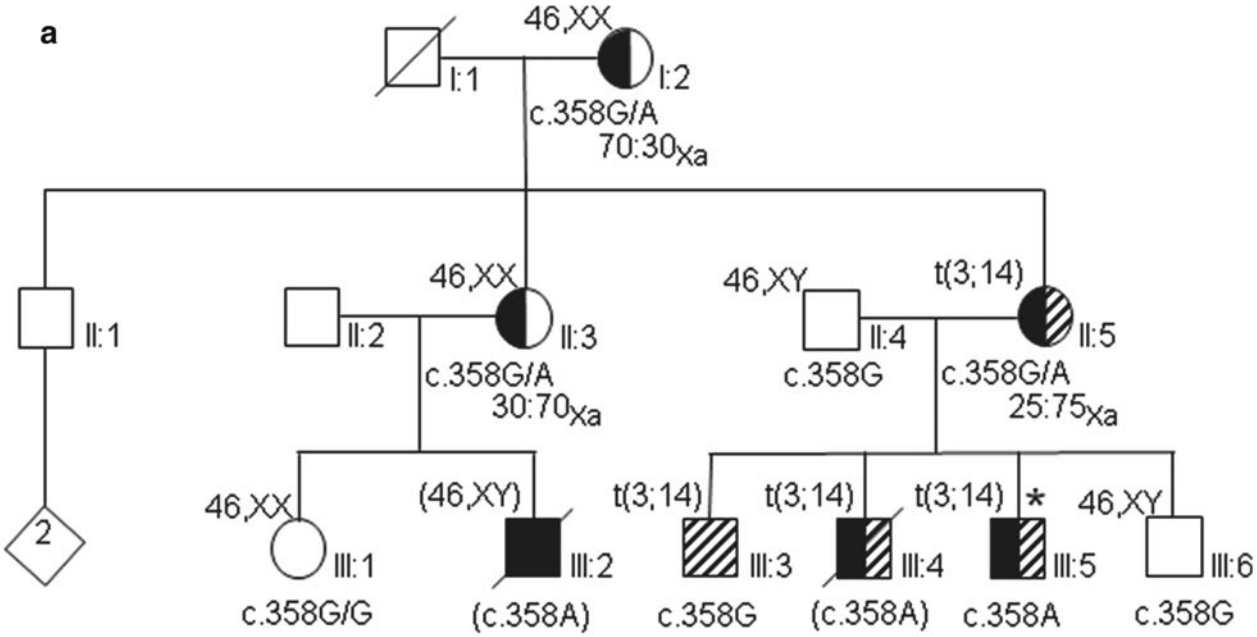
a
46,XX
I:1
I:2
c.358G/A
70:30Xa
II:1
II:2
46,XX
II:3
c.358G/A
30:70Xa
46,XY
II:4
c.358G
t(3;14)
II:5
c.358G/A
25:75Xa
2
46,XX
III:1
c.358G/G
(46,XY)
III:2
(c.358A)
t(3;14)
III:3
c.358G
t(3;14)
III:4
(c.358A)
t(3;14)
*
III:5
c.358A
46,XY
III:6
c.358G

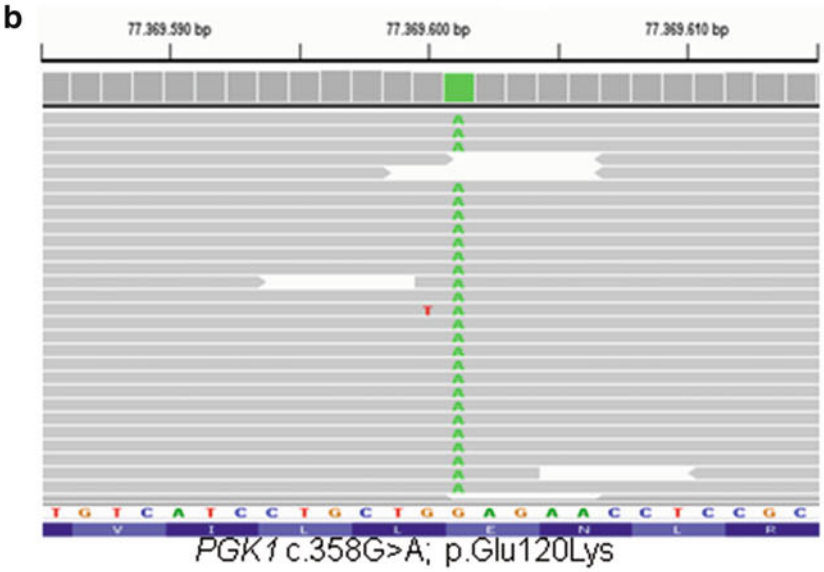
b
77.369.590 bp
77.369.600 bp
77.369.610 bp
PGK1 c.358G>A; p.Glu120Lys

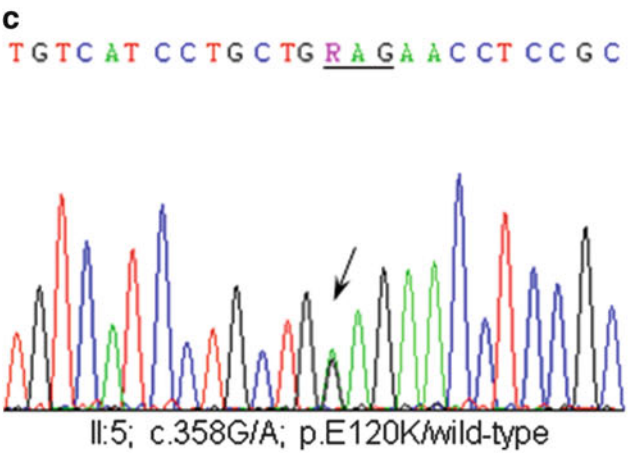
c
TGTCATCCTGCTGRAGAACCTCCGC
II:5; c.358G/A; p.E120K/wild-type

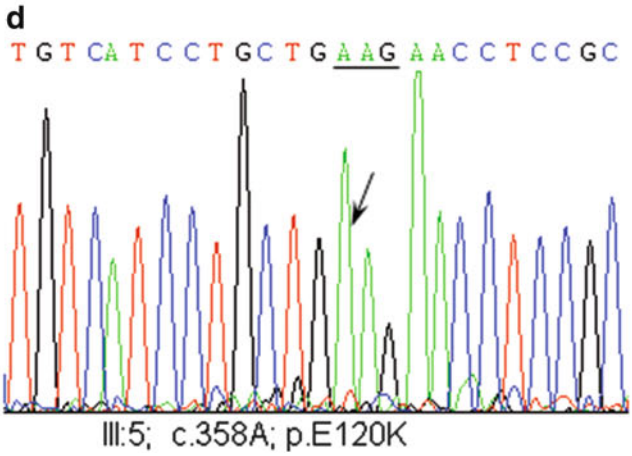
d
TGTCATCCTGCTGAAGAACCTCCGC
III:5; c.358A; p.E120K

**Table 1** Clinical features in subject carriers of either the *PGK1* c.358A mutation or the t(3;14) translocation alone or in association

| Clinical features | III:2 PGK1 c.358A | III:4 PGK1 c.358A&t(3;14) | III:5 PGK1 c.358A&t(3;14) | III:3 t(3;14) | NUBPL [a]252010 | CCDC39 [a]613807 | DNAJC19 [a]610198 |
|---|---|---|---|---|---|---|---|
| Hemolytic anemia | Severe | Severe | Severe | No | NR | NR | Normochromic microcytic |
| Erythroblastosis fetalis | Yes | Yes | Yes | No | – | – | NR |
| Jaundice | Yes | Yes | Yes | No | – | – | NR |
| Hyperbilirubinemia | Yes | Yes | Yes | No | – | – | NR |
| Hemolytic crisis | Severe | Severe | Severe | No | – | – | NR |
| Hepatosplenomegaly | Yes | Yes | Yes | No | – | – | NR |
| Splenectomy | ND | No | Yes | No | – | – | NR |
| Hemoglobin | Decreased | Decreased | Decreased | No | – | – | NR |
| MCV | Normal | Decreased | Decreased | No | – | – | Decreased |
| Neurological dysfunction | Yes | Yes | Yes | No | Characteristic | NR | Described |
| Neonatal hypotonia | No | Yes | Yes | No | – | – | NR |
| Developmental delay | Moderate | Yes | Yes | No | Characteristic | – | Described |
| Intellectual disability | Mild | Severe | Severe | No | Described | – | Described |
| Speech | Delayed | Absent | Absent | Normal | Described | – | Reported |
| Seizures, epilepsy | Severe | Severe | Severe | No | Reported | – | NR |
| Encephalopathy | Yes | Yes | Yes | No | Described | – | NR |
| Ataxia | NR | NR | NR | Transient | Described | – | Reported |
| Myopathy | Yes | Yes | Yes | No | Characteristic | NR | Cardiomyopathy |
| Muscular dystrophy | No | Severe | Severe | No | – | – | – |
| Weakness | Yes | Yes | Yes | Yes | Yes | – | Yes |
| Unsupported walking | Walk with help | Never sit or walk | Never walked | No | Characteristic | – | Characteristic |
| Spastic muscular tone | Yes | Yes | Yes | No | Described | – | – |
| Nuchal and dorsal muscle hypotonia | Yes | Yes | Yes | No | – | – | – |
| Swallow, tube feeding | Yes | Yes | Yes | No | Described | – | – |
| Horizontal nystagmus | Unknown | Yes | Yes | No | Characteristic | – | Reported |
| Infection | Repeated | Repeated | Repeated | No | – | Characteristic | – |

[a] OMIM number
*NR* not reported (see also Table S2)

The 3q26.33 breakpoint is at position g.180,278,286_180,278,294delTTCTGCA, 41.6 kb upstream of the 5′ region of tetratricopeptide repeat domain 14 (*TTC14*), a gene whose function is presently unknown (Fig. S3). Additional genes localized further distal from the breakpoint are (1) the coiled-coil domain containing 39 (*CCDC39*) localized only at 53.5 kb, (2) the *FXR1*, and (3) the DnaJ (Hsp40) homologue, subfamily C, member 19 (*DNAJC19*). This gene encodes an important protein for mitochondrial physiology. Located at the inner mitochondrial membrane, it has been shown to function as a chaperone for mitochondrial protein import system. Defects in this gene are reported to cause an autosomal recessive secondary 3-methylglutaconic aciduria (OMIM #610198), a disorder that partially overlaps with that of reported subjects (Table 1) (Wortmann et al. 2012, 2013;

**Fig. 1** (continued) Pedigree of the family, WES, and confirmation of the X-linked *PGK1* c.358G>A, p.E120K mutation. (**a**) Pedigree illustrating the segregation of the t(3;14)(q26.3;q12) and *PGK1* mutation. The index patient is indicated by *asterisk*. Translocation carriers are shown as hatched or half-hatched symbols, whereas filled and half-filled symbols denote the segregation of *PGK1* mutation. Data in parentheses are inferred. The ratio of X-chromosome inactivation of PGK1 mutation carrier females is indicated (Xa: active X chromosome). (**b**) Alignment of WES reads visualized using IGV tool indicating the homozygous single base substitution in exon 4 of *PGK1*. (**c**, **d**) Confirmation of the missense mutation c.358G>A; p.E120K by Sanger sequencing in subjects II:5 and III:5

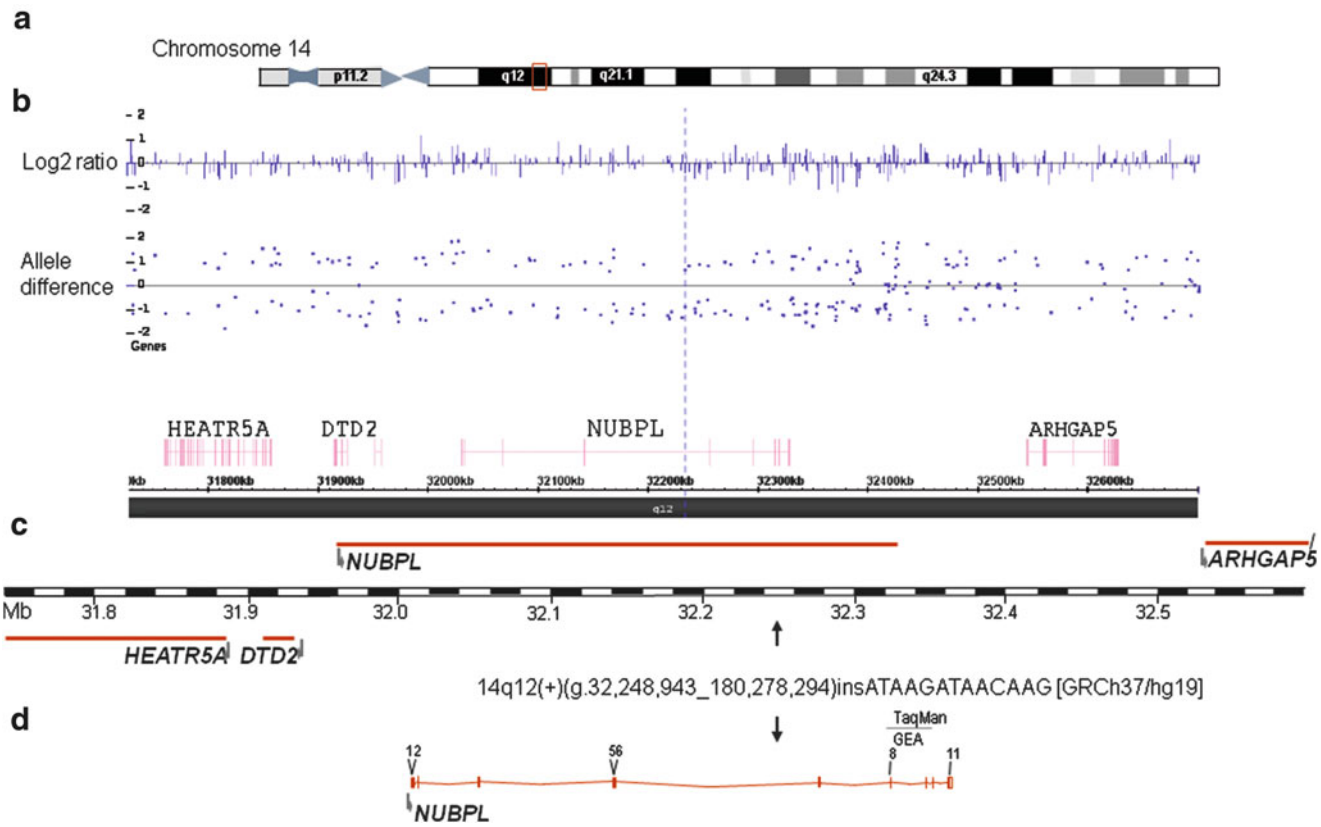


**Fig. 2** Overview of the chromosome 14q12 breakpoint region. (**a**) Schematic ideogram of chromosome 14; the breakpoint region is highlighted by a *box*. (**b**) Array analysis of the 14q12 breakpoint region using the Genome-Wide Human SNP array 6.0. A *dashed line* highlights the position of the breakpoint; Log2 ratios and allele differences are shown from the region (each *dot point* represents an oligonucleotide probe). Below, genes within this interval are depicted. No genomic imbalance can be identified within this region. (**c**) Detailed physical map across the breakpoint region. *Horizontal lines with folded gray arrows* indicate the position of genes in sense (above the map) and antisense (below the map) orientation. (**d**) Detailed map of *NUBPL* (RefSeq NM_025152.2) indicating the position of breakpoint at nucleotide resolution and the positions of TaqMan gene expression assay probe

Davey et al. 2006). Therefore, serum and urine amino acid and urine organic acid levels were determined (see Table S3A and S3B). In subject III:3, 3-hydroxybutyric acid was especially increased, but also 3-methylglutaconic acid (3-MGA) and 3-methylglutaric acid (3-MG) were slightly increased.

The 14q12 breakpoint is at position g.32,248,943_32,248,944dupATAAGATAACAAG, within IVS6 of *NUBPL* (Fig. 2), a member of the Mrp/NBP35 ATP-binding protein family, and critical for the assembly of human respiratory mitochondrial CI (Sheftel et al. 2009). Recently, recessive mutations in *NUBPL* have been implicated in the genetic etiology of CI deficiency [OMIM #252010], a mitochondrial respiratory chain defect that is caused by mutations in multiple different nuclear, mitochondrial, or X-linked genes (Calvo et al. 2010; Fassone and Rahman 2012). Additionally, in subjects with pediatric neurological disorders, three deletions encompassing this gene were reported ($p = 0.135$) (Cooper et al. 2011).

## Exclusion of Genomic Imbalance and Identification of the Additional Genetic Defect

Pathogenic genomic imbalance that could explain the phenotypic inconsistency observed among translocation carriers was excluded by SNP 6.0 array analysis.

Subsequently, reevaluation of the family history revealed that the maternal cousin (III:2; Fig. 1a) presented a clinical phenotype resembling that of index subject. Based on this, two possible disorders, X-linked PGK1 and triosephosphate isomerase 1 (*TPI1*; OMIM #190450, 12p13.31) deficiencies, were suggested. Furthermore, X-chromosome segregation analysis among siblings using array-based SNP data corroborated the possibility of PGK1 deficiency (data not shown).

Consequently, WES of the index subject revealed a novel missense mutation c.358G>A that leads to a change from glutamic acid to lysine at position 120 of PGK1 (p.E120K) within exon 4 (Fig. 1b). Segregation study confirmed this alteration in the index subject and showed that female subjects I:2, II:3, and II:5 are asymptomatic carriers (Fig. 1a, c and d), whereas the remaining family members are normal. Substitution of the highly conserved, solvent-exposed, negatively charged glutamic acid 120 by positively charged lysine (E120K; Table S7, Figs. S4 and S7) increases the net charge of the protein by two units (from 2.8 to 4.8 at pH 7.4) and certainly strongly argues in favor of this being the disease-causing mutation.

Borderline skewed X-chromosome inactivation toward the normal allele (25:75) was observed in female II:5, the only mutation carrier that presented symptoms during pregnancy (data not shown).

## Functional Characterization of the PGK1 p.E120K Variant

The specific activity of the purified PGK1-E120K variant was 10.2 U/mg compared to that of 816 U/mg of PGK1-WT (Chiarelli et al. 2012).

Kinetic analysis showed that, like PGK1-WT, PGK1-E120K variant was activated by high substrate concentrations (Fig. 3a and b) (Chiarelli et al. 2012). The mutant enzyme turned out to be severely affected in its kinetic properties (Table S4), showing a reduction of two orders of magnitude of its apparent $k_{cat}$ values toward both substrates. The apparent $K_m$ value toward 3-PG was sevenfold increased with respect to that of PGK1-WT, whereas that toward Mg-ATP was practically unchanged.

Interestingly, the variant's thermal inactivation rate curve was biphasic, with an increased slope after 5 min incubation, suggesting that it underwent heat-induced molecular change leading to the loss of enzyme activity (Fig. S5).

## Gene Expression Studies

Expression array profiling of LCLs from translocation carriers (only one of them affected by the *PGK1* mutation) did not reveal significantly altered expression of genes from the breakpoints (Table S5). The expression level of the disrupted *NUBPL* was only reduced by ~1 SD.

Subsequently, expression levels of three of these genes were also analyzed in subjects II:5, III:5, III:3, III:6, and controls by RT-qPCR (Fig. 4a, Table S5, Fig. S6A and B). By this analysis, a statistically significant 2.6-fold reduction of the *NUBPL* expression level ($P = 0.0001$; 0.061 vs. 0.156) was observed.

Additionally, systematic analysis of array expression data of mitochondrial CI subunits did not show considerable alteration in their expression (Table S6).

## SDS-PAGE Western Blot Analysis

Levels of the five OXPHOS complexes as well as the NUBPL assembly factor were determined by SDS-PAGE Western blot in LCLs, as our attempt to establish a fibroblast cell line from the index subject was unsuccessful.

NUBPL levels were reduced in all translocation carriers although at different extent (Fig. 4b). No significant changes were observed in the levels of the five complexes

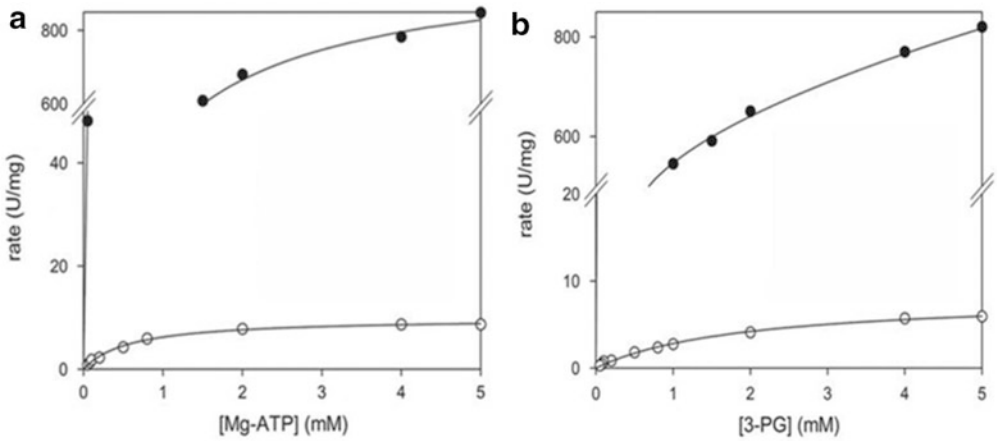


**Fig. 3** Kinetic profile of PGK1-E120K variant vs. wild-type enzyme. Steady-state kinetics of PGK1-E120K variant and wild-type as function of (**a**) Mg-ATP at fixed 5 mM 3-PG concentration and (**b**) as of 3-PG at fixed 5 mM Mg-ATP concentration. *Open circles* represent the PGK1-E120K variant, whereas filled circles represent the wild type. Like the wild type, the PGK1-E120K variant presents a biphasic kinetic behavior toward the two substrates; therefore, the linear region (0–5 mM substrates, range of physiological concentration) was considered to extrapolate the kinetic parameters

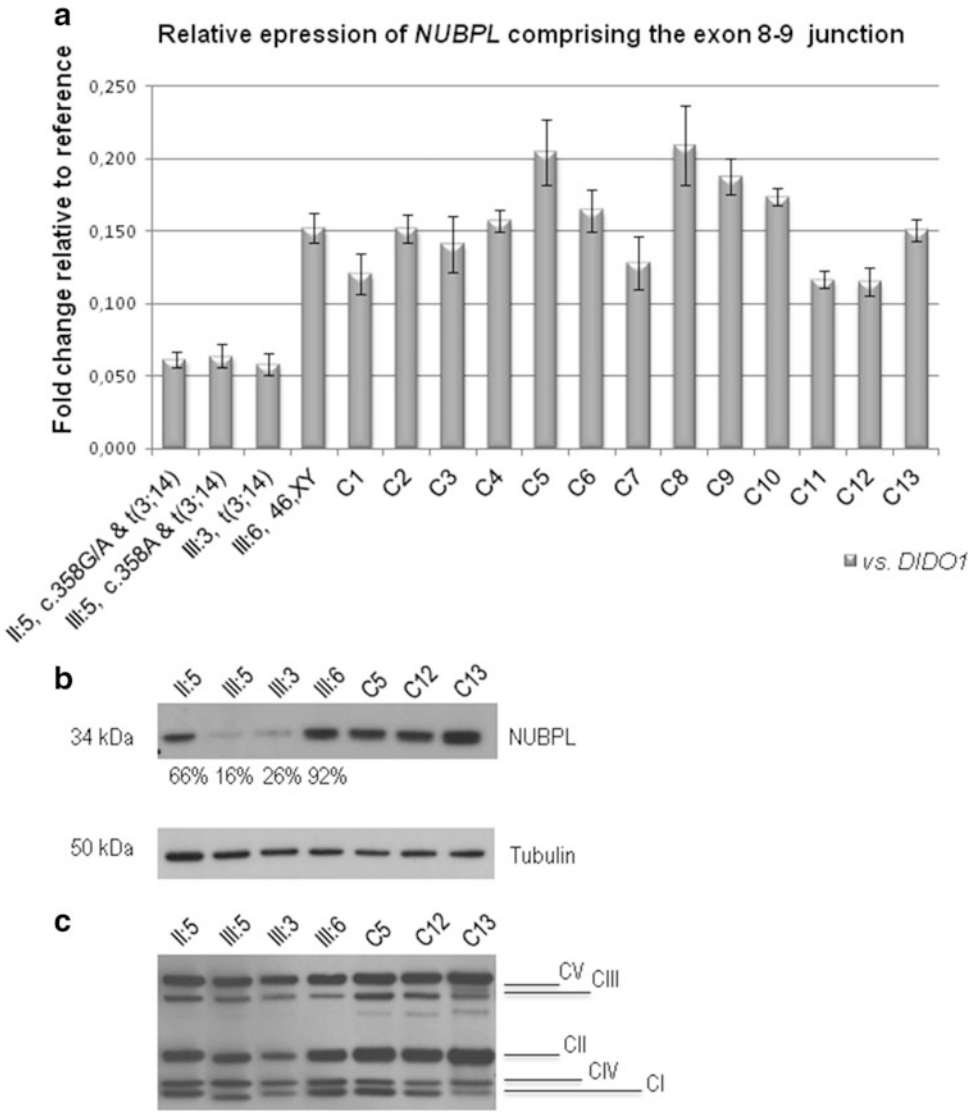


**Fig. 4** Quantification of *NUBPL* mRNA and protein in LCLs of translocation carriers and controls. (**a**) Bar graph depicting the relative expression of the *NUBPL* transcript comprising the exon 8–9 junction. Expression levels were normalized to the internal control (*DIDO1*). Fold change relative to reference is given in 2ΔCt. *Error bars* represent standard deviation, and C1 to C13 are control LCLs from unrelated subjects. (**b**) SDS-PAGE Western blot of NUBPL and alpha tubulin (loading control) in the family members and control LCLs showing significant reduction of NUBPL in the individuals affected by the translocation. NUBPL expression levels were normalized to the loading control. (**c**) SDS-PAGE Western blot of MitoProfile Total OXPHOS Human WB antibody cocktail

by the OXPHOS antibody cocktail (Fig. 4c). The dissimilar reduction of NUBPL protein in translocation carriers is in striking contrast with the evenly reduced mRNAs levels (Fig. 4a).

## Discussion

Alleged association of the familial translocation t(3;14) (q26;q12) with a particularly severe hemolytic anemia and neuromyopathy led us to map the translocation breakpoints, at nucleotide resolution.

Given the absence of genomic imbalance that could explain the phenotypic inconsistency observed among translocation carriers, and taking into account previously unreported family medical history data, the presence of an additional genetic defect was hypothesized. Segregation analysis of X chromosome and WES revealed that the index subject is also affected by a novel X-linked *PGK1* mutation (c.358G>A, p.E120K) within a highly conserved region.

Biochemical and functional characterization of the PGK1-E120K variant showed highly perturbed kinetic properties (Table S4). Very likely the p.E120K substitution

leads to a distorted local protein structure with detrimental indirect effect on the active site geometry, locking the enzyme in a more tight conformation and hindering proper domain movements required for its catalytic activity. Additionally, the variant turned out to have weakened protein stability (Fig. S4) most likely due to an intrinsic propensity of aggregating in a temperature- and time-dependent manner (Pey et al. 2013). These data led us to conclude that p.E120K is one of the most severely impaired PGK1 variants characterized thus far (Fermo et al. 2012; Chiarelli et al. 2012) and consequently the main genetic cause of the phenotype observed in this family.

Although rare, lethal forms of PGK1 deficiency during infancy have been reported in the literature (Beutler 2007). Even more infrequent are PGK1-deficient patients exhibiting the three distinguishing clinical features of this deficiency (hereditary non-spherocytic hemolytic anemia, neurological dysfunction, and myopathy). In the family reported here, all affected subjects (III:2, III:4, and III:5) presented the full clinical spectrum of PGK1 deficiency, and seemingly they are among the most severely affected PGK1-deficient patients reported to date.

The disruption of *NUBPL* by the 14q12 breakpoint led to a 60% reduction of the mRNA expression level of this CI assembly factor in three family members. Concomitant reduction of the protein level was also observed, being the index subject, the most affected one. The translocation per se is only associated with a subclinical state as the only clinical feature reported in translocation carriers (without PGK1 deficiency) is exercise intolerance due to premature fatigue, a common symptom of mitochondrial myopathy.

Interestingly, homozygous subjects for the branch-site mutation c.815-27T>C within IVS 9 of *NUBPL* are predicted to have ~30% of NUBPL expression. This mutation was excluded in the presently reported family (data not shown). The partially impaired CI function in these subjects is also sub-pathologic and certainly not associated to a mitochondrial CI disease (Tucker et al. 2012).

Although generally the clinical phenotype of family members carrying identical PGK1 mutations is reportedly similar, both translocation carriers (III:4 and III:5), unlike their translocation noncarrier cousin, show severe neuromyopathy with exacerbated muscular dystrophy.

In different tissues or pathogenic conditions, one of the two metabolic pathways, glycolysis or OXPHOS, is predominant over the other (Hu et al. 2012). Additionally, these pathways are interconnected as cytosolic NADH, the electron supplier that drives ATP synthesis via OXPHOS, is generated through glycolysis to pyruvate by glyceraldehyde-3-phosphate dehydrogenase (GAPDH) [see Glycolysis: Regulating Blood Glucose, http://themedicalbiochemistry-page.org/glycolysis.php] (Ramzan et al. 2013). Synergistic interactions, called synergistic heterozygosity, between defects in one or more different energy metabolism pathways have been reported as a common disease mechanism (Vockley et al. 2000). Such interaction between the reported genetic defects, both participating in cellular energy metabolism, seems obvious.

Although unlikely, we cannot exclude that other genes from the breakpoint regions, such as *DNAJC19*, may also contribute to the increased clinical severity of PGK1 deficiency in translocation carriers. The slight increase of both 3-MGA and 3-MG observed in the index subject can be related with several features of the clinical phenotype (metabolic disorder, mitochondrial dysfunction, progressive neuromuscular degeneration, and anemia) (Wortmann et al. 2013). Additionally, glycogen granules and granular structures in the mitochondria of endothelial cells and muscle fibers were reported in a PGK1-deficient subject (Schröder et al. 1996). Therefore, involvement of PGK1 deficiency in mitochondrial dysfunction seems likely and can also be related to the drastic reduction of NUBPL in the index subject.

Even more unlikely, but theoretically possible, is that the observed phenotype is exclusively the result of the novel PGK1 mutation, and the phenotype heterogeneity observed among translocation carriers and noncarriers is the outcome of each individual's genomic/epigenetic background.

In conclusion, the discordant inheritance of the allegedly translocation-associated severe phenotype, instead of being due to a genomic imbalance, is mainly explained by independent inheritance of a novel *PGK1* c.358G>A, p.E120K mutation. The pathogenicity of this mutation was confirmed by in vitro functional characterization of the variant. Furthermore, the t(3;14)(q26;q12) is only associated with a subclinical phenotype; nevertheless, disruption NUBPL, a component of the OXPHOS cellular energy pathway, most likely exacerbates the PGK1-deficient phenotype in subjects who are also translocation carriers. In addition, the case presented here constitutes a "beautiful" example of synergistic heterozygosity and a naturally occurring model to study the interactions between cellular energy pathways and their association with mitochondrial dysfunction. Therefore, further studies are warranted to clarify these additional aspects.

Additionally our data imply that synergistic interactions, involving heterozygous genomic and chromosome rearrangements, may contribute for the "missing" heritability

of inborn metabolic disorders. Last but not least, this study eloquently illustrates that even in our genomic era with WES and personalized genomics, a thorough family medical history is necessary in the elucidation of the molecular bases of rare diseases and their prevention.

**Acknowledgments** We are grateful to the family members and the referring physician, Matild Dobos, for their involvement in this study. We thank the Chrombios Molecular Cytogenetics GmbH (Raubling, Germany), the Gulbenkian Institute of Sciences (Oeiras, Portugal), and the DNAVision (Gosselies, Belgium) for carrying out chromosome sorting and processing Affymetrix SNP 6.0 arrays and WES, respectively. Additionally, we would like to thank Sara Malveiro for the technical support at the beginning of this work, to Catarina Fernandes for the segregation analysis of the novel PGK1 mutation, and to Barbara Marques for the fluorescence in situ hybridization (FISH). We are also grateful to Andreas Gal and João Lavinha for their comments on the manuscript.

*Funding*: C.A. was supported by the Ricardo Jorge Research Fellowship (BRJ/01/DG/2009) from the *Instituto Nacional de Saúde Dr Ricardo Jorge*. L.S.A is supported by the Portuguese Foundation for Science and Technology (FCT) fellowship (C2008/INSA/P4). This work was partially supported by FCT research grants PTDC/SAU-GMG/118140/2010 and PEst-OE/SAU/UI0009/2011 as well as by a Portuguese-Hungarian bilateral collaboration grant.

## Synopsis

An extremely severe non-spherocytic hemolytic anemia and neuromyopathy, hypothesized to be associated with chromosome translocation-associated genomic imbalance, were shown to be mainly caused by a novel pathogenic severe *PGK1* mutation and that the neuromyopathic symptoms of the deficiency are likely exacerbated by the disruption of mitochondrial complex I assembly factor, NUBPL.

## Compliance with Ethics Guidelines

### Conflict of Interest

Dezső David, Lígia S. Almeida, Maristella Maggi, Carlos Araújo, Stefan Imreh, Giovanna Valentini, György Fekete, and Irén Haltrich declare that they have no conflict of interest.

### Informed Consent

All procedures followed were in accordance with the ethical standards of the responsible committee on human experimentation (institutional and national) and with the Helsinki Declaration of 1975, as revised in 2000.

Informed consent was obtained from all subjects for being included in the study.

Additional informed consent was obtained for the patient for which identifying information (photograph) is included in this article.

## Details of the Contributions of Individual Authors

DD designed, oriented, and analyzed the results and wrote the manuscript, LSA performed immunodetection of NUBPL, MM and GV performed in vitro characterization of the PGK1 variant, CA carried out RT-qPCR and sequencing of the junction fragments, SI contributed to the WES, and GF and IH contributed with identification, clinical description, and samples from family members. All authors contributed to the manuscript.

## References

Beutler E (2007) PGK deficiency. Br J Haematol 136:3–11

Calvo SE, Tucker EJ, Compton AG et al (2010) High-throughput, pooled sequencing identifies mutations in NUBPL and FOXRED1 in human complex I deficiency. Nat Genet 42: 851–858

Chiarelli LR, Morera SM, Bianchi P, Fermo E, Zanella A, Galizzi A, Valentini G (2012) Molecular insights on pathogenic effects of mutations causing phosphoglycerate kinase deficiency. PLoS One 7:e32065

Cooper GM, Coe BP, Girirajan S (2011) A copy number variation morbidity map of developmental delay. Nat Genet 43:838–846

Davey KM, Parboosingh JS, McLeod DR et al (2006) Mutation of DNAJC19, a human homologue of yeast inner mitochondrial membrane co-chaperones, causes DCMA syndrome, a novel autosomal recessive Barth syndrome-like condition. J Med Genet 43:385–393

David D, Marques B, Ferreira C, Vieira P, Corona-Rivera A, Ferreira JC, van Bokhoven H (2009) Characterization of two ectrodactyly-associated translocation breakpoints separated by 2.5 Mb on chromosome 2q14.1-q14.2. Eur J Hum Genet 17:1024–1033

David D, Marques B, Ferreira C et al (2013) A familial t(8;13) translocation associated TRPS I and a novel expanded TRP syndrome most likely caused by cis-ruption and increased *TRPS1* expression. Hum Genet 132:1287–1299

De Gregori M, Ciccone R, Magini P et al (2007) Cryptic deletions are a common finding in "balanced" reciprocal and complex chromosome rearrangements: a study of 59 patients. J Med Genet 44: 750–762

Fassone E, Rahman S (2012) Complex I deficiency: clinical features, biochemistry and molecular genetics. J Med Genet 49: 578–590

Fermo E, Bianchi P, Chiarelli LR et al (2012) A new variant of phosphoglycerate kinase deficiency (p.I371K) with multiple tissue involvement: molecular and functional characterization. Mol Genet Metab 106:455–461

Hu Y, Lu W, Chen G et al (2012) K-rasG12V transformation leads to mitochondrial dysfunction and a metabolic switch from oxidative phosphorylation to glycolysis. Cell Res 22:399–412

Kevelam SH, Rodenburg RJ, Wolf NI et al (2013) NUBPL mutations in patients with complex I deficiency and a distinct MRI pattern. Neurology 80:1577–1583

Pey AL, Mesa-Torres N, Chiarelli LR, Valentini G (2013) Structural and energetic basis of protein kinetic destabilization in human phosphoglycerate kinase 1 deficiency. Biochemistry 52: 1160–1170

Ramzan R, Weber P, Linne U, Vogt S (2013) GAPDH: the missing link between glycolysis and mitochondrial oxidative phosphorylation? Biochem Soc Trans 41:1294–1297

Schäffer AA (2013) Digenic inheritance in medical genetics. J Med Genet 50:641–652

Schröder JM, Dodel R, Weis J, Stefanidis I, Reichmann H (1996) Mitochondrial changes in muscle phosphoglycerate kinase deficiency. Clin Neuropathol 15:34–40

Sheftel AD, Stehling O, Pierik AJ et al (2009) Human Ind1, an iron-sulfur cluster assembly factor for respiratory complex I. Mol Cell Biol 29:6059–6073

Tamai M, Kawano T, Saito R, Sakurai et al (2014) Phosphoglycerate kinase deficiency due to a novel mutation (c. 1180A>G) manifesting as chronic hemolytic anemia in a Japanese boy. Int J Hematol 100:393–397

Tucker EJ, Mimaki M, Compton AG, McKenzie M, Ryan MT, Thorburn DR (2012) Next-generation sequencing in molecular diagnosis: NUBPL mutations highlight the challenges of variant detection and interpretation. Hum Mutat 33:411–418

Vockley J, Rinaldo P, Bennett MJ, Matern D, Vladutiu GD (2000) Synergistic heterozygosity: disease resulting from multiple partial defects in one or more metabolic pathways. Mol Genet Metab 71: 10–18

Wortmann SB, Kluijtmans LA, Engelke UFH et al (2012) The 3-methylglutaconic acidurias: what's new? J Inherit Metab Dis 35: 13–22

Wortmann SB, Kluijtmans LA, Rodenburg RJ, et al (2013) 3-Methylglutaconic aciduria—lessons from 50 genes and 977 patients. *J Inherit Metab Dis* 36:913–921

JIMD Reports
DOI 10.1007/8904_2015_428

CASE REPORT

# Abnormal Newborn Screening in a Healthy Infant of a Mother with Undiagnosed Medium-Chain Acyl-CoA Dehydrogenase Deficiency

**Lise Aksglaede · Mette Christensen · Jess H. Olesen · Morten Duno · Rikke K.J. Olsen · Brage S. Andresen · David M. Hougaard · Allan M. Lund**

Received: 12 January 2015 / Revised: 05 February 2015 / Accepted: 18 February 2015 / Published online: 13 March 2015


**Abstract** A neonate with low blood free carnitine level on newborn tandem mass spectrometry screening was evaluated for possible carnitine transporter defect (CTD). The plasma concentration of free carnitine was marginally reduced, and the concentrations of acylcarnitines (including C6, C8, and C10:1) were normal on confirmatory tests. Organic acids in urine were normal. In addition, none of the frequent Faroese *SLC22A5* mutations (p.N32S, c.825-52G>A) which are common in the Danish population were identified. Evaluation of the mother showed low-normal free carnitine, but highly elevated medium-chain acylcarnitines (C6, C8, and C10:1) consistent with medium-chain acyl-CoA dehydrogenase deficiency (MCADD). The diagnosis was confirmed by the finding of homozygous presence of the c.985A>G mutation in *ACADM*.

Communicated by: Rodney Pollitt, PhD

Competing interests: None declared

L. Aksglaede (✉) · M. Christensen · J.H. Olesen · M. Duno · A.M. Lund
Centre for Inherited Metabolic Diseases, Department of Clinical Genetics, Copenhagen University Hospital, Copenhagen, Denmark
e-mail: lise.aksglaede@rh.regionh.dk

R.K.J. Olsen
Research Unit for Molecular Medicine, Aarhus University Hospital and Department of Clinical Medicine, Aarhus University, Aarhus, Denmark

B.S. Andresen
Department of Biochemistry and Molecular Biology, University of Southern Denmark, Odense, Denmark

D.M. Hougaard
Centre for Neonatal Screening, Department for Congenital Disorders, Statens Serum Institute, Copenhagen, Denmark

## Introduction

Medium-chain acyl-CoA dehydrogenase deficiency (MCADD) is the most common inborn error of fatty acid oxidation (Gregersen et al. 2008). MCADD presents with a characteristic acylcarnitine pattern that can easily be identified in dried blood spot samples by tandem mass spectrometry (Oerton et al. 2011), and taken together with the excellent prognosis upon early treatment, MCADD is therefore part of the newborn screening (NBS) program in several countries. In Denmark, MCADD has been part of the NBS program since 2002 (Lund et al. 2012).

Clinical manifestations of MCADD are diverse, but the disease usually presents in the first years of life with hypoketotic hypoglycemia and encephalopathy in relation to an intercurrent illness and/or insufficient energy intake. Undiagnosed/untreated these patients are at high risk of developing a life-threatening metabolic decompensation with sudden death or permanent neurological sequelae (Iafolla et al. 1994; Pollitt and Leonard 1998; Wilson et al. 1999).

Here we present the diagnosis of maternal MCADD on NBS of her newborn child.

## Case Report

The proband was born at term after an uneventful pregnancy. Birth weight was 3,816 g. She was the third child of healthy unrelated parents. NBS performed at age 2 days revealed a low blood free carnitine of 6.0 μmol/L (cut off <6.3 μmol/L), and the infant was suspected of having carnitine transporter deficiency (CTD). Confirmatory testing was performed according to the Danish

neonatal screening program (Lund et al. 2012) including analysis of plasma free carnitine and acylcarnitines and analysis of urine organic acids. Plasma acylcarnitine profile at age 15 days showed only a slightly decreased concentration of free carnitine (18 μmol/L, ref. 24–64 μmol/L) excluding CTD. She had a normal acylcarnitine profile (including C6, C8, and C10:1), and the urinary excretion of organic acids was normal, thereby excluding secondary depletion of carnitine. None of the frequent Faroese *SLC22A5* mutations known to segregate in the Danish population (c.95A>G, c.825-52G>A) nor the risk haplotype (Rasmussen et al. 2014) was identified. In parallel with the analyses in the infant, the mother (aged 36 years) was evaluated and turned out to have a normal free carnitine in plasma (30 μmol/L, ref. 24–64 μmol/L) and highly elevated medium-chain acylcarnitines (C6, C8, and C10:1) consistent with MCADD. Direct sequencing of exon 11 of the *ACADM* gene revealed homozygous presence of the prevalent c.985A>G mutation in the mother, confirming the MCADD diagnosis, whereas the newborn child was found to be heterozygous for the c.985A>G mutation.

The mother denied having any symptoms related to MCADD, and specifically she reported a normal fasting tolerance. However, she had never had any severe infections or diseases, and when she was a child, her parents used to give her high-carbohydrate drinks during intercurrent illness, which may have prevented metabolic crises.

Her diet was evaluated by a metabolic dietician, and it turned out that her intake of fat was 35.8%, and she was recommended to reduce it to a maximum of 30%. Furthermore, she was instructed in following a specific high-carbohydrate regimen in case of illness.

The mother had six healthy siblings who all were offered biochemical evaluation. None of the four sisters that turned up for evaluation had acylcarnitine profiles consistent with MCADD. Two sisters, however, had slightly elevated concentrations of C8 acylcarnitine, one of whom was later found to be heterozygous for the c.985A>G mutation in *ACADM*. Molecular testing was not performed in the remaining three sisters.

## Discussion and Conclusions

We report a case of an asymptomatic MCADD patient homozygous for the c.985A>G mutation detected incidentally through NBS due to low free carnitine. This result on NBS in the newborn most likely reflects poor carnitine stores in the mother. However, in our case the mother presented with low-normal free carnitine at the initial evaluation 16 days after delivery. Though the relation between free carnitine in plasma and carnitine stores is unclear, this result does not support low carnitine stores in the mother. It is well described that plasma carnitine decreases during pregnancy from the 12th week of gestation to term and may reach concentrations half the normal in healthy nonpregnant women. The decrease in total carnitine is mainly caused by a decrease in free carnitine (Schoderbeck et al. 1995) and is thought to be the consequence of a reduced rate of carnitine biosynthesis, possibly because of an inadequate iron status (Keller et al. 2009) or because of a low availability of precursors for carnitine (Ringseis et al. 2010). Interestingly, one study reported a complete normalization of plasma carnitine one month after delivery (Marzo et al. 1994), and our finding of low-normal free carnitine 16 days after delivery may reflect a partial normalization to concentrations often seen in patients with MCADD.

The finding of abnormal concentrations of specific acylcarnitines and low free carnitine on NBS has revealed various types of inborn errors of metabolism in undiagnosed mothers. Thus, maternal MCADD (Leydiker et al. 2011), CTD (De Biase et al. 2012; El-Hattab et al. 2010; Lee et al. 2010; Lund et al. 2012; Schimmenti et al. 2007; Vijay et al. 2006), glutaric acidemia type I (Crombez et al. 2008), and combined homocystinuria and methylmalonic aciduria (Lin et al. 2009) have all been detected through NBS by the finding of decreased free carnitine in the newborn. In addition, elevated specific acylcarnitines in newborns have revealed maternal 3-methylcrotonyl-CoA carboxylase deficiency (Gibson et al. 1998; Koeberl et al. 2003; Lund et al. 2012), very long-chain acyl-CoA dehydrogenase deficiency (McGoey and Marble 2011), holocarboxylase synthetase deficiency (Nyhan et al. 2009), and multiple acyl-CoA dehydrogenation deficiency due to a riboflavin transporter gene defect (Chiong et al. 2007; Ho et al. 2011). These cases illustrate the importance of taking a detailed maternal history and performing biochemical evaluation with acylcarnitine profile and urine organic acids and when appropriate molecular genetic follow-up in mothers of newborns with abnormal screening results if confirmatory testing shows that the newborn is normal.

After the introduction of MCADD to the NBS program, it has become clear that the incidence of MCADD is much higher than previously thought (Andresen et al. 2001; Maier et al. 2009; Maier et al. 2005). The incidence of MCADD detected by NBS in Denmark is 1 in 8,954, whereas the incidence of clinically presenting MCADD in Denmark during the preceding 10 years before screening was only 1 in 39,691 (Andresen et al. 2012). One explanation for this discrepancy is that the genotypes of the screened population differ from the genotypes in the clinically detected population. Thus, genotypes that have not been identified in clinically presenting cases have been identified in a significant number of screened infants, and

these genotypes have been associated with a milder biochemical phenotype (Andresen et al. 2012). Importantly, it has been shown that the proportion of newborns with the prevalent c.985A>G homozygous genotype is approximately 50% in a screened population (Andresen et al. 2012) as compared with 80% in a clinically presenting population (Tanaka et al. 1992), supporting the notion that c.985A>G homozygous MCADD has a higher penetrance than most other MCADD genotypes. This is also reflected in the biochemical phenotype, where c.985A>G homozygous newborns have higher mean and median C8 carnitine levels than newborns with other *ACADM* genotypes (Andresen et al. 2012; Oerton et al. 2011).

The correlation between genotype and clinical phenotype in MCADD is not clear (Andresen et al. 1997; Arnold et al. 2010). Several asymptomatic patients being homozygous for the c.985A>G mutation have been reported (Andresen et al. 2012; Duran et al. 1986; Leydiker et al. 2011). Identification of the asymptomatic mother in the present study represents one further example that c.985A>G homozygous individuals can remain without recognized symptoms until adulthood and that this can also explain some of the discrepancy between the number of clinically diagnosed patients with MCADD and the number of newborns identified by screening (Andresen et al. 2012).

On the other hand others have reported MCADD presenting in adulthood, some with fatal outcome (for review see Lang 2009) stressing the importance of diagnosing these individuals. It may also be of note that both our case and a similar case (Leydiker et al. 2011) are homozygous for the c.985A>G, indicating that low free carnitine in newborns requires this classic genotype in the mother.

In conclusion, the detection of asymptomatic MCADD and other maternal metabolic disorders is important in order to initiate proper management, family screening, and prevention of complications as sudden deterioration can occur with these disorders at any age. Our case underlines the importance of thorough biochemical evaluation of mothers of newborns with reduced free carnitine on NBS if confirmatory testing shows that the newborn is normal.

## Synopsis

Thorough biochemical evaluation of mothers of newborns with a reduced free carnitine on NBS is important if confirmatory testing shows that the newborn is normal.

## Conflict of Interest

Lise Aksglaede, Mette Christensen, Jess H Olesen, Morten Duno, Rikke KJ Olsen, Brage S Andresen, David M Hougaard, and Allan M Lund declare that they have no conflict of interest.

## Compliance with Ethics Guidelines

This article does not contain any studies with human or animal subjects performed by any of the authors.

## Author Contribution

LA: responsible for collecting medical records, gathering relevant literature, and drafting the article

MC, JHO, and DMH: performing biochemical analyses and revising the article critically for important intellectual content

MD, RKJO, and BSA: performing genetic investigations and revising the article critically for important intellectual content

AML: clinical examination and follow-up of case and revising the article critically for important intellectual content

## References

Andresen BS, Bross P, Udvari S et al (1997) The molecular basis of medium-chain acyl-CoA dehydrogenase (MCAD) deficiency in compound heterozygous patients: is there correlation between genotype and phenotype? Hum Mol Genet 6(5):695–707

Andresen BS, Dobrowolski SF, O'Reilly L et al (2001) Medium-chain acyl-CoA dehydrogenase (MCAD) mutations identified by MS/MS-based prospective screening of newborns differ from those observed in patients with clinical symptoms: identification and characterization of a new, prevalent mutation that results in mild MCAD deficiency. Am J Hum Genet 68(6):1408–1418

Andresen BS, Lund AM, Hougaard DM et al (2012) MCAD deficiency in Denmark. Mol Genet Metab 106(2):175–188

Arnold GL, Saavedra-Matiz CA, Galvin-Parton PA, Erbe R, Devincentis E, Kronn D (2010) Lack of genotype-phenotype correlations and outcome in MCAD deficiency diagnosed by newborn screening in New York State. Mol Genet Metab 99(3):263–268

Chiong MA, Sim KG, Carpenter K, Rhead W, Ho G, Olsen RK (2007) Transient multiple acyl-CoA dehydrogenation deficiency in a newborn female caused by maternal riboflavin deficiency. Mol Genet Metab 92(1–2):109–114

Crombez EA, Cederbaum SD, Spector E, Chan E, Salazar D, Neidich J (2008) Maternal glutaric acidemia, type I identified by newborn screening. Mol Genet Metab 94(1):132–134

De Biase I, Champaigne NL, Schroer R, Pollard LM, Longo N, Wood T (2012) Primary carnitine deficiency presents atypically with long QT syndrome: a case report. J Inherit Metab Dis Rep 2:87–90

Duran M, Hofkamp M, Rhead WJ, Saudubray JM, Wadman SK (1986) Sudden child death and 'healthy' affected family members with medium-chain acyl-coenzyme A dehydrogenase deficiency. Pediatrics 78(6):1052–1057

El-Hattab AW, Li FY, Shen J et al (2010) Maternal systemic primary carnitine deficiency uncovered by newborn screening: clinical, biochemical, and molecular aspects. Genet Med 12(1):19–24

Gibson KM, Bennett MJ, Naylor EW, Morton DH (1998) 3-Methylcrotonyl-coenzyme A carboxylase deficiency in Amish/Mennonite adults identified by detection of increased acylcarnitines in blood spots of their children. J Pediatr 132(3 Pt 1):519–523

Gregersen N, Andresen BS, Pedersen CB, Olsen RK, Corydon TJ, Bross P (2008) Mitochondrial fatty acid oxidation defects remaining challenges. J Inherit Metab Dis 31(5):643–657

Ho G, Yonezawa A, Masuda S et al (2011) Maternal riboflavin deficiency, resulting in transient neonatal-onset glutaric aciduria Type 2, is caused by a microdeletion in the riboflavin transporter gene GPR172B. Hum Mutat 32(1):E1976–E1984

Iafolla AK, Thompson RJ Jr, Roe CR (1994) Medium-chain acyl-coenzyme A dehydrogenase deficiency: clinical course in 120 affected children. J Pediatr 124(3):409–415

Keller U, van der Wal C, Seliger G, Scheler C, Ropke F, Eder K (2009) Carnitine status of pregnant women: effect of carnitine supplementation and correlation between iron status and plasma carnitine concentration. Eur J Clin Nutr 63(9):1098–1105

Koeberl DD, Millington DS, Smith WE et al (2003) Evaluation of 3-methylcrotonyl-CoA carboxylase deficiency detected by tandem mass spectrometry newborn screening. J Inherit Metab Dis 26 (1):25–35

Lang TF (2009) Adult presentations of medium-chain acyl-CoA dehydrogenase deficiency (MCADD). J Inherit Metab Dis 32 (6):675–683

Lee NC, Tang NL, Chien YH et al (2010) Diagnoses of newborns and mothers with carnitine uptake defects through newborn screening. Mol Genet Metab 100(1):46–50

Leydiker KB, Neidich JA, Lorey F et al (2011) Maternal medium-chain acyl-CoA dehydrogenase deficiency identified by newborn screening. Mol Genet Metab 103(1):92–95

Lin HJ, Neidich JA, Salazar D et al (2009) Asymptomatic maternal combined homocystinuria and methylmalonic aciduria (cblC) detected through low carnitine levels on newborn screening. J Pediatr 155(6):924–927

Lund AM, Hougaard DM, Simonsen H et al (2012) Biochemical screening of 504,049 newborns in Denmark, the Faroe Islands and Greenland-experience and development of a routine program for expanded newborn screening. Mol Genet Metab 107 (3):281–293

Maier EM, Gersting SW, Kemter KF et al (2009) Protein misfolding is the molecular mechanism underlying MCADD identified in newborn screening. Hum Mol Genet 18(9):1612–1623

Maier EM, Liebl B, Roschinger W et al (2005) Population spectrum of ACADM genotypes correlated to biochemical phenotypes in newborn screening for medium-chain acyl-CoA dehydrogenase deficiency. Hum Mutat 25(5):443–452

Marzo A, Cardace G, Corbelletta C et al (1994) Plasma concentration, urinary excretion and renal clearance of L-carnitine during pregnancy: a reversible secondary L-carnitine deficiency. Gynecol Endocrinol 8(2):115–120

McGoey RR, Marble M (2011) Positive newborn screen in a normal infant of a mother with asymptomatic very long-chain Acyl-CoA dehydrogenase deficiency. J Pediatr 158(6):1031–1032

Nyhan WL, Willis M, Barshop BA, Gangoiti J (2009) Positive newborn screen in the biochemically normal infant of a mother with treated holocarboxylase synthetase deficiency. J Inherit Metab Dis 32(Suppl 1):S79–S82

Oerton J, Khalid JM, Besley G et al (2011) Newborn screening for medium chain acyl-CoA dehydrogenase deficiency in England: prevalence, predictive value and test validity based on 1.5 million screened babies. J Med Screen 18(4):173–181

Pollitt RJ, Leonard JV (1998) Prospective surveillance study of medium chain acyl-CoA dehydrogenase deficiency in the UK. Arch Dis Child 79(2):116–119

Rasmussen J, Lund AM, Risom L et al (2014) Residual OCTN2 transporter activity, carnitine levels and symptoms correlate in patients with primary carnitine deficiency. Mol Genet Metab Rep 1:241–248

Ringseis R, Hanisch N, Seliger G, Eder K (2010) Low availability of carnitine precursors as a possible reason for the diminished plasma carnitine concentrations in pregnant women. BMC Pregnancy Childbirth 10:17

Schimmenti LA, Crombez EA, Schwahn BC et al (2007) Expanded newborn screening identifies maternal primary carnitine deficiency. Mol Genet Metab 90(4):441–445

Schoderbeck M, Auer B, Legenstein E et al (1995) Pregnancy-related changes of carnitine and acylcarnitine concentrations of plasma and erythrocytes. J Perinat Med 23(6):477–485

Tanaka K, Yokota I, Coates PM et al (1992) Mutations in the medium chain acyl-CoA dehydrogenase (MCAD) gene. Hum Mutat 1 (4):271–279

Vijay S, Patterson A, Olpin S et al (2006) Carnitine transporter defect: diagnosis in asymptomatic adult women following analysis of acylcarnitines in their newborn infants. J Inherit Metab Dis 29 (5):627–630

Wilson CJ, Champion MP, Collins JE, Clayton PT, Leonard JV (1999) Outcome of medium chain acyl-CoA dehydrogenase deficiency after diagnosis. Arch Dis Child 80(5):459–462

JIMD Reports
DOI 10.1007/8904_2015_429

CASE REPORT

# Cobalamin C Disease Missed by Newborn Screening in a Patient with Low Carnitine Level

**Rebecca C. Ahrens-Nicklas · Esra Serdaroglu · Colleen Muraresku · Can Ficicioglu**

Received: 21 January 2015 / Revised: 12 February 2015 / Accepted: 18 February 2015 / Published online: 13 March 2015


**Abstract** Cobalamin C (CblC) disease is the most common inherited disorder of intracellular cobalamin metabolism. It is a multisystemic disorder mainly affecting the eye and brain and characterized biochemically by methylmalonic aciduria, low methionine level, and homocystinuria. We report a patient found to have CblC disease who initially presented with low carnitine and normal propionylcarnitine (C3) levels on newborn screen. Newborn screening likely failed to detect CblC in this patient because of both his low carnitine level and the presence of a mild phenotype.

## Introduction

Cobalamin C (CblC) disease is the most common inborn error of intracellular cobalamin metabolism. The disorder is caused by mutations in *MMACHC*. Pathogenesis is due to an inability to convert cobalamin to the active forms, methylcobalamin and adenosylcobalamin. Methylcobalamin is required for the conversion of homocysteine to methionine by methionine synthase. Adenosylcobalamin is required for the conversion of methylmalonyl-CoA to succinyl-CoA by methylmalonyl-CoA mutase (Martinelli et al. 2011). Therefore, CblC disease is characterized by elevated levels of homocysteine, low methionine level, and elevated methylmalonic acid (MMA).

CblC disease has a spectrum of severity with two distinct phenotypic forms: early and late onset. Early-onset patients present with intrauterine growth retardation (IUGR), microcephaly, failure to thrive, developmental delay, hypotonia, progressive retinopathy, and maculopathy (Fischer et al. 2014). Early-onset patients usually present in the first months of life and have an unfavorable prognosis (Carrillo-Carrasco et al. 2011). Late-onset CblC patients usually present with extrapyramidal and neuropsychiatric symptoms in any decade of life (Rosenblatt et al. 1997). Late-onset patients are less likely to have ocular involvement (Gerth et al. 2008).

Tandem mass spectrometry-based newborn screening (NBS) aims to detect patients with inborn errors of metabolism prior to the onset of symptoms. Based on the results of 5 years of expanded newborn screening in New York State, the estimated prevalence of CblC is 1:100,000 (Weisfeld-Adams et al. 2010). Elevated levels of propionylcarnitine (C3) and a high C3/C2 (acetyl) ratio could suggest a variety of disorders of propionate metabolism such as methylmalonic acidemia, propionic acidemia, and congenital cobalamin defects including CblC disease. These results require emergent evaluation by a metabolic specialist. Rapid diagnosis and therapy is crucial in the prevention of long-term complications of these disorders.

Here we present a case of CblC that was originally missed by NBS. However, NBS did indicate a low carnitine level, which in turn prompted further investigation leading to diagnosis of CblC.

Communicated by: Rodney Pollitt, PhD

Competing interests: None declared

R.C. Ahrens-Nicklas · E. Serdaroglu · C. Muraresku · C. Ficicioglu
Section of Metabolic Disease, Philadelphia, PA, USA

R.C. Ahrens-Nicklas · C. Muraresku
Division of Human Genetics, The Children's Hospital of Philadelphia, Philadelphia, PA, USA

R.C. Ahrens-Nicklas · C. Ficicioglu (✉)
Department of Pediatrics, Perelman School of Medicine at the University of Pennsylvania, Philadelphia, PA, USA
e-mail: Ficicioglu@email.chop.edu

E. Serdaroglu
Department of Pediatric Neurology, Ihsan Dogramac Children's Hospital Hacettepe University Ankara, Ankara, Turkey

## Clinical Report

The male patient was a full-term infant born to a 19-year-old G1P0 mother via normal spontaneous vaginal delivery after an uneventful pregnancy. He had no complications in the neonatal period and was discharged home on the third day of life. His parents were healthy, nonconsanguineous, and of Mexican descent. There was no known family history of metabolic disease. His NBS collected on his second day of life demonstrated an inconclusive result for a low carnitine (C0) level (9 μmol/L, normal >10.46) and normal C3 level. A repeat NBS on his fourteenth day again reported a normal C3 level and a low C0 level (10.26 μmol/L, normal >10.46) (Table 1).

Given the two low carnitine levels, he was referred to an outside hospital for evaluation of low carnitine at 7 weeks of life. His physical and development examinations were normal at this time. Diagnostic testing at 7–8 weeks of life confirmed the low carnitine level (20 μmol/L, normal 32–62). The metabolic work-up (Table 1) also revealed significantly elevated blood C3 acylcarnitine, total and free homocysteine, and urine and blood MMA. His vitamin B12 level was normal. These findings are consistent with a cobalamin defect. Interestingly, he had a normal methionine level. Methionine is often low in patients with cobalamin defects because they are unable to convert homocysteine to methionine. He was started on carnitine therapy and referred to our center for further evaluation and management.

His diagnosis of CblC was confirmed with fibroblast complementation assays. Gene sequencing of *MMACHC* demonstrated two mutations: c.482G>A (p.R161Q) and c.608G>A (p.W203X).

Therapy was initiated with hydroxycobalamin (1 mg IM three times per week) and levocarnitine (50 mg/kg/day). His biochemical markers of disease improved substantially after initiation of hydroxycobalamin therapy (Table 1). Within five days of his first injection, he had a roughly fivefold reduction in total homocysteine and urine and blood MMA levels. The mainstay of therapy for patients with CblC is parental hydroxycobalamin; this is often combined with oral betaine, carnitine, folate, and methionine as needed. He was also initially started on a low-protein diet that was subsequently liberalized. Hydroxycobalamin, rather than dietary therapy, is the definitive treatment for CblC (Martinelli et al. 2011).

Given his excellent response to hydroxycobalamin, he has not required therapy with betaine. His last exam was at 30 months of age; he has continued on 1 mg/week of IM hydroxycobalamin and has remained in good metabolic control (Table 1) with no episodes of acute metabolic decompensation.

At his 30-month visit, he had normal growth parameters. His examination demonstrated pseudostrabismus and a

**Table 1** Metabolic laboratory values

| Metabolite | Newborn screen #1<br>2 days of life | Newborn screen #2<br>14 days of life | Confirmatory testing<br>2 months of life | Response to OH-cobalamin<br>5 days after first injection | Follow-up values<br>30 months of life |
|---|---|---|---|---|---|
| C0 | 9 μmol/L (borderline <10.46) | 10.26 μmol/L (borderline <10.46) | | | |
| C3 | 2.44 μmol/L (borderline >5.94) | 2.74 μmol/L (borderline >5.94) | 6.14 μmol/L (<0.94) | 5.13 μmol/L (0–1.60) | 1.99 μmol/L (0–1.60) |
| C3/C2 | 0.21 (borderline >0.2, positive >0.26) | 0.4 (borderline >0.2, positive >0.26) | | | |
| Total carnitine | | | 20 μmol/L (32–62) | | 58.5 μmol/L (25–69) |
| Total homocysteine | | | 70.43 μmol/L (<15) | 14.75 μmol/L (<15) | 15.04 μmol/L (<15) |
| Free homocystine | | | 3.3 μmol/L (0) | | <2 μmol/L (0) |
| Methionine | | | 30.3 μmol/L (8–49) | | 41.1 μmol/L (8-49) |
| Blood MMA | | | 15.8 μmol/L (0.1–0.37) | 3.4 μmol/L (0.1–0.37) | 4.8 μmol/L (0.1–0.37) |
| Urine MMA | | | 387.8 mmol MMA/mol Cr (<4) | 61.3 mmol MMA/mol Cr (<4) | Not detected |

speech delay. Ophthalmologic exam demonstrated myopic astigmatism but no other abnormalities.

## Discussion

On newborn screening, elevations in C3 and the C3/C2 ratio are markers for disorders of propionate metabolism including CblC disease. Confirmatory testing including acylcarnitine profile, measurements of homocysteine and MMA, and urine organic acids can help identify an individual's specific diagnosis. Given the wide spectrum of clinical presentations of CblC disease, it is possible that cases could be missed on newborn screening. In a recent review of missed newborn screening cases in New South Wales, Australia, 11/15 missed cases could be attributed to mild phenotypes. Two of these cases were CblC patients (Estrella et al. 2014).

This is a unique case of a missed CblC disease because the patient was ultimately diagnosed through evaluation of a low carnitine level on newborn screen. Low carnitine may lead to a lower C3 acylcarnitine level. Therefore, depending on screening cutoffs, CblC patients with late-onset, mild mutations and low total carnitine levels could be missed on newborn screening.

Genotype-phenotype correlation of *MMACHC* mutations has been reported. While more than 50 mutations have been described, three common mutations exist, which demonstrate genotype-specific age of onset. The c.271dupA and c.331C>T mutations are associated with early-onset disease, while the c.394C>T mutation typically leads to late-onset disease (Lerner-Ellis et al. 2005). Genotypic differences in age of onset are likely due to mRNA stability and transcript levels. Individual variability in residual protein levels and activity results in variable levels of detectable diagnostic metabolites.

Our patient had two previously reported *MMACHC* mutations, c.482G>A (p.R161Q) and c.608G>A (p.W203X). The missense c.482G>A mutation is reported to be a late-onset mutation, with patients generally presenting in second or third decade (Lerner-Ellis et al. 2005, 2009; Morel et al. 2006; Thauvin-Robinet et al. 2007). A case series of five patients identified through NBS with homozygous c.482G>A mutations demonstrated that all were clinically well at age 2.5 months (Lin et al. 2009). Only one of the five patients had elevated blood MMA and homocysteine levels. Compound heterozygous patients carrying the c.482G>A mutation with an early-onset mutation (e.g., c.271dupA) have a milder phenotype than patients with homozygous early-onset mutations (Morel et al. 2006; Carrillo-Carrasco et al. 2011).

The nonsense c.608G>A (p.W203X) mutation found in our case has been previously described in patients of Hispanic origin with early-onset form of CblC (Lerner-Ellis et al. 2005, 2009; Weisfeld-Adams et al. 2010). A similar nonsense mutation, c.609G>A, is the most common mutation in patients of Chinese descent. Severity of disease and age of onset in compound heterozygotes carrying c.609G>A depend on the severity of the other mutation (Wang et al. 2010). Given our patient's compound heterozygosity for a late- and an early-onset mutation, he would be predicted to have a mild clinical presentation.

In addition to a mild mutation, low total carnitine likely masked this patient's diagnosis of CblC disease. Low carnitine can be due to primary carnitine disease or a secondary cause, such as prematurity, (Honzík et al. 2005) or low maternal carnitine levels since carnitine is transferred across the placenta (Stanley 2004). Unfortunately, we were unable to obtain a carnitine sample from our patient's mother. Low carnitine can also be seen in a number of fatty acid oxidation defects and organic acidemias, as free carnitine is consumed by excessive accumulating acyl-CoA species. Therefore this could contribute to missed newborn screens in patients with a variety of inborn errors of metabolism.

To increase the sensitivity of newborn screening for CblC disease, the threshold for labeling C3 as abnormal could be lowered. However, this would greatly increase the rate of false-positive tests. The C3/C2 ratio can also be used as a marker for CblC (McHugh et al. 2011). In retrospective analysis, this ratio was actually elevated in our patient (Table 1). However, in the state where the NBS was performed, the C3/C2 ratio is only reported if the C3 level is elevated. This case suggests that the C3/C2 ratio (and perhaps other ratios such as C3/C0) should be used as a second tier testing marker for disorders of propionate metabolism when the total carnitine level is low.

Some researchers have suggested that NBS reports additional markers, such as methionine and homocysteine, in samples with elevated C3. This could help increase the specificity of screening for cobalaminopathies (Chace et al. 2001; Tortorelli et al. 2010) and differentiate C3 elevations due to cobalaminopathies from methylmalonic acidemia or propionic acidemia. However, it is unclear that the addition of these markers would help increase the sensitivity of the NBS for CblC given that in mild cases these markers, like C3, could be normal.

Given that two NBS failed to detect CblC in our patient, metabolic evaluation and definitive therapy were delayed. Early diagnosis and treatment can improve outcomes but cannot prevent all complications of CblC disease (Rosenblatt et al. 1997; Andersson et al. 1999; Boxer et al. 2005; Smith et al. 2006; Thauvin-Robinet et al. 2007; Martinelli et al. 2011; Aleman et al. 2014). Early therapy may be particularly beneficial for late-onset patients, as it can be started prior to the development of any organ damage (Huemer et al. 2014). However, recent studies have

demonstrated residual neurodevelopmental delays and progression of ocular disease in patients identified by newborn screening and treated since birth (Weisfeld-Adams et al. 2013).

In our case, ordering plasma acylcarnitine profile and urine organic acids (UOA) in addition to blood and urine carnitine levels helped to detect CblC disease. Although the current recommended work-up is to measure blood and urine carnitine levels to rule out primary and nutritional carnitine deficiency in babies with low carnitine level on newborn screen, this case suggests the benefits of adding plasma acylcarnitine and UOA.

In conclusion, newborn screening may not be able to detect all patients with CblC disease. This case report about a newborn with CblC suggests that medical providers should consider CblC in older patients with multisystemic symptoms of unclear etiology such as cognitive decline, neuropsychiatric disease, and unexpected thrombosis.

## Synopsis

A CblC patient may be missed on newborn screening if he carries a late-onset, mild mutation and has low total carnitine levels.

## Compliance with Ethics Guidelines

Conflict of Interest

Rebecca Ahrens-Nicklas declares she has no conflicts of interest.

Esra Serdaroglu declares she has no conflicts of interest.

Colleen Muraresku declares she has no conflicts of interest.

Can Ficicioglu declares he has no conflicts of interest.

This article does not contain any studies with human or animal subjects performed by any of the authors.

## Contributions

Concept/design: RA, ES, CM, CF

Drafting of article: RA, ES

Revision of article: RA, ES, CM, CF

Approval of article: RA, ES, CM, CF

## References

Aleman TS, Brodie F, Garvin C et al (2014) Retinal structure in cobalamin c disease: mechanistic and therapeutic implications. Ophthalmic Genet 2014:1–10. doi:10.3109/13816810.2014.885059

Andersson HC, Marble M, Shapira E (1999) Long-term outcome in treated combined methylmalonic acidemia and homocystinemia. Genet Med 1:146–150. doi:10.1097/00125817-199905000-00006

Boxer AL, Kramer JH, Johnston K et al (2005) Executive dysfunction in hyperhomocystinemia responds to homocysteine-lowering treatment. Neurology 64:1431–1434. doi:10.1212/01.WNL.0000158476.74580.A8

Carrillo-Carrasco N, Chandler RJ, Venditti CP (2011) Combined methylmalonic acidemia and homocystinuria, cblC type. I. Clinical presentations, diagnosis and management. J Inherit Metab Dis 35:91–102. doi:10.1007/s10545-011-9364-y

Chace DH, DiPerna JC, Kalas TA et al (2001) Rapid diagnosis of methylmalonic and propionic acidemias quantitative tandem mass spectrometric analysis of propionylcarnitine in filter-paper blood specimens obtained from newborns. Clin Chem 47:2040–2044

Estrella J, Wilcken B, Carpenter K et al (2014) Expanded newborn screening in New South Wales: missed cases. J Inherit Metab Dis 37:881–887. doi:10.1007/s10545-014-9727-2

Fischer S, Huemer M, Baumgartner M et al (2014) Clinical presentation and outcome in a series of 88 patients with the cblC defect. J Inherit Metab Dis 37:831–840. doi:10.1007/s10545-014-9687-6

Gerth C, Morel CF, Feigenbaum A, Levin AV (2008) Ocular phenotype in patients with methylmalonic aciduria and homocystinuria, cobalamin C type. YMPA 12:591–596. doi:10.1016/j.jaapos.2008.06.008

Honzík T, Chrastina R, HansíkovÄ H et al (2005) Carnitine concentrations in term and preterm newborns at birth and during the first days of life. Prague Med Rep 106:297–306

Huemer M, Scholl-Bürgi S, Hadaya K et al (2014) Three new cases of late-onset cblC defect and review of the literature illustrating when to consider inborn errors of metabolism beyond infancy. Orphanet J Rare Dis 9:161. doi:10.1186/s13023-014-0161-1

Lerner-Ellis JP, Anastasio N, Liu J et al (2009) Spectrum of mutations in MMACHC, allelic expression, and evidence for genotype-phenotype correlations. Hum Mutat 30:1072–1081. doi:10.1002/humu.21001

Lerner-Ellis JP, Tirone JC, Pawelek PD et al (2005) Identification of the gene responsible for methylmalonic aciduria and homocystinuria, cblC type. Nat Genet 38:93–100. doi:10.1038/ng1683

Lin HJ, Neidich JA, Salazar D et al (2009) Asymptomatic maternal combined homocystinuria and methylmalonic aciduria (cblC) detected through low carnitine levels on newborn screening. J Pediatr 155:924–927. doi:10.1016/j.jpeds.2009.06.046

Martinelli D, Deodato F, Dionisi-Vici C (2011) Cobalamin C defect: natural history, pathophysiology, and treatment. J Inherit Metab Dis 34:127–135. doi:10.1007/s10545-010-9161-z

McHugh DMS, Cameron CA, Abdenur JE et al (2011) Clinical validation of cutoff target ranges in newborn screening of metabolic disorders by tandem mass spectrometry: a worldwide collaborative project. Genet Med 13:230–254. doi:10.1097/GIM.0b013e31820d5e67

Morel CF, Lerner-Ellis JP, Rosenblatt DS (2006) Combined methylmalonic aciduria and homocystinuria (cblC): Phenotype–genotype correlations and ethnic-specific observations. Mol Genet Metab 88:315–321. doi:10.1016/j.ymgme.2006.04.001

Rosenblatt DS, Aspler AL, Shevell MI et al (1997) Clinical heterogeneity and prognosis in combined methylmalonic aciduria and homocystinuria (cblC). J Inherit Metab Dis 20:528–538. doi:10.1023/A:1005353530303

Smith SE, Kinney HC, Swoboda KJ, Levy HL (2006) Subacute combined degeneration of the spinal cord in cblC disorder

despite treatment with B12. Mol Genet Metab 88:138–145. doi:10.1016/j.ymgme.2006.02.007

Stanley CA (2004) Carnitine deficiency disorders in children. Ann N Y Acad Sci 1033:42–51. doi:10.1196/annals.1320.004

Thauvin-Robinet C, Roze E, Couvreur G et al (2007) The adolescent and adult form of cobalamin C disease: clinical and molecular spectrum. J Neurol Neurosurg Psychiatry 79:725–728. doi:10.1136/jnnp.2007.133025

Tortorelli S, Turgeon CT, Lim JS et al (2010) Two-tier approach to the newborn screening of methylenetetrahydrofolate reductase deficiency and other remethylation disorders with tandem mass spectrometry. J Pediatr 157:271–275. doi:10.1016/j.jpeds.2010.02.027

Wang F, Han L, Yang Y et al (2010) Clinical, biochemical, and molecular analysis of combined methylmalonic acidemia and hyperhomocysteinemia (cblC type) in China. J Inherit Metab Dis 33:435–442. doi:10.1007/s10545-010-9217-0

Weisfeld-Adams JD, Bender HA, Miley-Åkerstedt A et al (2013) Neurologic and neurodevelopmental phenotypes in young children with early-treated combined methylmalonic acidemia and homocystinuria, cobalamin C type. Mol Genet Metab 110:241–247. doi:10.1016/j.ymgme.2013.07.018

Weisfeld-Adams JD, Morrissey MA, Kirmse BM et al (2010) Molecular genetics and metabolism. Mol Genet Metab 99:116–123. doi:10.1016/j.ymgme.2009.09.008

JIMD Reports
DOI 10.1007/8904_2015_432

RESEARCH REPORT

# Adverse Effects of Genistein in a Mucopolysaccharidosis Type I Mouse Model

**Sandra D.K. Kingma · Tom Wagemans · Lodewijk IJlst · Jurgen Seppen · Marion J.J. Gijbels · Frits A. Wijburg · Naomi van Vlies**

Received: 16 December 2014 / Revised: 10 March 2015 / Accepted: 11 March 2015 / Published online: 09 April 2015


**Abstract** Mucopolysaccharidosis type I (MPS I) is a lysosomal storage disorder characterized by diminished degradation of the glycosaminoglycans heparan sulfate (HS) and dermatan sulfate (DS). Patients present with a variety of symptoms, including severe skeletal disease. Current therapeutic strategies have only limited effects on bone disease. The isoflavone genistein has been studied as a potential therapy for the mucopolysaccharidoses because of its putative ability to inhibit GAG synthesis and subsequent accumulation. Cell, animal, and clinical studies, however, showed variable outcomes. To determine the effects of genistein on MPS I-related bone disease, wild-type (WT) and MPS I mice were fed a genistein-supplemented diet (corresponding to a dose of approximately 160 mg/kg/day) for 8 weeks. HS and DS levels in bone and plasma remained unchanged after genistein supplementation, while liver HS levels were decreased in genistein-fed MPS I mice as compared to untreated MPS I mice. Unexpectedly, genistein-fed mice exhibited significantly decreased body length and femur length. In addition, 60% of genistein-fed MPS I mice developed a scrotal hernia and/or scrotal hydrocele, manifestations ,which were absent in WT or untreated MPS I mice. In contrast to studies in MPS III mice, our study in MPS I mice demonstraes no beneficial but even potential adverse effects of genistein supplementation. Our results urge for a cautious approach on the use of genistein, at least in patients with MPS I.

Communicated by: Ashok Vellodi

S.D.K. Kingma · T. Wagemans · F.A. Wijburg (✉) · N. van Vlies
Department of Pediatrics and Amsterdam Lysosome Centre "Sphinx", Academic Medical Center, University of Amsterdam, Amsterdam, The Netherlands
e-mail: f.a.wijburg@amc.uva.nl

S.D.K. Kingma · T. Wagemans · L. IJlst · N. van Vlies
Laboratory of Genetic Metabolic Diseases, Department of Clinical Chemistry and Pediatrics, Academic Medical Center, University of Amsterdam, Amsterdam, The Netherlands

J. Seppen
Tytgat Institute for Liver and Intestinal Research, Academic Medical Center, University of Amsterdam, Amsterdam, The Netherlands

M.J.J. Gijbels
Department of Medical Biochemistry, Academic Medical Center, University of Amsterdam, Amsterdam, The Netherlands

M.J.J. Gijbels
Department of Molecular Genetics and Department of Pathology, Cardiovascular Research Institute Maastricht, Maastricht, The Netherlands

## Introduction

Mucopolysaccharidosis type I (MPS I, OMIM 252800) is a lysosomal storage disease (LSD) caused by α-L-iduronidase (IDUA, EC 3.2.1.76) deficiency, resulting in impaired degradation and subsequent accumulation of the glycosaminoglycans (GAGs) heparan sulfate (HS) and dermatan sulfate (DS). Patients may present with cardiac and pulmonary disease, inguinal and umbilical hernias, corneal clouding, and progressive central nervous system (CNS) disease which significantly limits life expectancy (Muenzer 2011). In addition, skeletal dysplasia, generally referred to as dysostosis multiplex, is a striking feature and a major cause of morbidity. Patients show progressive loss of range of joint motion with contractures, growth arrest, kyphosis, scoliosis, hip dysplasia, and hypoplastic vertebral bodies resulting in spinal cord compression (Muenzer 2011; White 2011). Current therapies, including hematopoietic stem cell transplantation (HSCT) and enzyme replacement therapy, effectively treat many features of MPS I but have limited effects on bone disease (Weisstein et al. 2004; Sifuentes et al. 2007).

Several factors contribute to this lack of effect. Firstly, the inability of the relatively large enzyme to traffic through the poorly vascularized matrix of growth plates and other cartilaginous tissue to target cells (Aldenhoven et al. 2009; Baldo et al. 2013). Secondly, cartilage cells are derived from mesenchymal stem cells, which are not transplanted in sufficient amounts by HSCT (Koç et al. 2002). Thirdly, therapy is started after the onset of irreversible bone lesions, which may already exist before birth (Martin and Ceuterick 1983; Hinek and Wilson 2000). An alternative treatment strategy for LSDs is substrate reduction therapy, which aims to reduce the synthesis of the accumulating material, thereby preventing or halting lysosomal storage. This approach has been used successfully in Gaucher disease and Niemann–Pick disease type C (Hollak and Wijburg 2014).

The isoflavone genistein has several biological activities. It is an antioxidant, has estrogenic activity, and inhibits the activity of tyrosine kinase receptors including the epidermal growth factor receptor (EGFR) (Akiyama et al. 1987; Dixon and Ferreira 2002). Genistein has been shown to reduce GAG synthesis in MPS fibroblasts, at least partly via the latter mechanism (Jakóbkiewicz-Banecka et al. 2009). An in vivo study with a high dose of genistein in MPS IIIB mice showed reduced GAG levels in brain and impressive amelioration of neurological symptoms (Malinowska et al. 2010). Although genistein appears to be well tolerated in high doses, adverse effects, which are associated with its potential antiproliferative and estrogenic actions, have been reported and may include hepatotoxicity and hormonal disbalance (Kim et al. 2013; Singh et al. 2014). The only study on the effects of genistein on MPS-related bone disease showed increased range of joint motion in genistein-treated MPS II patients, suggesting that genistein at least reaches the surrounding connective and muscle tissue of the joints (Marucha et al. 2011). Because genistein can reach the bone tissue (Coldham and Sauer 2000), we fed MPS I mice a high-dose genistein diet to evaluate its potential for the treatment of MPS I-related bone disease.

## Materials and Methods

### Animals

MPS I mice (B6.129-*Idua*$^{tm1Clk}$/J, (Clarke et al. 1997)) were purchased from Jackson Laboratory and maintained as a heterozygote line on an inbred C57BL/6J background at the Academic Medical Center. The mice were housed at 21 ± 1°C, 40–50% humidity, on a 12 h light–dark cycle, with ad libitum access to water and food. Genotypes were identified by PCR using a protocol provided by Jackson Laboratory.

An AIN93M diet (Reeves 1997) with 3.7% sunflower oil and 0.3% rapeseed oil instead of 4% soy oil was produced (Research Diet Services BV). For the genistein-fed group, genistein aglycone (kind gift from Axcentua) was added to the diet in a concentration of 0.1% (w/w). Assuming a food intake of 0.16 g food per gram of body weight per day, this diet results in a dose of 160 mg/kg/day, which is similar to other studies on the effects of a high dose of genistein in MPS mice (Malinowska et al. 2009, 2010). One week before weaning, mice received the soy-free diet. At 3 weeks of age, male wild-type (WT) and MPS I mice were weaned on the soy-free diet or the genistein-supplemented diet ($n = 10$ per group). Every week, mice were weighed and examined for general pathological manifestations. If scrotal abnormalities were observed, scrotal hydrocele and/or scrotal hernias were objectified by macroscopic inspection, transillumination, and/or ultrasound by a skilled animal technician and macroscopic inspection of the scrotum and abdominal and pelvic cavity after sacrifice. At 11 weeks of age, mice were anesthetized with an intraperitoneal injection of 100 mg/kg pentobarbital and euthanized by exsanguination via cardiac puncture. Body length and femur length were measured, and blood and tissues collected.

All animal experiments were approved by the animal institutional review board at the Academic Medical Center, University of Amsterdam.

### Tissue Processing

Blood was collected into EDTA tubes, kept on ice, and centrifuged at 240 g for 10 min. Plasma was collected and stored at −80°C until analysis. Mouse livers were snap-freezed in liquid nitrogen and stored at −80°C. Before analysis, mouse livers were homogenized in PBS, and protein concentration was determined using Pierce® BCA Protein Assay Reagent A (Thermo Scientific) as described by the manufacturer. Mouse humeri were collected and placed in 0.9% NaCl containing complete mini protease inhibitor cocktail (Roche Applied Science) at 4°C for >1 day. Next, soft tissue was removed, and humeri were stored at −80°C. Before analysis, humeri were homogenized in PBS, sonificated twice for 15 s on 40 joules/watt/second using a Vibra Cell sonicator (Sonics & Materials Inc.), and centrifuged for 1 min at 400 g. Protein concentration of the supernatant was determined as described above.

### GAG Analysis

GAG levels in mouse plasma, liver, and humerus homogenates were determined using HPLC-MS/MS, as described previously (de Ru et al. 2013), with one modification for tissue samples: 12.5 µg protein of liver or humerus

homogenates were used. Genistein supplementation did not alter HS or DS disaccharide composition; therefore, only values of the most abundant HS derived disaccharide D0A0 and DS derived disaccharide D0a4 are given.

### Genistein Measurement

Genistein levels were determined by ultrahigh performance liquid chromatography (UHPLC) with a protocol modified from Seppen et al. (2012). 40 µl of plasma or humerus homogenate was acidified with 5 µl 1M 4-morpholineethanesulfonic acid. Genistein was hydrolyzed by adding 2.5 µl β-glucuronidase (Sigma Aldrich) and 2.5 µl sulfatase (10 mg/ml in PBS, Sigma Aldrich) and incubated at 37°C for 20 h. Protein was precipitated by adding 100 µl methanol and samples were centrifuged at 8,000g for 2 min. The supernatant was vaporized using a Techne® Dri-block® heater (Bibby Scientific) and the residue dissolved in 20% v/v acetonitrile.

UHPLC was performed on a Dionex UltiMate 3000 UHPLC, equipped with a PolarAdvantage C18 column (Thermo Scientific), variable wavelength detector set at 260 nm, 5 µl injection, and a flow rate of 0.5ml/min. The following program was used with solvent A (A, 0.1% v/v formic acid in water) and solvent B (B, 0.1% v/v formic acid in acetonitrile): start 30% B, $t = 5$ 55% B, $t = 5.1$ 100% B, $t = 6.1$ 30% B, and $t = 10$ 30% B. Linear gradients were employed and $t$ is in minutes. Dionex Chromeleon software (Thermo Scientific) was used to integrate the chromatograms, and genistein level was calculated using a calibration curve of genistein dissolved in dimethyl sulfoxide, diluted in mouse plasma.

### Morphology of Testes

The morphology of testicular cells and structures was analyzed by routine hematoxylin/eosin (HE) staining.

### Statistical Analysis

Statistical analysis was performed using Mann–Whitney $U$ tests for nonparametric analysis with SPSS Statistics software version 21 (IBM Corp.). Significance was assumed where $p$ values were $<0.05$.

## Results

### Genistein Decreases GAG Levels in the Liver but Not in the Bone or Plasma

As expected, analysis of GAG levels revealed significantly higher levels in MPS I plasma and tissues ($p < 0.0001$), as compared to WT (Fig. 1). Genistein supplementation did not affect GAG levels in WT or MPS I bone or plasma (Fig. 1a, b). HS levels in the liver from genistein-fed MPS I mice were 25% decreased ($p < 0.01$), as compared to untreated mice. No difference in liver DS levels was observed between genistein-fed and untreated MPS I mice (Fig. 1c).

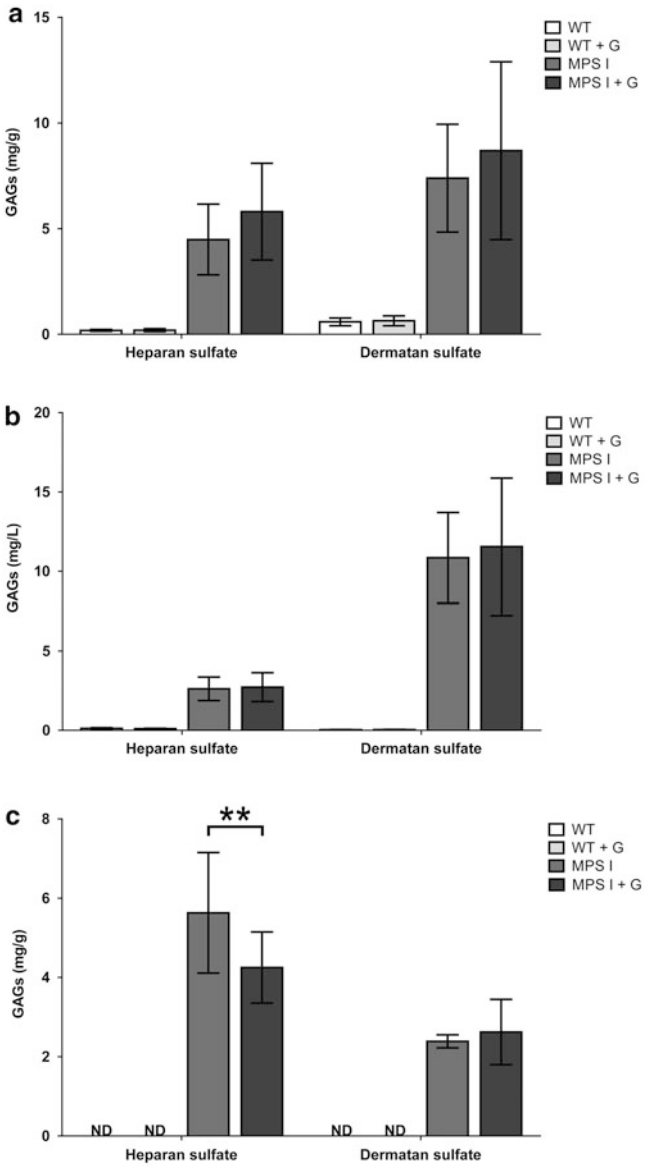


**Fig. 1** GAG levels. GAG levels in the bone (**a**), plasma (**b**), and liver (**c**) in control and genistein-supplemented mice. The results are expressed as milligrams GAGs per gram of protein for the liver and bone or as milligrams GAGs per liter of plasma. All values are mean ± standard deviation of 10 mice. Each sample was analyzed in duplicate, $^{**}p < 0.01$, ND not detectable, G genistein supplementation

### Genistein Was Present in the Plasma but Undetectable in the Bone

Genistein levels in the plasma of genistein-fed MPS I mice were 782 nM ±503. In the control group, genistein concentration in the plasma was below the limit of quantification (data not shown). Genistein levels in the bone were below detection level in all MPS I mice (data not shown).

### Genistein Causes Decreased Skeletal Growth and Scrotal Hernia/Hydrocele in MPS I Mice

Total body weight of MPS I mice was 11% increased ($p < 0.05$), as compared to WT mice (Fig. 2a). Total body weight of genistein-fed MPS I mice was decreased by 16% ($p < 0.001$) (Fig. 2a), as compared to untreated MPS I mice. Following genistein supplementation, total body length was 4% ($p < 0.05$) and 6% ($p < 0.001$) decreased in WT and MPS I mice (Fig. 2b), respectively, as compared to untreated mice. Femur length of MPS I mice was 4% decreased ($p < 0.05$), as compared to WT mice (Fig. 2c). Femur length of genistein-fed mice were 3% ($p < 0.01$) and 7% ($p < 0.001$) decreased in WT and MPS I mice (Fig. 2c), respectively, compared to untreated mice. Surprisingly, 60% of the genistein-fed MPS I mice had an enlarged scrotum (Fig. 3) with redness of the overlying skin, and the mice showed a wide-based gait. None of the WT or untreated MPS I mice showed scrotal abnormalities. The scrotal enlargements were observed to be due to either scrotal hernia and/or scrotal hydrocele. HE staining of testes revealed no morphological changes of testicular cells and structures in genistein-fed or untreated mice (results not shown).

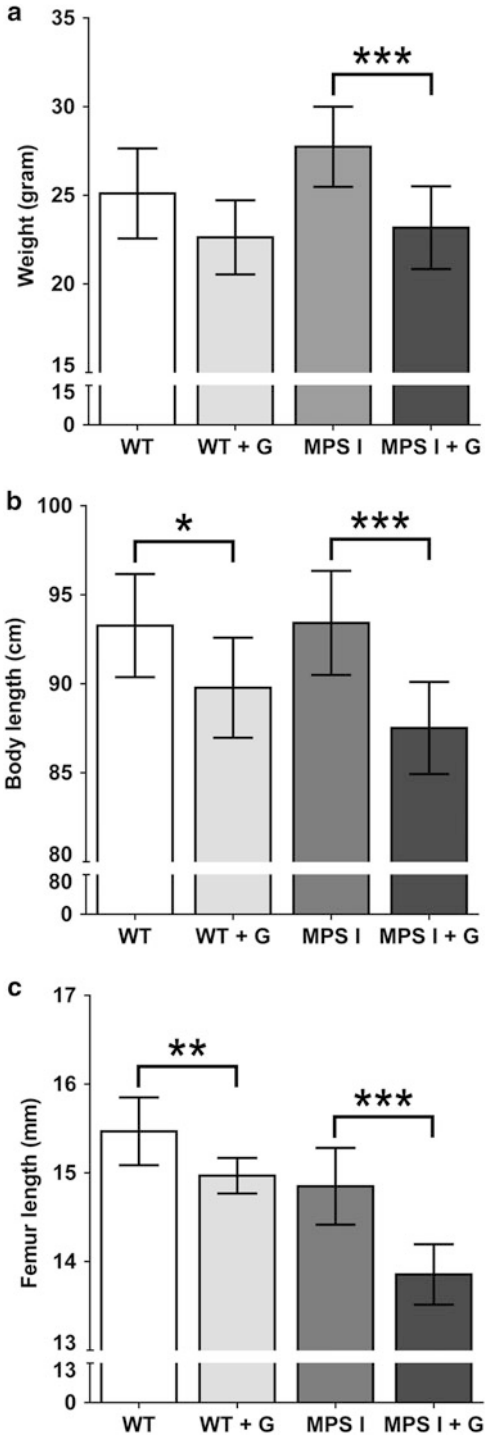


**Fig. 2** Weight, body length, and femur length. Weight (**a**), body length (**b**), and femur length (**c**) in control and genistein-supplemented mice. All values are mean ± standard deviation of 10 mice, *$p < 0.05$, **$p < 0.01$, ***$p < 0.001$, G genistein supplementation

## Discussion

Skeletal disease is one of the most prevalent and incapacitating disease manifestations in patients suffering from the MPSs and frequently results in the need for multiple surgical interventions (Muenzer 2011; White 2011). Current disease-modifying therapies for the management of MPS I ameliorate a number of clinical signs and symptoms but have a limited effect on the progression of skeletal disease (Weisstein et al. 2004; Sifuentes et al. 2007). Therefore, therapeutic strategies targeting bone disease are urgently needed.

The isoflavone genistein inhibits the activity of tyrosine kinase receptors, thereby modulating the expression of several genes, including some involved in GAG synthesis (Akiyama et al. 1987; Moskot et al. 2014). Genistein is being investigated for its potential benefit in the treatment of CNS disease in MPS III, as it passes the blood–brain barrier, and an in vivo study showed that genistein may reduce GAG accumulation in the brain and corrects behavioral abnormalities in MPS III mice (Tsai 2005;


**Fig. 3** Scrotal abnormalities. Scrotum of a MPS I mouse on control diet (**a**) and a MPS I mouse on genistein diet (**b**). 60% of MPS I mice with genistein had either scrotal hydrocele or scrotal hernia, as depicted in (**b**). All other mice had scrota as depicted in (**a**)

Malinowska et al. 2010; Langford-Smith et al. 2011). As prevention of GAG accumulation in the cartilage and bone might halt the progression of skeletal disease in the MPSs, we investigated the effects of genistein on GAG accumulation in MPS I mice in order to evaluate its potential for the treatment of MPS I-related bone disease.

In agreement with results of previously published studies on the effects of genistein in MPS mice (Malinowska et al. 2009; Friso et al. 2010), GAG levels were significantly decreased in the liver of genistein-fed MPS I mice. Surprisingly, we observed no effect on GAGs in the bone or plasma. The effect of genistein on GAG levels in the bone or plasma of MPS III mice has not been described in previous studies (Malinowska et al. 2009, 2010; Friso et al. 2010). In rats, genistein is known to reach bone in approximately 17 times lower quantities when compared to plasma levels, 2 h after administration of 4 mg/kg genistein (Coldham and Sauer 2000) (in the current study, we used 160 mg/kg/day oral supplementation). Although plasma genistein concentrations in our study were comparable with or even higher than the concentrations reported in other studies on the effects of genistein in mice (Santell et al. 2000; Mentor-Marcel et al. 2001), genistein concentrations in the bone in our study were below detection level. These results suggest that the treatment duration and/or dosage of genistein may have been insufficient to treat the bone. In our study, mice were treated from 3 weeks of age, for a period of 8 weeks as, at 11 weeks of age, the growth plate is almost closed and skeletal development almost completed. Therefore, we do not expect any additional effect on the bone with a longer supplementation period. Earlier initiation of genistein supplementation is not feasible as mice are weaned at 3 weeks of age.

Our observation that genistein supplementation led to decreased body weight in mice was not surprising. Although not decreased previously in MPS III mice (Malinowska et al. 2009, 2010; Friso et al. 2010), the effect of genistein on decreasing lipid deposition and body weight has been reported earlier in mice and rats and may be due to the estrogenic effect of increasing lipoprotein lipase activity (Naaz et al. 2003) or decreased food intake (Seppen 2012). Genistein-fed mice in our study, however, also exhibited decreased skeletal growth, including decreased femur length, which has not been described previously. In addition, 60% of genistein-fed MPS I mice developed a scrotal hernia and/or a scrotal hydrocele. The cause of the decrease in skeletal growth and the observed scrotal hernia/hydroceles is unclear. Increased levels of DS, an abundant GAG in connective tissue, may have contributed to the development of adverse effects, as our recently published study showed that genistein can increase HS and DS storage in MPS I chondrocytes and fibroblasts (but not in osteoblasts) (Kingma et al. 2014). In the present study, GAG levels were analyzed in complete bones, and chondrocytes only make up a small portion of the entire bone. This might explain the fact that no increase in GAG levels was observed in the bones of genistein-treated MPS I mice, while these animals did show a decrease in femur length. Increased GAG storage in certain cell types might further stimulate the pathophysiological mechanisms causing bone and connective tissue disease in MPS I. In addition, patients with MPS I already frequently display hernias and hydroceles (Arn et al. 2009). Genistein may thus lead to a more severe MPS I phenotype, at least in mice. Therefore, increasing the dose of genistein or prolonging the supplementation period likely will not result in amelioration of bone disease in MPS I mice. The only study in patients on the effects of a high dose, i.e., 150 mg/kg/day, of (synthetic) genistein (at least 1-year treatment of 22 MPS III patients) concluded that genistein is safe but did report elevation of liver enzymes, breast development in

boys or young girls, menstrual irregularities, and bilateral deep vein thrombosis in a 20-year-old woman with several other risk factors for thrombosis (Kim et al. 2013). This study did not report on growth rate.

In conclusion, our study suggests that high doses of genistein might lead to decreased growth and increased incidence of scrotal hydroceles and hernias, at least in MPS I. These data, in combination with other potential adverse effects reported in previous studies (Kim et al. 2013; Singh et al. 2014), support a cautious approach to the introduction of high doses of genistein in patients with various MPSs and underscores the need for well-designed and controlled clinical trials allowing the collection of all potential adverse effects over longer periods of time.

**Acknowledgments** We thank Ronald Wanders, Henk van Lenthe, Wim Kulik, and Jos Ruijter for technical assistance and helpful discussions. We thank Axcentua for providing genistein. This work was financially supported by the foundation "Steun Emma Kinderziekenhuis AMC" and the "WE Foundation."

## Take-Home Message

Genistein-fed mucopolysaccharidosis type I mice exhibit scrotal hernias/hydroceles and decreased skeletal growth, emphasizing the need for caution when using genistein in patients with MPS.

## Compliance with Ethics Guidelines

Conflicts of Interest

Sandra Kingma, Tom Wagemans, Lodewijk IJlst, Jurgen Seppen, Marion Gijbels, Frits Wijburg, and Naomi van Vlies declare that they have no conflicts of interest.

## Informed Consent

This article does not contain any studies with human subjects performed by any of the authors.

## Animal Rights

All institutional and national guidelines for the care and use of laboratory animals were followed.

## Contributions of the Individual Authors

Sandra D.K. Kingma: designing, conducting, reporting, and revising the work described in the article.

Tom Wagemans: conducting the work described in the article.

Lodewijk IJlst: designing and revising the work described in the article.

Jurgen Seppen: conducting and revising the work described in the article.

Marion J.J. Gijbels: conducting and revising the work described in the article.

Frits A. Wijburg: designing, reporting, and revising the work described in the article.

Naomi van Vlies: designing, reporting, and revising the work described in the article.

## References

Akiyama T, Ishida J, Nakagawa S et al (1987) Genistein, a specific inhibitor of tyrosine-specific protein kinases. J Biol Chem 262: 5592–5595

Aldenhoven M, Sakkers RJB, Boelens J, de Koning TJ, Wulffraat NM (2009) Musculoskeletal manifestations of lysosomal storage disorders. Ann Rheum Dis 68:1659–1665

Arn P, Wraith JE, Underhill L (2009) Characterization of surgical procedures in patients with mucopolysaccharidosis type I: findings from the MPS I Registry. J Pediatr 154:859–64.e3

Baldo G, Mayer FQ, Martinelli BZ et al (2013) Enzyme replacement therapy started at birth improves outcome in difficult-to-treat organs in mucopolysaccharidosis I mice. Mol Genet Metab 109: 33–40

Clarke LA, Russell CS, Pownall S et al (1997) Murine mucopolysaccharidosis type I: targeted disruption of the murine alpha-L-iduronidase gene. Hum Mol Genet 6:503–511

Coldham NG, Sauer MJ (2000) Pharmacokinetics of [(14)C]Genistein in the rat: gender-related differences, potential mechanisms of biological action, and implications for human health. Toxicol Appl Pharmacol 164:206–215

De Ru MH, van der Tol L, van Vlies N et al (2013) Plasma and urinary levels of dermatan sulfate and heparan sulfate derived disaccharides after long-term enzyme replacement therapy (ERT) in MPS I: correlation with the timing of ERT and with total urinary excretion of glycosaminoglycans. J Inherit Metab Dis 36: 247–255

Dixon RA, Ferreira D (2002) Genistein. Phytochemistry 60:205–211

Friso A, Tomanin R, Salvalaio M, Scarpa M (2010) Genistein reduces glycosaminoglycan levels in a mouse model of mucopolysaccharidosis type II. Br J Pharmacol 159:1082–1091

Hinek A, Wilson SE (2000) Impaired elastogenesis in Hurler disease: dermatan sulfate accumulation linked to deficiency in elastin-binding protein and elastic fiber assembly. Am J Pathol 156: 925–938

Hollak CEM, Wijburg FA (2014) Treatment of lysosomal storage disorders: successes and challenges. J Inherit Metab Dis 37: 587–598

Jakóbkiewicz-Banecka J, Piotrowska E, Narajczyk M, Barańska S, Wegrzyn G (2009) Genistein-mediated inhibition of glycosaminoglycan synthesis, which corrects storage in cells of patients suffering from mucopolysaccharidoses, acts by influencing an epidermal growth factor-dependent pathway. J Biomed Sci 16:26

Kim KH, Dodsworth C, Paras A, Burton BK (2013) High dose genistein aglycone therapy is safe in patients with mucopolysaccharidoses involving the central nervous system. Mol Genet Metab 109:382–385

Kingma SDK, Wagemans T, IJlst L, Wijburg FA, van Vlies N (2014) Genistein increases glycosaminoglycan levels in mucopolysaccharidosis type I cell models. J Inherit Metab Dis 37:813–821

Koç ON, Day J, Nieder M, Gerson SL, Lazarus HM, Krivit W (2002) Allogeneic mesenchymal stem cell infusion for treatment of metachromatic leukodystrophy (MLD) and Hurler syndrome (MPS-IH). Bone Marrow Transplant 30:215–222

Langford-Smith A, Malinowska M, Langford-Smith KJ et al (2011) Hyperactive behaviour in the mouse model of mucopolysaccharidosis IIIB in the open field and home cage environments. Genes Brain Behav 10:673–682

Malinowska M, Wilkinson FL, Bennett W et al (2009) Genistein reduces lysosomal storage in peripheral tissues of mucopolysaccharide IIIB mice. Mol Genet Metab 98:235–242

Malinowska M, Wilkinson FL, Langford-Smith KJ et al (2010) Genistein improves neuropathology and corrects behaviour in a mouse model of neurodegenerative metabolic disease. PLoS One 5:e14192

Martin JJ, Ceuterick C (1983) Prenatal pathology in mucopolysaccharidoses: a comparison with postnatal cases. Clin Neuropathol 2:122–127

Marucha J, Tylki-Szymańska A, Jakóbkiewicz-Banecka J, Piotrowska E, Kloska A, Czartoryska B, Węgrzyn G (2011) Improvement in the range of joint motion in seven patients with mucopolysaccharidosis type II during experimental gene expression-targeted isoflavone therapy (GET IT). Am J Med Genet A 155A:2257–2262

Mentor-Marcel R, Lamartiniere CA, Eltoum I, Greenberg NM, Elgavish A (2001) Genistein in the Diet Reduces the Incidence of Poorly Differentiated Prostatic Adenocarcinoma in Transgenic Mice (TRAMP). Cancer Res 61:6777–6782

Moskot M, Montefusco S, Jakóbkiewicz-Banecka J et al (2014) The phytoestrogen genistein modulates lysosomal metabolism and transcription factor EB (TFEB) activation. J Biol Chem 289: 17054–17069

Muenzer J (2011) Overview of the mucopolysaccharidoses. Rheumatol (Oxford, England)) 50(Suppl 5):v4–v12

Naaz A, Yellayi S, Zakroczymski M (2003) The soy isoflavone genistein decreases adipose deposition in mice. Endocrinology 144:3315–3320

Reeves PG (1997) Components of the AIN-93 diets as improvements in the AIN-76A diet. J Nutr 127:838S–841S

Santell RC, Kieu N, Helferich WG (2000) Genistein inhibits growth of estrogen-independent human breast cancer cells in culture but not in athymic mice. J Nutr 130:1665–1669

Seppen J (2012) A diet containing the soy phytoestrogen genistein causes infertility in female rats partially deficient in UDP glucuronyltransferase. Toxicol Appl Pharmacol 264:335–342

Sifuentes M, Doroshow R, Hoft R et al (2007) A follow-up study of MPS I patients treated with laronidase enzyme replacement therapy for 6 years. Mol Genet Metab 90:171–180

Singh P, Sharma S, Rath SK (2014) Genistein induces deleterious effects during its acute exposure in Swiss mice. Biomed Res Int 2014:619617

Tsai T-H (2005) Concurrent measurement of unbound genistein in the blood, brain and bile of anesthetized rats using microdialysis and its pharmacokinetic application. J Chromatogr A 1073:317–322

Weisstein JS, Delgado E, Steinbach LS, Hart K, Packman S (2004) Musculoskeletal manifestations of Hurler syndrome: long-term follow-up after bone marrow transplantation. J Pediatr Orthop 24:97–101

White KK (2011) Orthopaedic aspects of mucopolysaccharidoses. Rheumatology 50(Suppl 5):v26–v33

JIMD Reports
DOI 10.1007/8904_2015_434

CASE REPORT

# Expanding the Clinical and Magnetic Resonance Spectrum of Leukoencephalopathy with Thalamus and Brainstem Involvement and High Lactate (LTBL) in a Patient Harboring a Novel *EARS2* Mutation

**Roberta Biancheri · Eleonora Lamantea · Mariasavina Severino · Daria Diodato · Marina Pedemonte · Denise Cassandrini · Alexandra Ploederl · Federica Trucco · Chiara Fiorillo · Carlo Minetti · Filippo M. Santorelli · Massimo Zeviani · Claudio Bruno**

Received: 02 February 2015 / Revised: 23 February 2015 / Accepted: 06 March 2015 / Published online: 09 April 2015


**Abstract** Leukoencephalopathy with thalamus and brainstem involvement and high lactate (LTBL) is a novel mitochondrial disease caused by mutations in *EARS2*, which encodes the mitochondrial glutamyl-tRNA synthetase (mtGluRS). A distinctive brain MRI pattern is the hallmark of the disease.

A 6-year-old boy presented at 3 months with feeding difficulties and muscle hypotonia. Brain MRI, at 8 months, showed hyperintensity of the deep cerebral and cerebellar white matter, thalamus, basal ganglia, brainstem, and thin corpus callosum. From the second year of life onward, the child reported global clinical improvement, parallel to partial resolution of brain MRI pattern. However, the last neuroimaging assessment revealed novel lesions within the left caudate and pallidum nuclei. DNA genomic sequencing analysis identified a novel *EARS2* mutation.

This case expands the clinical and neuroradiological phenotype of LTBL presenting intermediate clinical manifestations between the severe and milder forms of the disease and previously unreported brain MRI features.

Communicated by: Nicole Wolf, MD PhD

Competing interests: None declared

R. Biancheri · A. Ploederl
Child Neurology and Psychiatry, Istituto Giannina Gaslini, Genoa, Italy

E. Lamantea · D. Diodato · M. Zeviani
Unit of Molecular Neurogenetics Pierfranco and Luisa Mariani Center for the Study of Mitochondrial Disorders in Children, Fondazione IRCCS Istituto Neurologico "Carlo Besta", Milan, Italy

M. Severino
Neuroradiology Unit, Istituto Giannina Gaslini, Genoa, Italy

M. Pedemonte · F. Trucco · C. Minetti
Pediatric Neurology Unit, Istituto Giannina Gaslini, Genoa, Italy

D. Cassandrini · C. Fiorillo · F.M. Santorelli
Neuromuscular and Molecular Medicine Unit, IRCCS Stella Maris, Pisa, Italy

C. Bruno (✉)
Department of Neuroscience, Center of Myology and Neurodegenerative Disorders, Istituto Giannina Gaslini, Genoa, Italy
e-mail: claudio2246@gmail.com

## Introduction

Leukoencephalopathy with thalamus and brainstem involvement and high lactate (LTBL) has been recently defined as a novel mitochondrial disease condition characterized by early onset of neurologic symptoms, a biphasic clinical course, and peculiar neuroimaging (Steenweg et al. 2012a).

LTBL is caused by mutations in *EARS2* gene, encoding mitochondrial glutamyl-tRNA synthetase (mtGluRS) (Steenweg et al. 2012a).

We identified a novel *EARS2* mutation in a patient whose clinical and brain MRI features expand the phenotypic spectrum of LTBL.

## Case Report

A 6-year-old boy, only child of healthy unrelated parents, was born at term after uneventful pregnancy and normal

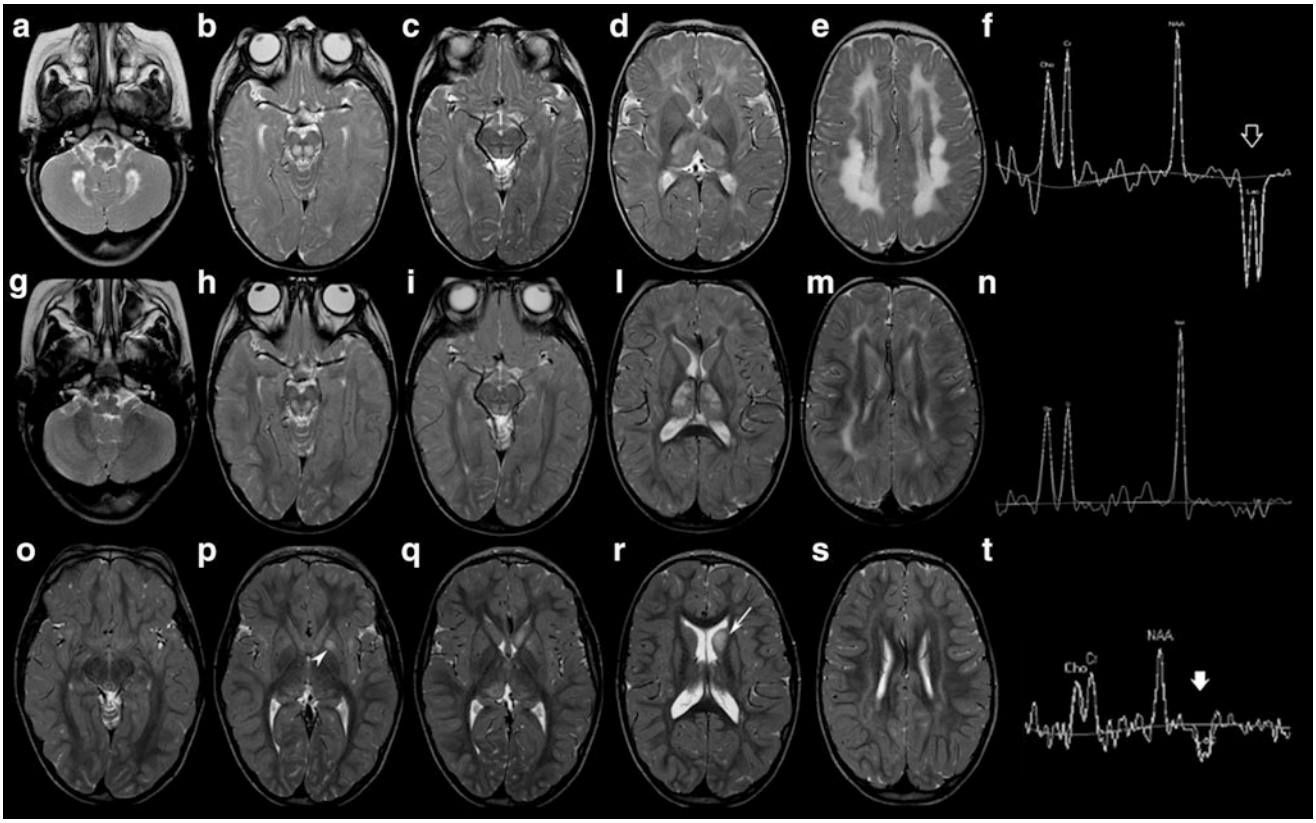


**Fig. 1** Brain MRI and MRS at age 8 months (**a**–**f**), 29 months (**g**–**n**), and 5 years and 10 months (**o**–**t**). Axial T2-weighted images show symmetrical T2 hyperintensity of the deep cerebral white matter, thalamus, basal ganglia, brainstem, cerebellar white matter, and dentate nuclei (**a**–**e**). MRS of the cerebral white matter shows markedly increased lactate (*empty arrow*, **f**). At age 29 months, axial T2-weightwed images show a substantial improvement of the signal abnormalities (**g**–**m**). MRS of the cerebral white matter reveals significantly reduced lactate (**n**). Three years later, axial T2-weighted images depict further improvement of these lesions (**o**–**s**). New signal abnormalities of the left caudate (*arrow*) and globus pallidus (*arrowhead*) are evident. MRS shows high lactate in the left caudate head (*thick arrow*, **t**)

delivery. Birth weight was 3,430 g. Perinatal period was normal (APGAR score 9/10). At age 3 months, he presented with feeding difficulties, vomiting, failure to thrive, and muscle hypotonia. At age 8 months, his neurological examination showed developmental delay, axial muscle hypotonia, brisk tendon reflexes in all limbs, poor head control, and inability of sitting unaided. Laboratory investigations showed increased levels of lactate in plasma (46.4 mg/dl; normal range 8–22 mg/dl) but not in urine. EEG was normal. Brain MRI showed symmetrical T2 hyperintensities with restricted diffusion of the cerebral deep white matter, thalami, midbrain, dorsal part of the pons and medulla oblongata, dentate nuclei, and cerebellar white matter. A periventricular white matter rim was spared. The corpus callosum was thin (Fig. 1a–e). Single-voxel proton MR spectroscopy (MRS) showed markedly increased lactate (Fig. 1f).

At 10 months, a muscle biopsy revealed ragged-red and cytochrome c oxidase-negative fibers (Fig. 2), whereas spectrophotometric determination of respiratory chain complexes showed reduced activities of complexes I, III, and IV in the muscle homogenate.

The patient was treated with riboflavin (10 mg/day), thiamine (100 mg/day), and CoQ10 (100 mg/day).

At 14 months, neurological examination showed normal head circumference, mild axial muscle hypotonia, increased muscle tone in lower limbs, and brisk tendon reflexes in all limbs, but the child had acquired the ability of sitting without support and of standing with support.

Over the following 2 years, the clinical course showed significant improvement with the child being able to walk with support at the age of 21 months and without aid at 24 months. Nonetheless, the Griffiths developmental scale performed at 21 months showed a global development age of 11 months. At 29 months, neurological examination confirmed the presence of pyramidal signs with autonomous toe walking and widened base gait; the Griffiths developmental scale showed a development age of 15 months.

A brain MRI at age 30 months revealed striking improvement of the signal abnormalities and marked

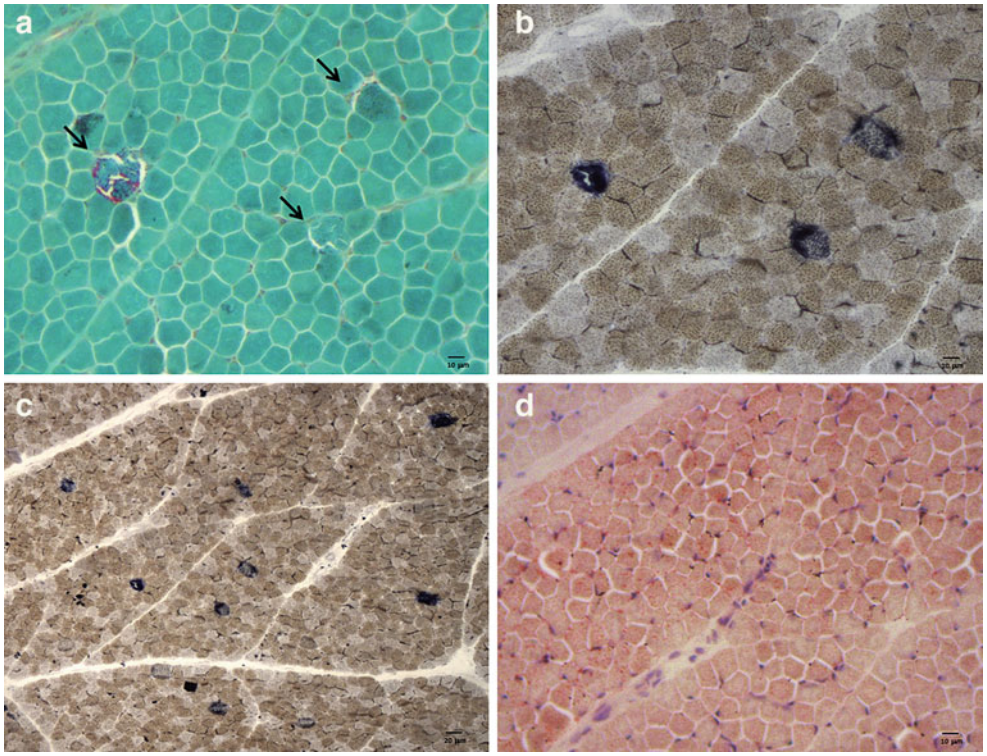


**Fig. 2** Muscle biopsy. (**a**) Trichrome staining showing three ragged-red fibers (*arrows*). (**b**) Combined COX–SDH staining (magnification 20×) confirms the same ragged-red fibers as COX-negative–SDH-positive fibers. (**c**) Combined COX–SDH staining (magnification 10×) highlighting several scattered COX-negative–SDH-positive fibers. (**d**) Oil red O staining showing lipid accumulation

reduction of lactate in single-voxel proton MRS. Restricted diffusion persisted only in the thalami and posterior part of the pons (Fig. 1g–n).

During the following years, the patient showed progressive improvement of motor functions and never suffered from seizures. Blood lactate values progressively lowered from 46.4 mg/dl at 8 months to 33.4 mg/dl at 14 months, 32.5 mg/dl at 21 months, 33.3 mg/dl at 4 years, 19.4 mg/dl at 5 years, and 16.7 mg/dl at 6 years. Cardiac (including ECG and echocardiography), funduscopy, and hearing assessments were normal, as well as sensory and motor nerve conduction velocity studies. The last brain MRI, performed at the age of 5 years and 10 months, showed further improvement, although new areas of T2 hyperintensity without diffusion restriction were present within the head of the left caudate nucleus and pallidum, with a lactate peak on multi-voxel proton MRS (Fig. 1o–t). At this time the child showed mild generalized muscle weakness and unsupported toe walking gait with widened base.

At 6 years, cognitive assessment (WISC-IV) revealed a highly disharmonic profile with the following results: verbal comprehension index (VCI 92), perceptual organization index (POI 58), processing speed index (PSI 56), and working memory index (WMI 64) resulting into total intelligence quotient (IQ 58), i.e., mild mental retardation.

Since the MRI pattern and the muscle biopsy findings corresponded to those reported in leukoencephalopathy with thalamus and brainstem involvement and high lactate (LTBL), after receiving written informed consent from the parents of the patient, in agreement with the Declaration of Helsinki and approved by the Ethical Committees of the Fondazione IRCCS Istituto Neurologico "C. Besta," Milan, Italy, we analyzed the nucleotide sequence of the exons and exon–intron boundaries of EARS2 gene. We found a new homozygous variant (c.902G>C/p.Gly301Ala) in EARS2. The mutation was heterozygous in the healthy parents and absent in the public single-nucleotide polymorphism databases, including dbSNP (http://www.ncbi.nlm.nih.gov/projects/SNP) and EVS (http://evs.gs.washington.edu/EVS), which altogether contain approximately 12,000 alleles. In addition, the p.Gly301Ala change scored very highly for likelihood to be deleterious according to ad hoc software for pathogenicity prediction (damaging for Polyphen2, $p = 0.960$; Panther, 0.95; MutPred, 0.969; SIFT and MutationTaster).

## Discussion

Two distinct presentations and clinical courses have been reported in LTBL. The severe form is characterized by early-onset hypotonia, delayed psychomotor development, seizures, and persistent lactate elevation. In the mild form, clinical manifestations usually occur after the age of 6

months, with irritability and psychomotor regression, but clinical and biochemical improvement takes place from the second year of life without further clinical deterioration (Steenweg et al. 2012a, b; Talim et al. 2013). Respiratory chain enzyme activities in muscle have been found either reduced or normal in individual patients (Steenweg et al. 2012a). The clinical picture correlates well with the severity of neuroimaging. Although extensive symmetrical deep white matter abnormalities and signal changes of the thalami, brainstem, and cerebellar white matter together with increased lactate on MRS are the hallmark of LTBL (Steenweg et al. 2012a, b; Talim et al. 2013), significant improvement without new lesions and normalization of MRS have been observed in the mild form, whereas patients with the severe forms undergo progressive atrophy of the affected structures. However, long-term clinical and radiological follow-up has still to be completely elucidated. A rapidly progressive and fatal disease has recently been reported in an infant harboring a homozygous mutation in *EARS2* in association with severe combined deficiency of respiratory chain complexes I and IV in skeletal muscle and dysgenesis in the posterior part of the corpus callosum at brain MRI (Talim et al. 2013).

Our patient carrying a new mutation in *EARS2* showed a presentation of intermediate severity between the two aforementioned forms. Early-onset feeding difficulties, muscle hypotonia, and developmental delay were reflected by the severe brain MRI pattern detected at 3 months of age, which spontaneously improved from the second year of life onward, parallel to a slowly progressive clinical improvement, with the acquisition of motor milestones such as sitting and walking unaided in the second year of life. Interestingly, at 6 years, cognitive assessment revealed normal verbal index and impaired nonverbal functions, leading to a severely irregular neuropsychological profile with impossibility of obtaining a reliable total IQ. Indeed, although it was consistent with the diagnosis of mild mental retardation, the normality of verbal functioning allowed him to compensate the gaps in the performance field. It is likely that these data correlate with the documented neuroimaging improvement. Interestingly, we also documented asymptomatic lesions within the left caudate and pallidum nuclei during the most recent MRI, at age 5 years and 10 months; these lesions were not previously reported in LTBL. The appearance of new brain lesions, even with a transient and reversible pattern, has been described during the course of other mitochondrial disorders such as pyruvate dehydrogenase complex deficiency (Giribaldi et al. 2012). However, they typically occur during episodes of metabolic crisis that did not occur in our patient.

Mutations in different mitochondrial tRNA synthetases appear to be associated with a spectrum of syndromes characterized by striking tissue specificity, the heart (AARS2), the kidney (SARS2), or the peripheral nervous system (GARS2 and KARS2) (Konovalova and Tyynismaa 2013). The involvement of the brain reveals remarkable segmental involvement of specific tracts and nuclei in association with mutations in different genes: for instance, DARS2 mutations are typically linked to leukoencephalopathy with brainstem and spinal cord involvement and high lactate (LBSL) (Scheper et al. 2007), *RARS2* mutations to pontocerebellar hypoplasia type 6 (PCH6) (Edvardson et al. 2007), and EARS2 to LTBL. The mechanistic basis of this specificity, particularly in the central nervous system, remains unexplained, being possibly related to difference in mitochondrial translation throughout organ development (Konovalova and Tyynismaa 2013; Scheper et al. 2007; Edvardson et al. 2007; Diodato et al. 2014). Recently, experimental studies have shown that cell-type-specific differences in the sensitivity to mutations may explain the selective vulnerability of specific white matter tracts in LBSL despite the ubiquitous distribution of the mitochondrial aspartyl-tRNA synthetase encoded by *DARS2* (van Berge et al. 2012). A similar mechanism is postulated in PCH6 (Cassandrini et al. 2013) and might also apply to LTBL.

In conclusion, our study expands the clinical and neuroradiological phenotype of LTBL. Further studies are needed to define the phenotypic spectrum of this novel disorder and to better understand the factors influencing mitochondrial translation in different tissues.

**Acknowledgments** We wish to thank Paolo Broda and Annagloria Incontrera for technical assistance.

The financial supports of Telethon Italy (Grant no. GUP09004) and of Pierfranco and Luisa Mariani Foundation, Italy, are gratefully acknowledged.

## Take-Home Message

In this report, we present the first long-term clinical and neuroradiological follow-up of a LTBL/EARS2 patient, showing previously unreported brain MRI features.

## Compliance with Ethics Guidelines

Roberta Biancheri, Eleonora Lamantea, Mariasavina Severino, Daria Diodato, Marina Pedemonte, Denise Cassandrini, Alexandra Ploederl, Federica Trucco, Chiara Fiorillo, Carlo Minetti, Filippo M. Santorelli, Massimo Zeviani, and Claudio Bruno declare that they have no conflict of interest.

## Informed Consent

All procedures followed were in accordance with the ethical standards of the responsible committee on human experimenta-

tion (institutional and national) and with the Helsinki Declaration of 1975, as revised in 2000. Informed consent was obtained from all patients for being included in the study.

## Author Contributions

Study concept and design: Biancheri and Bruno

Acquisition of data: Biancheri, Lamantea, Severino Diodato, Cassandrini, Pedemonte, Trucco, Fiorillo, Ploederl, and Bruno

Analysis and interpretation of data: Biancheri, Lamantea, Santorelli, Zeviani, and Bruno

Drafting of the manuscript: Biancheri, Zeviani, and Bruno

Critical revision of the manuscript for important intellectual content: Minetti, Santorelli, Zeviani, and Bruno

Obtained funding: Zeviani

Administrative, technical, and material support: Bruno

Study supervision: Biancheri, Lamantea, and Bruno

## References

Cassandrini D, Cilio MR, Bianchi M et al (2013) Pontocerebellar hypoplasia type 6 caused by mutations in *RARS2*: definition of the clinical spectrum and molecular findings in five patients. J Inherit Metab Dis 36:43–53

Diodato D, Ghezzi D, Tiranti V (2014) The mitochondrial aminoacyl tRNA synthetases: genes and syndrome. Int J Cell Biol 2014:787956

Edvardson S, Shaag A, Kolesnikova O et al (2007) Deleterious mutation in the mitochondrial arginyl-transfer RNA synthetase gene is associated with pontocerebellar hypoplasia. Am J Hum Genet 81:857–862

Giribaldi G, Doria-Lamba L, Biancheri R et al (2012) Intermittent-relapsing pyruvate dehydrogenase complex deficiency: a case with clinical, biochemical, and neuroradiological reversibility. Dev Med Child Neurol 54:472–476

Konovalova S, Tyynismaa H (2013) Mitochondrial aminoacyl-tRNA synthetases in human disease. Mol Genet Metab 108:206–211

Scheper GC, van der Klok T, van Andel RJ et al (2007) Mitochondrial aspartyl-tRNA synthetase deficiency causes leukoencephalopathy with brain stem and spinal cord involvement and lactate elevation. Nat Genet 39:534–539

Steenweg ME, Ghezzi D, Haack T et al (2012a) Leukoencephalopathy with thalamus and brainstem involvement and high lactate 'LTBL' caused by *EARS2* mutations. Brain 135:1387–1394

Steenweg ME, Vanderver A, Ceulemans B et al (2012b) Novel infantile-onset leukoencephalopathy with high lactate level and slow improvement. Arch Neurol 69:718–722

Talim B, Pyle A, Griffin H et al (2013) Multisystem fatal infantile disease caused by a novel homozygous *EARS2* mutation. Brain 136:e228

van Berge L, Dooves S, van Berkel CG et al (2012) Leukoencephalopathy with brain stem and spinal cord involvement and lactate elevation is associated with cell-type-dependent splicing of mtAspRS mRNA. Biochem J 44:955–962

JIMD Reports
DOI 10.1007/8904_2015_438

RESEARCH REPORT

# Mitochondrial DNA Depletion and Deletions in Paediatric Patients with Neuromuscular Diseases: Novel Phenotypes

**Tuomas Komulainen • Milla-Riikka Hautakangas • Reetta Hinttala • Salla Pakanen • Vesa Vähäsarja • Petri Lehenkari • Päivi Olsen • Päivi Vieira • Outi Saarenpää-Heikkilä • Johanna Palmio • Hannu Tuominen • Pietari Kinnunen • Kari Majamaa • Heikki Rantala • Johanna Uusimaa**

Communicated by: Johannes Häberle

**Electronic supplementary material:** The online version of this chapter (doi:10.1007/8904_2015_438) contains supplementary material, which is available to authorized users.

T. Komulainen (✉) · M.-R. Hautakangas · R. Hinttala · S. Pakanen · P. Olsen · P. Vieira · H. Rantala · J. Uusimaa
PEDEGO Research Group and Medical Research Center Oulu, University of Oulu, P.O. Box 5000, FIN-90014 Oulu, Finland
e-mail: mikakomu@student.oulu.fi

T. Komulainen · M.-R. Hautakangas · R. Hinttala · S. Pakanen · P. Olsen · P. Vieira · H. Rantala · J. Uusimaa
Department of Children and Adolescents, Division of Pediatric Neurology, Oulu University Hospital, PO Box 23, FI-90029 OYS Oulu, Finland

V. Vähäsarja
Department of Children and Adolescents, Division of Pediatric Surgery, Oulu University Hospital, PO Box 23, FI-90029 OYS Oulu, Finland

T. Komulainen · M.-R. Hautakangas · R. Hinttala · S. Pakanen · P. Lehenkari · K. Majamaa · H. Rantala · J. Uusimaa
Medical Research Center Oulu, University of Oulu and Oulu University Hospital, P.O. Box 5000, FIN-90014 Oulu, Finland

P. Lehenkari · P. Kinnunen
Department of Surgery, Oulu University Hospital, PO Box 21, FI-90029 OYS Oulu, Finland

O. Saarenpää-Heikkilä
Department of Pediatrics, Tampere University Hospital, PO Box 2000, FI-33521 Tampere, Finland

J. Palmio
Department of Neurology, Tampere University Hospital, PO Box 2000, FI-33521 Tampere, Finland

H. Tuominen
Department of Pathology, Oulu University Hospital, PO Box 50, FI-90029 OYS Oulu, Finland

K. Majamaa
Clinical Neuroscience Center, University of Oulu, P.O. Box 5000, FIN-90014 Oulu, Finland

K. Majamaa
Department of Neurology, Oulu University Hospital, PO Box 20, FIN-90029 OYS Oulu, Finland

Received: 25 October 2014 / Revised: 02 March 2015 / Accepted: 31 March 2015 / Published online: 05 May 2015


**Abstract Objective**: To study the clinical manifestations and occurrence of mtDNA depletion and deletions in paediatric patients with neuromuscular diseases and to identify novel clinical phenotypes associated with mtDNA depletion or deletions.

**Methods**: Muscle DNA samples from patients presenting with undefined encephalomyopathies or myopathies were analysed for mtDNA content by quantitative real-time PCR and for deletions by long-range PCR. Direct sequencing of mtDNA maintenance genes and whole-exome sequencing were used to study the genetic aetiologies of the diseases. Clinical and laboratory findings were collected.

**Results**: Muscle samples were obtained from 104 paediatric patients with neuromuscular diseases. mtDNA depletion was found in three patients with severe early-onset encephalomyopathy or myopathy. Two of these patients presented with novel types of mitochondrial DNA depletion syndromes associated with increased serum creatine kinase (CK) and multiorgan disease without mutations in any of the known mtDNA maintenance genes; one patient had pathologic endoplasmic reticulum (ER) membranes in muscle. The third patient with mtDNA depletion was diagnosed with merosine-deficient muscular dystrophy caused by a homozygous mutation in the *LAMA2* gene. Two patients with an early-onset Kearns-Sayre/Pearson-like phenotype harboured a large-scale mtDNA deletion, minor multiple deletions and high mtDNA content.

**Conclusions**: Novel encephalomyopathic mtDNA depletion syndrome with structural alterations in muscle ER was identified. mtDNA depletion may also refer to

secondary mitochondrial changes related to muscular dystrophy. We suggest that a large-scale mtDNA deletion, minor multiple deletions and high mtDNA content associated with Kearns-Sayre/Pearson syndromes may be secondary changes caused by mutations in an unknown nuclear gene.

**Abbreviations**

| | |
|---|---|
| CK | Creatine kinase |
| ER | Endoplasmic reticulum |
| mtDNA | Mitochondrial DNA |
| MDDS | Mitochondrial DNA depletion syndrome |
| nDNA | Nuclear DNA |
| PCIAA | Phenol-chloroform-isoamyl alcohol extraction |
| qRT-PCR | Real-time quantitative PCR |
| XL-PCR | Long-range PCR |

## Introduction

Mitochondrial DNA depletion syndromes (MDDS) are a clinically and genetically heterogeneous group of typically recessively inherited diseases with early or juvenile onset that are characterized by a severe reduction of mtDNA content (Alberio et al. 2007). Based on affected tissues and their mtDNA content, the clinical presentations of MDDS can be classified into three different forms: encephalomyopathic, myopathic and hepatocerebral. For clinical purposes, mtDNA depletion has been defined as mtDNA content of $<0.30$ relative to age-matched controls (Rahman and Poulton 2009). However, measuring intracellular mtDNA content is technically challenging and the amount of mtDNA is age- and tissue-related (Dimmock et al. 2010; Morten et al. 2007). Numerous pathogenic mutations have been found in the 12 nuclear genes responsible for encoding proteins vital to mtDNA maintenance (El-Hattab and Scaglia 2013; Suomalainen and Isohanni 2010).

Mitochondrial DNA (mtDNA) deletions are qualitative mitochondrial genome defects that come from the loss of mtDNA molecule fragments (Krishnan et al. 2008). They are most likely to be caused by defects that occur during the repair or replication of mtDNA (Krishnan et al. 2008; Yu-Wai-Man and Chinnery 2012). mtDNA deletions are associated with several clinical syndromes, but they also increase with age (Krishnan et al. 2007). Mutations in nuclear genes involved in mtDNA replication and maintenance, e.g., *POLG1* (NM_001126131.1) encoding the catalytic subunit of mitochondrial DNA polymerase γ, can cause accumulation of mtDNA point mutations and deletions throughout life (Chan and Copeland 2009). The most common single large-scale mtDNA deletion is 4,977 base pairs (bp) spanning between the genes for cytochrome B (*CytB*) and cytochrome c oxidase subunit II (*COXII*) (Krishnan et al. 2007; Remes et al. 2005).

The aim of this study was to investigate the occurrence of mtDNA depletions and deletions in muscle biopsy samples of paediatric patients with undefined encephalomyopathy or myopathy, in order to estimate the role of mtDNA rearrangements in pathogenesis of these diseases. Further objective was to identify novel clinical phenotypes associated with mtDNA depletion or deletions.

## Subjects and Methods

### Patients and Controls

Skeletal muscle biopsy samples were taken as a part of the diagnostic protocol and collected from patients under 18 years with undefined encephalomyopathy or myopathy, who were examined at the Department of Paediatrics of Oulu University Hospital between 1990 and 2012 by the protocol including both clinical assessments and histological, biochemical and/or molecular genetic analyses (Uusimaa et al. 2000). All 104 patients were screened for the eight common *POLG1* mutations (p.T251I, p.A467T, p.N468N, p.G517V, p.P587L, p.R722H, p.W748S and p.Y955C) and the common MELAS m.3423A>G, MERRF m.8834A>G and NARP m.8993T>G mutations in mtDNA. The control muscle samples were collected by the Department of Paediatrics at Oulu University Hospital between the years 2008 and 2012. The samples were taken from patients with no signs of mitochondrial or other neurological diseases during surgical treatments for orthopaedic conditions where mitochondrial function has not been shown to play a major role. Muscle biopsies of 0.25–0.5 $cm^3$ in diameter were performed during an operation requiring an incision through muscle tissue. The biopsies were only done if unnecessary trauma could be avoided. The collection of muscle tissue samples did not interfere with the result of the operation or the recovery of the patient.

The study protocol has been approved by the Ethics Committee of the Faculty of Medicine at the University of Oulu and the Ethics Committee of the Northern Ostrobothnia Hospital District and it is in compliance with the Helsinki Declaration. Written informed consent was given by the guardians of the subjects prior to the study.

### DNA Extraction from Muscle Biopsy Samples and Fibroblasts

Total genomic DNA was extracted from skeletal muscle samples using standard phenol-chloroform-isoamyl alcohol

extraction (PCIAA) and ethanol precipitation or by using a commercially available Wizard Genomic DNA Purification kit (Promega, Madison, WI, USA). All extracted DNA samples were aliquoted into small fractions and stored in −80°C. DNA for whole-exome sequencing was extracted from patient fibroblasts by using a commercially available QIAamp DNA Mini Kit (Qiagen, Hilden, Germany) and ethanol precipitation. Fibroblasts were cultured in Dulbecco's Modified Eagle's Medium (DMEM) (Sigma-Aldrich, St. Louis, MO, USA) including 5 mM glucose, sodium bicarbonate and pyridoxine and supplemented with 10% FBS, 1 mM sodium pyruvate, 2 mM L-glutamine, 100 IU/mL penicillin and 100 μg/mL streptomycin.

### Real-Time Quantitative PCR of Muscle DNA Samples

Real-time quantitative PCR (qRT-PCR) was used to determine the amount of mtDNA relative to nuclear DNA in both patient and control muscle samples and was shown as an mtDNA/nDNA ratio. mtDNA was amplified using PCR primers targeted at the mitochondrial NADH dehydrogenase 1 (*ND1*) gene as described by He et al. (He et al. 2002). The values were normalized using the nuclear-encoded brain natriuretic peptide (*BNP*) gene as a single-copy nuclear gene. Amplification products were detected by sequence-specific 6FAM/TAMRA-labelled fluorogenic probes (Sigma-Genosys, Suffolk, UK). The sequences of the primers and probes and description of reaction conditions are available on request. The PCR programme was performed and amplification products were detected by an iCycler thermal cycler and an iQ5 Multicolor Real-Time PCR Detection System (Bio-Rad Laboratories Inc., Hercules, CA, USA). The mtDNA/nDNA ratio was calculated with the ΔCT method described by Pfaffl (Pfaffl 2001). mtDNA depletion was defined as an mtDNA ratio of $<0.30$ relative to median of age-matched controls (Rahman and Poulton 2009). Unfortunately, we were not able to obtain controls below 5 years of age. Thus, patients below 5 years were compared to median of 5-year-old controls.

### Detection of Mitochondrial DNA Deletions in Muscle DNA Samples

Deletions of mitochondrial DNA were detected by long-range PCR (XL-PCR) amplification of mtDNA using Phusion DNA polymerase (New England Biolabs, Ipswich, MA, USA). The amplification reaction was carried out with light-strand primer starting from the nucleotide 10 (L10) and heavy-strand primer starting from the nucleotide 16496 (H16496). The sequences of the primers and probes and description of reaction conditions are available on request. The PCR products, along with a GeneRuler λ mix ladder and 1 kb ladder (New England Biolabs, Ipswich, MA, USA), were electrophoresed on 0.7% agarose gel stained with a SYBR Safe DNA gel stain (Invitrogen, Eugene, OR, USA).

### Molecular Genetic Studies on Patients with Mitochondrial DNA Depletion or Deletions

Based on the clinical phenotype and muscle histology findings, one patient (Patient 3) was analysed for laminin subunit alpha 2 (*LAMA2*) gene. All other patients with mtDNA depletion or deletions (Patients 1–2 and 4–5) were analysed for all the exons and intron-exon boundaries of the *POLG1*, *C10orf2* and thymidine kinase 2 (*TK2*) genes and the entire mtDNA coding region by direct sequencing. In addition, two patients (Patients 4–5) with a large single mtDNA deletion associated with Kearns-Sayre/Pearson-like phenotypes were analysed also for ADP/ATP translocase 1 (*ANT1*) gene.

Whole-exome sequencing was performed in two patients with novel MDDS phenotypes with unknown genetic aetiology (Patients 1–2) and patients with single large-scale mtDNA deletions and minor multiple deletions (Patients 4–5). For whole-exome sequencing, total genomic DNA was extracted from skin fibroblasts. DNA samples of Patients 1–2 were analysed by the commercially available Agilent SureSelect in-solution target enrichment system (Agilent SureSelect Human All Exon V5, Agilent Technologies, Santa Clara, CA, USA) with mean sequencing coverage of 30× using the Illumina HiSeq sequencing platform at the FIMM Technology Center, Helsinki, Finland, as described by Sulonen et al. (Sulonen et al. 2011). DNA samples of Patients 4–5 were analysed using Agilent SureSelect Human All Exon Kit V1 (Agilent Technologies) and sequenced on the Illumina GAIIx sequencing platform at the McGill University, Montreal, Canada, and Genome Quebec Innovation Center, Montreal, Canada. Bioinformatics of the whole-exome sequencing data (variant filtering and interpretation) on these four patients (Patients 1–2 and 4–5) was performed by Dr. Javad Nadaf, Dr. Somayyeh Fahiminiya and Prof. Jacek Majewski at the Department of Human Genetics, McGill University, and Genome Quebec Innovation Center.

## Results

### Characteristics of Patient and Control Cohorts

Muscle samples were obtained from 104 paediatric patients with encephalomyopathy or myopathy. The median age was 4.1 years (range of 1 month to 17 years). Control muscle samples were obtained from 14 subjects under 18 years with no suspicion of mitochondrial or other neurological diseases. The median age of controls was 12 years (range of 5–16 years). Muscle mtDNA content of the controls is presented in Fig. 1a.

### Molecular Studies and Clinical Features of the Patients

Among the 104 paediatric patients with neuromuscular disorders, we identified three patients (Patients 1–3 in Table 1) with mtDNA depletion (Fig. 1b). Two of them presented with severe multiorgan phenotype of MDDS and increased serum creatine kinase (CK) levels. Muscle histology of Patient 2 disclosed myopathic muscle tissue with rounded fibres and endomysial collagen and electron micrograph (EM) showed disordered myofibrillar structure, pathologic ER membranes and accumulation of glycogen and extracellular collagen fibres (Fig. 2a, b). Molecular genetic studies including whole-exome sequencing did not reveal any mtDNA point mutations or mutations in any of the known mtDNA maintenance genes. Patient 3 presenting with severe myopathy and mtDNA depletion was diagnosed with merosine-deficient muscular dystrophy (MDC1A) based on histological and clinical features. This patient was found to harbour a homozygous p.G1591X mutation creating a stop codon in the *LAMA2* gene.

Two patients (Patients 4 and 5; Table 2) harboured a major large-scale 5 kb deletion and minor multiple deletions (Fig. 3a, b). In addition, qRT-PCR of these two patients showed high mtDNA content (4.9- and 6.9-fold increases, respectively) relative to the median of age-matched controls (Fig. 1a, b). The clinical features of both patients included early-onset external ophthalmoplegia, sensorineural hearing impairment, progressive tremor, severe ataxia, migraine and dysarthria. Furthermore, Patient 5 presented with transient anaemia and granulocytopaenia, pigmentary retinopathy and a trifascicular cardiac conduction block requiring a pacemaker in connection to Kearns-Sayre and Pearson syndromes. Muscle histology of both patients disclosed ragged-red fibres and COX-negative fibres as demonstrated in Fig. 2c. In addition, EM of muscle biopsy of Patient 5 revealed accumulation of mitochondria with pathologic internal structure and abnormal cristae (Fig. 2d). Respiratory chain activity measurement showed decreased activity of complexes I and I + III in muscle of Patient 5. Molecular genetic studies including whole-exome sequencing did not disclose any mtDNA point mutations or mutations in any of the known mtDNA maintenance genes.

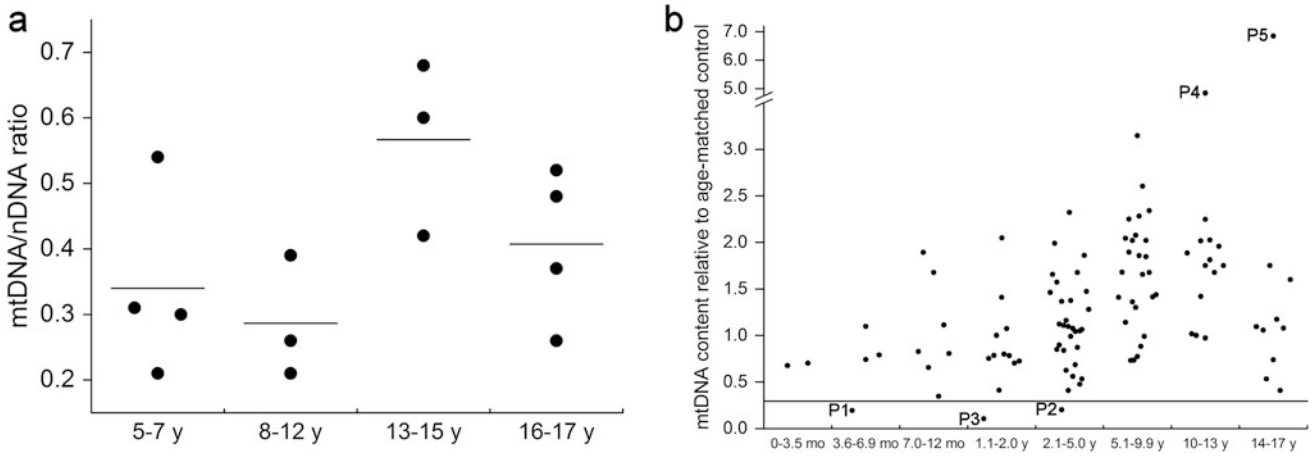


**Fig. 1** mtDNA content determined using quantitative real-time PCR. (**a**) Muscle mitochondrial DNA content of the control samples. The results are presented as mitochondrial DNA/nuclear DNA ratio. Each *dot* represents one sample. (**b**) Muscle mitochondrial DNA content of paediatric patients with encephalomyopathies and myopathies ($N = 104$) compared to median muscle mtDNA content of the age-matched control samples. mtDNA depletion was determined as mtDNA content <0.30 of age-matched controls. The cutoff point at 0.30 is marked with a *horizontal line*. Three patients with mtDNA depletion were identified (Patients 1–3). Two samples present with marked increase in mtDNA content relative to median of age-matched controls: a single sample in the age group 10–13 years (Patient 4) presents with a 4.9-fold increase and another sample in the age group 14–17 years (Patient 5) show a 6.9-fold increase in mtDNA content relative to age-matched controls. *mo* months, *y* years

**Table 1** Clinical features of paediatric patients with neuromuscular diseases associated with mtDNA depletion (Patients 1–3)

| Patient | Age at onset | Age at biopsy | Deletion status | mtDNA/nDNA ratio (± S.D.) | mtDNA relative to control | Enc | Myo | Hep | FTT | Epi | Ata | Others | Laboratory findings | OXPHOS activity | Muscle histology | Genetic aetiology |
|---|---|---|---|---|---|---|---|---|---|---|---|---|---|---|---|---|
| P1 | Newborn | 5 mo | No | 0.06 ± 0.05 | 0.19 | + | – | – | + | + | – | Spasticity, microcephaly EEG, burst suppression; MRI, white matter necrosis, basal ganglia and thalamic lesions | L: + CFSL: + P: + CK: + UAA: + | N | Atr, F | Unknown |
| P2 | Newborn | 3 y 5 mo | No | 0.06 ± 0.02 | 0.2 | + | + | – | + | – | – | Optic atrophy, pigmentary retinopathy, nystagmus, SNHI, death at age 4 y 8 mo | L: N P: N CK: + | N.A. | Gly, ER, Fib, | Unknown |
| P3 | 9 mo | 1 y 10 mo | No | 0.03 ± 0.01 | 0.1 | – | + | – | – | – | – | Merosine-deficient muscular dystrophy (MDC1A), severe muscular hypotonia ENMG: myopathy Brain MRI: leukodystrophy | CK: + | N.A. | Atr, F, Fib | *LAMA2* p. G1591X +/+ |

Abbreviations for clinical features: *Enc* encephalopathy, *Myo* myopathy, *Hep* hepatopathy, *FTT* failure to thrive, *Epi* epilepsy, *Ata* ataxia, *EEG* electroencephalography, *MRI* magnetic resonance imaging, *SNHI* sensorineural hearing impairment

Abbreviations for laboratory findings and OXPHOS activity: *CK* creatine kinase, *L* blood lactate, *CSFL* cerebrospinal fluid lactate, *P* blood pyruvate, *N* normal, + elevated, – decreased, *UAA* + in patient P1 generalized aminoaciduria, *OXPHOS* respiratory chain, *N.A.* not available

Abbreviations for histology: *N* normal, *Atr* atrophy, *F* fat excess, *Gly* increased glycogen, *ER* pathologic endoplasmic reticulum membranes, *Fib* accumulation of extracellular collagen fibres, *N.A.* not available

Abbreviations and footnotes: *y* years, *mo* months

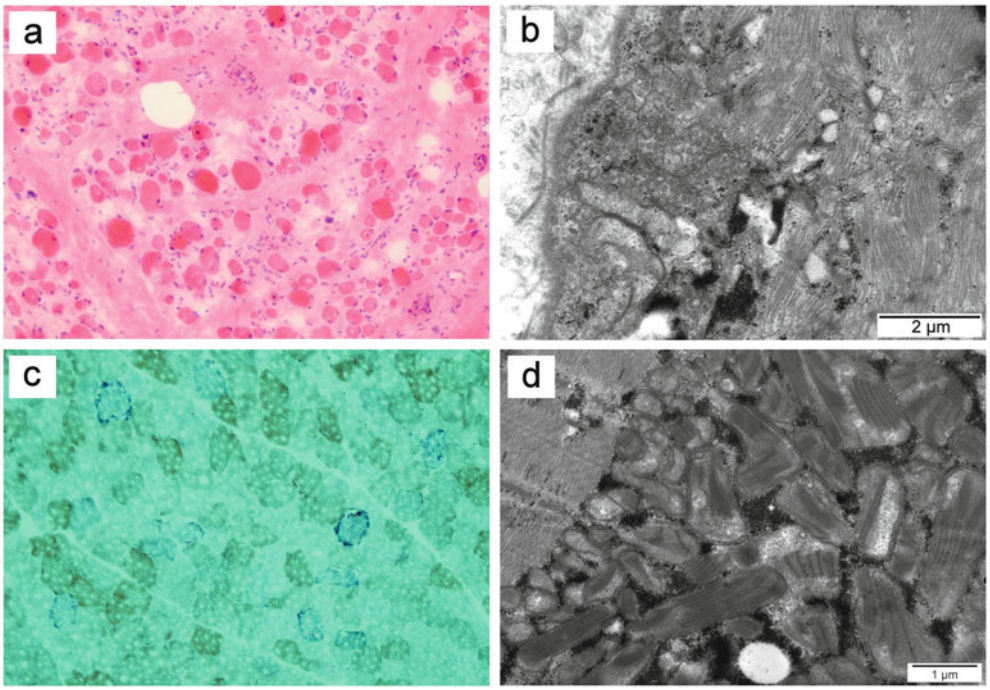


**Fig. 2** Histological findings in skeletal muscle biopsies associated with mtDNA depletion or deletions. (**a**) Muscle histology of Patient 2 disclosed myopathic muscle tissue with rounded fibres and endomysial collagen. HE staining. (**b**) Electron micrograph of the muscle of Patient 2 showing disordered myofibrillar structure, pathologic endoplasmic reticulum membranes, accumulation of glycogen and extracellular collagen fibres. (**c**) Muscle histology of Patient 5 demonstrated COX-negative fibres. SDH-COX staining. (**d**) Electron micrograph of the muscle of Patient 5 displayed accumulation of mitochondria with pathologic internal structure and abnormal cristae

## Discussion

We investigated mtDNA depletion and deletion in relation to paediatric neuromuscular diseases. As it is not ethically justifiable to collect muscle biopsies from healthy children with a sole intention to obtain control samples, the control samples had to be collected from patients who underwent surgical operation. This obviously had an effect on the selection process. Thus, we were unfortunately lacking control muscle samples from healthy children younger than 5 years old, but as presented by Dimmock et al. (Dimmock et al. 2010), muscle mtDNA content is relatively stable between 0 and 6 years of age. Therefore, mtDNA ratio of patients under 5 years was determined relative to median of 5-year-old controls. In all, we identified 4 patients with a typical presentation of a mitochondrial disorder in association with mtDNA depletion or deletions. Furthermore, mtDNA depletion was found as a secondary finding in hereditary muscular dystrophy.

Two patients with mtDNA depletion (Patients 1–2) presented with novel types of mitochondrial DNA depletion syndromes manifesting with multiorgan disease. The clinical features of these two patients with the severe MDDS associated with increased CK levels suggested mutations in the *TK2* gene (Lesko et al. 2010), but sequencing of *TK2* gene disclosed no mutations. Patient 1 manifested with a severe progressive metabolic encephalomyopathy and the brain MRI of Patient 1 disclosed white matter degeneration as well as basal ganglia and thalamic lesions resembling Leigh syndrome. Similar encephalopathic phenotypes have been described in MDDS caused by several mtDNA maintenance genes including in *SUCLA2* and *SUCLG1* (Ostergaard et al. 2007a, b; Carrozzo et al. 2007; Elpeleg et al. 2005), *DGUOK* (Mandel et al. 2001; Dimmock et al. 2008) and *RRM2B* (Bornstein et al. 2008; Acham-Roschitz et al. 2009; Kollberg et al. 2009). Patient 1 was also found with generalized aminoaciduria that has previously been described in MDDS patients (Uusimaa et al. 2014). Patient 2 presented with a novel early-onset and fatal MDDS phenotype including encephalopathy, optic atrophy, pigmentary retinopathy, sensorineural hearing impairment and pathologic ER membranes in histologically disordered muscle with accumulation of glycogen and extracellular collagen fibres (Fig. 2b). A patient with mtDNA depletion and similar clinical features has previously been described to harbour a missense mutation in *MFN2* gene encoding mitofusin 2, a protein essential in mitochondrial network dynamics (Renaldo et al. 2012). As ER and mitochondria are functionally related (Kornmann

**Table 2** Clinical features of patients with Kearns-Sayre/Pearson syndrome associated with a single large-scale deletion and minor multiple mtDNA deletions and high mtDNA content (Patients 4–5)

| Patient | Aget at onset | Age at biopsy | Deletion status | mtDNA/nDNA ratio (± S.D.) | mtDNA relative to control | CPEO | Pt | Mig | SNHI | Myo | Ata | Others | Laboratory findings | Muscle histology | Genetic aetiology |
|---|---|---|---|---|---|---|---|---|---|---|---|---|---|---|---|
| P4 | 5 y | 12 y | Single 11 kb band + M | 1.89 ± 0.25 | 4.9 | + | – | + | + | – | + | Progressive tremor<br>Brain CT: subcortical and cerebellar hypodensity<br>Brain MRI: T2-weighted lesions in globus pallidus and thalamic and frontal subcortical regions | L: +<br>CFSL: +<br>P: N<br>CK: N | C–, RRF, F, Fib | Unknown |
| P5 | 1 y | 16 y | Single 11 kb band + M | 2.81 ± 0.89 | 6.9 | + | + | + | + | + | + | Transient anaemia and granulocytopaenia, pigmentary retinopathy, growth retardation, progressive cognitive impairment, trifascicular conduction block<br>Ultrasound: echogenic liver and kidneys<br>Brain MRI: symmetric T2-weighted lesions in inferior colliculi and right thalamic and frontal subcortical regions | LE: +<br>OXPHOS: CI + III and CIII– | C–, RRF, Mito, Cr | Unknown |

Abbreviations for mtDNA deletion status: *M* multiple deletions

Abbreviations for clinical features: *CPEO* chronic external ophthalmoplegia, *Pt* bilateral ptosis, *Mig* migraine, *SNHI* sensorineural hearing impairment, *Myo* myopathy, *Ata* ataxia, *CT* computed tomography, *MRI* magnetic resonance imaging

Abbreviations for laboratory findings: *L* blood lactate, *CSFL* cerebrospinal fluid lactate, *P* blood pyruvate, *CK* creatine kinase, *LE* liver enzymes, *OXPHOS C* respiratory chain complex activity, *N* normal, + elevated, – decreased, *N.A.* not available

Abbreviations for histology: *C–* COX-negative fibres, *RRF* ragged-red fibres, *F* fat excess, *Fib* fibrosis, *Mito* pathologic inner mitochondrial structures, *Cr* abnormal cristae in mitochondria, *N.A.* not available

Abbreviations and footnotes: *y* years, *mo* months

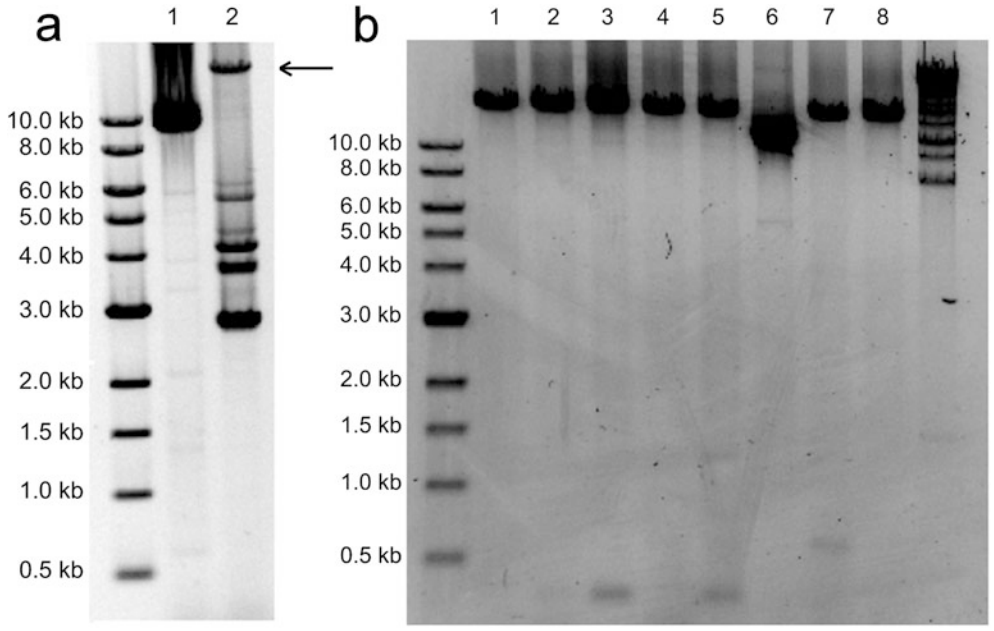


**Fig. 3** Long-range PCR of muscle DNA. (**a**) Lane 1, patient 4 presenting with Kearns-Sayre/Pearson-like syndrome; lane 2, a positive control for mtDNA deletions. Intact 16.6 kb mtDNA is marked with a *black arrow*. (**b**) Lanes 1 and 8, 5-year-old healthy control; lanes 2–5, patient samples with unspecific deletion bands; lane 6, Patient 5 presenting with a single large-scale deletion with no intact 16.6 kb mtDNA band. In addition, smaller deletion bands are visible signifying multiple mtDNA deletions; lane 7, a patient sample with unspecific 0.5 kb band

2013), the muscle histology of Patient 2 suggests involvement of ER in the pathogenesis of the disease.

Two patients (Patients 4 and 5) harboured a large-scale mtDNA deletion in addition to minor deletions in muscle DNA (Fig. 3). Although XL-PCR is not a quantitative method for mtDNA deletion analysis, we were not able to detect intact 16.6 kb mtDNA in an XL-PCR assay of these patients suggesting a very high heteroplasmy rate of the mutated mtDNA molecule. Most interestingly, we found markedly increased muscle mtDNA content with the qRT-PCR analysis in both cases referring to overamplification of mtDNA as a compensation mechanism for large-scale mtDNA deletion. These patients developed ophthalmoplegia at a young age along with other neurological symptoms including sensorineural hearing loss, muscle hypotonia and ataxia. Patient 5 also presented with pigmentary retinopathy and cardiac conduction block associated with KSS (#OMIM 530000), as well as transient anaemia and granulocytopaenia suggesting Pearson syndrome (OMIM #557000). In the previous literature, we found only one similar case of mtDNA overamplification associated with mtDNA deletions. This case was a female patient presenting with KSS (Wong et al. 2003) including progressive external ophthalmoplegia, ptosis and pigmentary retinopathy; the atypical onset of the disease happened at 30 years of age. She harboured a 3,078 bp mtDNA deletion with a 92% proportion of mutant mtDNA and partial mtDNA duplication. Ragged-red fibres were seen in muscle histology of this patient, but respiratory chain activity was normal. Quantitative analysis showed a ninefold increase in muscle mtDNA content, thus suggesting compensatory amplification of mtDNA due to a high deletion mutant load.

KSS is commonly associated with 4,977 bp mtDNA deletion (Remes et al. 2005). It has also been suggested that mtDNA duplications can be a typical feature of early-onset KSS (Poulton 1992; Odoardi et al. 2003). Consideration of the role of mtDNA duplications in KSS raises a question whether the high mtDNA content in qRT-PCR is actually an artefact caused by duplicated target gene in mtDNA molecules. In this work we did not analyse the DNA samples for duplications, but previous studies (Wong et al. 2003; Odoardi et al. 2003) suggest that the *ND1* gene, the target gene for qRT-PCR in our study, is not situated in common locations of either mtDNA deletions or duplications. This may indicate that the high mtDNA content found in our two KSS patients actually refers to a high copy number in the muscle suggesting compensatory overamplification of mtDNA, which is also suggested in the previous study (Wong et al. 2003). In addition, muscle histology of Patient 5 showed mitochondrial inclusion bodies, which could be related to high mtDNA content observed in quantitative analysis.

In general, in 40% of cases of mtDNA-related clinical syndromes, the genetic aetiology remains unsolved even after whole-exome sequencing (Calvo et al. 2012). In this study, with whole-exome sequencing, we did not identify

pathogenic mutations in any of the known mtDNA maintenance genes (El-Hattab and Scaglia 2013; Suomalainen and Isohanni 2010) to disclose the genetic aetiology of the disease in Patients 1 and 2, but further studies are ongoing to evaluate the role of the candidate genes identified by whole-exome sequencing (unpublished data provided by Dr. Javad Nadaf, Dr. Somayyeh Fahiminiya and Prof. Jacek Majewski, Department of Human Genetics, McGill University and Genome Quebec Innovation Center, Montreal, Canada) associated with these novel MDDS phenotypes. Most single mtDNA deletions are thought to be sporadic and thus not genetically transmitted (Chinnery et al. 2004), but multiple mtDNA deletions can be inherited as an autosomal dominant or recessive trait (Zeviani et al. 1990; Nishino et al. 1999). Our two patients with a KSS/Pearson-like phenotype presented with minor multiple deletions in addition to a major large-scale mtDNA deletion, which led us to suggest a genetic origin of the mtDNA arrangements leading to these clinical phenotypes. Whole-exome sequencing was performed in Patients 4–5, but no mutations in the known mtDNA maintenance genes were found. These circumstances could refer to mutations in a yet unknown nuclear gene responsible for mtDNA maintenance.

Patient 3, presenting with severe mtDNA depletion (mtDNA content only 0.10 compared to the age-matched controls) and severe myopathy with muscle fibrosis and atrophy, was diagnosed with merosine-deficient muscular dystrophy (MDC1A) based on further histological and clinical examinations. Molecular studies on this patient disclosed homozygous p.G1591X mutation in the *LAMA2* gene. Secondary mtDNA rearrangements have been previously found in neuromuscular disorders that are not primary mitochondrial diseases (Katsetos et al. 2013), but so far only a few studies concerning mtDNA rearrangements in the pathogenesis of muscle dystrophies have been performed. mtDNA deletions have been described in myotonic dystrophy (Sahashi et al. 1992) and oculopharyngeal muscular dystrophy (Lezza et al. 1997; Muqit et al. 2008). Another study on congenital myotonic dystrophy associated mtDNA depletion to a minor degree with the disease, but no evidence of mtDNA rearrangements in the pathogenesis was found and therefore mild mtDNA depletion was suggested to be secondary to the disease (Poulton et al. 1995).

In conclusion, we describe two novel early-onset phenotypes associated with mtDNA depletion, one of them presenting with pathologic endoplasmic reticulum membranes. In addition, we suggest that Kearns-Sayre and Pearson syndrome can present with multiple deletions and may be caused by mutations in an unknown mtDNA maintenance gene. Furthermore, mtDNA depletion can be a secondary finding in hereditary muscular dystrophy.

**Acknowledgements** The authors thank Ms. Anja Heikkinen and Ms. Pirjo Keränen for their expert assistance. The work was supported by grants from the Research Council for Health of the Academy of Finland (JU, Decision number 138566; KM, Decision number 127764; RH, Decision number 266498 and 273790), the Sigrid Juselius Foundation, the Finnish Medical Foundation, the Arvo ja Lea Ylppö Foundation, the Foundation for Pediatric Research, the Alma and K.A. Snellman Foundation, the Emil Aaltonen Foundation, National Graduate School of Clinical Investigation (CLIGS), a Marie Curie International Outgoing Fellowship of the European Union's Seventh Framework Programme under the grant agreement number 273669 (BioMit), Special State Grants for Health Research in the Department of Pediatrics and Adolescence and the Department of Neurology at Oulu University Hospital, Oulu, Finland.

## Synopsis

Novel phenotypes associated with mtDNA depletion and deletions without mutations in the known mtDNA maintenance genes.

## Compliance with Ethics Guidelines

### Conflict of Interest

Tuomas Komulainen, Milla-Riikka Hautakangas, Reetta Hinttala, Salla Pakanen, Vesa Vähäsarja, Petri Lehenkari, Päivi Olsen, Päivi Vieira, Outi Saarenpää-Heikkilä, Johanna Palmio, Hannu Tuominen, Pietari Kinnunen, Kari Majamaa, Heikki Rantala and Johanna Uusimaa declare that they have no conflict of interest.

### Informed Consent

All procedures followed were in accordance with the ethical standards of the responsible committee on human experimentation (institutional and national) and with the Helsinki Declaration of 1975, as revised in 2000. Informed consent was obtained from all patients or their guardian for being included in the study.

### Authors' Contributions

Tuomas Komulainen is responsible for the study design, gathering, analysing and interpreting the data and drafting the manuscript. Reetta Hinttala and Johanna Uusimaa are responsible for the study design, gathering, analysing and interpreting the data and revising the manuscript for important intellectual content. Milla-Riikka Hautakangas, Reetta Hinttala, Salla Pakanen, Vesa Vähäsarja, Petri Lehenkari, Päivi Olsen, Päivi Vieira, Outi Saarenpää-Heikkilä, Johanna Palmio, Hannu Tuominen, Pietari Kin-

nunen, Kari Majamaa and Heikki Rantala are responsible for gathering, analysing and interpreting the data and revising the manuscript for important intellectual content.

## References


Acham-Roschitz B, Plecko B, Lindbichler F, Bittner R, Mache CJ, Sperl W, Mayr JA (2009) A novel mutation of the RRM2B gene in an infant with early fatal encephalomyopathy, central hypomyelination, and tubulopathy. Mol Genet Metab 98:300–304

Alberio S, Mineri R, Tiranti V, Zeviani M (2007) Depletion of mtDNA: syndromes and genes. Mitochondrion 7:6–12

Bornstein B, Area E, Flanigan KM et al (2008) Mitochondrial DNA depletion syndrome due to mutations in the RRM2B gene. Neuromuscul Disord 18:453–459

Calvo SE, Compton AG, Hershman SG et al (2012) Molecular diagnosis of infantile mitochondrial disease with targeted next-generation sequencing. Sci Transl Med 4(118):118ra10. doi:10.1126/scitranslmed.3003310

Carrozzo R, Dionisi-Vici C, Steuerwald U et al (2007) SUCLA2 mutations are associated with mild methylmalonic aciduria, Leigh-like encephalomyopathy, dystonia and deafness. Brain 130:862–874

Chan SS, Copeland WC (2009) DNA polymerase gamma and mitochondrial disease: understanding the consequence of POLG mutations. Biochim Biophys Acta 1787:312–319

Chinnery PF, DiMauro S, Shanske S et al (2004) Risk of developing a mitochondrial DNA deletion disorder. Lancet 364:592–596

Dimmock DP, Zhang Q, Dionisi-Vici C et al (2008) Clinical and molecular features of mitochondrial DNA depletion due to mutations in deoxyguanosine kinase. Hum Mutat 29:330–331

Dimmock D, Tang LY, Schmitt ES, Wong LJ (2010) Quantitative evaluation of the mitochondrial DNA depletion syndrome. Clin Chem 56:1119–1127

El-Hattab AW, Scaglia F (2013) Mitochondrial DNA depletion syndromes: review and updates of genetic basis, manifestations, and therapeutic options. Neurotherapeutics 10:186–198

Elpeleg O, Miller C, Hershkovitz E et al (2005) Deficiency of the ADP-forming succinyl-CoA synthase activity is associated with encephalomyopathy and mitochondrial DNA depletion. Am J Hum Genet 76:1081–1086

He L, Chinnery PF, Durham SE et al (2002) Detection and quantification of mitochondrial DNA deletions in individual cells by real-time PCR. Nucleic Acids Res 30, e68

Katsetos CD, Koutzaki S, Melvin JJ (2013) Mitochondrial dysfunction in neuromuscular disorders. Semin Pediatr Neurol 20:202–215

Kollberg G, Darin N, Benan K et al (2009) A novel homozygous RRM2B missense mutation in association with severe mtDNA depletion. Neuromuscul Disord 19:147–150

Kornmann B (2013) The molecular hug between the ER and the mitochondria. Curr Opin Cell Biol 25:443–448

Krishnan KJ, Greaves LC, Reeve AK, Turnbull DM (2007) Mitochondrial DNA mutations and aging. Ann N Y Acad Sci 1100:227–240

Krishnan KJ, Reeve AK, Samuels DC et al (2008) What causes mitochondrial DNA deletions in human cells? Nat Genet 40:275–279

Lesko N, Naess K, Wibom R et al (2010) Two novel mutations in thymidine kinase-2 cause early onset fatal encephalomyopathy and severe mtDNA depletion. Neuromuscul Disord 20:198–203

Lezza AM, Cormio A, Gerardi P et al (1997) Mitochondrial DNA deletions in oculopharyngeal muscular dystrophy. FEBS Lett 418:167–170

Mandel H, Szargel R, Labay V et al (2001) The deoxyguanosine kinase gene is mutated in individuals with depleted hepatocerebral mitochondrial DNA. Nat Genet 29:337–341

Morten KJ, Ashley N, Wijburg F et al (2007) Liver mtDNA content increases during development: a comparison of methods and the importance of age- and tissue-specific controls for the diagnosis of mtDNA depletion. Mitochondrion 7:386–395

Muqit MM, Larner AJ, Sweeney MG et al (2008) Multiple mitochondrial DNA deletions in monozygotic twins with OPMD. J Neurol Neurosurg Psychiatry 79:68–71

Nishino I, Spinazzola A, Hirano M (1999) Thymidine phosphorylase gene mutations in MNGIE, a human mitochondrial disorder. Science 283:689–692

Odoardi F, Rana M, Broccolini A et al (2003) Pathogenic role of mtDNA duplications in mitochondrial diseases associated with mtDNA deletions. Am J Med Genet A 118A:247–254

Ostergaard E, Christensen E, Kristensen E, Mogensen B, Duno M, Shoubridge EA, Wibrand F (2007a) Deficiency of the alpha subunit of succinate-coenzyme A ligase causes fatal infantile lactic acidosis with mitochondrial DNA depletion. Am J Hum Genet 81:383–387

Ostergaard E, Hansen FJ, Sorensen N et al (2007b) Mitochondrial encephalomyopathy with elevated methylmalonic acid is caused by SUCLA2 mutations. Brain 130:853–861

Pfaffl MW (2001) A new mathematical model for relative quantification in real-time RT-PCR. Nucleic Acids Res 29, e45

Poulton J (1992) Duplications of mitochondrial DNA: implications for pathogenesis. J Inherit Metab Dis 15:487–498

Poulton J, Harley HG, Dasmahapatra J, Brown GK, Potter CG, Sykes B (1995) Mitochondrial DNA does not appear to influence the congenital onset type of myotonic dystrophy. J Med Genet 32:732–735

Rahman S, Poulton J (2009) Diagnosis of mitochondrial DNA depletion syndromes. Arch Dis Child 94:3–5

Remes AM, Majamaa-Voltti K, Karppa M et al (2005) Prevalence of large-scale mitochondrial DNA deletions in an adult Finnish population. Neurology 64:976–981

Renaldo F, Amati-Bonneau P, Slama A et al (2012) MFN2, a new gene responsible for mitochondrial DNA depletion. Brain 135: e223, 1–4, author reply e224, 1–3

Sahashi K, Tanaka M, Tashiro M, Ohno K, Ibi T, Takahashi A, Ozawa T (1992) Increased mitochondrial DNA deletions in the skeletal muscle of myotonic dystrophy. Gerontology 38:18–29

Sulonen AM, Ellonen P, Almusa H et al (2011) Comparison of solution-based exome capture methods for next generation sequencing. Genome Biol 12:R94

Suomalainen A, Isohanni P (2010) Mitochondrial DNA depletion syndromes–many genes, common mechanisms. Neuromuscul Disord 20:429–437

Uusimaa J, Remes AM, Rantala H et al (2000) Childhood encephalopathies and myopathies: a prospective study in a defined population to assess the frequency of mitochondrial disorders. Pediatrics 105:598–603

Uusimaa J, Evans J, Smith C et al (2014) Clinical, biochemical, cellular and molecular characterization of mitochondrial DNA depletion syndrome due to novel mutations in the MPV17 gene. Eur J Hum Genet 22:184–191

Wong LJ, Perng CL, Hsu CH et al (2003) Compensatory amplification of mtDNA in a patient with a novel deletion/duplication and high mutant load. J Med Genet 40, e125

Yu-Wai-Man P, Chinnery PF (2012) Dysfunctional mitochondrial maintenance: what breaks the circle of life? Brain 135:9–11

Zeviani M, Bresolin N, Gellera C et al (1990) Nucleus-driven multiple large-scale deletions of the human mitochondrial genome: a new autosomal dominant disease. Am J Hum Genet 47:904–914

JIMD Reports
DOI 10.1007/8904_2015_439

RESEARCH REPORT

# Medium-Chain Acyl-CoA Dehydrogenase Deficiency: Evaluation of Genotype-Phenotype Correlation in Patients Detected by Newborn Screening

**Gwendolyn Gramer · Gisela Haege · Junmin Fang-Hoffmann · Georg F. Hoffmann · Claus R. Bartram · Katrin Hinderhofer · Peter Burgard · Martin Lindner**

Received: 18 February 2015 / Revised: 27 March 2015 / Accepted: 31 March 2015 / Published online: 05 May 2015


**Abstract Background**: Medium-chain acyl-CoA dehydrogenase deficiency (MCADD) is included in many newborn screening programmes worldwide. In addition to the prevalent mutation c.985A>G in the *ACADM* gene, potentially mild mutations like c.199T>C are frequently found in screening cohorts. There is ongoing discussion whether this mutation is associated with a clinical phenotype.

**Methods**: In 37 MCADD patients detected by newborn screening, biochemical phenotype (octanoylcarnitine (C8), ratios of C8 to acetylcarnitine (C2), decanoylcarnitine (C10) and dodecanoylcarnitine (C12) at screening and confirmation) and clinical phenotype (inpatient emergency treatment, metabolic decompensations, clinical assessments, psychometric tests) were assessed in relation to genotype.

**Results**: 16 patients were homozygous for c.985A>G (group 1), 11 compound heterozygous for c.199T>C and c.985A>G/another mutation (group 2) and 7 compound heterozygous for c.985A>G and mutations other than c.199T>C (group 3) and 3 carried neither c.985A>G nor c.199T>C but other known homozygous mutations (group 4). At screening C8/C2 and C8/C10, at confirmation C8/C2, C8/C10 and C8/C12 differed significantly between patients compound heterozygous for c.199T>C (group 2) and other genotypes. C8, C10 and C8/C2 at screening were strongly associated with time of sampling in groups 1 + 3 + 4, but not in group 2. Clinical phenotype did not differ between genotypes. Two patients compound heterozygous for c.199T>C and a severe mutation showed neonatal decompensation with hypoglycaemia.

**Conclusion**: Biochemical phenotype differs between MCADD patients compound heterozygous for c.199T>C with a severe mutation and other genotypes. In patients detected by newborn screening, clinical phenotype does not differ between genotypes following uniform treatment recommendations. Neonatal decompensation can also occur in patients with the presumably mild mutation c.199T>C prior to diagnosis.

## Introduction

Medium-chain acyl-CoA dehydrogenase deficiency (MCADD) is the most common inborn error of fatty acid oxidation, which affects about 1:20,000 to 1:8,000 newborns (Andresen et al. 2001; Grosse et al. 2006; Saudubray et al. 2012). It is included in many newborn screening programmes worldwide (National Newborn Screening and Genetics Resource Center, Austin, Texas; Bundesausschuss 2005; Wilcken et al. 2007). Outcome is predominantly excellent following presymptomatic diagnosis, if prolonged fasting is avoided and adequate emergency management is performed during episodes of metabolic stress (Wilcken et al. 2007; Lindner et al. 2011). In cohorts

Communicated by: Rodney Pollitt, PhD

G. Gramer (✉) · G. Haege · J. Fang-Hoffmann · G.F. Hoffmann · P. Burgard · M. Lindner
Department of General Paediatrics, Division for Neuropaediatrics and Metabolic Medicine, Centre for Paediatric and Adolescent Medicine, University of Heidelberg, Im Neuenheimer Feld 430, 69120 Heidelberg, Germany
e-mail: gwendolyn.gramer@med.uni-heidelberg.de

C.R. Bartram · K. Hinderhofer
Institute of Human Genetics, University of Heidelberg, Im Neuenheimer Feld 366, 69120 Heidelberg, Germany

diagnosed symptomatically, about 20% of patients died from their first metabolic decompensation, 20% showed severe neurological sequelae (Derks et al. 2006). In these cohorts, the c.985A>G mutation in the *ACADM* gene accounted for about 90% of disease-causing alleles (Gregersen et al. 1991; Yokota et al. 1991; Derks et al. 2006). In addition to this most common mutation in Europe, in screening cohorts other mutations, especially c.199T>C, are frequently found (Ziadeh et al. 1995; Andresen et al. 2001; Maier et al. 2005; Waddell et al. 2006; Hsu et al. 2008). There is ongoing discussion, whether patients with this potentially mild mutation would ever show any clinical phenotype (Andresen et al. 2001) or might not require treatment at all (Sturm et al. 2012). However, findings on associations between genotype and biochemical phenotype in MCADD are divergent (Andresen et al. 1997; Maier et al. 2005; Rhead 2006; Sturm et al. 2012). A straightforward correlation between clinical phenotype and genotype could not be demonstrated so far (Wilcken et al. 1994; Andresen et al. 1997).

## Methods

### Patients

From 1999 until 2012, MCADD was detected in 119 newborns at the Newborn Screening Center in Heidelberg. According to our current protocol, MCADD recall is performed in all cases with C8 > 1 μmol/L and cases with C8 > 0.28 μmol/L if C8/C10 is > P 99, C8/C2 > P 99.5 and C8/12 > P 99.5. Minimal criteria for confirmation of MCADD are a characteristic acylcarnitine profile in dried blood and presence of hexanoylglycine in urine or an informative genotype or reduced enzyme activity. In this study we report follow-up data based on the biochemical and clinical phenotypes of 37 patients with MCADD who took part in a study on long-term outcome of patients with inborn errors of metabolism detected by newborn screening (Lindner et al. 2011) and in whom information on genotype (both alleles) was available.

The recommended time for newborn screening blood sampling in Germany was day 3–5 before 2002 and 36–72 h thereafter (Harms et al. 2002).

After confirmation of MCADD, all families received counselling by a metabolic specialist. Recommendations included regular feeds, avoidance of prolonged fasting and immediate contact to the metabolic centre in case of intercurrent infections to decide on further management. All children received a personalised emergency card.

Mean age of patients (17 male, 20 female) at evaluation was 7.0 years (SD 4.2, range 0.6–14.4).

### Genotype

Genotype analysis was performed at the Institute of Human Genetics, University of Heidelberg. All exons and parts of the neighbouring intron regions of the *ACADM* gene (NM_000016.4) were analysed by direct sequencing (Zschocke et al. 2001). Mutations are described according to the recommendations of HGVS (http://www.hgvs.org/mutnomen/). The conventional nomenclature on protein level skips the first 25 amino acids of the precursor peptide and starts numbering with codon 26. Mutation analysis in patients' parents was not routinely performed, but compound heterozygosity was assumed in these biochemically well-characterised patients carrying two mutations.

### Biochemical Parameters

Acylcarnitine profiles were measured from dried blood spots as previously described (Schulze et al. 2003). Levels of octanoylcarnitine (C8) and ratios of C8 to acetylcarnitine (C2), decanoylcarnitine (C10) and dodecanoylcarnitine (C12) at screening and confirmation were used for further evaluation.

Analysis of organic acids in urine was performed using gas chromatography/mass spectrometry (Hoffmann et al. 1989). For selected patients, e.g., with mutations not previously described, enzyme activity in lymphocytes was analysed by Prof. Wanders, AMC, Amsterdam, the Netherlands (patients 18, 29), or by Prof. Spiekerkötter, University Children's Hospital, Düsseldorf, Germany (patients 17, 28).

### Clinical Parameters

Standardised clinical status examination investigated 32 clinically relevant signs related to the central nervous system, peripheral nervous system, muscle, heart, eye, liver, skin, kidney, haematopoiesis and growth. A critical subset of signs relevant to MCADD was defined (available upon request). Most recent clinical assessments were evaluated, and assessments with at least one disease relevant finding were classified as abnormal. Intellectual development was evaluated by standardised psychometric instruments appropriate for age: 1.5 years Denver test or Bayley Scales of Infant Development (BSID-II), 3.5 years K-ABC or WPPSI-III and >5 years SON-R 2.5–7 or WISC-IV. IQ ≥ 85 was considered normal; results <85 and Denver results not appropriate for age were scored subnormal.

### Statistical Analysis

Differences of acylcarnitine markers between groups were tested for significance by randomised one-way ANOVA

(Edgington 1995; Howell 2001; Smucker et al. 2007). Cohen's $d = \sqrt{\frac{\sum_{i=1}^{k}(\hat{\mu}_i - \hat{\mu})^2/k}{MS_{error}}}$ was computed as measure for the size of the differences. For group comparison of "presence of hexanoylglycine" and clinical parameters, Fisher's exact test was used (IBM SPSS Statistics 20.0).

For analysis of acylcarnitines in relation to time of sampling, curve fitting and nonlinear regression were performed using *R* (Spiess 2012; Elzhov et al. 2013). Akaike weights were used as criterion for model selection (Spiess and Neumeyer 2010). Adjusted $R^2_{adj}$ was used as measure of strength of association between time and acylcarnitine marker (strong association assumed if $R^2_{adj} > 0.6$). The Anderson-Darling test was computed using *R* (Scholz 2011).

Due to the explorative nature of the analysis, no adjustment of alpha error was performed. *P*-values $\leq 0.05$ were considered statistically significant, values $>0.05$ and $\leq 0.1$ reported as trends.

## Results

### Genotypes

Sixteen patients were homozygous for c.985A>G (genotype group 1), eleven patients (group 2) compound heterozygous for c.199T>C in combination with c.985A>G ($n = 8$) or another mutation ($n = 3$) and seven patients compound heterozygous for c.985A>G and mutations other than c.199T>C (group 3) and three patients carried neither c.985A>G nor c.199T>C but other known homozygous mutations (group 4). Thus, c.985A>G was the most frequent disease-causing allele accounting for 63.5%, followed by c.199T>C with 14.9% of all alleles.

Information on individual patients and assumed severity of mutations other than c.985A>G or c.199T>C according to literature (Andresen et al. 2001; Waddell et al. 2006; ter Veld et al. 2009; Smith et al. 2010; Yusupov et al. 2010; Sturm et al. 2012) is given in Table 1.

In one patient of German origin, a previously unreported mutation (HGMD 2013) was found. Patient 29 carried c.985A>G and c.721G>A/p.(Gly241Ser) (conventional nomenclature: Gly216Ser). A pathogenetic relevance of c.721G>A seems likely, as glycine at position 241 lies in a conserved region. Enzyme activity in lymphocytes (AMC Amsterdam) was <0.06 nmol/min mg protein (norm 0.43–1.63). The patient never showed a symptomatic episode, but was so far admitted five times for emergency treatment during intercurrent infections.

Patient 18 carried c.403_405delATT/p.(Ile135del) (conventional nomenclature: Ile110del), causing loss of isoleucine at position 135, together with c.199T>C. Enzyme activity in lymphocytes (AMC Amsterdam) was 0.18 nmol/min mg protein (norm 0.43–1.63). The patient never showed a symptomatic episode and never required inpatient emergency treatment. Sturm et al. described this mutation under a different nomenclature as c.397_399delATT in a homozygous patient associated with residual enzyme activity of 3% (Sturm et al. 2012).

Patient 27 carried c.199T>C and c.1140_1141insG, the latter being a sequence variant of unknown clinical significance. Theoretically it causes frame shift and a premature stop codon and is therefore a presumably severe mutation. Enzyme activity in this patient was 13.9% according to ter Veld et al. (2009). This patient never showed a symptomatic episode.

Of the patients in genotype group 4 (neither c.985A>G nor c.199T>C), two were homozygous for c.799G>A/p.(Gly267Arg) (conventional nomenclature: Gly242Arg), and one was homozygous for c.583G>A/p.(Gly195Arg) (conventional nomenclature: Gly170Arg). All patients were of Turkish origin.

### Biochemical Parameters

Levels of C8, C8/C2, C8/C10 and C8/C12 at screening and confirmation in genotype groups 1–4 are shown in Table 2. At screening C8/C2 ($F(3,34) = 3.26$, $p = 0.049$, $d = 0.44$) and C8/C10 ($F(3,34) = 37.28$, $p < 0.001$, $d = 1.58$) differed significantly between genotype groups. For both ratios, post hoc comparisons were significant between groups 1 and 2, 2 and 3, and 2 and 4 (all *p*-values $\leq 0.03$). There was a trend towards a difference in C8 levels ($F(3,33) = 2.24$, $p = 0.096$, $d = 0.37$) and C8/C12 ($F(3,33) = 2.49$, $p = 0.087$, $d = 0.39$) between genotype groups.

At confirmation C8/C2 ($F(3,27) = 3.42$, $p = 0.033$, $d = 0.51$), C8/C10 ($F(3,28) = 29.80$, $p < 0.001$, $d = 1.49$) and C8/C12 ($F(3,26) = 4.89$, $p = 0.008$, $d = 0.66$) differed significantly between genotype groups. Post hoc comparisons were significant between groups 1 and 2 and 2 and 3 for all ratios and between 2 and 4 only for C8/C10 and C8/C12 (all *p*-values $\leq 0.022$).

Comparing only patients from genotype group 1 and 2, all acylcarnitine parameters evaluated were significantly higher (all *p*-values $\leq 0.018$) in group 1 at screening and confirmation (compare Table 2). The best discriminative parameter between these two groups was C8/C10, both at screening and confirmation, as there was no overlap between the two groups.

**Table 1** Genotypes, biochemical and clinical phenotypes

| Pat. No. | Mutation 1 | Mutation severity | Mutation 2 | Mutation severity | Genotype group | C8 NBS | C8 confirmation | HG at confirmation (0 = not detectable 1 = detectable) | Number of symptomatic episodes | If symptomatic episode: hypoglycaemia (1 = yes, 0 = no) | If symptomatic episode: impaired consciousness (1 = yes, 0 = no) | Clinical status (1 = abnormal, 0 = normal) | IQ | Age at evaluation (years) |
|---|---|---|---|---|---|---|---|---|---|---|---|---|---|---|
| 1 | c.985A>G | S | c.985A>G | S | 1 | 1.73 | 1.91 | 0 | 0 | | | 0 | 128 | 14.4 |
| 2 | c.985A>G | S | c.985A>G | S | 1 | 7.14 | 1.3 | 1 | 1[a] | 1 | 1 | 0 | 109 | 13.7 |
| 3 | c.985A>G | S | c.985A>G | S | 1 | 1.05 | 5.33 | 0 | 0 | | | 0 | 102 | 13.7 |
| 4 | c.985A>G | S | c.985A>G | S | 1 | 7.58 | 10.1 | 1 | 1 | 0 | 1 | 0 | 79 | 12.3 |
| 5 | c.985A>G | S | c.985A>G | S | 1 | 6.49 | mv | mv | 1[a] | mv | 1 | 0 | 105 | 12.3 |
| 6 | c.985A>G | S | c.985A>G | S | 1 | 22.46 | 2.31 | mv | 0 | | | nd | nd | 11.3 |
| 7 | c.985A>G | S | c.985A>G | S | 1 | 23.19 | 5.5 | mv | 0 | | | 0 | 106 | 11.2 |
| 8 | c.985A>G | S | c.985A>G | S | 1 | 3.05 | 4.03 | mv | 0 | | | 0 | 104 | 9.9 |
| 9 | c.985A>G | S | c.985A>G | S | 1 | 4.69 | 1.73 | 1 | 0 | | | 0 | 104 | 6.4 |
| 10 | c.985A>G | S | c.985A>G | S | 1 | 1.87 | 3.1 | 1 | 0 | | | nd | 76 | 6.2 |
| 11 | c.985A>G | S | c.985A>G | S | 1 | 4.9 | 3.39 | 1 | 2 | mv | 1 | 0 | 119 | 6.8 |
| 12 | c.985A>G | S | c.985A>G | S | 1 | 6.43 | 3.96 | 1 | 0 | | | 0 | 118 | 5.9 |
| 13 | c.985A>G | S | c.985A>G | S | 1 | 3.92 | 3.06 | 1 | 0 | | | 0 | 120 | 5.3 |
| 14 | c.985A>G | S | c.985A>G | S | 1 | 6.54 | 1.59 | 1 | 0 | | | 0 | AA | 2.4 |
| 15 | c.985A>G | S | c.985A>G | S | 1 | 40.22 | 0.97 | 1 | 1[a] | 1 | 0 | 0 | AA | 1.8 |
| 16 | c.985A>G | S | c.985A>G | S | 1 | 7.89 | 1.46 | 1 | 0 | | | 0 | nd | 1.2 |
| 17 | c.799G>A | S[b] | c.199T>C | M | 2 | 2.15 | 6.51[c] | 1 | 1[a] | 1 | 1 | 0 | 93 | 4.3 |
| 18 | c.403_405delATT | S[d] | c.199T>C | M | 2 | 2.51 | 0.39 | 1 | 0 | | | 0 | 114 | 9.9 |
| 19 | c.985A>G | S | c.199T>C | M | 2 | 1.7 | 1.34 | 0 | 0 | | | 0 | 108 | 14.1 |
| 20 | c.985A>G | S | c.199T>C | M | 2 | 2.2 | 0.5 | 1 | 0 | | | 0 | 127 | 8.4 |
| 21 | c.985A>G | S | c.199T>C | M | 2 | 2.21 | 1.13 | 1 | 1[a] | 1 | 0 | 0 | 100 | 8.4 |
| 22 | c.985A>G | S | c.199T>C | M | 2 | 3.1 | 0.53 | 0 | 0 | | | 0 | 92 | 7.8 |
| 23 | c.985A>G | S | c.199T>C | M | 2 | 1.36 | 0.35 | 1 | 0 | | | 0 | 122 | 7.7 |
| 24 | c.985A>G | S | c.199T>C | M | 2 | 0.97 | 1.94 | mv | 0 | | | 0 | 122 | 7.8 |
| 25 | c.985A>G | S | c.199T>C | M | 2 | 1.17 | 0.37 | 1 | 0 | | | 0 | AA | 1.9 |
| 26 | c.985A>G | S | c.199T>C | M | 2 | 1.94 | 0.28 | 1 | 0 | | | 0 | AA | 1.5 |
| 27 | c.1140_1141insG | U[e]/S | c.199T>C | M | 2 | 0.78 | 0.48 | mv | 0 | | | 0 | AA | 7.8 |
| 28 | c.985A>G | S | c.424_426delAAG | S[f] | 3 | 6.17 | 4.6 | mv | 0 | | | 0 | nd | 4.3 |
| 29 | c.985A>G | S | c.721G>A | U[g] | 3 | 14.38 | 5.72 | 1 | 0 | | | 0 | AA | 3.2 |

| | | | | | | | | | | | | | |
|---|---|---|---|---|---|---|---|---|---|---|---|---|---|
| 30 | c.985A>G | S | c.799G>A | S[b] | 3 | 6.47 | 1.52 | 1 | 0 | 0 | nd | 1.6 |
| 31 | c.985A>G | S | c.387+1G>A | S[h] | 3 | 4.97 | 1.06 | 1 | 0 | 1 | NAA | 3.9 |
| 32 | c.985A>G | S | c.362C>T | S[i] | 3 | 2.15 | 3.86 | 1 | 0 | nd | 107 | 7.1 |
| 33 | c.985A>G | S | c.244_245insT | S[i] | 3 | 10.82 | 3.88 | 1 | 0 | 0 | nd | 1.7 |
| 34 | c.985A>G | S | c.244_245insT | S[i] | 3 | 0.57 | 1.67 | 1 | 0 | 0 | nd | 0.6 |
| 35 | c.583G>A | S[j] | c.583G>A | S[j] | 4 | 9.27 | 3.82 | 1 | 0 | 0 | AA | 2.7 |
| 36 | c.799G>A | S[b] | c.799G>A | S[b] | 4 | 4.17 | 2.67 | 1 | 0 | 0 | 107 | 11.0 |
| 37 | c.799G>A | S[b] | c.799G>A | S[b] | 4 | 6.01 | 1.24 | mv | 0 | 0 | 90 | 7.7 |

[a] Decompensation in neonatal period
[b] Smith et al. (2010)
[c] Sample was taken in period of decompensation
[d] Sturm et al. (2012) (Nomenclature c.397_399delATT, enzyme activity 3%)
[e] Sequence variant of unknown clinical significance; theoretically causing frameshift and premature stop codon, therefore presumably severe mutation; enzyme activity in this patient 13.9% according to ter Veld et al. (2009)
[f] Enzyme activity in lymphocytes 0% (performed at the University Children's Hospital, Duesseldorf)
[g] Mutation not previously described
[h] Yusupov et al. (2010)
[i] Andresen et al. (2001)
[j] Waddell et al. (2006)

*AA* result of Denver test appropriate for age, *C8* octanoylcarnitine, *HG* hexanoylglycine in urine, *mv* missing value, *NAA* result of Denver test not appropriate for age, *NBS* newborn screening, *nd* not done, *S* severe (assumed mutation severity), *M* mild (assumed mutation severity), *U* mutation severity unknown

**Table 2** Biochemical parameters for the four genotype groups in the first newborn screening sample (upper lines) and at confirmation (lower lines)

| Genotype group | | C8 | C8/C2 | C8/C10 | C8/C12 |
|---|---|---|---|---|---|
| *Group 1* | | | | | |
| c.985A>G/c.985A>G | Mean | 9.32 | 0.42 | 10.99 | 95.55 |
| | SD | 10.47 | 0.41 | 2.43 | 114.74 |
| | Range | 1.05; 40.22 | 0.08; 1.83 | 6.41; 15.71 | 9.55; 449.20 |
| | Mean | 3.23 | 0.45 | 11.37 | 44.39 |
| | SD | 2.44 | 0.39 | 2.95 | 28.52 |
| | Range | 0.97; 10.10 | 0.08; 1.29 | 6.30; 18.25 | 5.80; 82.00 |
| *Group 2* | | | | | |
| c.199T>C/c.985A>G or another mutation | Mean | 1.83 | 0.07 | 2.67 | 13.21 |
| | SD | 0.71 | 0.03 | 0.44 | 7.20 |
| | Range | 0.78; 3.10 | 0.03; 0.14 | 1.87; 3.33 | 5.86; 31.38 |
| | Mean | 1.26 | 0.06 | 2.14 | 8.84 |
| | SD | 2.14 | 0.05 | 0.65 | 4.11 |
| | Range | 0.28; 6.51 | 0.01; 0.20 | 1.55; 4.12 | 4.41; 15.50 |
| *Group 3* | | | | | |
| c.985A>G/other than c.199T>C | Mean | 6.50 | 0.27 | 10.97 | 46.43 |
| | SD | 4.78 | 0.16 | 2.99 | 22.53 |
| | Range | 0.57; 14.38 | 0.10; 0.55 | 7.68; 15.06 | 14.25; 79.99 |
| | Mean | 2.95 | 0.23 | 10.35 | 42.49 |
| | SD | 1.82 | 0.12 | 2.59 | 19.31 |
| | Range | 1.06; 5.72 | 0.07; 0.36 | 7.24; 13.62 | 21.20; 71.50 |
| *Group 4* | | | | | |
| Neither c.985A>G nor c.199T>C | Mean | 6.48 | 0.29 | 8.49 | 46.90 |
| | SD | 2.58 | 0.26 | 1.98 | 28.33 |
| | Range | 4.17; 9.27 | 0.03; 0.55 | 6.20; 9.70 | 14.38; 66.21 |
| | Mean | 3.25 | 0.20 | 9.29 | 28.49 |
| | SD | 0.81 | 0.21 | 0.86 | 8.82 |
| | Range | 1.24; 3.82 | 0.04; 0.35 | 8.68; 9.89 | 22.25; 34.73 |

Presence of hexanoylglycine in urine did not differ between genotype groups (Fisher's exact test, $p = 0.741$).

## Time of Sampling

Median age at blood sampling for screening was 3.0 days (mean 3.5, SD 2.2, range 1.5–14.1) and at confirmation 10.5 days (mean 12.9, SD 10.3, range 4.0–56.0). There was no significant difference between genotype groups regarding the distribution of time of blood sampling for screening (Anderson-Darling test adjusted for ties: AD ($N = 37$) $= -0.93$, $p = 0.693$) and confirmation (AD ($N = 36$) $= 0.80$, $p = 0.182$). Regression equations and models for curve fitting are shown for parameters at screening for genotype groups 1 + 3 + 4 vs. group 2 in Fig. 1. At screening, in genotype groups 1 + 3 + 4, C8, C8/C2 and C10 were strongly associated with age at sampling (C8, $R^2_{adj} = 0.679$; C8/C2, $R^2_{adj} = 0.778$; C10, $R^2_{adj} = 0.737$). In genotype group 2, there was no association between time of sampling and any of the parameters assessed (maximum $R^2_{adj} = 0.058$ ). At confirmation none of the parameters showed an association with time of sampling in any genotype group (maximum $R^2_{adj} = 0.18$).

## Clinical Outcome

Symptomatic episodes, defined as episodes with hypoglycaemia and/or reduced consciousness, occurred in 7 of 37 patients (18.9%; details in Table 1). None of these episodes resulted in death. Four patients showed an episode with

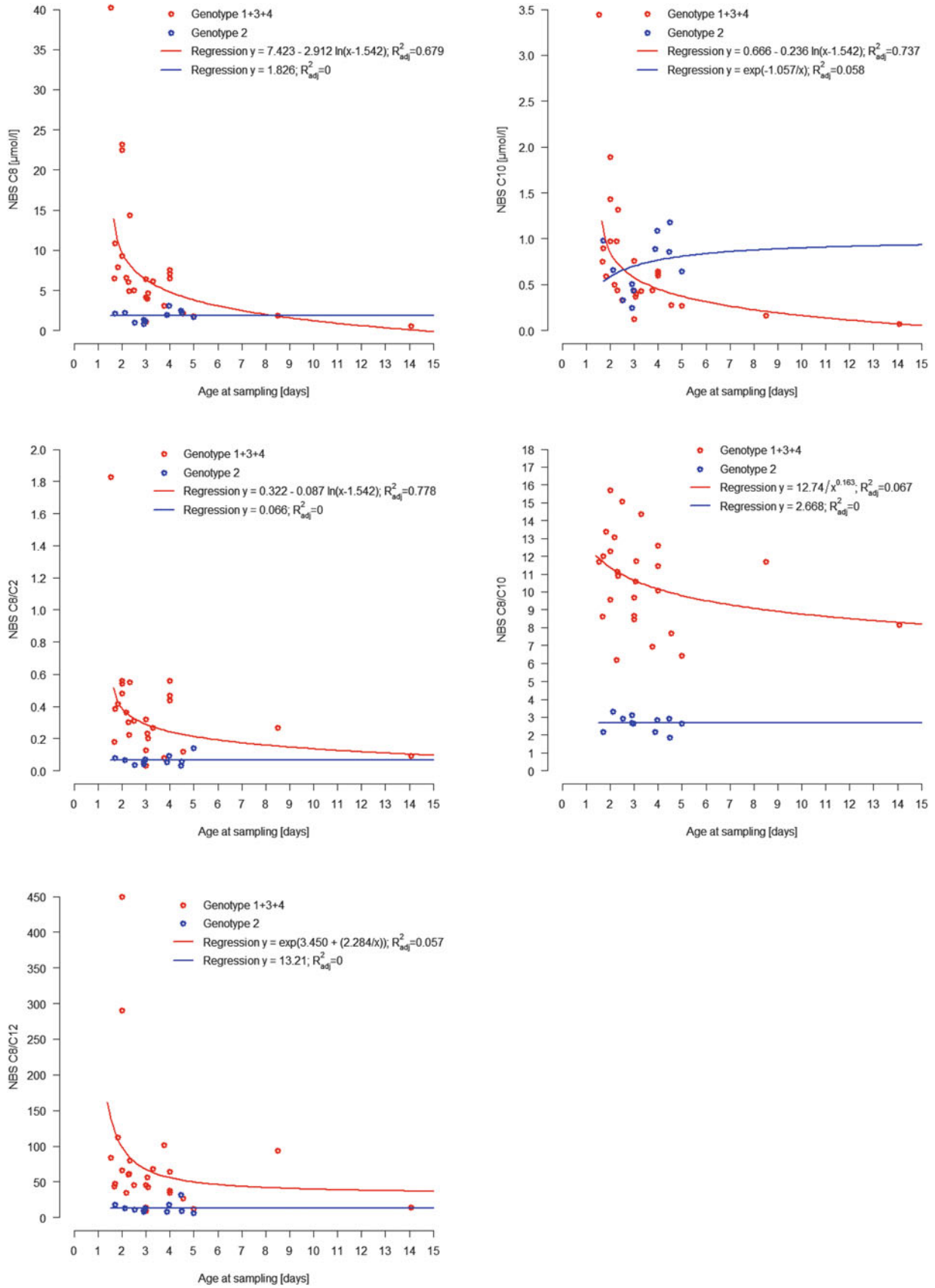


**Fig. 1** Biochemical parameters at first screening in relation to age at sampling in genotype groups 1 + 3 + 4 and 2. Regression equations and regression models for nonlinear curve fitting are shown for C8 (logarithmic and linear model), C10 (logarithmic and S-model), C8/C2 (logarithmic and linear model), C8/C10 (hyperbolic and linear model) and C8/C12 (S-model and linear model)

hypoglycaemia (Patients 2, 15, 17, 21), all in the neonatal period before screening results were available. Two of these patients were homozygous for c.985A>G (patients 2 and 15), one compound heterozygous for c.799G>A and c.199T>C (patient 17) and one for c.985A>G and c.199T>C (patient 21). Patient 17 was admitted to hospital on day 4 of life because of pronounced weight loss and tachypnea and showed metabolic acidosis, hypoglycaemia (blood glucose 2 mmol/L) and ketonuria (ketonstix +++). Residual enzyme activity in lymphocytes was 19% (University Children's Hospital, Düsseldorf). Patient 21 showed postnatal hypoglycaemia (blood glucose 1.2 mmol/L) and was treated on the neonatal intensive care unit with oral feeds of carbohydrates on the first day of life. Patients 2 and 17 also showed reduced consciousness in these episodes.

Three patients, all c.985A>G homozygous, had episodes with reduced consciousness without hypoglycaemia or without information on blood glucose level. Patient 11 showed two episodes (aged 20 and 21 months) with reduced consciousness after 12 h overnight fast. Blood glucose was not measured, but after application of glucose polymer by the parents, the patient was reported to have recovered quickly and to be vigilant again. Patient 4 was admitted to intensive care aged 5 weeks with severe dehydration and reduced consciousness, but normal blood glucose. Patient 5 showed neonatal decompensation with coma and need for resuscitation. This event took place at an external hospital, and unfortunately we do not have information on blood glucose levels from this episode.

The number of symptomatic episodes ($p = 0.675$) and hospital admissions for emergency treatment ($p = 0.392$) did not differ between genotype groups. Except for delayed speech development in patient 31, there were no relevant pathological findings in clinical status in any of the patients. Results of developmental tests were normal in 90.3% of patients (28 of 31), which is not different from a standard cohort (about 16% IQ < 85). Percentage of subnormal developmental test results or abnormal clinical findings did not differ between genotype groups. Patient 5 who had experienced neonatal decompensation with coma and need for resuscitation showed normal clinical status and intellectual development (IQ 105).

## Discussion

MCADD is widely accepted as suitable condition for newborn screening, as death or neurological sequelae can mostly be prevented by prophylactic measures (Nennstiel-Ratzel et al. 2005; Wilcken et al. 2007; Lindner et al. 2011). This finding could be replicated in our follow-up study. As for many other conditions, also in MCADD the number of patients identified by screening is higher than the number of patients identified clinically (Derks et al. 2005; Wilcken et al. 2007; Wilcken et al. 2009). The genotypic spectrum in screened cohorts includes presumably mild mutations like c.199T>C (Andresen et al. 2001; Maier et al. 2005), and there is ongoing discussion about genotype-phenotype correlation. In our study we assessed biochemical and clinical phenotype in relation to genotype in patients detected by newborn screening.

### Biochemical Phenotype

We found significant differences and trends between genotype groups in several acylcarnitine markers at screening and confirmation. Patients compound heterozygous for c.199T>C and c.985A>G or another mutation showed lower acylcarnitine markers than the other genotype groups, which is in line with previous reports (Maier et al. 2005; Waddell et al. 2006). In contrast to results from an Australian cohort (Waddell et al. 2006), we found no difference between patients homozygous for c.985A>G and compound heterozygous for c.985A>G in combination with mutations other than c.199T>C. This is in accordance with the report by Maier and colleagues (2005). Other authors (Sturm et al. 2012) reported a lack of association between genotype and octanoylcarnitine levels at screening due to an overlap between patients homozygous for c.985A>G and compound heterozygous for c.985A>G and c.199T>C. However, this study did not consider ratios between acylcarnitines and did not apply statistical methods to compare biochemical parameters between genotypes.

In our study, patients carrying neither c.985A>G nor c.199T>C but other known homozygous mutations did not differ biochemically from patients carrying c.985A>G (homozygous or in combination with mutations other than c.199T>C), but from patients carrying c.199T>C compound heterozygous with c.985A>G or another mutation. Two of these three patients were homozygous for c.799G>A, which has been described as severe (Smith et al. 2010; Sturm et al. 2012) and has been found in symptomatic patients (Yokota et al. 1991; Andresen et al. 1997). In contrast to only mild elevations of acylcarnitine markers found in three patients homozygous for c.799G>A reported by Maier et al. (2005), which lay in the range of patients carrying c.199T>C and another mutation, C8 levels in our patients homozygous for c.799G>A lay above the range of patients carrying c.199T>C and another mutation.

In our patient collective, we found C8/C10 to best discriminate between patients homozygous for c.985A>G and compound heterozygous for c.199T>C and c.985A>G or another mutation, which is in line with other reports (Maier et al. 2009; Smith et al. 2010).

### Time of Sampling

It has been reported that time of sampling affects octanoylcarnitine levels in MCADD (Rhead 2006; Maier et al. 2009), but not in unaffected newborns (Khalid et al. 2010). As age at sampling did not differ between genotype groups, our collective was eligible for assessment of both the association between biochemical parameters and genotype and biochemical parameters and time of sampling. Only octanoylcarnitine, C8/C2 and C10 at screening showed a strong association with age at sampling in patients with genotypes not including c.199T>C, with both levels decreasing with time. In patients compound heterozygous for c.199T>C and c.985A>G or another mutation, no association was found between time of sampling and any of the parameters at screening. At confirmation, none of the parameters showed an association with time in any of the genotype groups. It is important to be aware of this age dependency in interpretation of screening results, especially if the first sample has been drawn later than the recommended age of 36–72 h.

### Clinical Phenotype

Previous studies have come to the conclusion that in MCADD, correlation between genotype and clinical phenotype is not straightforward (Wilcken et al. 1994; Heptinstall et al. 1995; Andresen et al. 1997) and that clinical variation may result from differences in metabolic stress experienced rather than differences in genotype (Andresen et al. 1997). In our study neonatal episodes of hypoglycaemia were also documented for two patients carrying the presumably mild mutation c.199T>C. So far it had been stated that patients compound heterozygous for c.199T>C and another mutation had never been found to be symptomatic (Andresen et al. 2001; Maier et al. 2005; Waddell et al. 2006; Smith et al. 2010; Sturm et al. 2012). O'Reilly reported that patients carrying c.199T>C compound heterozygous with c.985A>G had shown significant lethargy without hypoglycaemia in an episode of vomiting, requiring hospital admission (O'Reilly et al. 2004). Both our patients carried a known disease-causing mutation on the second allele (patient 17 c.199T>C and c.799G>A; patient 21 c.199T>C and c.985A>G). The mutation c.799G>A has been found in patients detected asymptomatically by newborn screening (Zschocke et al. 2001), as well as in symptomatic patients (Yokota et al. 1991; Andresen et al. 1997). This mutation has been classified as severe (Smith et al. 2010; Sturm et al. 2012). Residual enzyme activity of 19% in our patient 17 (c.199T>C and c.799G>A) was in the range of disease-causing mutations.

Sturm et al. (2012) found residual enzyme activities in patients compound heterozygous for c.199T>C and a severe mutation between 28% and 49% and discussed that c.199T>C may be an innocuous polymorphism without clinical relevance. As a consequence of hypoglycaemia in our two patients carrying c.199T>C and a severe mutation, it should be considered that also patients with presumably mild mutations might become symptomatic under metabolic stress. Thus, it does not seem safe to predict a completely asymptomatic clinical phenotype from the milder biochemical phenotype. Neonatal hypoglycaemia or death has been reported in patients with MCADD diagnosed symptomatically (Wilcken et al. 1994; Derks et al. 2006; Wilcken et al. 2007). However, it could be discussed that neonatal hypoglycaemia in our patients might have been unrelated to MCADD. Neonatal hypoglycaemia affects 5–15% of otherwise healthy newborns (Harris et al. 2013). Patient 17 showed ketotic hypoglycaemia, which is not typical for MCADD, but has been reported in a relevant number of MCADD patients before (Iafolla et al. 1994). This finding can be explained by some residual MCAD function. Hsu also reported a patient with MCADD (c.985A>G and c.127G>A) with marked ketonuria during an intercurrent infection (Hsu et al. 2008).

In our study, reduced consciousness was documented in one patient homozygous for c.985A>G without hypoglycaemia. Reduced vigilance might be explained by severe dehydration in this patient. However, some authors postulate that in MCADD episodes of reduced consciousness can occur without hypoglycaemia due to accumulation of free fatty acids and their carnitine and CoA esters (Mayell et al. 2007; Saudubray et al. 2012).

So far, all our patients with MCADD detected by newborn screening receive uniform recommendations regarding feeding intervals and emergency management. Under this prophylactic treatment, no difference was found between different genotype groups concerning number of metabolic decompensations, inpatient emergency treatment and the overall excellent clinical outcome. Concerning clinical evaluation, the finding of delayed speech development in one patient – who had never experienced a metabolic decompensation – may well be unrelated to MCADD, as it is common in the general population (Gottschling et al. 2012). The percentage of MCADD patients with subnormal psychometric test results (10%) was not higher than expected in the general population.

### Conclusion

Patients with MCADD homozygous for c.985A>G did not differ biochemically from patients compound heterozygous

for c.985A>G and mutations other than c.199T>C. Patients carrying c.199T>C in combination with c.985A>G or another mutation showed significantly lower acylcarnitine markers compared to other genotypes and thus a "milder" biochemical phenotype. Evaluation of clinical phenotype of our patients showed – to our knowledge for the first time – that neonatal decompensation with hypoglycaemia can also occur in patients carrying c.199T>C and a severe mutation prior to diagnosis. Therefore, it does not seem safe to predict an asymptomatic clinical phenotype from the milder biochemical phenotype. This leads to the conclusion that also in patients carrying c.199T>C compound heterozygous with a severe mutation, there may be the risk of MCADD-associated hypoglycaemia under severe metabolic stress. Given uniform treatment recommendations, no differences were found in clinical phenotype between different genotypes.

**Acknowledgements** This study was made possible by the continuous and generous support of the Dietmar Hopp Foundation, St. Leon-Rot.

The authors thank all patients and their families for their participation and trust.

Many thanks to all the colleagues who provided information on their patients: U. Wendel, E. Thimm (Düsseldorf), E. Mengel (Mainz), F.K. Trefz (Reutlingen) and M. Baumgartner (Zürich).

Enzyme activity in patients 18 and 29 was analysed by Prof. Wanders, AMC, Amsterdam, the Netherlands, and in patients 17 and 28 by Prof. Spiekerkötter at the University Children's Hospital, Düsseldorf, Germany.

## Take-Home Message

Biochemical but not clinical phenotype differs between MCADD patients with different genotypes detected by newborn screening following uniform treatment recommendations. Neonatal decompensation can also occur in patients carrying the presumably mild mutation c.199T>C compound heterozygous with a severe mutation prior to diagnosis.

## Compliance with Ethics Guidelines

### Conflict of Interest

*Authors' Disclosures*

G. Gramer received support for travel expenses to a scientific meeting from Merck Serono.

G. Haege reports no disclosures.

J. Fang-Hoffmann reports no disclosures.

G.F. Hoffmann received lecture fees from Nutricia, Friedrichsdorf i.T.

C. R. Bartram reports no disclosures.

K. Hinderhofer reports no disclosures.

P. Burgard is member of an advisory board for Merck Serono, Darmstadt, and received lecture fees from Merck Serono, Darmstadt; Vitaflo, Bad Homburg; and Nutricia, Friedrichsdorf i.T.

M. Lindner received lecture fees from Orphan Europe, Milupa and Nutricia.

### Conflict of Interest

None

### Informed Consent

All procedures followed were in accordance with the ethical standards of the responsible committee on human experimentation (institutional and national) and with the Helsinki Declaration of 1975, as revised in 2000. Informed consent was obtained from all patients/their parents for being included in the study. The study was approved by the University Hospital Heidelberg ethical committee (IRB code 104/2005).

### Authors' Contributions

G. Gramer: Study design; recruitment of patients; collection, evaluation and interpretation of data; drafting and writing the manuscript

G. Haege: Statistical analysis; evaluation and interpretation of data; writing and revision of the manuscript

J. Fang-Hoffmann: Data collection; revision of the manuscript

G. F. Hoffmann: Study design; evaluation and interpretation of data; revision of the manuscript

C. R. Bartram: Molecular genetic analyses; revision of the manuscript

K. Hinderhofer: Molecular genetic analyses; revision of the manuscript

P. Burgard: Study design; recruitment of patients; collection, evaluation and interpretation of data; statistical analysis; revision of the manuscript

M. Lindner: Study design; recruitment of patients; collection, evaluation and interpretation of data; revision of the manuscript

*All authors approved the final version of the manuscript*.

G. Gramer serves as guarantor for the article.

### Funding

This study was supported by the Dietmar Hopp Foundation, St. Leon-Rot, Germany. The authors confirm independence

from the sponsor; the content of the article has not been influenced by the sponsor.

G. Gramer was supported by a research scholarship (Olympia Morata Programme) of the Medical Faculty of the University of Heidelberg.

## References

Andresen BS, Bross P, Udvari S et al (1997) The molecular basis of medium-chain acyl-CoA dehydrogenase (MCAD) deficiency in compound heterozygous patients: is there correlation between genotype and phenotype? Hum Mol Genet 6:695–707

Andresen BS, Dobrowolski SF, O'Reilly L et al (2001) Medium-chain acyl-CoA dehydrogenase (MCAD) mutations identified by MS/MS-based prospective screening of newborns differ from those observed in patients with clinical symptoms: identification and characterization of a new, prevalent mutation that results in mild MCAD deficiency. Am J Hum Genet 68:1408–1418

Bundesausschuss GBdÄuKG (2005) Beschluss über eine Änderung der Richtlinen des Bundesausschusses der Ärzte und Krankenkassen über die Früherkennung von Krankheiten bei Kindern bis zur Vollendung des 6. Lebensjahres (Kinder-Richtlinien) zur Einführung des erweiterten Neugeborenen-Screenings, 2011. http://www.g-ba.de/informationen/beschluesse/zur-richtlinie/15/#170

Derks TG, Duran M, Waterham HR, Reijngoud DJ, Ten Kate LP, Smit GP (2005) The difference between observed and expected prevalence of MCAD deficiency in The Netherlands: a genetic epidemiological study. Eur J Hum Genet 13:947–952

Derks TG, Reijngoud DJ, Waterham HR et al (2006) The natural history of medium-chain acyl CoA dehydrogenase deficiency in the Netherlands: clinical presentation and outcome. J Pediatr 148:665–670

Edgington ES (1995) Randomization tests. Marcel-Dekker, New York

Elzhov TV, Mullen KM, Spiess A, Bolker B (2013) Minpack.lm: R interface to the Levenberg-Marquardt nonlinear least-squares algorithm found in MINPACK, plus support for bounds. http://cran.r-project.org/web/packages/minpack.lm/index.html

Gottschling A, Franze M, Hoffmann W (2012) Entwicklungsverzögerungen bei Kindern: Screening als Grundlage für eine gezielte Förderung. Dtsch Arztebl 3:123–125

Gregersen N, Blakemore AI, Winter V et al (1991) Specific diagnosis of medium-chain acyl-CoA dehydrogenase (MCAD) deficiency in dried blood spots by a polymerase chain reaction (PCR) assay detecting a point-mutation (G985) in the MCAD gene. Clin Chim Acta 203:23–34

Grosse SD, Khoury MJ, Greene CL, Crider KS, Pollitt RJ (2006) The epidemiology of medium chain acyl-CoA dehydrogenase deficiency: an update. Genet Med 8:205–212

Harms E, Roscher A, Grüters A et al (2002) Neue Screening-Richtlinien - Richtlinien zur Organisation und Durchführung des Neugeborenenscreenings auf angeborene Stoffwechselstörungen und Endokrinopathien in Deutschland. Monatsschr Kinderheilkd 150:1424–1440

Harris DL, Weston PJ, Signal M, Chase JG, Harding JE (2013) Dextrose gel for neonatal hypoglycaemia (the Sugar Babies Study): a randomised, double-blind, placebo-controlled trial. Lancet 382:2077–2083

Heptinstall LE, Till J, Wraith JE, Besley GT (1995) Common MCAD mutation in a healthy parent of two affected siblings. J Inherit Metab Dis 18:638–639

HGMD THGMD (2013) The Human gene mutation database HGMD. Retrieved 13 June, 2013 from http://www.hgmd.cf.ac.uk/ac/index.php

Hoffmann G, Aramaki S, Blum-Hoffmann E, Nyhan WL, Sweetman L (1989) Quantitative analysis for organic acids in biological samples: batch isolation followed by gas chromatographic-mass spectrometric analysis. Clin Chem 35:587–595

Howell DC (2001) Resampling Procedures Version 1.3. http://www.uvm.edu/~dhowell/StatPages/Resampling/ResamplingPackage.zip. Accessed 9 Nov 2010

Hsu HW, Zytkovicz TH, Comeau AM et al (2008) Spectrum of medium-chain acyl-CoA dehydrogenase deficiency detected by newborn screening. Pediatrics 121:e1108–e1114

Iafolla AK, Thompson RJ Jr, Roe CR (1994) Medium-chain acyl-coenzyme A dehydrogenase deficiency: clinical course in 120 affected children. J Pediatr 124:409–415

Khalid JM, Oerton J, Besley G et al (2010) Relationship of octanoylcarnitine concentrations to age at sampling in unaffected newborns screened for medium-chain acyl-CoA dehydrogenase deficiency. Clin Chem 56:1015–1021

Lindner M, Gramer G, Haege G et al (2011) Efficacy and outcome of expanded newborn screening for metabolic diseases-report of 10 years from South-West Germany. Orphanet J Rare Dis 6:44

Maier EM, Liebl B, Roschinger W et al (2005) Population spectrum of ACADM genotypes correlated to biochemical phenotypes in newborn screening for medium-chain acyl-CoA dehydrogenase deficiency. Hum Mutat 25:443–452

Maier EM, Pongratz J, Muntau AC et al (2009) Dissection of biochemical borderline phenotypes in carriers and genetic variants of medium-chain acyl-CoA dehydrogenase deficiency: implications for newborn screening [corrected]. Clin Genet 76:179–187

Mayell SJ, Edwards L, Reynolds FE, Chakrapani AB (2007) Late presentation of medium-chain acyl-CoA dehydrogenase deficiency. J Inherit Metab Dis 30:104

National Newborn Screening & Genetics Resource Center Austin Texas. National Newborn Screening & Genetics Resource Center, Austin, Texas. http://genes-r-us.uthscsa.edu/

Nennstiel-Ratzel U, Arenz S, Maier EM et al (2005) Reduced incidence of severe metabolic crisis or death in children with medium chain acyl-CoA dehydrogenase deficiency homozygous for c.985A>G identified by neonatal screening. Mol Genet Metab 85:157–159

O'Reilly L, Bross P, Corydon TJ et al (2004) The Y42H mutation in medium-chain acyl-CoA dehydrogenase, which is prevalent in babies identified by MS/MS-based newborn screening, is temperature sensitive. Eur J Biochem 271:4053–4063

Rhead WJ (2006) Newborn screening for medium-chain acyl-CoA dehydrogenase deficiency: a global perspective. J Inherit Metab Dis 29:370–377

Saudubray JM, Van den Berghe G, Walter JH (eds) (2012) Inborn metabolic diseases. Springer, Berlin

Scholz F (2011) adk: Anderson-Darling K-sample test and combinations of such tests. Retrieved 27 Sept 2013 from http://cran.r-project.org/web/packages/adk/index.html

Schulze A, Lindner M, Kohlmüller D, Olgemöller K, Mayatepek E, Hoffmann GF (2003) Expanded newborn screening for inborn errors of metabolism by electrospray ionization-tandem mass spectrometry: results, outcome, and implications. Pediatrics 111:1399–1406

Smith EH, Thomas C, McHugh D et al (2010) Allelic diversity in MCAD deficiency: the biochemical classification of 54 variants identified during 5 years of ACADM sequencing. Mol Genet Metab 100:241–250

Smucker MD, Allan J, Carterette B (2007) A comparison of statistical significance tests for information retrieval evaluation. Conference

on information and knowledge management (CIKM). ACM Press, Lisbon

Spiess A (2012) qpcR: modelling and analysis of real-time PCR data. http://cran.r-project.org/web/packages/qpcR/index.html.

Spiess AN, Neumeyer N (2010) An evaluation of R2 as an inadequate measure for nonlinear models in pharmacological and biochemical research: a Monte Carlo approach. BMC Pharmacol 10:6

Sturm M, Herebian D, Mueller M, Laryea MD, Spiekerkoetter U (2012) Functional effects of different medium-chain acyl-CoA dehydrogenase genotypes and identification of asymptomatic variants. PLoS One 7, e45110

ter Veld F, Mueller M, Kramer S et al (2009) A novel tandem mass spectrometry method for rapid confirmation of medium- and very long-chain acyl-CoA dehydrogenase deficiency in newborns. PLoS One 4, e6449

Waddell L, Wiley V, Carpenter K et al (2006) Medium-chain acyl-CoA dehydrogenase deficiency: genotype-biochemical phenotype correlations. Mol Genet Metab 87:32–39

Wilcken B, Hammond J, Silink M (1994) Morbidity and mortality in medium chain acyl coenzyme A dehydrogenase deficiency. Arch Dis Child 70:410–412

Wilcken B, Haas M, Joy P et al (2007) Outcome of neonatal screening for medium-chain acyl-CoA dehydrogenase deficiency in Australia: a cohort study. Lancet 369:37–42

Wilcken B, Haas M, Joy P et al (2009) Expanded newborn screening: outcome in screened and unscreened patients at age 6 years. Pediatrics 124:e241–e248

Yokota I, Coates PM, Hale DE, Rinaldo P, Tanaka K (1991) Molecular survey of a prevalent mutation, 985A-to-G transition, and identification of five infrequent mutations in the medium-chain Acyl-CoA dehydrogenase (MCAD) gene in 55 patients with MCAD deficiency. Am J Hum Genet 49:1280–1291

Yusupov R, Finegold DN, Naylor EW, Sahai I, Waisbren S, Levy HL (2010) Sudden death in medium chain acyl-coenzyme a dehydrogenase deficiency (MCADD) despite newborn screening. Mol Genet Metab 101:33–39

Ziadeh R, Hoffman EP, Finegold DN et al (1995) Medium chain acyl-CoA dehydrogenase deficiency in Pennsylvania: neonatal screening shows high incidence and unexpected mutation frequencies. Pediatr Res 37:675–678

Zschocke J, Schulze A, Lindner M et al (2001) Molecular and functional characterisation of mild MCAD deficiency. Hum Genet 108:404–408

JIMD Reports
DOI 10.1007/8904_2015_440

RESEARCH REPORT

# Rhabdomyolysis-Associated Mutations in Human *LPIN1* Lead to Loss of Phosphatidic Acid Phosphohydrolase Activity

**George G. Schweitzer · Sara L. Collier · Zhouji Chen · James M. Eaton · Anne M. Connolly · Robert C. Bucelli · Alan Pestronk · Thurl E. Harris · Brian N. Finck**

Received: 23 February 2015 / Revised: 06 April 2015 / Accepted: 08 April 2015 / Published online: 13 May 2015


**Abstract** Rhabdomyolysis is an acute syndrome due to extensive injury of skeletal muscle. Recurrent rhabdomyolysis is often caused by inborn errors in intermediary metabolism, and recent work has suggested that mutations in the human gene encoding lipin 1 (*LPIN1*) may be a common cause of recurrent rhabdomyolysis in children. Lipin 1 dephosphorylates phosphatidic acid to form diacylglycerol (phosphatidic acid phosphohydrolase; PAP) and acts as a transcriptional regulatory protein to control metabolic gene expression. Herein, a 3-year-old boy with severe recurrent rhabdomyolysis was determined to be a compound heterozygote for a novel c.1904T>C (p.Leu635-Pro) substitution and a previously reported genomic deletion of exons 18–19 (E766-S838_del) in *LPIN1*. Western blotting with patient muscle biopsy lysates demonstrated a marked reduction in lipin 1 protein, while immunohistochemical staining for lipin 1 showed abnormal subcellular localization. We cloned cDNAs to express recombinant lipin 1 proteins harboring pathogenic mutations and showed that the E766-S838_del allele was not expressed at the RNA or protein level. Lipin 1 p.Leu635Pro was expressed, but the protein was less stable, was aggregated in the cytosol, and was targeted for proteosomal degradation. Another pathogenic single amino acid substitution, lipin 1 p.Arg725His, was well expressed and retained its transcriptional regulatory function. However, both p.Leu635Pro and p.Arg725His proteins were found to be deficient in PAP activity. Kinetic analyses demonstrated a loss of catalysis rather than diminished substrate binding. These data suggest that loss of lipin 1-mediated PAP activity may be involved in the pathogenesis of rhabdomyolysis in lipin 1 deficiency.

Communicated by: Robin Lachmann, PhD FRCP

Competing interests: None declared

**Electronic supplementary material:** The online version of this chapter (doi:10.1007/8904_2015_440) contains supplementary material, which is available to authorized users.

G.G. Schweitzer · S.L. Collier · Z. Chen · B.N. Finck (✉)
Department of Medicine, Division of Geriatrics and Nutritional Sciences, Washington University School of Medicine, 660 S. Euclid Ave, Box 8031, St. Louis, MO 63110, USA
e-mail: bfinck@dom.wustl.edu

J.M. Eaton · A.M. Connolly
Department of Pediatrics, Washington University School of Medicine, 660 S. Euclid Ave, Box 8031, St. Louis, MO 63110, USA

A.M. Connolly · R.C. Bucelli · A. Pestronk
Department of Neurology, Washington University School of Medicine, 660 S. Euclid Ave, Box 8031, St. Louis, MO 63110, USA

A. Pestronk
Department of Pathology and Immunology, Washington University School of Medicine, 660 S. Euclid Ave, Box 8031, St. Louis, MO 63110, USA

T.E. Harris
Department of Pharmacology, University of Virginia, Charlottesville, VA, USA

## Introduction

Mutations in the gene encoding lipin 1 (*LPIN1*) have been identified as a cause of recurrent, early-onset, pediatric rhabdomyolysis and myoglobinuria (OMIM#268200) (Zeharia et al. 2008; Michot et al. 2010, 2012). Rhabdomyolysis is an acute syndrome due to extensive injury of skeletal muscle resulting in the release of intracellular metabolites and proteins, including creatine kinase and myoglobin, into the systemic circulation. Clinical features

may include myalgia, weakness, pigmenturia, renal failure, and secondary injury to other organ systems. Untreated rhabdomyolysis can result in death from renal, cardiac, or hematologic dysfunction.

Although there are many common acquired causes of acute rhabdomyolysis, hereditary etiologies should be considered in the setting of recurrent rhabdomyolysis or in the setting of rhabdomyolysis with positive family history. Classes of inherited metabolic disorders associated with recurrent rhabdomyolysis include glycogen storage diseases, fatty acid oxidation defects, and mitochondrial disorders (Tonin et al. 1990; Kelly and Strauss 1994; Bennett 2010; Zutt et al. 2014). Recently, homozygous mutations in *LPIN1* were identified as a common cause of recurrent rhabdomyolysis in pediatric patients, and more than 50% of infants and children with unexplained severe rhabdomyolysis in a European population may have pathologic mutations in *LPIN1* (Zeharia et al. 2008; Michot et al. 2010, 2012).

Lipin 1 regulates intermediary metabolism by multiple mechanisms. Lipin 1 is a lipid phosphatase converting phosphatidic acid (PA) to diacylglycerol (DAG) (PAP activity) (Han et al. 2006) through a catalytic site and other critical accessory haloacid dehalogenase (HAD) domains in the protein's C-terminus (Figs. 1a and S1). Lipin 1 also traffics to the nucleus to interact with DNA-bound transcription factors regulating expression of genes encoding mitochondrial fatty acid oxidation enzymes (Finck et al. 2006) through a nuclear receptor interaction domain (NRID) also in the protein's C-terminus (Figs. 1a and S1). Of the 19 distinct mutations in *LPIN1* associated with rhabdomyolysis, most are frameshift mutations leading to loss of expression or generating truncated proteins lacking both HAD catalytic sites and the NRID. It is unknown whether defects in lipin 1 PAP activity or transcriptional regulatory function, or both, underlie the pathogenesis of rhabdomyolysis in people with *LPIN1* mutations.

In the present study, we detected a novel missense mutation and a known exon deletion in *LPIN1* in a young boy presenting to our institution with severe recurrent rhabdomyolysis, which may be the first report of *LPIN1* mutations in a North American patient. We assessed the expression and molecular function of recombinant human lipin 1 proteins harboring rhabdomyolysis-associated mutations. We found that single amino acid substitution mutations in lipin 1 known to be present in patients with rhabdomyolysis led to loss of PAP activity via loss of catalysis, but did not always affect transcriptional regulatory function. These findings link the loss of lipin 1-mediated PAP activity to the etiology of recurrent rhabdomyolysis.

## Materials and Methods

Detailed methods and source material are described in Supplementary Materials.

### Generation and Overexpression of Mutant Alleles

Human lipin 1 cDNA in the pENTR™ vector was a gift of Andrew Morris. Changes in nucleotide sequence corresponding to known lipin 1 mutations were introduced into the cDNA by using site-directed mutagenesis. WT and mutant cDNAs were transferred to pcDNA3.1/nV5-DEST™ fusing a V5 epitope tag to the N-terminus of the protein (Life Technologies/Invitrogen, Carlsbad, CA). HEK293 cells were transfected with vectors driving expression of WT or mutant proteins for analysis of mRNA and protein expression, subcellular localization, protein half-life, and PAP activity. For kinetic analyses, WT, p.Leu635Pro, and p.Arg725His lipin 1 cDNA were transferred to pCMVTAG2 (Agilent) and then inserted into the pAdTRACK-CMV vector for adenoviral production using the AdEasy system.

### Immunohistochemistry/Fluorescent Staining

For human tissue, 10 μm sections of frozen muscle biopsies were placed on microscope slides, fixed, blocked, stained with lipin 1 antibody against the C-terminal region (Harris et al. 2007), stained with appropriate secondary antibodies, and coverslip mounted with DAPI. For human muscle histochemistry, cryostat sections of rapidly frozen muscle were processed as previously described (Mozaffar and Pestronk 2000). For cultured cell staining and cellular distribution analysis, Cos7 cells were plated and lipin 1 WT and mutant expression vectors were transfected. Twenty-four hours later, cells were fixed and incubated with DAPI, anti-V5, and anti-calnexin (cytoplasmic marker). Cells were stained with appropriate secondary antibodies and visualized by fluorescence for subcellular protein distribution analysis as described previously (Ren et al. 2010).

### Protein and RNA Analysis

Protein from cultured cells was isolated and subjected to SDS-PAGE. After blotting, WT and lipin 1 mutant protein was determined from an antibody against lipin 1, and alpha-tubulin antibody was used to demonstrate equal loading. Total RNA was isolated from cultured cells and subjected to reverse transcription, and lipin 1 gene expression was determined and normalized to 36B4 expression.

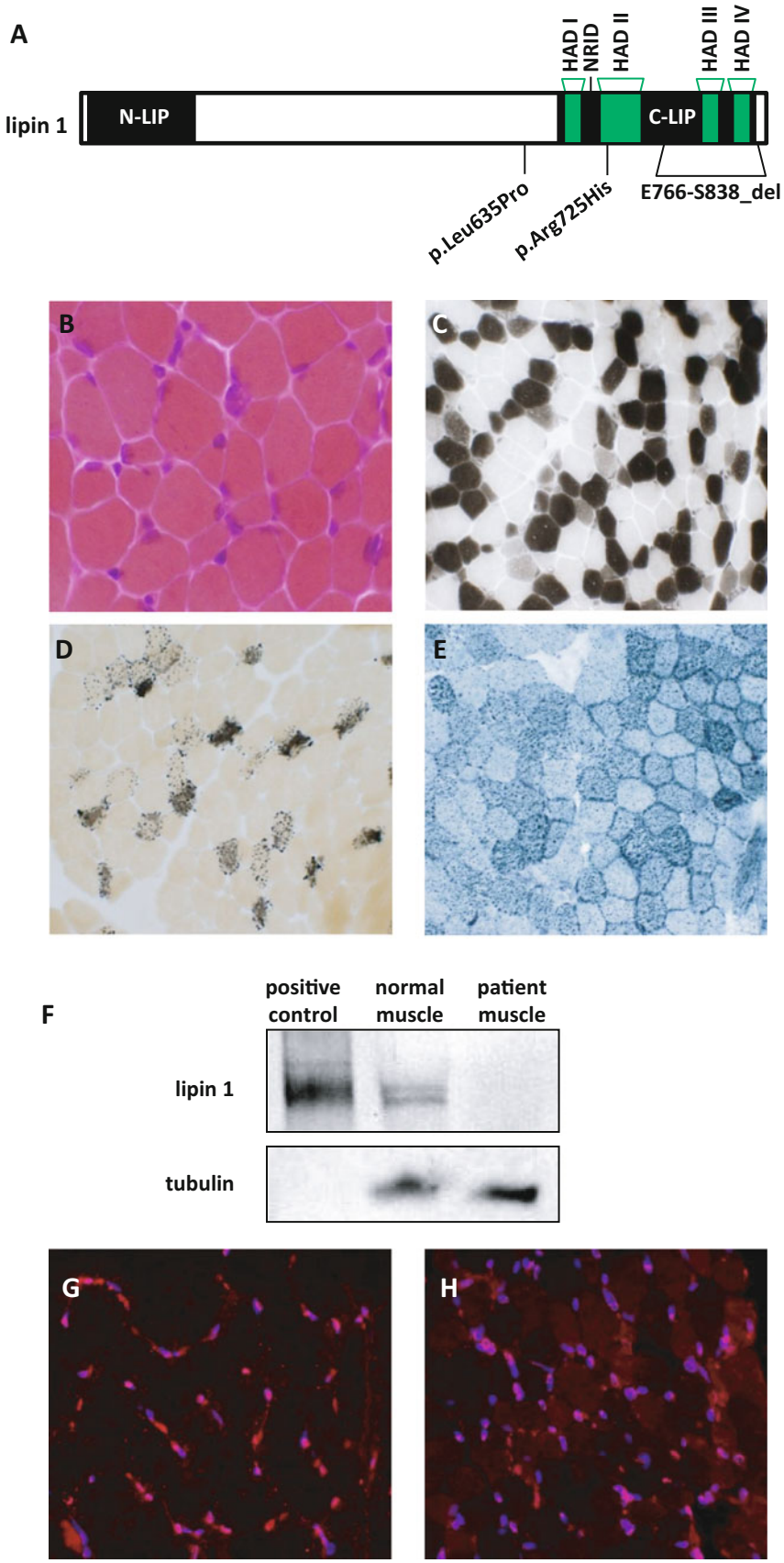


**Fig. 1** *LPIN1* mutations in a boy with recurrent rhabdomyolysis. (**a**) Diagram of *LPIN1* gene. The haloacid dehalogenase (HAD) domains that are important for regulating PAP activity are noted. The nuclear receptor interaction domain (NRID) is important for transcriptional

### Protein Half-Life

Pulse-chase labeling of the HEK293cells containing WT and lipin 1 mutant expression vectors was achieved by incubating the cells with [$^{35}$S]Cys/Met followed by chase media consisting of DMEM containing 10 mM Met and 3 mM Cys for 0, 1, 2, or 4 h. Lysates were collected in homogenization buffer as described in Supplementary Material and incubated with lipin 1 antibody overnight at 4°C. The protein-antibody complex was pulled down, subjected to SDS-PAGE, and analyzed by autoradiography.

### Transcriptional Regulation

The ability of lipin 1 to coactivate overexpressed Gal4-PGC-1α and MEF2A was assayed by cotransfection of Cos7 cells with WT and mutant lipin proteins with the Gal4-reponsive UAS thymidine kinase luciferase construct.

### PAP Activity

PAP-1 activity was assessed as described (Martin et al. 1987) with modifications. In brief, transfected cultured cells were incubated with $^{14}$C-phosphatidic acid (PA), PA salt, phosphatidylcholine, and $MgCl_2$ without or with *N*-ethylmaleimide to determine PAP-1 and PAP-1-independent activity, respectively.

### Kinetic Analysis

FLAG-tagged WT, p.Leu635Pro, and p.Arg725His lipin 1 proteins were expressed in HeLa cells with 72 h adenoviral infection, harvested, lysed, incubated with anti-FLAG beads for 2–4 h, and column purified. Lipin 1 proteins were quantified, and PAP assays were performed at pH 7.5 with Triton X-100/PA mixed micelles as previously described (Eaton et al. 2013).

### Statistical analysis

Data were expressed as means ± SEM. Unpaired t-tests were used to determine significant differences. *P* values of $<0.05$ was considered statistically significant. The Michaelis-Menten equation $k_{cat}$ was calculated by $k_{cat} = V_{max}/E_t$, where $E_t$ = enzyme catalytic site concentration.

## Results

### Patient with Novel c.1904T>C (p.Leu635Pro) Mutation

A 3-year-old boy with normal motor and cognitive development was evaluated at our institution for severe, recurrent rhabdomyolysis with myoglobinuria. His first episode of rhabdomyolysis occurred at age 16 months. After several hours of play, he developed an unsteady gait with eventual refusal to walk and tea-colored urine. Examination showed that he was afebrile and in obvious discomfort, with no evidence of hepatosplenomegaly or scleral icterus. Neurologic examination showed generalized weakness with retention of antigravity strength in all muscle groups. He would not sit or stand. During the hospital course, he remained afebrile, his discomfort slowly resolved, and his strength steadily improved with a complete return to his normal baseline within 1 month of presentation.

His laboratory studies included a markedly elevated plasma creatine kinase (CK, peak 498,800 U/L), urine myoglobin (peak 8,277,000 ng/mL), aspartate aminotransferase (peak > 8000 IU/L), and alanine aminotransferase (peak 3762 IU/L). The remainder of the laboratory testing was normal and included cerebrospinal fluid (CSF) analysis, serum and CSF lactate/pyruvate, serum ammonia, total and free plasma carnitine, acylcarnitine profile, serum and CSF amino acids, urine organic acids, leukocytic coenzyme Q10, and peroxisomal profile. Pathogenic mutations were not present in *RYR1 or PYGM*. Cardiac and abdominal ultrasounds were normal. Muscle ultrasound demonstrated diffusely increased echogenicity in the bilateral hip adductor compartments with a relative increase in signal heterogeneity on the right side. The findings were not specific to any one etiology, but were deemed consistent with the clinical history of rhabdomyolysis. A muscle biopsy was obtained 6 weeks after a second episode of rhabdomyolysis and revealed changes consistent with recent rhabdomyolysis. Increased lipid was detected with normal mitochondrial stains (Fig. 1b–e) and enzymatic

**Fig. 1 (Continued)** regulatory function. Locations of *LPIN1* mutations of the patient (p.Leu635Pro and E766-S838_del) are included with the location of another reported mutation (p. Arg725His). (**b**–**h**) A muscle biopsy was performed 6 weeks after the patient's second episode of rhabdomyolysis and processed for routine histochemical staining. All photomicrographs were obtained at 20× magnification. (**b**) H&E demonstrated moderate variation in fiber size with occasional basophilic fibers; (**c**) ATPase 4.3 revealed an excessive number of Type IIC muscle fibers; (**d**) alkaline phosphatase with increased number of positive staining fibers; (**e**) Sudan black with moderately increased lipid. (**f**) Western blot demonstrating near absence of lipin 1 expression in the same patient. (**g**) Lipin 1 immunostaining in a pediatric control muscle shows strong nuclear staining of lipin 1. (**h**) Lipin 1 immunostaining in the p.Leu635Pro; E766-S838_del compound heterozygote muscle shows significantly reduced lipin 1 staining with an abnormal stippled or perinuclear staining pattern for the small amount of protein that is present (*Blue*: DAPI, *Red*: lipin 1)

activities (data not shown). He had two additional episodes of myoglobinuria (one associated with 9 h of continuous play outside his home and the other associated with an upper respiratory tract infection) and once again made complete recoveries after each episode. Serum CK values with the subsequent episodes peaked at 477,791 U/L. Between episodes, when asymptomatic, his CK nadir was 164 U/L (normal < 300 U/L).

*LPIN1* genetic testing revealed compound heterozygosity for a novel c.1904T>C (p.Leu635Pro; Figs. 1a and S1) variant and a previously reported pathogenic genomic deletion of exons 18–19 (E766-S838_del). The p.Leu635-Pro variant was classified as "likely pathogenic" based on Polymorphism Phenotyping (PolyPhen) and Sorting Intolerant From Tolerant (SIFT) software (Ng and Henikoff 2001; Ramensky et al. 2002). Indeed, whereas lipin 1 protein was readily detectable by immunohistochemical staining and by western blotting using muscle homogenate from a control pediatric patient (Fig. 1f, g), very little lipin 1 protein was detected in the patient with *LPIN1* mutations by western blot (Fig. 1f). Immunohistochemical staining with a lipin 1 antibody showed reduced staining with abnormal subcellular localization in the patient section (Fig. 1h). Whereas lipin 1 staining in the normal patient was distributed throughout the cell with relatively greater signal in the nucleus, the patient section exhibited perinuclear aggregation of lipin 1 with reduced nuclear staining.

## LPIN1 Exon Deletion Impairs Expression of the Lipin 1 Protein

The most common lipin 1 mutation in Caucasians (Michot et al. 2012) is an exon deletion that is predicted to delete amino acids E766-S838 in the C-terminus of the lipin 1 protein (Figs. 1a and S1). When the analogous deletion was made in a human V5-tagged lipin 1 cDNA in an expression vector (V5 tag on the N-terminus), very little V5-tagged lipin 1 protein was expressed when the expression vector was transfected into HEK293 cells (Fig. 2a). The mRNA encoded by this mutant allele was also poorly expressed (Fig. 2b), and very little $^{35}$S-methionine-containing protein was synthesized in pulse-chase experiments (Fig. 2c). This indicates that the mutation resulting in the E766-S838_del is likely a complete loss of function allele.

## Single Amino Acid Substitutions in Lipin 1

We also examined the expression and activity of two single amino acid substitution mutations in lipin 1 associated with recurrent rhabdomyolysis in children, including the novel p. Leu635Pro variant identified in the child described above. The protein abundance of p.Leu635Pro was lower than WT lipin 1 protein (Fig. 2a), though the p.Leu635Pro mRNA was more abundant (Fig. 2b). The lower abundance of the protein was due to reduced protein stability as pulse-chase analyses demonstrated diminished protein half-life (Fig. 2c). Predictions of protein secondary structure generated by using the online PSIPRED tool (Jones 1999; Buchan et al. 2013) suggested that Leu635 is located within an α-helix (Fig. 2d). The p.Leu635Pro substitution was predicted to disrupt this α-helix and may cause formation of a β-strand just upstream of the mutation. Incubation with the proteasomal inhibitor, ALLN, promoted the accumulation of the mutant protein (Fig. 2e). This suggests that lipin 1 p. Leu635Pro protein is expressed, but is less stable, may be misfolded, and is targeted for proteasomal degradation.

Another previously reported lipin 1 single amino acid substitution associated with rhabdomyolysis (p.Arg725His) (Michot et al. 2012) was well expressed at the RNA and protein level (Fig. 2a, b). Since the p.Arg725His and p. Leu635Pro proteins were expressed, functional analysis of these mutant lipin 1 alleles might yield clues to the molecular basis for disease in lipin 1-deficient patients.

## Analysis of the Subcellular Localization and Transcriptional Regulatory Function of Lipin 1 Mutant Proteins

Lipin 1 protein has been visualized across a variety of cellular compartments. Within a given cell, lipin 1 may be predominantly cytoplasmic (very little in the nucleus), equally distributed in the nucleus and cytoplasm, or predominantly nuclear (Fig. 3a). Comparison of the subcellular distribution WT and p.Arg725His protein detected no differences in the proportions of cells with lipin 1 staining in cytoplasmic, nuclear, or both compartments (Fig. 3a). Compared to WT lipin 1, the ability of p. Arg725His to coactivate MEF2A and PGC-1α, which are transcriptional regulators relevant to skeletal muscle, was also not affected (Fig. 3b). However, p.Leu635Pro protein was predominantly localized to the cytoplasm (Fig. 3a) and did not significantly coactivate MEF2A or PGC-1α activity (Fig. 3b). The perinuclear staining pattern of p.Leu635Pro is also consistent with the immunohistochemical staining results of the patient biopsy (Fig. 1h).

## PAP Activity of Lipin 1 Mutant Proteins

We compared the intrinsic PAP activity of lipin 1 mutant proteins to the activity of WT lipin 1 protein. Overexpressing the WT lipin 1 allele in HEK-293 cells markedly increased cellular PAP activity (Fig. 4a). Transfection of the p. Leu635Pro expression construct did not increase PAP activity compared to vector control-transfected cells, with the caveat that the p.Leu635Pro protein expressed at lower levels compared to than WT lipin 1. Treating p.Leu635Pro-

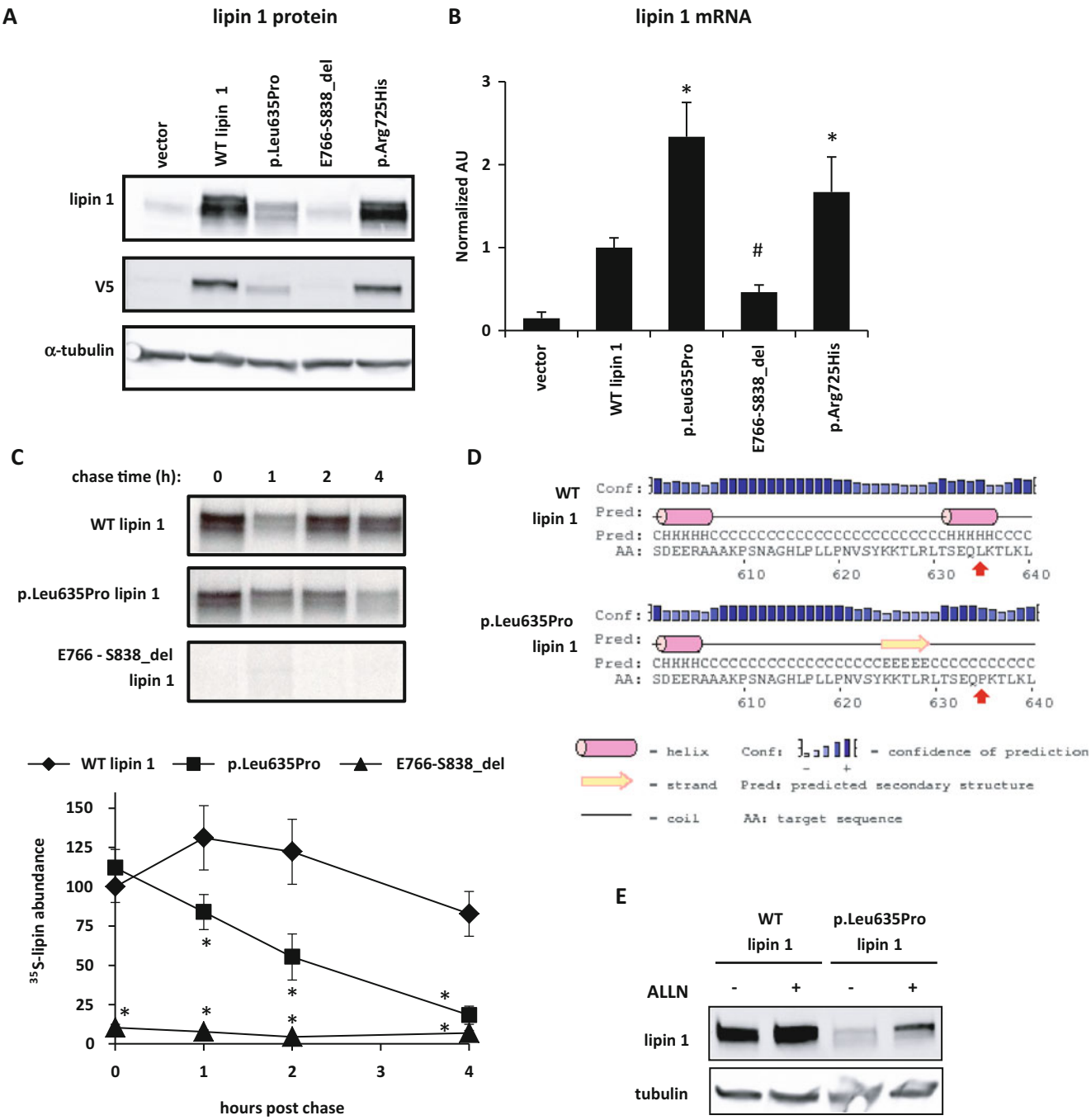


**Fig. 2** Lipin 1 proteins with disease-associated mutations have reduced protein abundance despite increased RNA levels and reduced protein stability. (**a**) Representative western blots using lysates from HEK293 cells transfected with V5-tagged lipin 1 (wild-type or mutant) or vector-only control are shown using antibodies against lipin 1, V5, and α-tubulin. (**b**) Lipin 1 mRNA expression of HEK293 cells transfected with V5-tagged lipin 1 (wild type or mutant) or vector only. Compared to WT lipin 1, p.Leu635Pro and p.Arg725His have significantly greater (*$P < 0.05$, *t*-test) and E766-S838 has significantly lower mRNA (#$P < 0.05$, *t*-test) expression. (**c**) A representative autoradiograph and average percent of radiolabeled lipin 1 abundance relative to WT lipin 1 from pulse-chase studies calculated from three separate gels are shown. Protein half-life of p. Leu635Pro was significantly lower than WT lipin 1 at 1, 2, and 4 h (*$P < 0.05$, *t*-test). (**d**) The panel depicts the results of PSIPRED prediction of the secondary structures of the affected region of lipin 1 proteins. The *red arrows* indicate the affected amino acids. p. Leu635Pro mutation results in disruption of a predicted α-helix and possible formation of a β-strand. (**e**) Representative western blots of HEK293 cells with overexpressed V5-tagged lipin 1 and p.Leu635Pro are shown. Cells were treated for 4 h with 26 μM ALLN prior to harvest

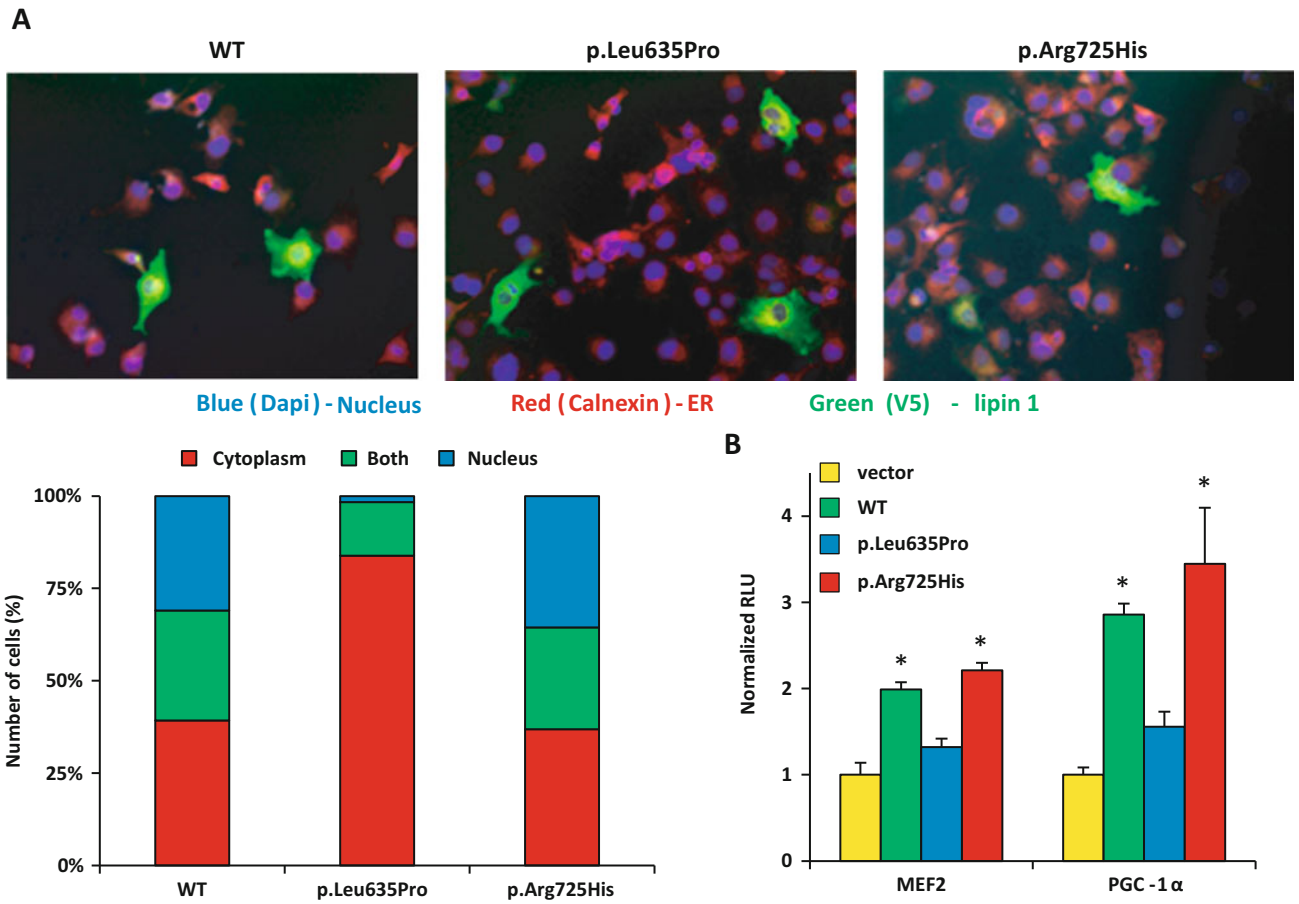


**Fig. 3** Nuclear localization and transcriptional regulatory function of lipin 1 mutant proteins. (**a**) COS7 cells transfected with V5-tagged lipin 1 (wild type or mutant) to examine its subcellular localization with the nuclear marker (DAPI) and the endoplasmic reticulum marker (calnexin). The percentage of the number of cells analyzed that localized to the cytoplasm, nucleus, or both was measured in at least 60 cells in at least 15 distinct fields. L365P had very little nuclear localization compared to WT and p.Arg725His. (**b**) Coactivation of Gal4-MEF2A and PGC-1α in COS7 cells cotransfected with a Gal4-responsive UAS-TK-luciferase reporter construct and cDNAs to express lipin 1 (WT or p.Arg725His), Gal4-MEF2A, Gal4-PGC-1α, or vector control. *$p < 0.05$ vs. vector control

transfected cells with ALLN caused p.Leu635Pro lipin 1 protein accumulation, but did not increase PAP activity in these cells (Fig. 4b). Transfection of p.Arg725His lipin 1, which was well expressed, also did not increase PAP activity. These results indicate that the two lipin 1 mutant proteins are deficient in PAP activity. To further investigate the defect in lipin 1 activity in the amino acid substitution mutants, the kinetic activities of purified WT, p.Leu635Pro, and p.Arg725His were examined. We found that the maximum velocity of the p.Arg725His and p.Leu635Pro proteins was markedly reduced, whereas the affinity for substrate was unaffected, compared to WT lipin 1 protein (Fig. 4c). This suggests that the defect in PAP activity of the p.Arg725His mutant is due to loss of catalysis and not substrate binding. Collectively, these data suggest that disease-associated mutations in lipin 1 lead to deficiency in intrinsic PAP activity.

## Discussion

The molecular basis for the pathogenesis of recurrent rhabdomyolysis associated with *LPIN1* mutations in humans is poorly understood. Previous work showed that PAP activity was markedly reduced in isolated myocytes from three patients with lipin 1 mutations, including the E766-S838_del mutation studied herein (Michot et al. 2013). However, those cells exhibited a complete loss of lipin 1 mRNA expression, and a distinction regarding impaired transcriptional regulatory function or PAP activity could not be made. In this study, by using recombinant lipin 1 proteins, we show that pathogenic, single amino acid substitutions in human lipin 1 disrupt PAP activity, but may not always affect nuclear transcriptional regulator function. A caveat to this conclusion is that only two single amino acid substitutions in *LPIN1* linked to rhabdomyolysis,

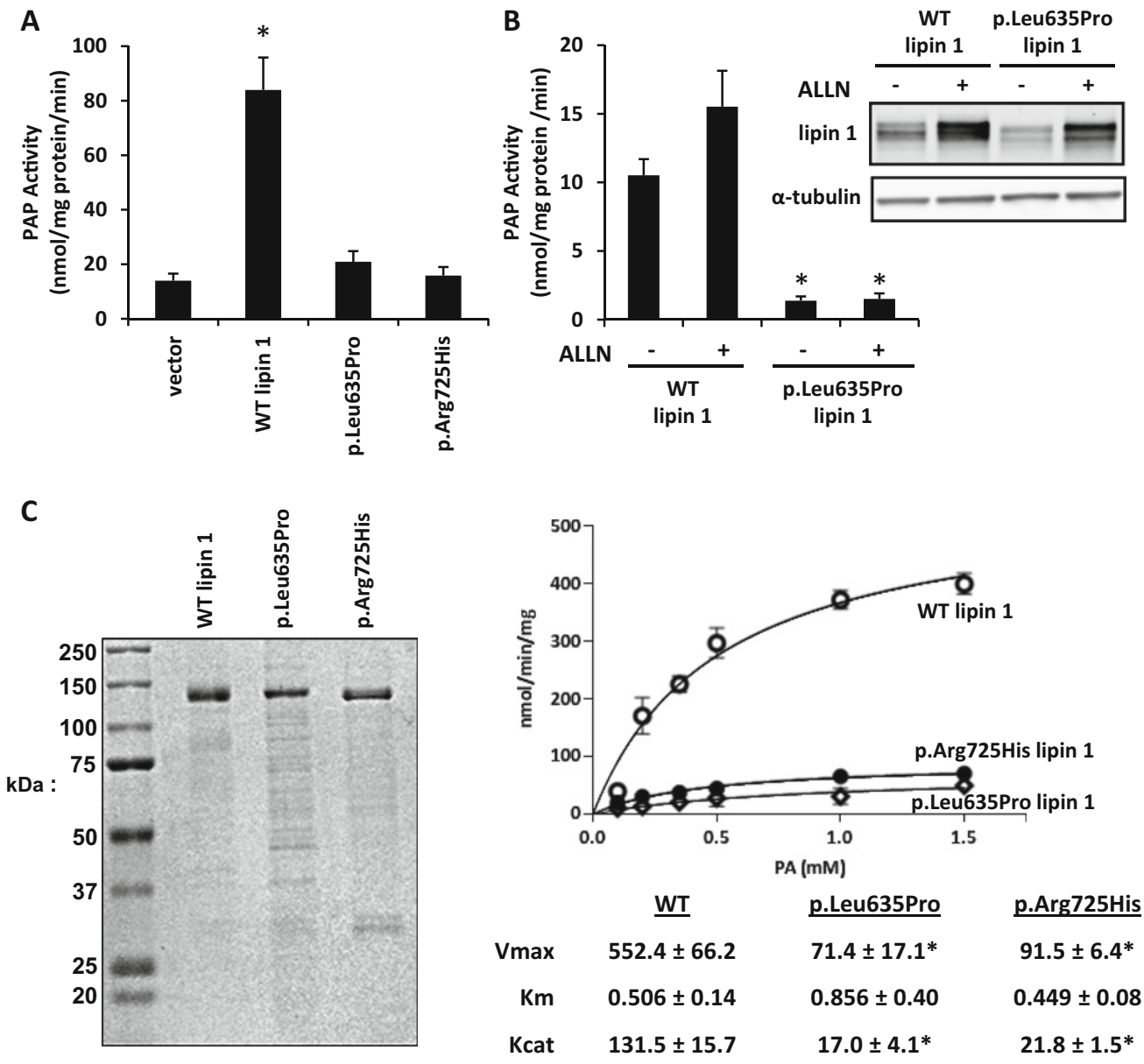


| | WT | p.Leu635Pro | p.Arg725His |
|---|---|---|---|
| Vmax | 552.4 ± 66.2 | 71.4 ± 17.1* | 91.5 ± 6.4* |
| Km | 0.506 ± 0.14 | 0.856 ± 0.40 | 0.449 ± 0.08 |
| Kcat | 131.5 ± 15.7 | 17.0 ± 4.1* | 21.8 ± 1.5* |

**Fig. 4** Lipin 1 proteins with disease-associated mutations lack PAP activity. (**a**) PAP activity of HEK293 cells overexpressing lipin 1 and lipin 1 mutants. PAP activity of WT lipin 1 was significantly greater than vector, p.Leu635Pro, and p.Arg725His (*$P < 0.05$, *t*-test). (**b**) PAP activity of HEK293 cells overexpressing lipin 1 and p.Leu635Pro incubated with ALLN. PAP activity of untreated WT lipin 1 was significantly greater than ALLN-treated and ALLN-untreated p. Leu635Pro (*$P < 0.05$, *t*-test). (**c**) Coomassie stain and PAP activity of purified recombinant WT lipin 1, p.Leu635Pro, and p.Arg725His. PAP activity was measured using Triton X-100/PA mixed micelles at pH 7.5. WT lipin 1 had approx. sixfold higher $V_{max}$ than p.Leu635Pro and p.Arg725His with no change in $K_m$

including the novel mutation identified herein, have been characterized, and thus, broad generalizations regarding this conclusion should be tempered accordingly.

The data presented herein suggest that abnormalities in PAP activity, and potentially resulting effects on glycerolipid content or partitioning, play a role in myocyte injury and necrosis leading to the rhabdomyolysis of lipin 1 deficiency. Clear links between the loss of lipin 1-mediated PAP activity and myocyte damage can be drawn. Conversion of PA to DAG is required for synthesis of triglyceride and phospholipids that are major constituents of cell membranes. Mutations in lipin 1 PAP activity would be predicted to increase the cellular PA concentration, which may be toxic and/or activate inflammatory MAPK signaling cascades (Nadra et al. 2008). PA also activates mTORC1 kinase (Sun and Chen 2008; Mitra et al. 2013), which has been linked to development of muscle injury and myopathy (Castets et al. 2013). A number of mitochondrial defects

lead to recurrent rhabdomyolysis (Bennett 2010; Zutt et al. 2014), and lipin 1 PAP activity impacts mitochondrial function by regulating fission and fusion (Huang et al. 2011). Very recently, it was reported that lipin 1 deficiency in muscle of mice caused myopathy via impaired autophagy, and a link between lipin 1-mediated PAP activity and autolysosome maturation was defined (Zhang et al. 2014). Further exploration of the molecular mechanisms involved will undoubtedly be the focus of future work.

Our molecular characterization of the E766-S838_del and p.Leu635Pro alleles in vitro agrees with the characterization of lipin 1 in the patient biopsy. Neither allele was well expressed at the protein level in cultured cells. Consistent with this, we had difficulty detecting lipin 1 protein in the patient biopsy by western blotting analysis. The recombinant p.Leu635Pro lipin 1 protein that was expressed tended to aggregate in the cytosol, particularly in the perinuclear region, of Cos7 fibroblasts. Immunohistochemical staining of a section of the patient biopsy showed a remarkably similar pattern of staining. This mislocalization of the p.Leu635Pro lipin 1 protein may also prevent it from trafficking to its substrate, PA, which is embedded in the ER membrane, though this remains to be determined. We believe that this is the first characterization of recombinant lipin 1 proteins harboring pathogenic mutations, and our work provides a clear mechanistic basis for the loss of lipin 1 activity in this patient with recurrent rhabdomyolysis.

Our current understanding of lipin 1 structure-function relationships provides clues regarding why these single amino acid substitutions lead to loss of lipin 1 function. The loss of PAP activity in the p.Arg725His mutant, which was well expressed, is consistent with the location of this highly conserved arginine in the HAD II domain (Figs. 1a and S1), which is a canonical component of classic HAD domains (Kok et al. 2012). Kinetic analyses suggest that this mutant lacks catalytic activity rather than the ability to bind substrate, which is consistent with its location in a HAD domain rather than the polybasic region required for binding (Eaton et al. 2013). The p.Leu635Pro substitution falls outside of the highly conserved C-lipin domain (Peterfy et al. 2001). The proline insertion in a predicted α-helix domain disrupts the α-helix and may lead to protein misfolding and degradation. Pulse-chase studies demonstrated a reduced protein half-life for p.Leu635Pro protein, and proteosomal inhibition caused accumulation of the WT and mutant allele. This is consistent with recent work indicating that the yeast and mouse homologues of lipin 1 are degraded via a proteosomal pathway (Pascual et al. 2014; Zhang et al. 2014).

In conclusion, we believe that this is the first report of a pathogenic p.Leu635Pro mutation in *LPIN1* as well as the first report of a *LPIN1* mutation in a North American patient with recurrent myoglobulinuria. We present evidence that single amino acid substitutions in lipin 1, including the novel variant, that are associated with recurrent rhabdomyolysis result in loss of PAP catalytic activity. This may facilitate the identification of the pathogenic mechanisms leading to myocyte cell death and suggest targeted therapies to treat afflicted patients.

## One Sentence

Herein, we show that recurrent rhabdomyolysis in a pediatric patient was associated with mutations in the bifunctional lipin 1 protein and that pathogenic mutations in lipin 1 led to loss of intrinsic phosphatidic acid phosphohydrolase activity.

## Compliance with Ethics Guidelines

### Conflict of Interest

George G. Schweitzer, Sara L. Collier, Zhoujj Chen, James M. Eaton, Anne M. Connolly, Robert C. Bucelli, Alan Pestronk, Thurl E. Harris, and Brian N. Finck declare that they have no conflict of interest.

### Informed Consent

All procedures followed were in accordance with the ethical standards of the responsible committee on human experimentation (institutional and national) and with the Helsinki Declaration of 1975, as revised in 2000. Informed consent was obtained from all patients for being included in the study.

### Author Contributions

G.G.S. performed experiments, analyzed data, generated figures, and wrote the manuscript. S.L.C, Z.C., J.M.E. performed experiments, analyzed data, generated figures, and edited portions of the manuscript. A.M.C. worked with the patient, analyzed data, and edited the manuscript. R.C.B performed experiments, analyzed data, generated figures, and wrote portions of the manuscript. A.P., T.E.H., and B.N.F analyzed data and wrote portions of the manuscript.

## References

Bennett MJ (2010) Pathophysiology of fatty acid oxidation disorders. J Inherit Metab Dis 33:533–537

Buchan DW, Minneci F, Nugent TC, Bryson K, Jones DT (2013) Scalable web services for the PSIPRED protein analysis workbench. Nucleic Acids Res 41:W349–W357

Castets P, Lin S, Rion N et al (2013) Sustained activation of mTORC1 in skeletal muscle inhibits constitutive and starvation-induced autophagy and causes a severe, late-onset myopathy. Cell Metab 17:731–744

Eaton JM, Mullins GR, Brindley DN, Harris TE (2013) Phosphorylation of lipin 1 and charge on the phosphatidic acid head group control its phosphatidic acid phosphatase activity and membrane association. J Biol Chem 288:9933–9945

Finck BN, Gropler MC, Chen Z et al (2006) Lipin 1 is an inducible amplifier of the hepatic PGC-1alpha/PPARalpha regulatory pathway. Cell Metab 4:199–210

Han GS, Wu WI, Carman GM (2006) The Saccharomyces cerevisiae Lipin homolog is a Mg2+−dependent phosphatidate phosphatase enzyme. J Biol Chem 281:9210–9218

Harris TE, Huffman TA, Chi A et al (2007) Insulin controls subcellular localization and multisite phosphorylation of the phosphatidic acid phosphatase, lipin 1. J Biol Chem 282:277–286

Huang H, Gao Q, Peng X et al (2011) piRNA-associated germline nuage formation and spermatogenesis require MitoPLD profusogenic mitochondrial-surface lipid signaling. Dev Cell 20:376–387

Jones DT (1999) Protein secondary structure prediction based on position-specific scoring matrices. J Mol Biol 292:195–202

Kelly DP, Strauss AW (1994) Inherited cardiomyopathies. N Engl J Med 330:913–919

Kok BP, Venkatraman G, Capatos D, Brindley DN (2012) Unlike two peas in a pod: lipid phosphate phosphatases and phosphatidate phosphatases. Chem Rev 112:5121–5146

Martin A, Hales P, Brindley DN (1987) A rapid assay for measuring the activity and the Mg2+ and Ca2+ requirements of phosphatidate phosphohydrolase in cytosolic and microsomal fractions of rat liver. Biochem J 245:347–355

Michot C, Hubert L, Brivet M et al (2010) LPIN1 gene mutations: a major cause of severe rhabdomyolysis in early childhood. Hum Mutat 31:E1564–E1573

Michot C, Hubert L, Romero NB et al (2012) Study of LPIN1, LPIN2 and LPIN3 in rhabdomyolysis and exercise-induced myalgia. J Inherit Metab Dis 35:1119–1128

Michot C, Mamoune A, Vamecq J et al (2013) Combination of lipid metabolism alterations and their sensitivity to inflammatory cytokines in human lipin-1-deficient myoblasts. Biochim Biophys Acta 1832:2103–2114

Mitra MS, Chen Z, Ren H et al (2013) Mice with an adipocyte-specific lipin 1 separation-of-function allele reveal unexpected roles for phosphatidic acid in metabolic regulation. Proc Natl Acad Sci U S A 110:642–647

Mozaffar T, Pestronk A (2000) Myopathy with anti-Jo-1 antibodies: pathology in perimysium and neighbouring muscle fibres. J Neurol Neurosurg Psychiatry 68:472–478

Nadra K, de Preux Charles AS, Medard JJ et al (2008) Phosphatidic acid mediates demyelination in Lpin1 mutant mice. Genes Dev 22:1647–1661

Ng PC, Henikoff S (2001) Predicting deleterious amino acid substitutions. Genome Res 11:863–874

Pascual F, Hsieh LS, Soto-Cardalda AI, Carman GM (2014) Yeast Pah1p phosphatidate phosphatase is regulated by proteasome-mediated degradation. J Biol Chem

Peterfy M, Phan J, Xu P, Reue K (2001) Lipodystrophy in the fld mouse results from mutation of a new gene encoding a nuclear protein, lipin. Nat Genet 27:121–124

Ramensky V, Bork P, Sunyaev S (2002) Human non-synonymous SNPs: server and survey. Nucleic Acids Res 30:3894–3900

Ren H, Federico L, Huang H et al (2010) A phosphatidic acid binding/nuclear localization motif determines lipin1 function in lipid metabolism and adipogenesis. Mol Biol Cell 21:3171–3181

Sun Y, Chen J (2008) mTOR signaling: PLD takes center stage. Cell Cycle 7:3118–3123

Tonin P, Lewis P, Servidei S, DiMauro S (1990) Metabolic causes of myoglobinuria. Ann Neurol 27:181–185

Zeharia A, Shaag A, Houtkooper RH et al (2008) Mutations in LPIN1 cause recurrent acute myoglobinuria in childhood. Am J Hum Genet 83:489–494

Zhang P, Verity MA, Reue K (2014) Lipin-1 regulates autophagy clearance and intersects with statin drug effects in skeletal muscle. Cell Metab 20:267–279

Zutt R, van der Kooi AJ, Linthorst GE, Wanders RJ, de Visser M (2014) Rhabdomyolysis: review of the literature. Neuromuscul Disord 24:651–659

JIMD Reports
DOI 10.1007/8904_2015_442

RESEARCH REPORT

# Dup-24 bp in the *CHIT1* Gene in Six Mexican Amerindian Populations

**T.D. Da Silva-José · K.J. Juárez-Rendón · J.A. Juárez-Osuna · A. Porras-Dorantes · A. Valladares-Salgado · M. Cruz · M. Gonzalez-Ibarra · A.G. Soto · M.T. Magaña-Torres · L. Sandoval-Ramírez · José Elías García-Ortiz**

Received: 18 February 2015 / Revised: 03 April 2015 / Accepted: 09 April 2015 / Published online: 13 May 2015


**Abstract** Chitotriosidase (CHIT, EC 3.2.1.14) is an enzyme secreted by activated macrophages with the ability to hydrolyze the chitin of pathogens. The high activity of this enzyme has been used as a secondary biomarker of response to treatment in patients with Gaucher disease (OMIM 230800). Within the world's population, approximately 6% is homozygous and 35% is heterozygous for the most common polymorphism in the *CHIT1* gene, a 24-bp duplication (dup-24 bp), with homozygosity of this duplication causing inactivation of the enzyme but without major consequences for health. To determine the frequency of the dup-24 bp *CHIT1* gene in indigenous populations from Mexico, 692 samples were analyzed: Purepecha (49), Tarahumara (97), Huichol (97), Mayan (139), Tenek (97), and Nahua (213). We found that the groups were in Hardy-Weinberg equilibrium. The dup-24 bp allele frequency was found to be (in order of highest to lowest) 37% (Mayan), 34% (Huichol and Nahua), 33% (Purepecha), 31% (Tenek), and 29% (Tarahumara).

Communicated by: Daniela Karall

Competing interests: None declared

T.D. Da Silva-José · K.J. Juárez-Rendón · J.A. Juárez-Osuna · A. Porras-Dorantes · M.T. Magaña-Torres · L. Sandoval-Ramírez · J.E. García-Ortiz (✉)
División de Genética, Centro de Investigación Biomédica de Occidente, CMNO-IMSS, Sierra Mojada 800, Col. Independencia, Guadalajara 44340, Jalisco, Mexico
e-mail: jose.elias.garcia@gmail.com

T.D. Da Silva-José · J.A. Juárez-Osuna · A. Porras-Dorantes
Doctorado en Genética Humana, Centro Universitario de Ciencias de la Salud, Universidad de Guadalajara, Guadalajara, Jalisco, Mexico

A. Valladares-Salgado · M. Cruz · M. Gonzalez-Ibarra · A.G. Soto
Unidad de Investigación Médica en Bioquímica Centro Médico Nacional, "Siglo XXI" IMSS, México, D.F., Mexico

## Introduction

Chitinases comprise a family of enzymes that hydrolyze chitin and have been found in a wide variety of organisms such as plants, nematodes, bacteria, fungi, insects, and mammals (Boot et al. 1995). Human chitinase (CHIT, EC 3.2.1.14) is a 50-kDa enzyme containing a C-terminal chitin-binding domain and is secreted from activated macrophages. This enzyme is proteolytically processed to a C-terminally truncated 39-kDa isoform characterized by hydrolase activity and is primarily thought to play a role in the body's defense against chitin-containing pathogens (Renkema et al. 1997; Boot et al. 1999). CHIT activity has been used in the diagnostic screening of several lysosomal storage diseases, in which this enzyme is usually highly elevated, making this enzyme a useful secondary biomarker for the treatment monitoring of Gaucher disease (OMIM 230800), Niemann-Pick disease (OMIM 257200), Krabbe disease (OMIM 245200), and thalassemia (OMIM 603141) (Guo et al. 1995; Boot et al. 1999).

The *CHIT1* gene (OMIM 600031.0001), localized on chromosome 1q32.1, consists of 11 exons and spans approximately 14 kb of genomic DNA coding a protein of 466 amino acids [UCSC Genomic coordinates (GRCh37): 1:203,185,206–203,198,859]. CHIT enzyme deficiency is recessively inherited, with widely different prevalence rates in various world populations (Boot et al. 1999). Currently, five genomic polymorphisms have been associated with

diminished CHIT activity: p.G102S (rs2297950), p.G354R (rs9943208), p.A442G/V (rs1065761), a 4-bp deletion across the exon/intron-10 boundary (complex E/I −10) (rs9943208), and a 24-bp duplication (dup-24 bp) (rs3831317) in exon 10 (Lee et al. 2007; Arndt et al. 2013).

The use of CHIT as a secondary biomarker to monitor enzymatic replacement therapy (ERT) in patients with Gaucher disease is common worldwide; however, ruling out the presence of null activity of CHIT is mandatory. The dup-24 bp polymorphism is possibly the most frequent explanation for a deficiency in chitotriosidase activity, resulting from the aberrant splicing and deletion of amino acids 344–372 (Boot et al. 1999). The biologic significance of the very high frequency of this gene polymorphism remains unexplained, which suggests it may have a selective advantage not yet completely understood (Canudas et al. 2001; Lee et al. 2007). In the African population, the dup-24 bp homozygous state is rare, with an estimated frequency of 2% (Malaguarnera et al. 2003). In contrast, the frequency of the homozygous status is approximately 6% in Caucasians (Boot et al. 1999). In Asian groups, the highest frequencies of this polymorphism have been found in South China, followed by South Korea, Southeast Asia, Japan, and Taiwan, with homozygosity frequencies ranging from 45% to 64% (Lee et al. 2007). Regarding Latin American groups, Peruvian and Mexican populations have been studied. In Peruvian populations, the published homozygosity frequencies are 12% (Peruvian mestizo), 22% (indigenous Amerindian), 26% (Amazonian Amerindian), and 12% (Quechua indigenous) (Manno et al. 2014). In Mexican mestizos, the frequency of dup-24 bp has been estimated as 5.56% for homozygosity (Juárez-Rendón et al. 2012), with no known frequencies for Mexican Amerindian groups. Given that higher frequencies of the dup-24 bp polymorphism are observed in Asian populations and other Amerindian populations, in this study, we wanted to investigate the frequency of the dup-24 bp polymorphism in six Mexican Amerindian populations.

## Material and Methods

A total of 692 samples of random individuals belonging to six indigenous groups distributed within the Mexican political boundaries were collected for genetic analysis. The samples were composed of Purepecha ($n = 49$), Tarahumara ($n = 97$), Huichol ($n = 97$), Mayan ($n = 139$), Tenek ($n = 97$), and Nahua ($n = 213$). Informed consent was obtained for these analyses, and peripheral blood samples were obtained from the participants after the objectives of this study were discussed with every participant. The Institutional Review Board of our center approved the scientific and ethics procedures in this study.

DNA was extracted according to standard protocols from peripheral blood leucocytes (Miller et al. 1988). The molecular analysis for dup-24 bp in the *CHIT1 g*ene was carried out by endpoint polymerase chain reaction (PCR) (Sanguinetti et al. 1994; Juárez-Rendón et al. 2012).

### Statistical Analysis

Genotype and allele frequencies were determined by direct counting. Hardy-Weinberg equilibrium was calculated using the chi-square test. The allelic frequencies were compared with the data from eight reported population: Mexican mestizos, Peruvian mestizos, three Peruvian Amerindian populations, Asians, Europeans, and Africans. The distribution of the allelic frequencies between pairs of populations was analyzed with exact test of population differentiation, which is analogous to Fisher's exact test. One million of steps in Markov chain were used to obtain the $p$-value and a value of $p < 0.05$ being considered significant. Arlequin ver. 3.0 software was used for the statistical analysis (Laurent Excoffier et al. 2005).

## Results

We studied the dup-24 bp polymorphism of the *CHIT1* gene in 692 Mexican Amerindians from north (Tarahumara), west (Huichol, Purepecha, Nahua, and Tenek), and south (Mayan) areas of Mexico. In these indigenous groups, we found 308 (44.5%) individuals with a homozygous wild-type genotype (wt/wt), 306 (44.2%) individuals with a heterozygous genotype (wt/dup), and 78 (11.3%) individuals who were homozygous (dup/dup) for the 24-bp duplication. The frequency of dup/dup was observed in a range of 10% (Tarahumara and Nahua) to 14% (Purepecha). In contrast, the allele frequency of dup-24 bp was found to be highest in Mayan (37%) and lowest in Tarahumara (29%) (Table 1). The observed distribution of genotypes fell within the Hardy-Weinberg equilibrium.

In the distribution of the polymorphism genotype frequencies, the six Mexican indigenous groups showed no significant differences among them ($p < 0.05$). However, the Huichol, Mayan, and Nahua showed significant differences with the Mexican mestizo population. These differences are due mainly to an increase in the frequency of the heterozygous wt/dup genotype. Amerindians and Quechua indigenous groups did not differ with the Mexican indigenous populations, and Peruvian mestizos were similar to the Purepecha and Mayan populations.

**Table 1** Genotypic and allelic distribution of the dup-24 bp polymorphism in the *CHIT1* gene in Mexican Amerindian populations

| | | Genotype frequencies (%) | | | | | | Allele frequencies | | | | Hardy-Weinberg |
|---|---|---|---|---|---|---|---|---|---|---|---|---|
| Populations | Number | Wt/wt | % | Wt/Dup | % | Dup/Dup | % | Wt | % | Dup | % | *p*-value |
| Purepechas | 49 | 24 | 49 | 18 | 37 | 7 | 14 | 66 | 67 | 32 | 33 | 0.2487 |
| Tarahumaras | 97 | 50 | 52 | 37 | 38 | 10 | 10 | 137 | 71 | 57 | 29 | 0.4261 |
| Huicholes | 97 | 43 | 45 | 42 | 43 | 12 | 12 | 128 | 66 | 66 | 34 | 0.7265 |
| Mayas | 139 | 55 | 39 | 66 | 48 | 18 | 13 | 176 | 63 | 102 | 37 | 0.7948 |
| Tenek | 97 | 47 | 48 | 40 | 41 | 10 | 11 | 134 | 69 | 60 | 31 | 0.7316 |
| Nahua | 213 | 89 | 42 | 103 | 48 | 21 | 10 | 281 | 66 | 145 | 34 | 0.2618 |
| Mestizos[9] | 306 | 177 | 58 | 112 | 37 | 17 | 6 | 466 | 76 | 146 | 24 | 0.8961 |

Wild type (wt); duplication 24 bp (Dup)

In contrast, the Amazonian Indians, Asians, Europeans, and Africans were different from all of the Mexican populations (Table 2).

## Discussion

The use of CHIT as a secondary biomarker has been considered a useful tool for monitoring ERT on patients with Gaucher disease. However, one important caveat is the presence of individuals homozygous for dup-24 bp in *CHIT1* who will require other biomarkers to follow up on their response to ERT (Guo et al. 1995; Lee et al. 2007; Manno et al. 2014). The identification of this polymorphism should also be useful for establishing genetic relationships between populations.

The distribution of this polymorphism was homogeneous across the Mexican Amerindian populations studied, and the Mexican mestizo population was similar to the Purepecha, Tarahumara, and Tenek. We also found a high allelic frequency of the dup-24 bp polymorphism of the *CHIT1* gene, the highest reported for ethnic groups living in Mexico and one of the highest among world populations (Lee et al. 2007). This observation is in accordance with the primarily Asian origin of the American indigenous groups more than 10,000 years ago (Reich et al. 2012) and supports the hypothesis of a selective advantage associated with this gene variant (Lee et al. 2007) or a possible founder effect as well as other markers (Manno et al. 2014). Although the null clinical significance of the dup-24 bp polymorphism in the *CHIT1* gene has been established for some time now (Boot et al. 1998; Canudas et al. 2001; Piras et al. 2007), it has not been determined if there is a clinical significance of the high frequency of homozygosity of dup-24 bp in *CHIT1* in Amerindian populations. Some authors have proposed that a CHIT deficiency can increase the susceptibility to infections due to parasites containing chitin (Malaguarnera et al. 2003), but this implication has to be tested in a future study.

## Compliance with Ethics Guidelines

### Conflicts of Interest

Thiago Donizete Da Silva-José, Karina Janett Juárez-Rendón, Jesús Alejandro Juárez-Osuna, Angela Porras-Dorantes, Adán Valladares-Salgado, Miguel Cruz, Miriam Gonzalez-Ibarra, Ana G. Soto, María Teresa Magaña-Torres, Lucila Sandoval-Ramírez, and José Elías García-Ortiz declare that they have no conflict of interest.

### Originality

The authors state that this is an original article and has not been simultaneously presented to any other journal and thus is exclusive to *Journal of Inherited Metabolic Disease*.

### Contribution of the Authors

Thiago Donizete Da Silva-José participated in the study design, execution, data analysis, statistical analysis, manuscript drafting, and critical discussion. Karina Janett Juárez-Rendón participated in the study design, manuscript drafting, and critical discussion. Jesús Alejandro Juárez-Osuna and Angela Porras-Dorantes participated in the acquisition of data and study execution. Adán Valladares-Salgado, Miguel Cruz, Miriam Gonzalez-Ibarra, and Ana G. Soto participated in the acquisition of data and samples. María Teresa Magaña-Torres and Lucila Sandoval-Ramírez participated in the study design, data analysis, and critical discussion. José Elías García-Ortiz participated in the study

**Table 2** *p*-values of the comparison from allelic frequencies of the dup-24 bp polymorphism between pairs of populations analyzed*

| Population | Purepecha | Tarahumara | Huichol | Mayan | Tenek | Nahua | Mexican mestizo | Asiatic | European | African | Peruvian mestizos | Indigenous Amerindian | Indigenous Amazonian |
|---|---|---|---|---|---|---|---|---|---|---|---|---|---|
| Tarahumara | 0.77178 | | | | | | | | | | | | |
| Huichol | 0.75821 | 0.61851 | | | | | | | | | | | |
| Mayan | 0.42037 | 0.21000 | 0.76880 | | | | | | | | | | |
| Tenek | 0.74951 | 0.95429 | 0.82458 | 0.41009 | | | | | | | | | |
| Nauha | 0.28584 | 0.23058 | 0.61454 | 0.65843 | 0.47287 | | | | | | | | |
| Mestizo[9] | 0.08031 | 0.20447 | 0.01816 | 0.00041 | 0.12841 | 0.00108 | | | | | | | |
| Asiatic[10] | 0.00003 | 0.00000 | 0.00000 | 0.00000 | 0.00000 | 0.00000 | 0.00000 | | | | | | |
| European[10] | 0.00210 | 0.00258 | 0.00003 | 0.00000 | 0.00000 | 0.00000 | 0.05298 | 0.00000 | | | | | |
| African[10] | 0.00000 | 0.00000 | 0.00000 | 0.00000 | 0.00000 | 0.00000 | 0.00000 | 0.00000 | 0.00000 | | | | |
| Mestizos Peruvian[12] | 0.05939 | 0.00294 | 0.04577 | 0.10112 | 0.00901 | 0.00774 | 0.00000 | 0.07108 | 0.00000 | 0.00000 | | | |
| Indigenous Amerindian[12] | 0.72112 | 0.61021 | 0.25594 | 0.06524 | 0.43566 | 0.05416 | 0.19040 | 0.00000 | 0.02372 | 0.00000 | 0.00348 | | |
| Amazonian indigenous[12] | 0.04782 | 0.00251 | 0.02309 | 0.04107 | 0.00509 | 0.00334 | 0.0000 | 0.38909 | 0.00000 | 0.00000 | 0.84083 | 0.00334 | |
| Quechua indigenous[12] | 0.30761 | 0.19435 | 0.54261 | 0.72166 | 0.31844 | 0.64632 | 0.02705 | 0.05346 | 0.00000 | 0.00000 | 0.59694 | 0.08153 | 0.36634 |

*$p < 0.05$

design, execution, data analysis, statistical analysis, manuscript drafting, and critical discussion.

Informed Consent

All procedures were in accordance with ethical standards of the responsible committee on national human experimentation and with the Helsinki Declaration of 1975, as revised on 2000 and 2013. Written informed consent was obtained from all individuals for being included into the study.

## References


Arndt S, Hobbs A, Sinclaire I et al (2013) Chitotriosidase deficiency: a mutation update in an African population. JIMD Rep 10:11–16

Boot RG, Renekema GH, Stijiland A et al (1995) Cloning of a cDNA encoding chitotriosidase. A human chitinase produced by macrophages. J Biol Chem 270:26252–26256

Boot RG, Renkema GH, Verhoek M et al (1998) The human chitotriosidase gene. Nature of inherited enzyme deficiency. J Biol Chem 273:25680–25685

Boot RG, van Achterberg TA, van Aken BE et al (1999) Strong induction of members of the chitinase family of proteins in atherosclerosis: chitotriosidase and human cartilage gp-39 expressed in lesion macrophages. Artherioscler Thromb Vasc Biol 19:687–694

Canudas J, Cenarro A, Civeira F et al (2001) Chitotriosidase genotype and serum activity in subjects with combined hyperlipidemia: effect of the lipid-lowering agents, atorvastatin and bezafibrate. Metabolism 50:447–450

Excoffier L, Laval G, Schneider S (2005) Arlequin ver. 3.0: an integrated software package for population genetics data analysis. Evol Bioinform Online 1:47–50

Guo YF, He W, Boer AM et al (1995) Elevated plasma chitotriosidase activity in various lysosomal storage disorders. J Inherit Metab Dis 18:717–722

Juárez-Rendón KJ, Lara-Aguilar RA, García-Ortiz JE (2012) 24-bp duplication on CHIT1 gene in Mexican population. Rev Med Inst Mex Seguro Soc 50:375–377

Lee P, Waalen J, Crain K et al (2007) Human chitotriosidase polymorphisms G354R and A442V associated with reduced enzyme activity. Blood Cells Mol Dis 39:353–360

Malaguarnera L, Ohazuruike LN, Tsianaka C et al (2003) Human chitotriosidase polymorphism is associated with human longevity in Mediterranean nonagenarians and centenarians. J Hum Genet 55:8–12

Manno N, SHerratt S, Boartto F et al (2014) High prevalence of chitotriosidase deficiency in Peruvian Amerindians exposed to chitin-bearing food and enteroparasites. Carbohydr Polym 113: 607–614

Miller SA, Dikes DD, Polesky HF (1988) A simple salting out procedure for extracting DNA from human nucleated cells. Nucleic Acids Res 16:1215

Piras I, Melis A, Ghiani ME et al (2007) Human CHIT1 gene distribution: new data from Mediterranean and European populations. J Hum Genet 52:110–116

Reich D, Patterson N, Campbell D et al (2012) Reconstructing Native American population history. Nature 488:370–374

Renkema GH, Boot RG, Strijland A et al (1997) Synthesis, sorting and processing into distinct isoforms of human macrophage chitotriosidase. Eur J Biochem 244:279–285

Sanguinetti CJ, Dias Neto E, Simpson AJ (1994) Rapid silver staining and recovery of PCR products separated on polyacrylamide gels. Biotechniques 17:914–921